

Muscle stem cells and glycogen metabolism
as targets for therapy in Pompe disease.

Rodrigo Cañibano Fraile

Colofon

Cover design: Rodrigo Cañibano Fraile
Lay-out: Publiss | www.publiss.nl
Print: Ridderprint | www.ridderprint.nl

© Copyright 2022: Rodrigo Cañibano Fraile, Rotterdam, the Netherlands, 2022

All rights reserved. No part of this thesis may be reproduced, distributed, stored in a retrieval system, or transmitted in any forms or by any means, without written permission of the author or, when appropriate, the publisher of the publications.

The work presented in this thesis was conducted at the Department of Pediatrics and the Department of Clinical Genetics, Erasmus MC University Medical Center Rotterdam, the Netherlands.

Muscle Stem Cells and Glycogen Metabolism as Targets for Therapy in Pompe Disease

**Spierstamcellen en glycogeenmetabolisme als doelwit voor het
ontwikkelen van therapieën voor de ziekte van Pompe**

Thesis

to obtain the degree of Doctor from the
Erasmus University Rotterdam

By command of the
rector magnificus

Prof. dr. A.L. Bredenoord

and in accordance with the decision of the Doctoral Board.

The public defense will be held on
Wednesday 1st June 2022 at 10:30 hours

by

Rodrigo Cañibano Fraile

born in Burgos, Spain.

Doctoral committee

Promotor: Prof. dr. A.T. van der Ploeg

Other members: Dr. J.C. de Greef
Prof. dr. P.A. van Doorn
Dr. W.L. van der Pol

Co-promotors: Dr. G.J. Schaaf
Dr. W.W.M. Pijnappel

–¿Qué gigantes? –dijo Sancho Panza.

–Aquellos que allí ves –respondió su amo– de los brazos largos, que los suelen tener algunos de casi dos leguas.

–Mire vuestra merced –respondió Sancho– que aquellos que allí se parecen no son gigantes, si no molinos de viento, y lo que en ellos parecen brazos son las aspas, que, volteadas por el viento, hacen andar la piedra del molino.

“What giants?” said Sancho Panza.

“Those thou seest there,” answered his master, “with the long arms, and some have them nearly two leagues long.”

“Look, your worship,” said Sancho; “what we see there are not giants but windmills, and what seem to be their arms are the sails that turned by the wind make the millstone go.”

Miguel de Cervantes, El ingenioso hidalgo Don Quijote de la Mancha

To my family.

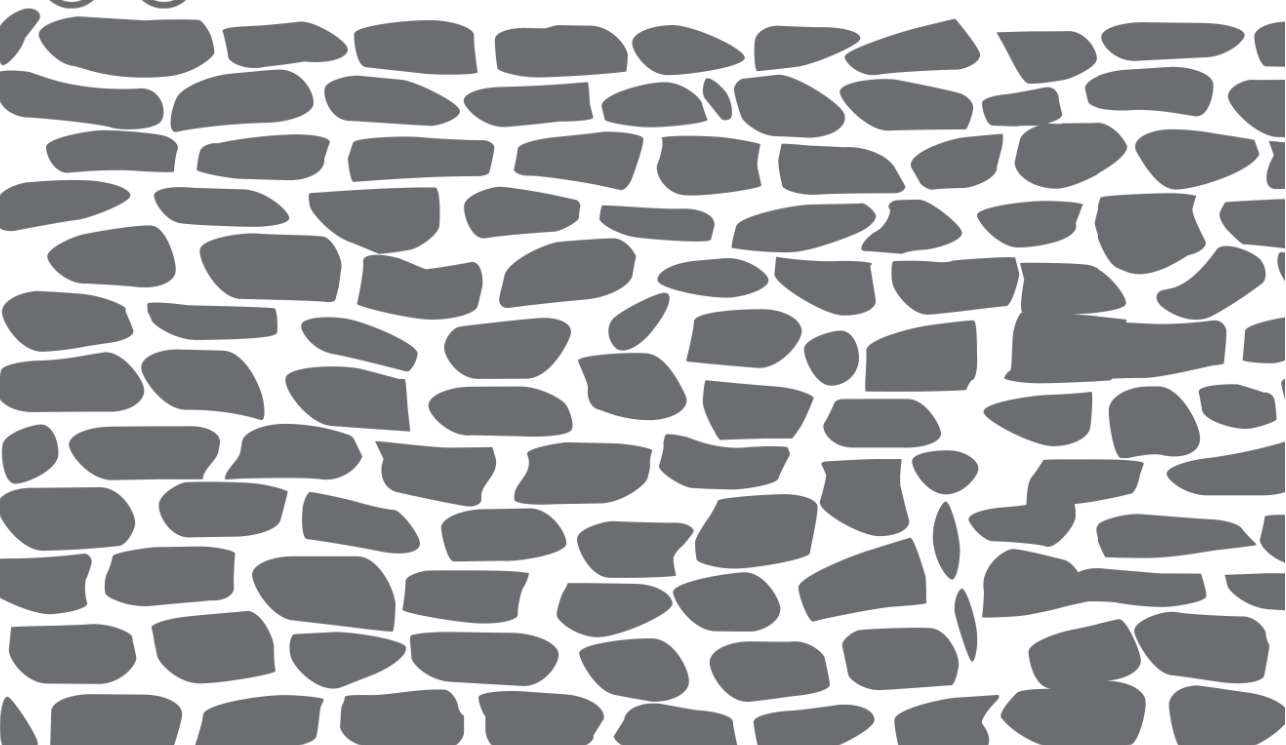
Table of Contents

List of abbreviations	8
Chapter 1: Introduction	11
Chapter 2: Lysosomal glycogen accumulation in Pompe disease results in disturbed cytoplasmic glycogen metabolism	51
Chapter 3: Restoring the regenerative balance in neuromuscular disorders: satellite cell activation as therapeutic target in Pompe disease	81
Chapter 4: An <i>in vitro</i> assay to quantify satellite cell activation using isolated mouse myofibers	109
Chapter 5: Provoked muscle regeneration transiently rescues the Pompe disease phenotype: the role of autophagy	137
Chapter 6: <i>Ex vivo</i> generation of reserve cell populations with enhanced muscle regenerative properties	169
Chapter 7: Discussion	211
Summary	238
Samenvatting	242
Resumen	246
<i>Curriculum vitae</i>	250
PhD portfolio	252
List of publications	254
Acknowledgements	255

List of abbreviations

AONs	Antisense oligonucleotides
AAV	Adeno-associated virus
BR	Brain
CRISPR	Clustered regularly interspaced short palindromic regions
CSA	Cross-sectional area
DEGs	Differentially expressed genes
DM	Differentiation medium
DMD	Duchenne muscle dystrophy
DP	Diaphragm
ECM	Extracellular matrix
EDL	<i>Extensor digitorum longus</i>
EdU	5-ethynyl-2'-deoxyuridine
EMA	European Medical Agency
ERT	Enzyme replacement therapy
EtOH	Ethanol
FAPs	Fibro-adipogenic progenitors
FCS	Fetal calf serum
FDA	Food and Drug Administration
FDR	False discovery rate
FGF2	Fibroblast growth factor 2
FRCs	Fast-adhering reserve cells
GAA	Acid α -glucosidase (protein)
GAA	Acid α -glucosidase (gene)
GAAGO	GAA knock out
GFP	Green fluorescent protein
GM	Proliferation medium
GMA	Glycolmethacrylate
GMP	Good manufacturing practice
GO	Gene ontology
GSDs	Glycogen storage diseases
GSDII	Glycogen storage disease Type II (Pompe disease)
HE	Hematoxylin-eosin (staining)
HHD	Hand-held dynamometry

HIV	Human immunodeficiency virus
HRT	Heart
HS	Horse serum
IGF-1	Insulin-like growth factor 1
IGFBPs	IGF binding proteins
iPSCs	Induced pluripotent stem cells
IVS1	c.32-13T>G disease associated variant
LSDs	Lysosomal storage disorders
MPS	Mucopolysaccharidosis
MRC	Medical Research Council (manual muscle testing function)
MRFs	Myogenic regulatory factors
MTT	Myoblast transfer therapy
MuSCs	Muscle stem cells
MyHC	Myosin heavy chain
NOD/SCID	Non-obese diabetic/Severe combined immunodeficiency
PAR	Parental cells
PAS	Periodic acid Schiff (staining)
PDEs	Phosphodiesterases
QF	<i>Quadriceps femoris</i>
RCs	Reserve cells
RT-qPCR	Reverse transcriptase quantitative polymerase chain reaction
SARS-CoV-2	Severe acute respiratory syndrome coronavirus 2
SMA	Spinal muscle atrophy
SPs	(Muscle) Side populations
SRCs	Slow-adhering reserve cells
SRT	Substrate reduction therapy
TA	<i>Tibialis anterior</i>
TALENs	Transcription activator-like effector nuclease
WT	Wild-type



Chapter 1

Introduction

While the 19th and the first half of the 20th centuries were dominated by advances in organic chemistry, the second half of the 20th and the 21st centuries are being led by astonishing developments in life-sciences. The current knowledge of biological processes is evolving faster than ever before. As a result, we are now able to understand, treat, and cure pathologies more effectively.

Fundamental research enables innovative discoveries with an enormous transformative power, while biotechnological and pharmaceutical industries thrive with the latest technical advances. Ultimately, all these efforts combined serve for the development of new approaches to treat disorders, some of which had no available therapy previously. However, this is not without many challenges. To date, many disorders remain without a treatment, and numerous questions still remain unanswered. In our research group, we aim to deepen the knowledge and provide answers to some of the questions that affect neuromuscular disorders, with a particular focus on Pompe disease, ultimately aiming to provide new alternatives to patients.

The purpose of this thesis is to study the molecular mechanisms that drive Pompe disease, as well as to investigate strategies to enhance muscle regeneration; ultimately aimed at the development of regenerative therapies for muscle disorders. We humbly hope that the work of this thesis contributes to the fulfillment of these goals in the future.

In this first chapter, we described fundamental notions on Pompe disease, a disease that is investigated in depth in chapters 2, 3, 4, and 5. We also provided the basic knowledge on skeletal muscle cell biology, necessary to provide the context to chapter 6. The concepts gathered in the lines below are relevant for the work performed in this thesis.

Pompe disease

Pompe disease, also known as glycogen storage disease Type II (GSDII), is a rare metabolic myopathy characterized by deficiency of acid α -glucosidase and is caused by disease-associated variants in the *GAA* gene. As a consequence, glycogen cannot be degraded inside the lysosome and accumulates [1,2]. In the classic infantile form of Pompe disease, its most severe form, *GAA* enzyme activity is practically absent. If left untreated, patients die of cardiorespiratory insufficiency usually before the age of 1 year. In childhood or adult onset patients, disease progression is slower and muscle weakness develops over time, eventually leading

to motor and respiratory function impairment. Patients often become wheelchair- and ventilator-dependent [2]. Enzyme replacement therapy is the standard care for Pompe disease since its approval by FDA/EMA in 2006 [3–5]. ERT consists of systemic administration of recombinant human acid α -glucosidase (rhGAA) (Lumizyme/Myozyme, Sanofi Genzyme). ERT improves survival and reduces cardiomyopathy in classic infantile patients. In childhood and adult onset patients it stabilizes respiratory function and ameliorates muscle function impairment, although variability in response to treatment exists between patients [6].

Glycogen metabolism in skeletal muscle

Deficiency of GAA in Pompe disease leads to lysosomal glycogen accumulation. Since skeletal muscle is the major organ for insulin-mediated glucose uptake, and most of the glucose is converted into glycogen for storage, it is essential to understand the biochemical regulation of glycogen synthesis in order to study its possible impact in the pathology.

Skeletal muscle takes up glucose from the bloodstream and converts it in glycogen that is stored both in the cytoplasm and in the lysosomes (Figure 1). This process also occurs in the liver. However, the main difference in glucose metabolism between skeletal muscle and liver is that the latter expresses glucose-6-phosphatase (G6Pase), allowing it to release (excess) of glucose into the bloodstream. Skeletal muscle does not, and excess of glucose is preferentially stored as glycogen. In the liver, glucose is taken up by glucose transporter 2 (GLUT2); while in skeletal muscle glucose is taken up from the blood by glucose transporter 1 (GLUT1) and 4 (GLUT4) (Figure 1). GLUT1 is a constitutive transporter, while GLUT4 is translocated to the sarcolemma in response to insulin to enhance glucose uptake [7]. When glucose enters the cytoplasm, it is phosphorylated to glucose-6-phosphate (G6P) by hexokinase (HK2), which can be used for either glycogen synthesis or glycolysis. If insulin levels are high, G6P enters the glycogen biosynthetic pathway. First, G6P is converted to glucose-1-phosphate (G1P) by phosphoglucomutase (PGM), then to UDP-glucose by UDP-glucose pyrophosphorylase (UGP2). Later, glycogenin-1 (GYG1) primes UDP-glucose for glycogen formation, and then glycogen synthase (GYS1) extends glycogen chains, while glycogen-branching enzyme (GBE1) catalyzes the branching of the growing glycogen molecules. When glucose is needed for metabolic tasks, cytosolic glycogen degradation is initiated by phosphorylase (PYGM) and glycogen debranching enzyme (AGL) [8]. Deficiency in most of these enzymes, either

biosynthetic or degradative, is associated with glycogen storage disorders. These include GSD0, II, III, IV, V, VIII, XIV, and XV in skeletal muscle. A similar case occurs in the liver, including GSDI, III, IV, VI, IX, XI, and XIV (Figure 1). Whereas certain diseases affect mainly one organ, such as GSDIIIb (affecting only the liver), others affect both, like it is the case in GSDIIIa, in which both liver and skeletal muscle are damaged. Glycogen is also stored in the lysosomes. The exact mechanism by which glycogen is transported to the lysosome is unknown. However, there are indications that this could be a form of autophagic or autophagy-like trafficking system [9]. Interestingly, previous reports as well as data presented in this thesis indicate that the metabolism of glycogen in the cytoplasm is disturbed in Pompe disease, ultimately favoring accumulation of cytoplasmic glycogen. These findings also suggest two scenarios: that disturbances in glycogen metabolism could affect disease progression or response to ERT treatment, or the reverse; that disease progression or response to treatment may influence the metabolism of glycogen [10–12].

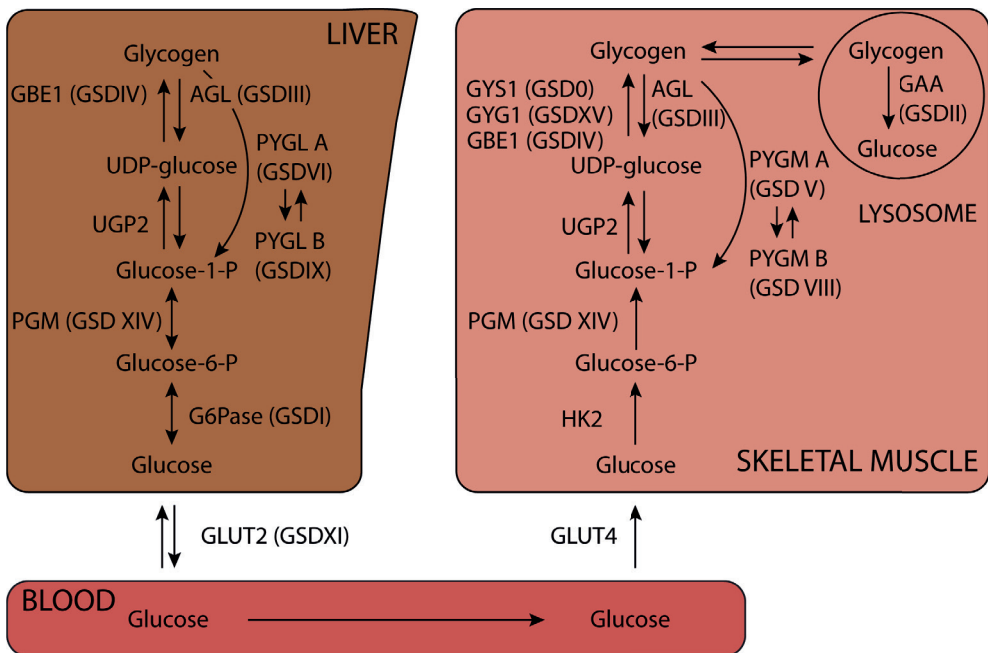


Figure 1. Schematic representation of the main steps in glycogen metabolism in liver and skeletal muscle. Arrows represent the direction in which each step takes place. Enzymes that catalyze each conversion are represented next to the arrows. GSDs caused by disease-causing variants in the enzymes were included between parenthesis.

Metabolic disturbances in GSDs other than Pompe disease

Disturbances in glycogen metabolism are not exclusive features of Pompe disease. Besides the main enzymatic deficiency that characterizes most GSDs, abnormal metabolism of glucose and/or glycogen has been described in several disorders. In GSDIa, one of the subtypes from the disorder known as von Gierke disease and characterized by deficiency of G6Pase activity (involved in the conversion of glucose-6-phosphate to glucose in the cytoplasm) in the liver, there is still a limited endogenous production of glucose despite the deficiency in G6Pase activity. This could indicate that glucose can still be synthesized or taken up by an alternative mechanism or group of mechanisms not yet identified [13]. Possibilities for glucose synthesis in this case include gluconeogenesis, uptake by the liver, or by degradation of glycogen via lysosomal GAA. A similar case may occur in GSD0, in which there is deficiency of glycogen synthase but only slightly reduced glycogen deposits, suggesting potential alternative pathways that lead to glycogen synthesis [14].

Disturbed metabolic activity in GSDs extend beyond glucose and glycogen metabolism, affecting other important cellular metabolic functions such as lipid metabolism, oxidative stress, or autophagy. The metabolism of lipids has been shown to be dysregulated in GSDI and GSDIII, GSDVI, and GSD IX [15–18]. Similarly, alterations of oxidative stress have been described in GSDIa and were recently reported also in Pompe disease [19,20]. Autophagy disturbances are known in Pompe disease (see below), and have also been reported in GSDIa [21]. Similarly, in Danon disease, a metabolic pathology with similar symptoms as those from Pompe disease characterized by loss of the lysosomal membrane protein LAMP2, autophagy is also impaired, further contributing to the clinical manifestations of the disease [22].

Autophagy

Autophagy is a process for lysosome-mediated degradation of cytoplasmic components such as damaged organelles and toxic protein aggregates. Together with the ubiquitin-proteasome system, the lysosomes are the major proteolytic systems in mammalian cells. Autophagy is a tightly regulated process, possibly with a narrow window of activity, as both inhibition and over-activation of autophagy are detrimental for muscle function [23]. Autophagy dysfunction is common among LSDs and GSDs, among them Pompe disease [24–26]. In Pompe disease, lysosomal dysfunction results in autophagic debris and a block of autophagic flux,

which could negatively affect endosomal trafficking, possibly influencing efficient delivery of ERT to the lysosomes [27,28].

Alternative therapeutic options for Pompe disease and other metabolic diseases

As mentioned before, ERT is the standard treatment for patients with Pompe disease since its approval in 2006. Enzyme replacement therapy was first proposed as a treatment option in the 60s, and was approved first as a treatment for Gaucher disease in 1991 [29–33]. Since then it has been successfully implemented as a treatment for seven lysosomal storage disorders, including Pompe disease [3–5,34]. Although not curative, the success and effectiveness of ERTs is undisputable. However, inefficient targeting to target tissues such as skeletal muscle, and immunogenicity are current drawbacks of ERT.

Next-generation ERTs

Similar as “classic” ERTs, next-generation ERTs are based on systemic delivery of the deficient enzyme. However, the use of new formulations, such as modification of the chemical structure of rhGAA to increase the levels of mannose-6-phosphate, and combination of rhGAA with pharmacological chaperons, showed improved tissue targeting, cellular uptake, and intracellular trafficking in mouse models of Pompe disease [35]. Similarly, chaperon therapy in combination with ERT showed promising results in Gaucher disease [36]. Next-generation ERT for Pompe disease is currently being tested in Phase III clinical trials (NCT03019406, NCT02782741).

Gene therapy

Gene therapy strategies aimed to introduce secretable forms of GAA have also showed promise to treat metabolic myopathies. Recent studies using AAV vectors showed promising data in Pompe disease models [37,38]. Early-phase clinical trials using AAV-mediated gene therapy have been conducted for the replacement of G6Pase in GSDI and GAA in Pompe disease, while two trials are currently ongoing (NCT02240407 and NCT03533673) [39]. Other gene therapy strategies using lentiviral vectors, which overcome some of the limitations inherent to AAV strategies, to target Pompe disease have shown great promise [39, manuscript submitted for publication].

Substrate reduction therapy

Although efforts have been mainly targeting the deficient enzyme, other therapies, such as substrate reduction therapy, have been proposed for LSDs. Substrate reduction therapy (SRT) is based on preventing storage not by correcting the original enzyme deficiency but by reducing the levels of biosynthesis of the accumulating substrate [41]. SRTs have successfully been approved such as miglustat and eliglustat tartrate for Gaucher disease [42,43]. The use of antisense oligonucleotide (AON)-mediated suppression of GYS1 in a mouse model of Pompe disease decreased the levels of lysosomal glycogen, and was suggested as an approach for SRT in Pompe disease [44]. Although they do not represent an alternative to ERTs, SRTs have proven able to overcome some challenges that ERTs could not, such as ability to cross the blood brain barrier, less immunogenicity issues, and ease of delivery through oral administration [45]. SRTs could have a synergic effect in combination with ERTs to maximize their effects and reduce disease progression.

Antisense oligonucleotides

One other promising therapeutic strategy for Pompe disease aim to modulate aberrant splicing through the use of chemically modified AONs. Splice switching AONs can be designed to restore normal splicing, which results in translation of functional copies of GAA [46]. In addition, the use of AON-mediated suppression of GYS1 in a mouse model of Pompe disease decreased the levels of lysosomal glycogen, and was suggested as an approach for SRT in Pompe disease [44]. Modulation of splicing has been successfully brought to the market by regulatory agencies for the treatment of DMD and SMA in recent years [47,48].

Skeletal muscle

Skeletal muscle is one of the most dynamic tissues in the human body. It accounts for 40-50% of the total body weight and is the largest protein reservoir, containing 50-75% of all proteins [49]. From a mechanical point of view its main function is to provide support and produce movement through the conversion of chemical energy into mechanical energy. Contraction capacity is what provides muscles with the ability and generate force and movement. Contractile systems based on actin-myosin mechanisms are a common feature of animal cells. However, these

systems are present in higher numbers, more complex, and in general more highly specialized in muscle cells. Mammals have four main types of muscle cells, all of them with contractile properties: skeletal muscle, cardiac muscle, smooth muscle, and myoepithelial cells.

Skeletal muscle is also eminently an endocrine organ that supports metabolic functions. It serves as the major tissue for insulin-stimulated glucose uptake, amino acid storage, and thermoregulation. In addition, muscle is also responsible for the secretion of myokines, which regulate metabolism in muscle, but also in other organs such as liver, brain, and adipose tissue [50]. Overall, skeletal muscle's central role in metabolic function highlights its relevance as an important organ for the prevention of common pathologic conditions and chronic diseases.

Muscle cells are highly specialized for rapid and efficient contraction. As a consequence of their specialization to perform contraction, muscle cells are post-mitotic, i.e. do not have capacity to divide [51]. Warren and Margaret Lewis reported in 1917 that myofibers increased in size without further nuclear division within the myofibers [52]. This was further validated by the discovery that skeletal muscle fibers are syncytial multinucleated cells [53,54]. See for an excellent review on the early years of the skeletal muscle research field [55].

The many nuclei of each muscle fiber are contained within the sarcoplasm, but most of the cytoplasm is made up of myofibrils, the basic contractile elements of the muscle cell. A myofibril is formed by a long chain of contractile units called sarcomeres. Each sarcomere is formed by an organized array of actin and myosin filaments, which slide past each other, producing the shortening or elongation of the sarcomere. Synchronized shortening of the thousands of sarcomeres in each myofibril is what gives muscle the capacity to contract rapidly.

Skeletal muscle is composed of several cell types: differentiated muscle cells, formed by many myonuclei in a syncytium within each myofiber, non-differentiated muscle cells or muscle stem cells, and non-muscle cells – such as fibroadipogenic progenitors (FAPs), immune cells, and endothelial cells – (Table 1). Muscle-resident stem cells are called satellite cells, and they play a fundamental role in the biology of skeletal muscle.

Satellite cells, the skeletal muscle stem cells

Satellite cells are *bona fide* muscle stem cells (MuSCs) [56] responsible for skeletal muscle growth and regeneration in response to stresses such as exercise, injury,

or disease [51]. They are located surrounding each myofiber, in a satellite-like position, between the sarcolemma and the basal lamina. Satellite cells were originally described by Alexander Mauro in 1961 by electron microscopy in muscle cells isolated from frog [57]. Satellite cells are characterized by the expression of transcription factors Pax7 – its most characteristic marker –, Pax3, and Myf5 (Figure 2) [58,59]. While Pax7 and Myf5 are involved in quiescence and activation of muscle stem cells, Pax3, a paralogue of Pax7, is expressed during embryonic myogenesis and downregulated by most satellite cells before birth [60–62]. Satellite cells are also defined by expression of a specific set of membrane proteins: M-cadherin, CD34, c-Met, CXCR4, NCAM1, VCAM1, and integrin α 7 β 1 [63] (Table 1). The first indication that satellite cells were muscle stem cells capable of generating myogenic progenitors date from the 70s [64,65]. These studies were later confirmed by experimentation using isolated fibers *in vitro*, which demonstrated the generation of pure myogenic cultures consisting of proliferating myoblasts. These studies indicated that satellite cells could proliferate and give rise to myogenic progenitors that, in turn, could differentiate further into myotubes [66–69]. In 2005, transplantation of myofibers into radiation-ablated muscles in mice with impaired regeneration proved that satellite cells were self-sufficient stem cells for muscle regeneration, as they were able to generate hundreds of myofibers, as well as new satellite cells that could regenerate muscle after subsequent rounds of regeneration [70].

Satellite cells lie in a quiescent state until they become activated in response to damage [64]. The specification of satellite cells to the myogenic lineage is mediated by myogenic regulatory factors (MRFs), a family of transcription factors formed by Myf5, MyoD, Mrf4, and myogenin [71]. When quiescent, satellite cells express Pax7 [58]. Upon activation, MyoD and Myf5 become expressed (Figure 2) [59,72–75]. Activated satellite cells acquire capacity to divide. Importantly, a subpopulation of activated satellite cells will continue lineage specification into proliferative myoblasts, progressively downregulating Pax7, while other subpopulation will regress to a quiescent state. The latter is termed self-renewal, the process by which stem cells generate other stem cells. The return to quiescence in satellite cells is characterized by Pax7 expression and absence of MyoD [71]. This process is influenced by MuSCs cell-intrinsic properties as well as by environmental cues. Self-renewal in MuSCs is regulated by the MAPK pathway [76]; with particular relevance, Spry1, an inhibitor of receptor tyrosine kinase signaling becomes expressed upon return to quiescence, while Spry1 depletion prevents MuSCs to self-renew [77,78]. Stem cells' self-renewal also depends on a specialized environmental, called

stem cell niche, that supports self-renewing activity [79]. In MuSCs, this niche, or environment, is highly influenced by interactions, mainly paracrine, between MuSCs and extracellular matrix (ECM) components present in the basal lamina, as well as and cell-cell interactions with muscle fibers [80,81]. Division of satellite cells into cells that either differentiate or self-renew is a result of a combined process of symmetric division, a cell division in which daughter cells have the same fate – e.g. both daughter cells acquire a stem cell fate, or both daughter cells differentiate –, and asymmetric division, in which each daughter cell acquires a different cell fate – i.e. one cell differentiates and the other acquires a stem cell fate – [82–85]. Through this process, satellite cells can repopulate the stem cell niche after activation and guarantee availability of stem cells for future rounds of myogenesis. Effective equilibrium and transition between self-renewal and differentiation by satellite cells is essential for efficient muscle regeneration [86].

As myoblasts progress in the lineage to mark the onset of differentiation, MyoD expression is reduced and myogenin expression is increased [71]. Myogenic cells at this moment do no longer support proliferative capacity and receive the name of myocytes. Myocytes acquire spindle-shaped morphology *in vitro* and have capacity to fuse with each other and form myotubes, or to fuse with existing myotubes. Myotubes are syncytial multinucleated cells characterized by the expression of myosin heavy chain (MyHC). MyHC is the motor protein of muscle thick filaments, and is considered a marker of late-stage differentiation [87]. Myotubes eventually mature into myofibers, which express several forms of myosins and are characterized by the acquisition of contractile capacity [88]. Muscle growth will occur as a result of addition of new myonuclei to pre-existing fibers and increase of the sarcoplasmic region [51].

In the last years, more evidence supported the hypothesis that satellite cells are not a uniform population, but rather a heterogeneous population of cells with different gene expression that conditions fate choice and functional properties [89–95]. This has been previously shown for other stem cell types, like hematopoietic, neural, and hair follicle specific populations [96–98]. In skeletal muscle, recent work showed satellite cell populations with distinct transcriptional profiles that are also functionally different [95,99,100]. Understanding the mechanisms that govern fate choices in skeletal muscle cells is paramount for their use for regenerative purposes.

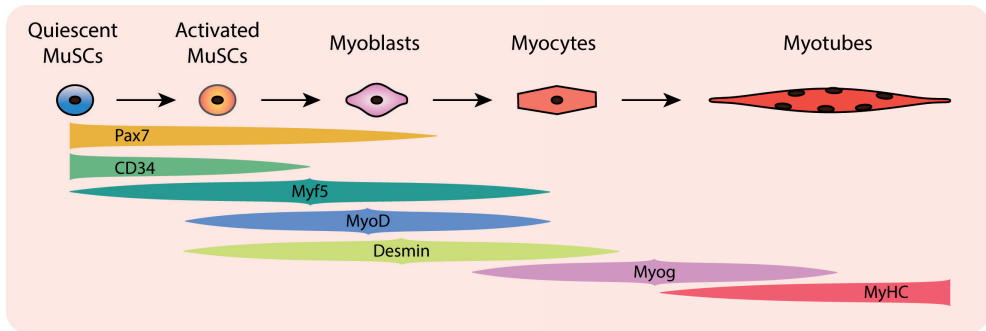


Figure 2. Schematic representation of myogenesis and characteristic markers during each stage.

Skeletal muscle regeneration

Skeletal muscle has an outstanding regenerative capacity. Muscle regeneration occurs as a consequence of aging, trauma, acquired diseases, or inherited myopathies. Skeletal muscle possesses several repair mechanisms. Minor damage to the myofibers' surface can be restored by muscle's membrane-patch repair, a surface membrane repair machinery [101–103]. Large damage or trauma to skeletal muscle is repaired in stem cell-mediated process, which is dependent on muscle resident stem cells or satellite cells. Satellite cells are essential for repair and regeneration of irreversibly damaged fibers [104–106]. Upon damage, satellite cells become active and start the myogenic program, eventually leading to efficient regeneration. Regeneration is, however, a complex process in which several other cell types intervene, such as inflammatory cells, fibroblasts, and adipogenic cells [51] (Table 1).

Immune cells have an initial pro-inflammatory response that eventually becomes a regenerative response through secretion of cytokines that promote myogenesis [107,108]. When injury occurs, immune cells such as monocytes and macrophages act synergistically with satellite cells to stimulate regeneration [109–111]. FAPs also play an essential role by maintaining an equilibrium between fibrosis and myogenesis; and regeneration is severely compromised in the absence of FAPs [112–114]. Fibroblasts are reported to communicate with myogenic progenitors to modify the ECM and stimulate regeneration [115,116]. Other cell types, like mesoangioblasts and bone marrow-derived cell progenitors have been reported to be myogenic both *in vitro* and *in vivo* [117,118]. However, it is not clear how this occurs and whether they are sources of myogenic cells during development [71].

Muscle regeneration is therefore better explained as a complex, orchestrated combination of multiple factors, involving several cell types, in which failure of any component will disturb muscle regeneration to varying degrees [86]. For this reason, *in vivo* models are usually most informative to understand the participation of other cell types and the role of the niche in muscle regeneration [119]. During disease, often one or several components of the regeneration machinery are compromised. Understanding these mechanisms is therefore essential to stimulate efficient regeneration in myopathies.

Cell type	Markers	References
MuSCs	Pax7, VCAM1, CXCR4, CD34, CD82, Itga7, Itgb1, SM/C2.6	[58,93,113,120–122]
FAPs	Sca1, PDGFR α , Tie2	[112,113]
Fibroblasts	α SMA, TCF4	[112,123,124]
PW1-interstitial cells (PICs)	PW1	[125]
Macrophages	CD45, CD11b, CD68, CD163, CD206, Arg1	[126–128]
Motor neurons	HB9, ChAT, VAcHT	[129]
Neutrophils	Ly6C/G	[107,130]
T cells	CD4, CD8, CD25, Foxp3	[128,131–133]
Endothelial cells	CD31, VE-Cad	[80,134,135]
Pericytes	NG2, ALP, PDGFR β , Cspg4, CD146, MCAM, Rgs5, Kcnj8	[136–138]

Table 1. Cells and signature markers present in skeletal muscle in homeostasis and during regeneration.

Skeletal muscle disorders

Although skeletal muscle has a remarkable capacity for regeneration in homeostasis, this function can be compromised as a result of physical inactivity, aging, trauma, or disease. These conditions are often characterized by muscle weakness, reduction in muscle elasticity, reduced protein synthesis, increased protein degradation, or impaired muscle regeneration; negatively affecting patients and causing personal, social, and economic burden [139]. Many efforts in research and industry are directed to understand the mechanisms of skeletal muscle regeneration in order to modulate them to fight disease.

The 2021 version of the gene table of neuromuscular disorders describes 1079 diseases for which 608 different causative genes are known [140]. Neuromuscular

disorders collectively impact 250,000 patients in the US only. Although together they affect a relatively large number of people, all neuromuscular disorders affect less than 40 patients per 100,000 persons in the EU (per 200,000 in the US), and are classified in the group of rare disorders [141].

As it is often the case for rare disorders, clinical trials and the development of effective treatments are scarce. Current treatments for neuromuscular disorders are not curative and are often economically very costly, amounting to more than 700,000\$ per patient per year in some cases [142]. Additional to the burden in the health of patients with neuromuscular disorders, this poses considerable stress in healthcare systems worldwide. These effects are more pronounced in developing and third world countries, which do not share solid healthcare systems. The consequences of this ultimately fall upon patients, which in some cases cannot access treatments at all.

Innovative treatment strategies for neuromuscular disorders

The number of FDA (Food and Drug Administration)/EMA (European Medical Agency) approved treatments and candidate therapies in clinical trials for neuromuscular disorders is growing rapidly in the last years. To set an example, the first treatment for spinal muscle atrophy (SMA), nusinersen, received FDA approval on 2016, while in 2020 two new treatments were approved for their commercialization [143]. Currently there are treatments approved by FDA and/or EMA for 6 neuromuscular disorders, including enzyme replacement therapy (ERT) for Pompe disease [144]. All of the treatments currently approved are disease-modifying treatments. This implies that, while they partially alleviate disease symptoms, in some cases considerably prolonging life span, ultimately, they are not curative. Although a significant improvement over the past, patients still require life-long treatments, suffer from treatment-associated side effects, and are often bound to regular visits to healthcare centers in order to receive their medication, negatively affecting their daily lives.

As a consequence, finding new, improved treatments becomes necessary. Currently, new treatments are reaching patients every year; however, the number of them is relatively low compared to the total number of patients and the need for new therapies. Research efforts around the globe have resulted in promising scientific discoveries, such as gene- and cell-therapies, and gene editing tools,

which hold great potential to develop curative treatments for some of these diseases in the future.

Gene therapy for muscle disorders

Gene therapy stands among the most promising treatments that are already reaching the market [145]. It relies on introducing a healthy copy of the disease-affected gene using a vector, which usually has a viral nature. It is particularly amenable as therapy for monogenic disorders, since it has potential to replace disease causing variations in a specific gene by healthy copies. Regarding neuromuscular disorders, in 2019 FDA approved the first gene therapy treatment for children with SMA [146]. In the case of Pompe disease, since acid α -glucosidase (GAA) is excreted and can be taken up by other cells by endocytosis, induction of functional copies of *GAA* in a given set of cells or organs could lead to cross-correction of the defective enzyme in other tissues. Currently, there are four candidate gene therapy approaches for Pompe disease in Phase I/II clinical trials that use adeno-associated virus (AAV) vectors (clinicaltrials.gov NCT02240407, NCT03533673, NCT04174105, NCT04093349). Similar approaches using lentiviral-mediated targeting are at pre-clinical stage being developed in our group [39, manuscript submitted for publication].

Gene editing in muscle disorders

The advent of gene-editing technology such as zinc finger nucleases, TALENs, and CRISPR/Cas has opened a new range of opportunities to treat disease. Gene-editing relies on cell's endogenous repair mechanisms to make very specific modifications in DNA, such as deletions, insertions, or gene knock outs [147]. As a consequence, it has potential to overcome some of the obstacles that other techniques such as ERTs and cell- or gene-therapies pose, such as safety and immunogenicity. Although clinical development of gene editing technology is progressing, it must overcome its own challenges, namely safety, especially regarding the presence of off-target effects, efficacy, and delivery. A number of clinical trials using gene-editing technology have been initiated for cancer, HIV, and β -thalassemia. At the moment of writing this thesis, there are two clinical trials for the treatment of lysosomal storage disorders (LSDs): mucopolysaccharidosis (MPS) type I and II (NCT02702115 and NCT03041324), while no trials have been started for Pompe disease [148].

Cell therapy for muscle disorders

Cell therapy consists on the use of the intrinsic properties of cells to regenerate and repair damaged tissues. It represents a promising strategy for the treatment of myopathies and is central in regenerative therapy approaches [149]. Cell-based therapies were originally established with the use of bone-marrow transplantations, performed firstly in 1968 [150]. Since then, bone marrow transplantation constitutes standard practice in the treatment of several forms of leukemia, where success rates higher than 90% are reached, as well as a treatment for Hurler syndrome, the most severe form of MPS type 1 [151]. In addition, cell-based therapies have been successfully implemented for other conditions, like skin and corneal burns [152–154].

Skeletal muscle represents a good model for implementation of cell therapy, given that the fusion of gene-corrected muscle cells with damaged fibers could, in principle, reconstitute the levels of deficient protein reverting the course of the disease. In addition, if transplanted cells harbor stem cell capacity, this would ensure their replenishment, guaranteeing long-term efficient regeneration. Currently, most of the data that discusses regenerative therapies for skeletal muscle disorders has been derived from *in vitro* studies or animal models.

Research on cell-based therapy for skeletal muscle started in the late 70s, when it was demonstrated for first time that donor myoblasts could fuse with host fibers [155]. A decade later, a series of studies showed engraftment of myoblasts and contribution to regeneration of dystrophin-positive muscle fibers in a Duchenne muscle dystrophy (DMD) mouse model [156–158]. In the 90s, myoblast transfer therapy clinical trials were performed in patients. Despite initially showing promising results through presence of dystrophin-positive muscle fibers, myoblast transfer therapy ultimately failed as a consequence of poor cell survival after transplantation, low migration capacity, production of immunogenic responses, low engraftment capacity, and lack of improvement of muscle function [159–166]. As a result of the low therapeutic efficacy, the use of myoblasts as sources for cell-based therapy for muscle disorders was abandoned.

After myoblasts failed for therapeutic use, satellite cells were subject of attention and were deemed better candidates as a source for regenerative therapy in skeletal muscle. In 2005 MuSCs were shown to be essential and self-sufficient for skeletal muscle regeneration after damage and were found to be capable of replenishing the stem cell pool [70]. In 2008, highly efficient functional engraftment of MuSCs was demonstrated in dystrophic mice [167,168]. Overall, satellite cells were

Study	Study type	Cell type	Donor	Genetic correction	Administration route	Immune suppression	Reference	Responsible institution
Transplantation of Myoblasts to DMD Patients	Phase I/II	Myoblasts	Allogeneic	No	IM	Yes (tacrolimus)	NCT02196467	CHU de Quebec-Universite Laval (Canada)
Mesoangioblast-mediated exon 51 skipping for genetic correction of dystrophin for DMD	Phase I/II	MABs	Allogeneic	Yes	IM	No	EudraCT 2019-001825-28	The University of Manchester (United Kingdom)
Bone marrow-derived autologous stem cells for the treatment of DMD	Phase I/II	MSCs	Autologous	?	?	?	NCT03067831	Stem Cells Arabia (Jordan)
Autologous muscle stem cell therapy for treatment of congenital urinary incontinence in epispadias patients	Phase I/II	MuSCs	Autologous	No	?	No	NCT04729582	Charite University, Berlin (Germany)

Table 2. Summary of currently ongoing clinical trials using cell therapy to treat skeletal muscle conditions. MABs: mesoangioblasts; MSCs: mesenchymal stromal cells; IM: intramuscular.

better candidates than myoblasts for: 1) greater capacity to differentiate and self-renew; 2) improved migration; 3) better survival after transplantation; 4) higher engraftment capacity (reviewed by [169]). A list of current clinical trials involving cell therapy for skeletal muscle is summarized in Table 2.

Satellite cells are, however, relatively scarce; accounting for 2-4% of total myonuclei. As mentioned above, often there is severe loss of muscle-regenerative cells soon after transplantation [170,171]. Consequently, in order to obtain clinically relevant numbers for therapy, muscle-regenerative cells need to be expanded. Expansion of satellite cells induces rapid loss of their regenerative properties soon after culture, which poses a major obstacle for the development of cell therapies to treat skeletal muscle disorders [168,172,173]. The main problem to date is the requirement of highly engraftable muscle regenerative cells that can be generated at sufficient numbers

for therapeutic application, which so far remains elusive. Expansion of stem cells that retain functional capacities is not solely a challenge in the skeletal muscle field. Similar efforts to achieve successful expansion of engraftable cells are also being done in other stem cell fields such as for the hematopoietic system [174].

In order to overcome this burden, research efforts have focused on finding methods to expand MuSCs with regenerative properties, and to find alternative cell types that retain MuSC-like properties, mainly: 1) capacity to contribute to fiber regeneration; 2) capacity to repopulate the stem cell niche to guarantee successive rounds of regeneration.

Sources of cells in cell therapy for skeletal muscle

Myoblasts/satellite cells

In order to maintain or re-induce regenerative properties in satellite cells and myoblasts expanded *ex vivo*, research efforts aim to faithfully recapitulate the MuSC niche. Efforts towards this aim include a variety of techniques: using extracellular matrix compounds [175,176], artificial elaboration of substrates that mimic the physiological rigidity of the MuSC environment [177,178], or creation of micropatterns [179]. 3D printing to design scaffolds to promote muscle regeneration is currently being explored [180]. Other approaches simulate the inflammatory milieu to stimulate muscle regeneration or muscle differentiation by using combined cultures of myogenic cells and other cell types such as macrophages [181], and fibro-adipogenic progenitors [113,182]. A number of methods aim to modulate myogenic cell fate with pharmacological treatments, for example, by using small molecules that target key signaling pathways for myogenesis, like inhibition of the p38/MAPK pathway [173,183,184], stimulation of the Wnt pathway [185] or stimulation of Notch signaling [186].

iPSCs

Induced pluripotent stem cells (iPSCs) can be generated from adult somatic cells after reprogramming with a cocktail of transcription factors that sets them into a pluripotent, embryonic-like state [187]. An advantage of these cells is that they can be indefinitely expanded, while maintaining their pluripotency. Through combination of several compounds in culture and isolation steps, these cells can then be efficiently converted into myogenic progenitors with capacity to engraft and regenerate skeletal muscle [188]. However, safety issues, particularly regarding transgene integration sites during the generation of iPSCs or myogenic progenitors

(e.g. transgene expression) should be addressed before they can be used in clinical trials [147,189].

Other cell types

Side population

The search for cells suitable for cell-therapy application resulted in the identification of a muscle side population (SP) distinct from the main population of muscle cells. Muscle SPs resemble bone marrow SPs in Sca1 expression and the capacity to efflux Hoechst 33342 dye, as well as the capacity to populate the hematopoietic compartment in irradiated mice. However, differently to bone marrow SPs, muscle SPs do not express c-Kit and CD45 [190]. *In vitro*, muscle SPs have low adhesion capacity compared to the main population of muscle cells and differentiate both into myotubes and fibroblasts [190]. *In vivo*, SP cells have capacity to reach skeletal muscle, contribute to fiber regeneration, and give rise to MuSCs after systemic delivery [191,192]. In addition, in combination with myogenic cells SP populations have also been shown to stimulate their regenerative properties [193]. Nevertheless, their regenerative capacity is limited to be considered optimal candidates for therapy [191].

Mesoangioblasts/Pericytes

Mesoangioblasts are mesodermal progenitors that in human express typical pericyte markers NG2 and ALP (Table 1). Mesoangioblasts are able to proliferate and differentiate into MyHC-positive myotubes when co-cultured with myogenic cells. Similarly to SP cells, upon systemic transplantation these cells had capacity to cross the vessel barrier, reach and regenerate skeletal muscle, and colonize the MuSC niche, expressing typical MuSC markers [117,136]. Despite the versatility of systemic administration, the capacity of pericytes to differentiate into non-myogenic cells upon transplantation and low dystrophin production upon transplantation in phase I/II clinical trials in DMD patients raised questions regarding their suitability for cell-based therapy for skeletal muscle [194,195].

Reserve cells

Reserve cells are a small subset of muscle cells that under differentiation conditions escape from terminal differentiation. These reserve cells downregulate MyoD

expression, express Pax7, and stop cycling, resembling a state of quiescence [196–202]. Reserve cells, have been identified in chick, mouse, and human [80,196,203]. Upon culture under proliferative conditions, these cells regain capacity to divide and form myotubes when differentiated [69]. Reserve cells have been partially characterized *in vitro* [199,202,204]. Although previous studies showed regenerative capacity of reserve cells upon transplantation, they did not study reserve cells' *in vivo* properties in detail, only showing limited engraftment efficacy and not showing capacity for stem cell engraftment and regeneration [170,203]. While the mechanisms by which reserve cells choose a stem cell fate instead of a differentiation fate have not been deciphered, evidence suggests that it could be influenced by factors such as cell cycle state at the moment of switch from proliferative to differentiating conditions [69], environmental cues, like membrane proteins and microenvironment signals [84], interaction of reserve cells with myotubes [178,205,206], and cell adhesion properties [78,179,207]. Pre-plating cells to select those with lower adhesion capacity was originally used to purify myogenic progenitors from heterogeneous cell populations [208–210]. In addition, previous studies showed that cells with reduced adhesion properties have increased stem cell properties [198,211–213].

Intramuscular delivery of muscle regenerative cells is not feasible for those disorders that affect a large collection of muscle groups, like Pompe disease. The current requirements for such therapy would imply to individually inject regenerative cells intramuscularly in each affected muscle, implying a surgical procedure, which would need to be periodically repeated in the case of limited stem cell function of transplanted cells. Nevertheless, targeting muscle groups that are severely affected, like diaphragm in Pompe disease, which has already been pursued for delivery of AAV-associated GAA [214], or in disorders that affect very localized muscle groups, such as the sphincter in the case of urinary incontinence, could be of higher relevance.

Regenerative defects in skeletal muscle pathology

In addition to a source of regenerative cells, the endogenous mechanisms of regeneration in skeletal muscle must be effective to develop a functional cell-based therapy. These mechanisms are often compromised in muscle-degenerative conditions. The cause for regenerative defects varies widely between different myopathies. In some disorders, such as DMD, successive rounds of degeneration

and regeneration as a consequence of dystrophin deficiency are thought to eventually exhaust the stem cell pool and replace muscle tissue with large numbers of fibroblasts and collagen deposits that prevent efficient myogenesis. This ultimately results in loss of proliferation by resident muscle stem cells, causing impaired regeneration [215]. Similar mechanisms have been proposed for other myopathies, like myotonic dystrophy and Emery-Dreifuss dystrophy [216,217]. Differently, in Pompe disease regeneration defects are caused by inefficient activation of the regenerative response, possibly due to the lack of robust sarcolemmal damage [218–220]. Thus, it is thought that the regenerative defect in Pompe disease is reversible and that successful activation of regeneration through external cues, such as exercise, could lead to improved myogenesis. Thus, in order to effectively develop new therapies, it is essential to understand the pathology behind the diseases, paying special attention to the regenerative response in the case of disorders that directly affect skeletal muscle.

Aims and scope of this thesis

Overall, this thesis explores pathology and metabolism of glycogen in Pompe disease. Furthermore, the work on this thesis aims to provide a deeper view of the regulation of skeletal muscle function at the cellular and molecular level, with a focus on the generation of expandable regenerative muscle cells towards a muscle regenerative therapy.

In **chapter 2**, the metabolism of glycogen in skeletal muscle of Pompe disease was analyzed in mouse and human patients. We found upregulation of enzymes involved in glycogen buildup in skeletal muscle, heart, and brain of mice with Pompe disease. In addition, changes were already present before onset of muscle pathology, while others developed through the life course of mice. Results in patients suggested that dysregulation of glycogen metabolism could also occur in humans, while ERT treatment resulted in a decrease in enzyme levels.

In **chapter 3**, we reviewed the literature on the role of satellite cell-mediated repair in neuromuscular disorders, with an emphasis in Pompe disease. We highlighted the differences between muscle dystrophies and Pompe disease and discussed potential targets for therapy, such as autophagy and satellite cell activation.

In **chapter 4**, we described a protocol that allows assessment of satellite cell activation *ex vivo* using isolated muscle fibers. Satellite cell activation – which is disturbed in several neuromuscular conditions including Pompe disease - is largely

dependent on signals from the satellite cell niche. An important aspect of the isolated fiber model is the preservation of the niche-satellite cell interaction, which is disrupted in virtually any other *ex vivo* model. We optimized the experimental parameters and show that the suggested approach preserves the satellite cell activation response to known muscle mitogens.

In **chapter 5**, we investigated the role of autophagy dysregulation – which is well-recognized to contribute to cellular pathology in Pompe disease- in muscle regeneration and satellite cell activation under GAA-deficient conditions. We found that dysregulation of key autophagy proteins occurs before the onset of muscle pathology, confirming a causative role in development of cellular pathology. Modulation of autophagic activity – as assessed in an *ex vivo* satellite cell activation assay – was not sufficient to restore the regenerative response. Alternatively, forcing muscle regeneration by inducing experimental muscle injury in the Pompe disease mouse model transiently restored muscle function and histology and concomitantly reduced the lysosomal load. These data suggest that modulating autophagy is not sufficient to overcome the satellite cell activation threshold that we observed in Pompe disease. However, the reverse appears possible, strategies to force satellite cell activation and initiation of muscle regeneration can overcome the autophagic block that characterizes Pompe disease.

In **chapter 6**, populations of muscle regenerative cells cultured *in vitro* were identified and studied. We described a new method to isolate and expand these cells, named reserve cells; a population of fast-adhering cells displayed a highly myogenic profile *in vitro*, while a population of slow-adhering cells showed increased properties associated to muscle stem cells. *In vivo*, fast-adhering reserve cells preferentially contributed to direct muscle regeneration after transplantation in pre-injured immunodeficient hosts. Slow-adhering reserve cells primarily engrafted as skeletal muscle cells, displaying enhanced regeneration properties after a second injury. In addition, we characterized the transcriptome of these fractions, and found signature markers for both populations, as well as differential regulation of pathways associated with promotion of stemness and myogenic properties.

Overall, this thesis presents new findings and developments in the field of Pompe disease and skeletal muscle regeneration, as well as an updated analysis of the current state-of-the-art and the future challenges of the field.

References

1. Reuser, A.J.J., Hirschhorn, R., and Kroos, M.A. (2018). Pompe disease: Glycogen storage disease type II, acid α -glucosidase (acid maltase) deficiency. In *The Online Metabolic and Molecular Bases of Inherited Disease. Lysosomal Storage Disorders.*, A. L. Beaudet, B. Vogelstein, K. W. Kinzler, S. E. Antonarakis, A. Ballabio, K. M. Gibson, and J. Mitchell, eds. (New York, NY: The McGraw-Hill Companies, INC).
2. van der Ploeg, A.T., and Reuser, A.J. (2008). Pompe's disease. *Lancet* 372, 1342–1353. Available at: <http://www.thelancet.com/article/S014067360861555X/fulltext> [Accessed October 12, 2015].
3. Van den Hout, H., Reuser, A.J., Vulto, A.G., Christa B Loonen, M., Cromme-Dijkhuis, A., and Van der Ploeg, A.T. (2000). Recombinant human α -glucosidase from rabbit milk in Pompe patients. *Lancet* 356, 397–398. Available at: <http://www.sciencedirect.com/science/article/pii/S0140673600025332> [Accessed November 11, 2015].
4. van der Ploeg, A.T., Clemens, P.R., Corzo, D., Escolar, D.M., Florence, J., Groeneveld, G.J., Herson, S., Kishnani, P.S., Laforet, P., Lake, S.L., et al. (2010). A randomized study of alglucosidase alfa in late-onset Pompe's disease. *N. Engl. J. Med.* 362, 1396–1406.
5. Kishnani, P.S., Corzo, D., Nicolino, M., Byrne, B., Mandel, H., Hwu, W.L., Leslie, N., Levine, J., Spencer, C., McDonald, M., et al. (2007). Recombinant human acid α -glucosidase: Major clinical benefits in infantile-onset Pompe disease. *Neurology* 68, 99–109. Available at: www.neurology.com [Accessed April 19, 2021].
6. de Vries, J.M., van der Beek, N.A., Hop, W.C., Karstens, F.P., Wokke, J.H., de Visser, M., van Engelen, B.G., Kuks, J.B., van der Kooij, A.J., Notermans, N.C., et al. (2012). Effect of enzyme therapy and prognostic factors in 69 adults with Pompe disease: an open-label single-center study. *Orphanet J. Rare Dis.* 7, 73. Available at: <http://ojrd.biomedcentral.com/articles/10.1186/1750-1172-7-73> [Accessed November 7, 2019].
7. Tarnopolsky, M.A. (2018). Myopathies Related to Glycogen Metabolism Disorders. *Neurotherapeutics* 15, 915–927.
8. Roach, P.J., Depaoli-Roach, A.A., Hurley, T.D., and Tagliabracci, V.S. (2012). Glycogen and its metabolism: some new developments and old themes. *Biochem. J* 441, 763–787.
9. Zirin, J., Nieuwenhuis, J., and Perrimon, N. (2013). Role of Autophagy in Glycogen Breakdown and Its Relevance to Chloroquine Myopathy. *PLoS Biol.* 11, 1001708. Available at: www.plosbiology.org [Accessed May 6, 2021].
10. Taylor, K.M., Meyers, E., Phipps, M., Kishnani, P.S., Cheng, S.H., Scheule, R.K., and Moreland, R.J. (2013). Dysregulation of multiple facets of glycogen metabolism in a murine model of Pompe disease. *PLoS One* 8, e56181. Available at: <http://www.ncbi.nlm.nih.gov/pubmed/23457523> [Accessed October 14, 2016].
11. Orth, M., and Mundegar, R.R. (2003). Effect of acid maltase deficiency on the endosomal/lysosomal system and glucose transporter 4. *Neuromuscul. Disord.* 13, 49–54. Available at: <http://www.nmd-journal.com/article/S0960896602001864/fulltext> [Accessed September 4, 2020].
12. Douillard-Guilloux, G., Raben, N., Takikita, S., Ferry, A., Vignaud, A., Guillet-Deniau, I., Favier, M., Thurberg, B.L., Roach, P.J., Caillaud, C., et al. (2009). Restoration of muscle functionality by genetic suppression of glycogen synthesis in a murine model of Pompe disease. *Hum. Mol. Genet.* 19, 684–696. Available at: <https://academic.oup.com/hmg/article/19/4/684/609722> [Accessed September 4, 2020].

13. Hijmans, B.S., Boss, A., Dijk, T.H. van, Soty, M., Wolters, H., Mutel, E., Groen, A.K., Derks, T.G.J., Mithieux, G., Heerschap, A., *et al.* (2017). Hepatocytes contribute to residual glucose production in a mouse model for glycogen storage disease type Ia. *Hepatology* 66, 2042–2054. Available at: <https://onlinelibrary.wiley.com/doi/full/10.1002/hep.29389> [Accessed November 1, 2021].
14. Ellingwood, S.S., and Cheng, A. (2018). Biochemical and Clinical Aspects of Glycogen Storage Diseases. *J. Endocrinol.* 238, R131. Available at: [/pmc/articles/PMC6050127/](https://pubmed.ncbi.nlm.nih.gov/31111111/) [Accessed November 13, 2021].
15. Bandsma, R., Smit, P., and Kuipers, F. (2002). Disturbed lipid metabolism in glycogen storage disease type I. *Eur. J. Pediatr.* 161 Suppl 1, S65–S69. Available at: <https://pubmed.ncbi.nlm.nih.gov/12373575/> [Accessed November 13, 2021].
16. Li, X.H., Gong, Q.M., Ling, Y., Huang, C., Yu, D.M., Gu, L.L., Liao, X.W., Zhang, D.H., Hu, X.Q., Han, Y., *et al.* (2014). Inherent lipid metabolic dysfunction in glycogen storage disease IIIa. *Biochem. Biophys. Res. Commun.* 455, 90–97.
17. Schmitz, G., Hohage, H., and Ullrich, K. (1993). Glucose-6-phosphate: a key compound in glycogenosis I and favism leading to hyper- or hypolipidaemia. *Eur. J. Pediatr.* 152 Suppl 1, 77–84. Available at: <https://pubmed.ncbi.nlm.nih.gov/8319730/> [Accessed December 2, 2021].
18. Beauchamp, N.J., Dalton, A., Ramaswami, U., Niinikoski, H., Mention, K., Kenny, P., Kolho, K.L., Raiman, J., Walter, J., Treacy, E., *et al.* (2007). Glycogen storage disease type IX: High variability in clinical phenotype. *Mol. Genet. Metab.* 92, 88–99.
19. Yiu, W.H., Mead, P.A., Jun, H.S., Mansfield, B.C., and Chou, J.Y. (2010). Oxidative stress mediates nephropathy in type Ia glycogen storage disease. *Lab. Invest.* 2010 904 90, 620–629. Available at: <https://www.nature.com/articles/labinvest201038> [Accessed November 2, 2021].
20. Tarallo, A., Damiano, C., Strollo, S., Minopoli, N., Indrieri, A., Polishchuk, E., Zappa, F., Nusco, E., Fecarotta, S., Porto, C., *et al.* (2021). Correction of oxidative stress enhances enzyme replacement therapy in Pompe disease. *EMBO Mol. Med.* 13, e14434. Available at: <https://onlinelibrary.wiley.com/doi/full/10.15252/emmm.202114434> [Accessed November 9, 2021].
21. Farah, B.L., Yen, P.M., and Koeberl, D.D. (2020). Links between autophagy and disorders of glycogen metabolism – Perspectives on pathogenesis and possible treatments. *Mol. Genet. Metab.* 129, 3–12.
22. Demirdas, S., van Slegtenhorst, M.A., Verdijk, R.M., Lee, M., van den Hout, H.M.P., Wessels, M.W., Frohn-Mulder, I.M.E., Gardeitchik, T., van der Ploeg, A.T., and Schaaf, G.J. (2019). Delayed Diagnosis of Danon Disease in Patients Presenting With Isolated Cardiomyopathy. *Circ. Genomic Precis. Med.* 12, e002395. Available at: <http://ahajournals.org> [Accessed April 26, 2021].
23. Sandri, M. (2010). Autophagy in skeletal muscle. *FEBS Lett.*
24. Seranova, E., Connolly, K.J., Zatyka, M., Rosenstock, T.R., Barrett, T., Tuxworth, R.I., and Sarkar, S. (2017). Dysregulation of autophagy as a common mechanism in lysosomal storage diseases. *Essays Biochem.* 61, 733–749. Available at: <https://doi.org/10.1042/EBC20170055> [Accessed April 21, 2021].
25. Fukuda, T., Roberts, A., Ahearn, M., Zaal, K., Ralston, E., Plotz, P.H., and Raben, N. (2006). Autophagy and lysosomes in Pompe disease. *Autophagy* 2, 318–320. Available at: <https://www.tandfonline.com/action/journalInformation?journalCode=kaup20> [Accessed April 21, 2021].

26. Nascimbeni, A.C., Fanin, M., Masiero, E., Angelini, C., and Sandri, M. (2012). The role of autophagy in the pathogenesis of glycogen storage disease type II (GSDII). *Cell Death Differ.* *19*, 1698–1708. Available at: www.nature.com/cdd [Accessed April 21, 2021].
27. Raben, N., Roberts, A., and Plotz, P.H. (2007). Role of autophagy in the pathogenesis of Pompe disease. *Acta Myol. myopathies cardiomyopathies Off. J. Mediterr. Soc. Myol.* *26*, 45–8. Available at: <http://www.ncbi.nlm.nih.gov/pubmed/17915569> [Accessed November 8, 2016].
28. Raben, N., and Plotz, P.H. (2008). A new look at the pathogenesis of Pompe disease. *Clin. Ther.* *30*, S86–S87. Available at: <http://www.clinicaltherapeutics.com/article/S0149291808003640/fulltext> [Accessed May 11, 2021].
29. Deduve, C. (1963). The lysosome. *Sci. Am.* *208*, 64–72. Available at: <https://www.scientificamerican.com/article/the-lysosome/> [Accessed April 19, 2021].
30. Brady, R.O., Kanfer, J.N., and Shapiro, D. (1965). Metabolism of glucocerebrosides II. Evidence of an enzymatic deficiency in Gaucher's disease. *Biochem. Biophys. Res. Commun.* *18*, 221–225.
31. Hers, H.G. (1965). Inborn Lysosomal Diseases. *Gastroenterology* *48*, 625–633.
32. Deduve, C. (1964). FROM CYTASES TO LYSOSOMES. *Fed. Proc.* *23*, 1045–1049. Available at: <https://europepmc.org/article/MED/14209796> [Accessed April 19, 2021].
33. Mechler, K., Mountford, W.K., Hoffmann, G.F., and Ries, M. (2015). Pressure for drug development in lysosomal storage disorders - A quantitative analysis thirty years beyond the US orphan drug act. *Orphanet J. Rare Dis.* *10*, 46. Available at: <http://www.ajrd.com/content/10/1/46> [Accessed April 19, 2021].
34. Li, M. (2018). Enzyme replacement therapy: A review and its role in treating lysosomal storage diseases. *Pediatr. Ann.* *47*, e191–e197.
35. Xu, S., Lun, Y., Frascella, M., Garcia, A., Soska, R., Nair, A., Ponery, A.S., Schilling, A., Feng, J., Tuske, S., et al. (2019). Improved efficacy of a next-generation ERT in murine Pompe disease. *JCI Insight* *4*. Available at: <https://insight.jci.org/articles/view/125358> [Accessed April 8, 2019].
36. Narita, A., Shirai, K., Itamura, S., Matsuda, A., Ishihara, A., Matsushita, K., Fukuda, C., Kubota, N., Takayama, R., Shigematsu, H., et al. (2016). Ambroxol chaperone therapy for neuronopathic Gaucher disease: A pilot study. *Ann. Clin. Transl. Neurol.* *3*, 200–215. Available at: <https://onlinelibrary.wiley.com/doi/full/10.1002/acn3.292> [Accessed June 3, 2021].
37. Colella, P., Sellier, P., Gomez, M.J., Biferi, M.G., Tanniou, G., Guerchet, N., Cohen-Tannoudji, M., Moya-Nilges, M., van Wittenberghe, L., Daniele, N., et al. (2020). Gene therapy with secreted acid alpha-glycosidase rescues Pompe disease in a novel mouse model with early-onset spinal cord and respiratory defects. *EBioMedicine* *67*. Available at: <https://pubmed.ncbi.nlm.nih.gov/33039711/> [Accessed June 3, 2021].
38. Puzzo, F., Colella, P., Biferi, M.G., Bali, D., Paulk, N.K., Vidal, P., Collaud, F., Simon-Sola, M., Charles, S., Hardet, R., et al. (2017). Rescue of Pompe disease in mice by AAV-mediated liver delivery of secretable acid α -glucosidase. *Sci. Transl. Med.* *9*, eaam6375. Available at: <http://www.ncbi.nlm.nih.gov/pubmed/29187643> [Accessed March 15, 2019].
39. Kishnani, P.S., Sun, B., and Koeberl, D.D. (2019). Gene therapy for glycogen storage diseases. *Hum. Mol. Genet.* *28*, R31–R41. Available at: <https://academic.oup.com/hmg/article/28/R1/R31/5520922> [Accessed June 3, 2021].

40. Van Til, N.P., Stok, M., Aerts Kaya, F.S.F., De Waard, M.C., Farahbakhshian, E., Visser, T.P., Kroos, M.A., Jacobs, E.H., Willart, M.A., Van Der Wegen, P., *et al.* (2010). Lentiviral gene therapy of murine hematopoietic stem cells ameliorates the Pompe disease phenotype. *Blood* 115, 5329–5337. Available at: <https://pubmed.ncbi.nlm.nih.gov/20385789/> [Accessed August 31, 2020].
41. Radin, N.S. (1996). Treatment of Gaucher disease with an enzyme inhibitor. *Glycoconj. J.* 13, 153–157.
42. Elstein, D., Dweck, A., Attias, D., Hadas-Halpern, I., Zevin, S., Altarescu, G., Aerts, J.F.M.G., Van Weely, S., and Zimran, A. (2007). Oral maintenance clinical trial with miglustat for type I Gaucher disease: Switch from or combination with intravenous enzyme replacement. *Blood* 110, 2296–2301. Available at: <http://ashpublications.org/blood/article-pdf/110/7/2296/483982/zh801907002296.pdf> [Accessed April 29, 2021].
43. Bennett, L.L., and Mohan, D. (2013). Gaucher disease and its treatment options. *Ann. Pharmacother.* 47, 1182–1193. Available at: <http://journals.sagepub.com/doi/10.1177/1060028013500469> [Accessed April 29, 2021].
44. Clayton, N.P., Nelson, C.A., Weeden, T., Taylor, K.M., Moreland, R.J., Scheule, R.K., Phillips, L., Leger, A.J., Cheng, S.H., and Wentworth, B.M. (2014). Antisense oligonucleotide-mediated suppression of muscle glycogen synthase 1 synthesis as an approach for substrate reduction therapy of pompe disease. *Mol. Ther. - Nucleic Acids* 3, e206. Available at: </pmc/articles/PMC4217081/> [Accessed March 19, 2021].
45. Coutinho, M., Santos, J., and Alves, S. (2016). Less Is More: Substrate Reduction Therapy for Lysosomal Storage Disorders. *Int. J. Mol. Sci.* 17, 1065. Available at: <http://www.mdpi.com/1422-0067/17/7/1065> [Accessed January 21, 2021].
46. Bergsma, A.J., In 't Groen, S.L., Verheijen, F.W., van der Ploeg, A.T., and Pijnappel, W.W.M.P. (2016). From Cryptic Toward Canonical Pre-mRNA Splicing in Pompe Disease: a Pipeline for the Development of Antisense Oligonucleotides. *Mol. Ther. Nucleic Acids* 5, e361. Available at: <http://www.ncbi.nlm.nih.gov/pubmed/27623443> [Accessed March 15, 2019].
47. Traynor, K. (2016). Eteplirsen approved for Duchenne muscular dystrophy. *Am. J. Heal. Pharm.* 73, 1719. Available at: <https://academic.oup.com/ajhp/article/73/21/1719/5102151> [Accessed May 6, 2021].
48. Haché, M., Swoboda, K.J., Sethna, N., Farrow-Gillespie, A., Khandji, A., Xia, S., and Bishop, K.M. (2016). Intrathecal Injections in Children with Spinal Muscular Atrophy: Nusinersen Clinical Trial Experience. *J. Child Neurol.* 31, 899–906. Available at: https://journals.sagepub.com/doi/10.1177/0883073815627882?url_ver=Z39.88-2003&rfr_id=ori%3Arid%3Acrossref.org&rfr_dat=cr_pub++0pubmed [Accessed May 6, 2021].
49. Frontera, W.R., and Ochala, J. (2015). Skeletal Muscle: A Brief Review of Structure and Function. *Behav. Genet.* 45, 183–195. Available at: <https://link.springer.com/article/10.1007/s00223-014-9915-y> [Accessed April 13, 2021].
50. Walowski, C.O., Braun, W., Maisch, M.J., Jensen, B., Peine, S., Norman, K., Müller, M.J., and Bosy-Westphal, A. (2020). Reference values for skeletal muscle mass – current concepts and methodological considerations. *Nutrients* 12, 1–36. Available at: </pmc/articles/PMC7146130/> [Accessed April 12, 2021].
51. Morgan, J., and Partridge, T. (2020). Skeletal muscle in health and disease. *DMM Dis. Model. Mech.* 13.

52. Lewis, W.H., and Lewis, M.R. (1917). Behavior of cross striated muscle in tissue cultures. *Am. J. Anat.* 22, 169–194. Available at: <http://doi.wiley.com/10.1002/aja.1000220202> [Accessed April 29, 2021].
53. Cooper, W.G., and Konigsberg, I.R. (1961). Dynamics of myogenesis in vitro. *Anat. Rec.* 140, 195–205. Available at: <http://doi.wiley.com/10.1002/ar.1091400305> [Accessed April 29, 2021].
54. Stockdale, F.E., and Holtzer, H. (1961). DNA synthesis and myogenesis. *Exp. Cell Res.* 24, 508–520.
55. Scharner, J., and Zammit, P.S. (2011). The muscle satellite cell at 50: the formative years. *Skelet. Muscle* 2011 11 7, 1–13. Available at: <https://skeletal-muscle-journal.biomedcentral.com/articles/10.1186/2044-5040-1-28> [Accessed September 6, 2021].
56. Chang, N.C., and Rudnicki, M.A. (2014). Satellite Cells: The Architects of Skeletal Muscle. In *Current Topics in Developmental Biology* (Academic Press Inc.), pp. 161–181.
57. Mauro, A. (1961). Satellite cell of skeletal muscle fibers. *J. Biophys. Biochem. Cytol.* 9, 493–5. Available at: <http://www.ncbi.nlm.nih.gov/pubmed/13768451> [Accessed June 26, 2016].
58. Seale, P., Sabourin, L.A., Girgis-Gabardo, A., Mansouri, A., Gruss, P., and Rudnicki, M.A. (2000). Pax7 is required for the specification of myogenic satellite cells. *Cell* 102, 777–86. Available at: <http://www.ncbi.nlm.nih.gov/pubmed/11030621> [Accessed March 4, 2015].
59. Rudnicki, M.A., Schnegelsberg, P.N., Stead, R.H., Braun, T., Arnold, H.H., and Jaenisch, R. (1993). MyoD or Myf-5 is required for the formation of skeletal muscle. *Cell* 75, 1351–9. Available at: <http://www.ncbi.nlm.nih.gov/pubmed/8269513> [Accessed September 25, 2017].
60. Kassam-Duchossoy, L., Giaccone, E., Gayraud-Morel, B., Jory, A., Gomès, D., and Tajbakhsh, S. (2005). Pax3/Pax7 mark a novel population of primitive myogenic cells during development. *Genes Dev.* 19, 1426–31. Available at: <http://www.ncbi.nlm.nih.gov/pubmed/15964993> [Accessed September 25, 2017].
61. Day, K., Shefer, G., Richardson, J.B., Enikolopov, G., and Yablonka-Reuveni, Z. (2007). Nestin-GFP reporter expression defines the quiescent state of skeletal muscle satellite cells. *Dev. Biol.* 304, 246–259. Available at: <http://pmc/articles/PMC1888564/> [Accessed April 29, 2021].
62. Relaix, F., Montarras, D., Zaffran, S., Gayraud-Morel, B., Rocancourt, D., Tajbakhsh, S., Mansouri, A., Cumano, A., and Buckingham, M. (2006). Pax3 and Pax7 have distinct and overlapping functions in adult muscle progenitor cells. *J. Cell Biol.* 172, 91–102. Available at: <http://www.jcb.org/cgi/> [Accessed April 29, 2021].
63. Negroni, E., Gidaro, T., Bigot, A., Butler-Browne, G.S., Mouly, V., and Trollet, C. (2015). Invited review: Stem cells and muscle diseases: advances in cell therapy strategies. *Neuropathol. Appl. Neurobiol.* 41, 270–87. Available at: <http://www.ncbi.nlm.nih.gov/pubmed/25405809> [Accessed July 9, 2016].
64. Schultz, E., Gibson, M.C., and Champion, T. (1978). Satellite cells are mitotically quiescent in mature mouse muscle: An EM and radioautographic study. *J. Exp. Zool.* 206, 451–456. Available at: <http://doi.wiley.com/10.1002/jez.1402060314> [Accessed April 7, 2020].
65. Moss, F.P., and Leblond, C.P. (1971). Satellite cells as the source of nuclei in muscles of growing rats. *Anat. Rec.* 170, 421–435. Available at: <http://doi.wiley.com/10.1002/ar.1091700405> [Accessed April 21, 2021].

66. Rosenblatt, J.D., Lunt, A.I., Parry, D.J., and Partridge, T.A. (1995). Culturing satellite cells from living single muscle fiber explants. *Vitr. Cell. Dev. Biol. - Anim. J. Soc. Vitr. Biol.* *31*, 773–779. Available at: <https://link.springer.com/article/10.1007/BF02634119> [Accessed April 21, 2021].
67. Konigsberg, U.R., Lipton, B.H., and Konigsberg, I.R. (1975). The regenerative response of single mature muscle fibers isolated in vitro. *Dev. Biol.* *45*, 260–275.
68. Beauchamp, J.R., Heslop, L., Yu, D.S., Tajbakhsh, S., Kelly, R.G., Wernig, A., Buckingham, M.E., Partridge, T.A., and Zammit, P.S. (2000). Expression of CD34 and Myf5 defines the majority of quiescent adult skeletal muscle satellite cells. *J. Cell Biol.* *151*, 1221–34. Available at: <http://www.ncbi.nlm.nih.gov/pubmed/11121437> [Accessed May 29, 2019].
69. Zammit, P.S., Golding, J.P., Nagata, Y., Hudon, V., Partridge, T.A., and Beauchamp, J.R. (2004). Muscle satellite cells adopt divergent fates: A mechanism for self-renewal? *J. Cell Biol.* *166*, 347–357. Available at: </pmc/articles/PMC2172269/?report=abstract> [Accessed September 2, 2020].
70. Collins, C. a., Olsen, I., Zammit, P.S., Heslop, L., Petrie, A., Partridge, T. a., and Morgan, J.E. (2005). Stem cell function, self-renewal, and behavioral heterogeneity of cells from the adult muscle satellite cell niche. *Cell* *122*, 289–301.
71. Zammit, P.S., Partridge, T.A., and Yablonka-Reuveni, Z. (2006). The skeletal muscle satellite cell: the stem cell that came in from the cold. *J. Histochem. Cytochem.* *54*, 1177–91. Available at: <http://www.ncbi.nlm.nih.gov/pubmed/16899758> [Accessed July 9, 2016].
72. FÜchtbauer, E.-M., and Westphal, H. (1992). MyoD and myogenin are coexpressed in regenerating skeletal muscle of the mouse. *Dev. Dyn.* *193*, 34–39. Available at: <http://doi.wiley.com/10.1002/aja.1001930106> [Accessed April 22, 2021].
73. Grounds, M.D., Garrett, K.L., Lai, M.C., Wright, W.E., and Beilharz, M.W. (1992). Identification of skeletal muscle precursor cells in vivo by use of MyoD1 and myogenin probes. *Cell Tissue Res.* *267*, 99–104. Available at: <https://pubmed.ncbi.nlm.nih.gov/1310442/> [Accessed April 22, 2021].
74. Olguin, H.C., and Olwin, B.B. (2004). Pax-7 up-regulation inhibits myogenesis and cell cycle progression in satellite cells: A potential mechanism for self-renewal. *Dev. Biol.* *275*, 375–388.
75. Rudnicki, M.A., Braun, T., Hinuma, S., and Jaenisch, R. (1992). Inactivation of MyoD in mice leads to up-regulation of the myogenic HLH gene Myf-5 and results in apparently normal muscle development. *Cell* *71*, 383–390. Available at: <http://www.cell.com/article/009286749290508A/fulltext> [Accessed April 22, 2021].
76. Jones, N.C., Tyner, K.J., Nibarger, L., Stanley, H.M., Cornelison, D.D.W., Fedorov, Y. V., and Olwin, B.B. (2005). The p38 α / β MAPK functions as a molecular switch to activate the quiescent satellite cell. *J. Cell Biol.* *169*, 105–116. Available at: <http://www.jcb.org/cgi/> [Accessed May 7, 2021].
77. Chakkalakal, J. V, Jones, K.M., Basson, M.A., and Brack, A.S. (2012). The aged niche disrupts muscle stem cell quiescence. *Nature* *490*, 355–60. Available at: <http://www.pubmedcentral.nih.gov/articlerender.fcgi?artid=3605795&tool=pmcentrez&rendertype=abstract> [Accessed November 19, 2014].
78. Shea, K.L., Xiang, W., LaPorta, V.S., Licht, J.D., Keller, C., Basson, M.A., and Brack, A.S. (2010). Sprouty1 regulates reversible quiescence of a self-renewing adult muscle stem cell pool during regeneration. *Cell Stem Cell* *6*, 117–29. Available at: <http://www.cell.com/article/S1934590909006389/fulltext> [Accessed October 19, 2015].

79. Bentzinger, C.F., Wang, Y.X., and Rudnicki, M.A. (2012). Building muscle: molecular regulation of myogenesis. *Cold Spring Harb. Perspect. Biol.* 4. Available at: <http://www.ncbi.nlm.nih.gov/pubmed/22300977> [Accessed July 1, 2016].
80. Abou-Khalil, R., Le Grand, F., Pallafacchina, G., Valable, S., Authier, F.J., Rudnicki, M. a., Cherardi, R.K., Germain, S., Chretien, F., Sotiropoulos, A., *et al.* (2009). Autocrine and Paracrine Angiopoietin 1/Tie-2 Signaling Promotes Muscle Satellite Cell Self-Renewal. *Cell Stem Cell* 5, 298–309.
81. Rozo, M., Li, L., and Fan, C.M. (2016). Targeting β 1-integrin signaling enhances regeneration in aged and dystrophic muscle in mice. *Nat. Med.* 22, 889–896. Available at: <https://www.nature.com/articles/nm.4116> [Accessed April 7, 2021].
82. Shinin, V., Gayraud-Morel, B., Gomès, D., and Tajbakhsh, S. (2006). Asymmetric division and cosegregation of template DNA strands in adult muscle satellite cells. *Nat. Cell Biol.* 8, 677–682. Available at: <https://www.nature.com/articles/ncb1425> [Accessed September 16, 2020].
83. Gurevich, D.B., Nguyen, P.D., Siegel, A.L., Ehrlich, O. V, Sonntag, C., Phan, J.M.N., Berger, S., Ratnayake, D., Hersey, L., Berger, J., *et al.* (2016). Asymmetric division of clonal muscle stem cells coordinates muscle regeneration in vivo. *Science*. Available at: <http://www.ncbi.nlm.nih.gov/pubmed/27198673> [Accessed May 22, 2016].
84. Kuang, S., Kuroda, K., Le Grand, F., and Rudnicki, M.A. (2007). Asymmetric self-renewal and commitment of satellite stem cells in muscle. *Cell* 129, 999–1010. Available at: <http://www.pubmedcentral.nih.gov/articlerender.fcgi?artid=2718740&tool=pmcentrez&rendertype=abstract> [Accessed May 9, 2015].
85. Conboy, M.J., Karasov, A.O., and Rando, T.A. (2007). High incidence of non-random template strand segregation and asymmetric fate determination in dividing stem cells and their progeny. *PLoS Biol.* 5, 1120–1126. Available at: www.plosbiology.org [Accessed May 5, 2021].
86. Dumont, N.A., Bentzinger, C.F., Sincennes, M.-C., and Rudnicki, M.A. (2015). Satellite Cells and Skeletal Muscle Regeneration. In *Comprehensive Physiology* (Hoboken, NJ, USA: John Wiley & Sons, Inc.), pp. 1027–1059. Available at: <http://doi.wiley.com/10.1002/cphy.c140068> [Accessed April 23, 2021].
87. Wells, L., Edwards, K.A., and Bernstein, S.I. (1996). Myosin heavy chain isoforms regulate muscle function but not myofibril assembly. *EMBO J.* 15, 4454–9. Available at: <http://www.ncbi.nlm.nih.gov/pubmed/8887536> [Accessed August 10, 2016].
88. Rudnicki, M.A., Le Grand, F., McKinnell, I., and Kuang, S. (2008). The molecular regulation of muscle stem cell function. *Cold Spring Harb. Symp. Quant. Biol.* 73, 323–31. Available at: <http://www.ncbi.nlm.nih.gov/pubmed/19329572> [Accessed July 9, 2016].
89. Tierney, M.T., and Sacco, A. (2016). Satellite Cell Heterogeneity in Skeletal Muscle Homeostasis. *Trends Cell Biol.*
90. Biressi, S., and Rando, T.A. (2010). Heterogeneity in the muscle satellite cell population. *Semin. Cell Dev. Biol.* 21, 845–854.
91. Rocheteau, P., Gayraud-Morel, B., Siegl-Cachedenier, I., Blasco, M.A., and Tajbakhsh, S. (2012). A subpopulation of adult skeletal muscle stem cells retains all template DNA strands after cell division. *Cell* 148, 112–125.

92. Evano, B., Gill, D., Hernando-Herraez, I., Comai, G., Stubbs, T.M., Commere, P.H., Reik, W., and Tajbakhsh, S. (2020). Transcriptome and epigenome diversity and plasticity of muscle stem cells following transplantation. *PLoS Genet.* *16*, e1009022. Available at: <https://doi.org/10.1371/journal.pgen.1009022> [Accessed May 20, 2021].
93. Sherwood, R.I., Christensen, J.L., Conboy, I.M., Conboy, M.J., Rando, T.A., Weissman, I.L., and Wagers, A.J. (2004). Isolation of adult mouse myogenic progenitors: Functional heterogeneity of cells within and engrafting skeletal muscle. *Cell* *119*, 543–554. Available at: <http://www.> [Accessed June 4, 2021].
94. Saber, J., Lin, A.Y.T., and Rudnicki, M.A. (2020). Single-cell analyses uncover granularity of muscle stem cells. *F1000Research* *9*, 31. Available at: <https://doi.org/10.12688/f1000research.20856.1> [Accessed May 24, 2021].
95. Barruet, E., Garcia, S.M., Striedinger, K., Wu, J., Lee, S., Byrnes, L., Wong, A., Xuefeng, S., Tamaki, S., Brack, A.S., et al. (2020). Functionally heterogeneous human satellite cells identified by single cell RNA sequencing. *Elife* *9*.
96. Chang, H.H., Hemberg, M., Barahona, M., Ingber, D.E., and Huang, S. (2008). Transcriptome-wide noise controls lineage choice in mammalian progenitor cells. *Nature* *453*, 544–547. Available at: <https://www.nature.com/articles/nature06965> [Accessed April 22, 2021].
97. Imayoshi, I., Isomura, A., Harima, Y., Kawaguchi, K., Kori, H., Miyachi, H., Fujiwara, T., Ishidate, F., and Kageyama, R. (2013). Oscillatory control of factors determining multipotency and fate in mouse neural progenitors. *Science* (80-.). *342*, 1203–1208. Available at: <https://science.sciencemag.org/content/342/6163/1203> [Accessed April 22, 2021].
98. Rompolas, P., Mesa, K.R., and Greco, V. (2013). Spatial organization within a niche as a determinant of stem-cell fate. *Nature* *502*, 513–518. Available at: <https://www.nature.com/articles/nature12602> [Accessed April 22, 2021].
99. Dell'Orso, S., Juan, A.H., Ko, K.-D., Naz, F., Gutierrez-Cruz, G., Feng, X., and Sartorelli, V. (2019). Single-cell analysis of adult skeletal muscle stem cells in homeostatic and regenerative conditions. *Development*, dev.174177. Available at: <http://dev.biologists.org/content/early/2019/03/18/dev.174177> [Accessed April 1, 2019].
100. Scaramozza, A., Park, D., Kollu, S., Beerman, I., Sun, X., Rossi, D.J., Lin, C.P., Scadden, D.T., Crist, C., and Brack, A.S. (2019). Lineage Tracing Reveals a Subset of Reserve Muscle Stem Cells Capable of Clonal Expansion under Stress. *Cell Stem Cell*. Available at: <https://www.sciencedirect.com/science/article/pii/S1934590919301195?via%3Dihub> [Accessed April 25, 2019].
101. Barthélémy, F., Defour, A., Lévy, N., Krahn, M., and Bartoli, M. (2018). Muscle Cells Fix Breaches by Orchestrating a Membrane Repair Ballet. *J. Neuromuscul. Dis.* *5*, 21–28.
102. Horn, A., Van Der Meulen, J.H., Defour, A., Hogarth, M., Sreetama, S.C., Reed, A., Scheffer, L., Chandel, N.S., and Jaiswal, J.K. (2017). Mitochondrial redox signaling enables repair of injured skeletal muscle cells. *Sci. Signal.* *10*. Available at: <http://stke.sciencemag.org/> [Accessed April 29, 2021].
103. Bansal, D., Miyake, K., Vogel, S.S., Groh, S., Chen, C.C., Williamson, R., McNeil, P.L., and Campbell, K.P. (2003). Defective membrane repair in dysferlin-deficient muscular dystrophy. *Nature* *423*, 168–172. Available at: www.nature.com/nature [Accessed May 5, 2021].
104. Lepper, C., Partridge, T. a, and Fan, C.-M. (2011). An absolute requirement for Pax7-positive satellite cells in acute injury-induced skeletal muscle regeneration. *Development* *138*, 3639–3646.

105. von Maltzahn, J., Jones, A.E., Parks, R.J., and Rudnicki, M.A. (2013). Pax7 is critical for the normal function of satellite cells in adult skeletal muscle. *Proc. Natl. Acad. Sci. U. S. A.* *110*, 16474–9. Available at: <http://www.ncbi.nlm.nih.gov/pubmed/24065826> [Accessed March 15, 2019].
106. Sambasivan, R., Yao, R., Kissenpfennig, A., van Wittenberghe, L., Paldi, A., Gayraud-Morel, B., Guenou, H., Malissen, B., Tajbakhsh, S., and Galy, A. (2011). Pax7-expressing satellite cells are indispensable for adult skeletal muscle regeneration. *Development* *138*, 3647–3656.
107. Tidball, J.G., and Villalta, S.A. (2010). Regulatory interactions between muscle and the immune system during muscle regeneration. *Am. J. Physiol. - Regul. Integr. Comp. Physiol.* *298*, 1173–1187. Available at: <http://www.ajpregu.org> [Accessed April 22, 2021].
108. Tidball, J.G., Dorshkind, K., and Wehling-Henricks, M. (2014). Shared signaling systems in myeloid cell-mediated muscle regeneration. *Dev.* *141*, 1184–1196.
109. Du, H., Shih, C.-H., Wosczyzna, M.N., Mueller, A.A., Cho, J., Aggarwal, A., Rando, T.A., and Feldman, B.J. (2017). Macrophage-released ADAMTS1 promotes muscle stem cell activation. *Nat. Commun.* *8*, 669. Available at: <http://www.nature.com/articles/s41467-017-00522-7> [Accessed February 19, 2019].
110. Tidball, J.G. (2017). Regulation of muscle growth and regeneration by the immune system. *Nat. Rev. Immunol.* Available at: <http://www.nature.com/doi/10.1038/nri.2016.150> [Accessed February 22, 2017].
111. Chazaud, B., Sonnet, C., Lafuste, P., Bassez, G., Rimaniol, A.C., Poron, F., Authier, F.J., Dreyfus, P.A., and Gherardi, R.K. (2003). Satellite cells attract monocytes and use macrophages as a support to escape apoptosis and enhance muscle growth. *J. Cell Biol.* *163*, 1133–1143. Available at: <http://www.jcb.org/cgi/doi/10.1083/jcb.200212046> [Accessed April 22, 2021].
112. Uezumi, A., Fukada, S.I., Yamamoto, N., Takeda, S., and Tsuchida, K. (2010). Mesenchymal progenitors distinct from satellite cells contribute to ectopic fat cell formation in skeletal muscle. *Nat. Cell Biol.* *12*, 143–152. Available at: <https://www.nature.com/articles/ncb2014> [Accessed April 22, 2021].
113. Joe, A.W.B., Yi, L., Natarajan, A., Le Grand, F., So, L., Wang, J., Rudnicki, M.A., and Rossi, F.M.V. (2010). Muscle injury activates resident fibro/adipogenic progenitors that facilitate myogenesis. *Nat. Cell Biol.* *12*, 153–163. Available at: <https://www.nature.com/articles/ncb2015> [Accessed April 22, 2021].
114. Murphy, M.M., Lawson, J.A., Mathew, S.J., Hutcheson, D.A., and Kardon, G. (2011). Satellite cells, connective tissue fibroblasts and their interactions are crucial for muscle regeneration. *Development* *138*, 3625–3637.
115. Fry, C.S., Kirby, T.J., Kosmac, K., McCarthy, J.J., and Peterson, C.A. (2017). Myogenic Progenitor Cells Control Extracellular Matrix Production by Fibroblasts during Skeletal Muscle Hypertrophy. *Cell Stem Cell* *20*, 56–69. Available at: <http://dx.doi.org/10.1016/j.stem.2016.09.010> [Accessed April 22, 2021].
116. Mackey, A.L., Magnan, M., Chazaud, B., and Kjaer, M. (2017). Human skeletal muscle fibroblasts stimulate in vitro myogenesis and in vivo muscle regeneration. *J. Physiol.* *595*, 5115–5127. Available at: <http://doi.wiley.com/10.1113/JP273997> [Accessed April 22, 2021].
117. Sampaolesi, M., Torrente, Y., Innocenzi, A., Tonlorenzi, R., D'Antona, G., Pellegrino, M.A., Barresi, R., Bresolin, N., De Angelis, M.G.C., Campbell, K.P., et al. (2003). Cell therapy of α -sarcoglycan null dystrophic mice through intra-arterial delivery of mesoangioblasts. *Science* (80-.). *301*, 487–492. Available at: <https://science.sciencemag.org/content/301/5632/487> [Accessed April 22, 2021].

118. Fukada, S., Miyagoe-Suzuki, Y., Tsukihara, H., Yuasa, K., Higuchi, S., Ono, S., Tsujikawa, K., Takeda, S., and Yamamoto, H. (2002). Muscle regeneration by reconstitution with bone marrow or fetal liver cells from green fluorescent protein-gene transgenic mice (The Company of Biologists).
119. Wosczyzna, M.N., and Rando, T.A. (2018). A Muscle Stem Cell Support Group: Coordinated Cellular Responses in Muscle Regeneration. *Dev. Cell* 46, 135–143. Available at: <https://doi.org/10.1016/j.devcel.2018.06.018> [Accessed April 22, 2021].
120. Liu, L., Cheung, T.H., Charville, G.W., and Rando, T. a (2015). Isolation of skeletal muscle stem cells by fluorescence-activated cell sorting. *Nat. Protoc.* 10, 1612–1624. Available at: <http://dx.doi.org/10.1038/nprot.2015.110>.
121. Fukada, S.I., Higuchi, S., Segawa, M., Koda, K.I., Yamamoto, Y., Tsujikawa, K., Kohama, Y., Uezumi, A., Imamura, M., Miyagoe-Suzuki, Y., *et al.* (2004). Purification and cell-surface marker characterization of quiescent satellite cells from murine skeletal muscle by a novel monoclonal antibody. *Exp. Cell Res.* 296, 245–255.
122. Alexander, M.S., Rozkalne, A., Colletta, A., Spinazzola, J.M., Johnson, S., Rahimov, F., Meng, H., Lawlor, M.W., Estrella, E., Kunkel, L.M., *et al.* (2016). CD82 Is a Marker for Prospective Isolation of Human Muscle Satellite Cells and Is Linked to Muscular Dystrophies. *Cell Stem Cell* 19, 800–807. Available at: <http://www.ncbi.nlm.nih.gov/pubmed/27641304> [Accessed April 6, 2018].
123. Tomasek, J.J., Gabbiani, G., Hinz, B., Chaponnier, C., and Brown, R.A. (2002). Myofibroblasts and mechano: Regulation of connective tissue remodelling. *Nat. Rev. Mol. Cell Biol.* 3, 349–363. Available at: <https://www.nature.com/articles/nrm809> [Accessed May 24, 2021].
124. Mathew, S.J., Hansen, J.M., Merrell, A.J., Murphy, M.M., Lawson, J.A., Hutcheson, D.A., Hansen, M.S., Angus-Hill, M., and Kardon, G. (2011). Connective tissue fibroblasts and Tcf4 regulate myogenesis. *Development* 138, 371–384. Available at: <http://genepath.med.harvard.edu/~cepko/protocol/xgalplap-> [Accessed May 24, 2021].
125. Mitchell, K.J., Pannérec, A., Cadot, B., Parlakian, A., Besson, V., Gomes, E.R., Marazzi, G., and Sassoon, D.A. (2010). Identification and characterization of a non-satellite cell muscle resident progenitor during postnatal development. *Nat. Cell Biol.* 12, 257–266. Available at: <https://www.nature.com/articles/ncb2025> [Accessed June 4, 2021].
126. Villalta, S.A., Nguyen, H.X., Deng, B., Gotoh, T., and Tidbal, J.G. (2009). Shifts in macrophage phenotypes and macrophage competition for arginine metabolism affect the severity of muscle pathology in muscular dystrophy. *Hum. Mol. Genet.* 18, 482–496. Available at: <https://academic.oup.com/hmg/article/18/3/482/2527316> [Accessed May 24, 2021].
127. Arnold, L., Henry, A., Poron, F., Baba-Amer, Y., Van Rooijen, N., Plonquet, A., Gherardi, R.K., and Chazaud, B. (2007). Inflammatory monocytes recruited after skeletal muscle injury switch into antiinflammatory macrophages to support myogenesis. *J. Exp. Med.* 204, 1057–1069. Available at: www.jem.org/cgi/doi/10.1084/jem.20070075 [Accessed May 24, 2021].
128. Ziemkiewicz, N., Hilliard, G., Pullen, N.A., and Garg, K. (2021). The Role of Innate and Adaptive Immune Cells in Skeletal Muscle Regeneration. *Int. J. Mol. Sci.* 22, 3265. Available at: <https://www.mdpi.com/1422-0067/22/6/3265> [Accessed May 4, 2021].
129. Wichterle, H., Lieberam, I., Porter, J.A., and Jessell, T.M. (2002). Directed differentiation of embryonic stem cells into motor neurons. *Cell* 110, 385–397. Available at: <http://www.cell.com/cgi/content/full/110/3/385/DC1> [Accessed June 4, 2021].

130. Dumont, N., Bouchard, P., and Frenette, J. (2008). Neutrophil-induced skeletal muscle damage: A calculated and controlled response following hindlimb unloading and reloading. *Am. J. Physiol. - Regul. Integr. Comp. Physiol.* 295, 1831–1838. Available at: www.ajpregu.org [Accessed May 24, 2021].
131. Tiemessen, M.M., Jagger, A.L., Evans, H.G., Van Herwijnen, M.J.C., John, S., and Taams, L.S. (2007). CD4+CD25+Foxp3+ regulatory T cells induce alternative activation of human monocytes/macrophages. *Proc. Natl. Acad. Sci. U. S. A.* 104, 19446–19451. Available at: www.pnas.org/cgi/doi/10.1073/pnas.0706832104 [Accessed May 24, 2021].
132. Burzyn, D., Kuswanto, W., Kolodin, D., Shadrach, J.L., Cerletti, M., Jang, Y., Sefik, E., Tan, T.G., Wagers, A.J., Benoist, C., et al. (2013). A Special Population of regulatory T Cells Potentiates muscle repair. *Cell* 155, 1282–1295.
133. Kuswanto, W., Burzyn, D., Panduro, M., Wang, K.K., Jang, Y.C., Wagers, A.J., Benoist, C., and Mathis, D. (2016). Poor Repair of Skeletal Muscle in Aging Mice Reflects a Defect in Local, Interleukin-33-Dependent Accumulation of Regulatory T Cells. *Immunity* 44, 355–367.
134. Christov, C., Chrétien, F., Abou-Khalil, R., Bassez, G., Vallet, G., Authier, F.J., Bassaglia, Y., Shinin, V., Tajbakhsh, S., Chazaud, B., et al. (2007). Muscle satellite cells and endothelial cells: Close neighbors and privileged partners. *Mol. Biol. Cell* 18, 1397–1409. Available at: <http://www.molbiolcell.org/cgi/doi/10.1091/mbc.E06> [Accessed May 24, 2021].
135. Wosczyzna, M.N., Biswas, A.A., Cogswell, C.A., and Goldhamer, D.J. (2012). Multipotent progenitors resident in the skeletal muscle interstitium exhibit robust BMP-dependent osteogenic activity and mediate heterotopic ossification. *J. Bone Miner. Res.* 27, 1004–1017. Available at: <https://asbmr.onlinelibrary.wiley.com/doi/full/10.1002/jbmr.1562> [Accessed May 24, 2021].
136. Dellavalle, A., Sampaolesi, M., Tonlorenzi, R., Tagliafico, E., Sacchetti, B., Perani, L., Innocenzi, A., Galvez, B.G., Messina, G., Morosetti, R., et al. (2007). Pericytes of human skeletal muscle are myogenic precursors distinct from satellite cells. *Nat. Cell Biol.* 9, 255–267. Available at: <https://www.nature.com/articles/hcb1542> [Accessed April 20, 2021].
137. Armulik, A., Genové, G., and Betsholtz, C. (2011). Pericytes: Developmental, Physiological, and Pathological Perspectives, Problems, and Promises. *Dev. Cell* 21, 193–215.
138. Scott, R.W., Arostegui, M., Schweitzer, R., Rossi, F.M.V., and Underhill, T.M. (2019). Hic1 Defines Quiescent Mesenchymal Progenitor Subpopulations with Distinct Functions and Fates in Skeletal Muscle Regeneration. *Cell Stem Cell* 25.
139. Wolfe, R.R. (2006). The underappreciated role of muscle in health and disease. *Am. J. Clin. Nutr.* 84, 475–482. Available at: <https://academic.oup.com/ajcn/article/84/3/475/464884> [Accessed April 13, 2021].
140. Benarroch, L., Bonne, G., Rivier, F., and Hamroun, D. (2020). The 2021 version of the gene table of neuromuscular disorders (nuclear genome). *Neuromuscul. Disord.* 30, 1008–1048. Available at: www.sciencedirect.com/www.elsevier.com/locate/nmd [Accessed April 12, 2021].
141. Understanding Neuromuscular Disease Care - IQVIA Available at: <https://www.iqvia.com/insights/the-iqvia-institute/reports/understanding-neuromuscular-disease-care> [Accessed April 13, 2021].
142. Pharmacoeconomic Review Report (Resubmission): NUSINERSEN (SPINRAZA) (2019). (Canadian Agency for Drugs and Technologies in Health) Available at: <http://www.ncbi.nlm.nih.gov/pubmed/31211527> [Accessed April 23, 2021].

143. Dangouloff, T., Botty, C., Beudart, C., Servais, L., and Hiligsmann, M. (2021). Systematic literature review of the economic burden of spinal muscular atrophy and economic evaluations of treatments. *Orphanet J. Rare Dis.* 16, 47. Available at: <https://ojrd.biomedcentral.com/articles/10.1186/s13023-021-01695-7> [Accessed April 23, 2021].
144. Cowling, B.S., and Thielemans, L. (2020). Translational medicine in neuromuscular disorders: From academia to industry. *DMM Dis. Model. Mech.* 13. Available at: <https://www.fda.gov>. [Accessed November 13, 2020].
145. Mendell, J.R., Al-Zaidy, S.A., Rodino-Klapac, L.R., Goodspeed, K., Gray, S.J., Kay, C.N., Boye, S.L., Boye, S.E., George, L.A., Salabarria, S., et al. (2021). Current Clinical Applications of In Vivo Gene Therapy with AAVs. *Mol. Ther.* 29, 464–488. Available at: <https://doi.org/10.1016/j.ymthe.2020.12.007>. [Accessed May 7, 2021].
146. Wirth, B. (2021). Spinal Muscular Atrophy: In the Challenge Lies a Solution. *Trends Neurosci.* 44, 306–322. Available at: <http://www.cell.com/article/S0166223620302745/fulltext> [Accessed April 23, 2021].
147. Broeders, M., Herrero-Hernandez, P., Ernst, M.P.T., van der Ploeg, A.T., and Pijnappel, W.W.M.P. (2020). Sharpening the Molecular Scissors: Advances in Gene-Editing Technology. *iScience* 23, 100789.
148. Ernst, M.P.T., Broeders, M., Herrero-Hernandez, P., Oussoren, E., van der Ploeg, A.T., and Pijnappel, W.W.M.P. (2020). Ready for Repair? Gene Editing Enters the Clinic for the Treatment of Human Disease. *Mol. Ther. - Methods Clin. Dev.* 18, 532–557. Available at: <https://linkinghub.elsevier.com/retrieve/pii/S2329050120301467> [Accessed July 28, 2020].
149. De Luca, M., Aiuti, A., Cossu, G., Parmar, M., Pellegrini, G., and Robey, P.G. (2019). Advances in stem cell research and therapeutic development. *Nat. Cell Biol.* 21, 801–811.
150. Gatti, R.A., Meuwissen, H.J., Allen, H.D., Hong, R., and Good, R.A. (1968). Immunological reconstitution of sex-linked lymphopenic immunological deficiency. *Lancet* 2, 1366–1369. Available at: <http://www.thelancet.com/article/S0140673668926731/fulltext> [Accessed April 19, 2021].
151. Hobbs, J.R., Barrett, A.J., Chambers, D., James, D.C.O., Hugh-Jones, K., Byrom, N., Henry, K., Lucas, C.F., Rogers, T.R., Benson, P.F., et al. (1981). Reversal of clinical features of Hurler's disease and biochemical improvement after treatment by bone-marrow transplantation. *Lancet (London, England)* 2, 709–712. Available at: <https://pubmed.ncbi.nlm.nih.gov/6116856/> [Accessed December 2, 2021].
152. Rama, P., Matuska, S., Paganoni, G., Spinelli, A., De Luca, M., and Pellegrini, G. (2010). Limbal Stem-Cell Therapy and Long-Term Corneal Regeneration. *N. Engl. J. Med.* 363, 147–155. Available at: <http://www.nejm.org/doi/abs/10.1056/NEJMoa0905955> [Accessed March 8, 2019].
153. Kondo, M., Wagers, A.J., Manz, M.G., Prohaska, S.S., Scherer, D.C., Beilhack, G.F., Shizuru, J.A., and Weissman, I.L. (2003). Biology of hematopoietic stem cells and progenitors: Implications for clinical application. *Annu. Rev. Immunol.* 21, 759–806. Available at: <https://pubmed.ncbi.nlm.nih.gov/12615892/> [Accessed September 2, 2020].
154. Hirsch, T., Rothoefter, T., Teig, N., Bauer, J.W., Pellegrini, G., De Rosa, L., Scaglione, D., Reichelt, J., Klausegger, A., Kneisz, D., et al. (2017). Regeneration of the entire human epidermis using transgenic stem cells. *Nature* 551, 327–332. Available at: <http://www.nature.com/doifinder/10.1038/nature24487> [Accessed December 1, 2017].
155. Lipton, B.H., and Schultz, E. (1979). Developmental fate of skeletal muscle satellite cells. *Science* 205, 1292–4. Available at: <http://www.ncbi.nlm.nih.gov/pubmed/472747>.

156. Partridge, T.A., Morgan, J.E., Coulton, G.R., Hoffman, E.P., and Kunkel, L.M. (1989). Conversion of mdx myofibres from dystrophin-negative to -positive by injection of normal myoblasts. *Nature* *337*, 176–179.
157. Karpati, G., Pouliot, Y., Zubrzycka-Gaarn, E., Carpenter, S., Ray, P.N., Worton, R.G., and Holland, P. (1989). Dystrophin is expressed in mdx skeletal muscle fibers after normal myoblast implantation. *Am. J. Pathol.* *135*, 27–32. Available at: <http://www.ncbi.nlm.nih.gov/pubmed/2672825> [Accessed June 25, 2016].
158. Takemitsu, M., Arahata, K., and Nonaka, I. (1990). [Muscle regeneration in mdx mouse, and a trial of normal myoblast transfer into regenerating dystrophic muscle]. *Rinshō shinkeigaku = Clin. Neurol.* *30*, 1066–72. Available at: <http://www.ncbi.nlm.nih.gov/pubmed/2279357> [Accessed June 25, 2016].
159. Law, P.K., Bertorini, T.E., Goodwin, T.G., Chen, M., Fang, Q.W., Li, H.J., Kirby, D.S., Florendo, J.A., Herrod, H.G., and Golden, G.S. (1990). Dystrophin production induced by myoblast transfer therapy in Duchenne muscular dystrophy. *Lancet (London, England)* *336*, 114–5. Available at: <http://www.ncbi.nlm.nih.gov/pubmed/1697393> [Accessed June 25, 2016].
160. Huard, J., Bouchard, J.P., Roy, R., Malouin, F., Dansereau, G., Labrecque, C., Albert, N., Richards, C.L., Lemieux, B., and Tremblay, J.P. (1992). Human myoblast transplantation: preliminary results of 4 cases. *Muscle Nerve* *15*, 550–60. Available at: <http://www.ncbi.nlm.nih.gov/pubmed/1584246> [Accessed June 25, 2016].
161. Miller, R.G., Sharma, K.R., Pavlath, G.K., Gussoni, E., Mynhier, M., Lanctot, A.M., Greco, C.M., Steinman, L., and Blau, H.M. (1997). Myoblast implantation in Duchenne muscular dystrophy: the San Francisco study. *Muscle Nerve* *20*, 469–78. Available at: <http://www.ncbi.nlm.nih.gov/pubmed/9121505> [Accessed June 25, 2016].
162. Law, P.K., Goodwin, T.G., Fang, Q., Deering, M.B., Duggirala, V., Larkin, C., Florendo, J.A., Kirby, D.S., Li, H.J., and Chen, M. (1993). Cell transplantation as an experimental treatment for Duchenne muscular dystrophy. *Cell Transplant.* *2*, 485–505. Available at: <http://www.ncbi.nlm.nih.gov/pubmed/8167934> [Accessed June 25, 2016].
163. Karpati, G., Ajdukovic, D., Arnold, D., Gledhill, R.B., Guttman, R., Holland, P., Koch, P.A., Shoubridge, E., Spence, D., and Vanasse, M. (1993). Myoblast transfer in Duchenne muscular dystrophy. *Ann. Neurol.* *34*, 8–17. Available at: <http://www.ncbi.nlm.nih.gov/pubmed/8517684> [Accessed June 25, 2016].
164. Tremblay, J.P., Bouchard, J.P., Malouin, F., Théau, D., Cottrell, F., Collin, H., Rouche, A., Gilgenkrantz, S., Abbadi, N., and Tremblay, M. (1993). Myoblast transplantation between monozygotic twin girl carriers of Duchenne muscular dystrophy. *Neuromuscul. Disord.* *3*, 583–92. Available at: <http://www.ncbi.nlm.nih.gov/pubmed/8186717> [Accessed June 25, 2016].
165. Tremblay, J.P., Malouin, F., Roy, R., Huard, J., Bouchard, J.P., Satoh, A., and Richards, C.L. (1993). Results of a triple blind clinical study of myoblast transplantations without immunosuppressive treatment in young boys with Duchenne muscular dystrophy. *Cell Transplant.* *2*, 99–112. Available at: <http://www.ncbi.nlm.nih.gov/pubmed/8143083> [Accessed June 25, 2016].
166. Mendell, J.R., Kissel, J.T., Amato, A.A., King, W., Signore, L., Prior, T.W., Sahenk, Z., Benson, S., McAndrew, P.E., and Rice, R. (1995). Myoblast transfer in the treatment of Duchenne's muscular dystrophy. *N. Engl. J. Med.* *333*, 832–8. Available at: <http://www.ncbi.nlm.nih.gov/pubmed/7651473> [Accessed June 25, 2016].

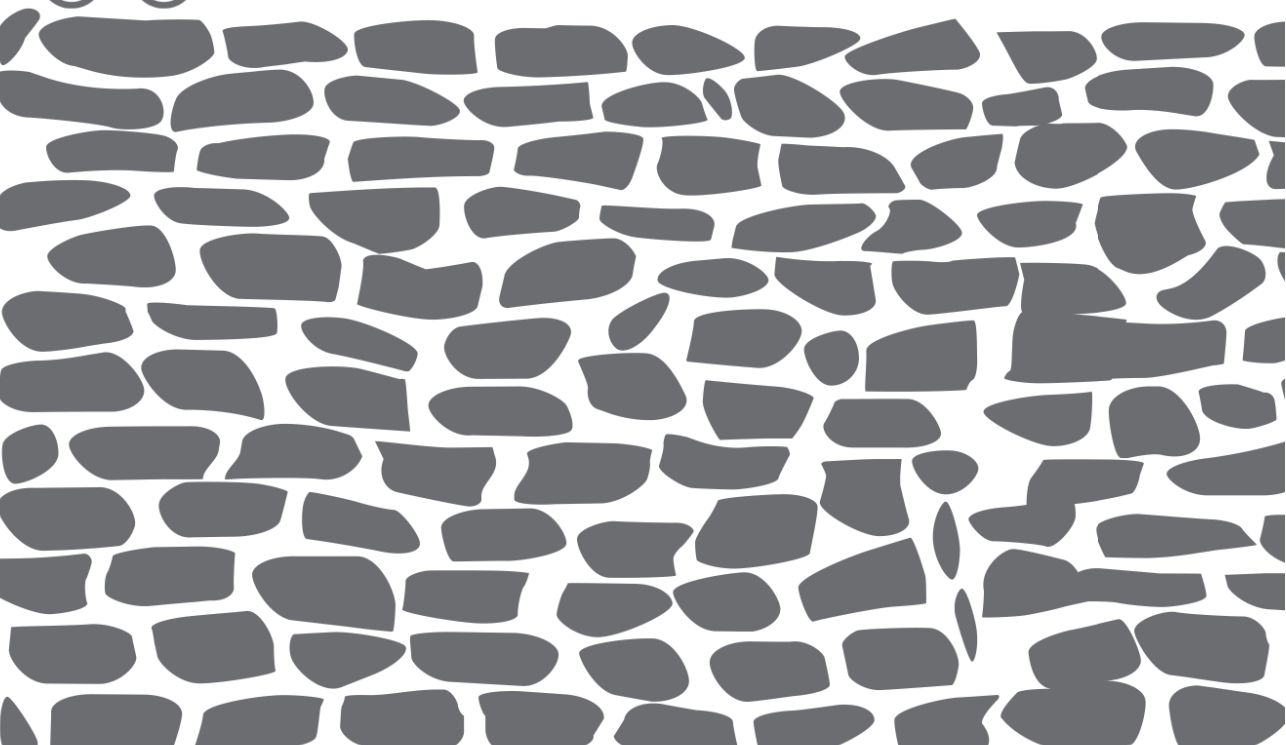
167. Cerletti, M., Jurga, S., Witczak, C. a., Hirshman, M.F., Shadrach, J.L., Goodyear, L.J., and Wagers, A.J. (2008). Highly Efficient, Functional Engraftment of Skeletal Muscle Stem Cells in Dystrophic Muscles. *Cell* 134, 37–47.
168. Sacco, A., Doyonnas, R., Kraft, P., Vitorovic, S., and Blau, H.M. (2008). Self-renewal and expansion of single transplanted muscle stem cells. *Nature* 456, 502–506.
169. Schaaf, G.J. (2012). Ex-vivo Expansion of Muscle-Regenerative Cells for the Treatment of Muscle Disorders. *J. Stem Cell Res. Ther.* 01. Available at: http://www.researchgate.net/publication/270011806_Ex-vivo_Expansion_of_Muscle-Regenerative_Cells_for_the_Treatment_of_Muscle_Disorders [Accessed November 12, 2015].
170. Beauchamp, J.R., Morgan, J.E., Pagel, C.N., and Partridge, T.A. (1999). Dynamics of myoblast transplantation reveal a discrete minority of precursors with stem cell-like properties as the myogenic source. *J. Cell Biol.* 144, 1113–1121.
171. Skuk, D., and Tremblay, J.P. (2017). Cell Therapy in Myology: Dynamics of Muscle Precursor Cell Death after Intramuscular Administration in Non-human Primates. *Mol. Ther. - Methods Clin. Dev.* 5, 232–240. Available at: <http://dx.doi.org/10.1016/j.omtm.2017.05.002>. [Accessed April 23, 2021].
172. Montarras, D., Morgan, J., Collins, C., Relaix, F., Zaffran, S., Cumano, A., Partridge, T., and Buckingham, M. (2005). Direct isolation of satellite cells for skeletal muscle regeneration. *Science* 309, 2064–7. Available at: <http://www.ncbi.nlm.nih.gov/pubmed/16141372> [Accessed August 12, 2015].
173. Charville, G.W., Cheung, T.H., Yoo, B., Santos, P.J., Lee, G.K., Shrager, J.B., and Rando, T.A. (2015). Ex Vivo Expansion and In Vivo Self-Renewal of Human Muscle Stem Cells. *Stem cell reports*. Available at: <http://www.sciencedirect.com/science/article/pii/S2213671115002386> [Accessed September 9, 2015].
174. Wilkinson, A.C., Ishida, R., Kikuchi, M., Sudo, K., Morita, M., Crisostomo, R.V., Yamamoto, R., Loh, K.M., Nakamura, Y., Watanabe, M., et al. (2019). Long-term ex vivo haematopoietic-stem-cell expansion allows nonconditioned transplantation. *Nature* 571, 117–121.
175. Rayagiri, S.S., Ranaldi, D., Raven, A., Mohamad Azhar, N.I.F., Lefebvre, O., Zammit, P.S., and Borycki, A.-G. (2018). Basal lamina remodeling at the skeletal muscle stem cell niche mediates stem cell self-renewal. *Nat. Commun.* 9, 1075. Available at: <http://www.nature.com/articles/s41467-018-03425-3> [Accessed April 4, 2018].
176. Ishii, K., Sakurai, H., Suzuki, N., Mabuchi, Y., Sekiya, I., Sekiguchi, K., and Akazawa, C. (2018). Recapitulation of Extracellular LAMININ Environment Maintains Stemness of Satellite Cells In Vitro. *Stem Cell Reports*. Available at: <http://www.sciencedirect.com/science/article/pii/S2213671117305611?via%3Dihub> [Accessed January 23, 2018].
177. Gilbert, P.M., Havenstrite, K.L., Magnusson, K.E.G., Sacco, a, Leonardi, N. a, Kraft, P., Nguyen, N.K., Thrun, S., Lutolf, M.P., and Blau, H.M. (2010). Substrate elasticity regulates skeletal muscle stem cell self-renewal in culture. *Science* 329, 1078–1081.
178. Quarta, M., Brett, J.O., DiMarco, R., De Morree, A., Boutet, S.C., Chacon, R., Gibbons, M.C., Garcia, V.A., Su, J., Shrager, J.B., et al. (2016). An artificial niche preserves the quiescence of muscle stem cells and enhances their therapeutic efficacy. *Nat. Biotechnol.* 34, 752–759.
179. Yennek, S., Burute, M., Théry, M., and Tajbakhsh, S. (2014). Cell adhesion geometry regulates non-random DNA segregation and asymmetric cell fates in mouse skeletal muscle stem cells. *Cell Rep.* 7, 961–970.

180. Baiguera, S., Del Gaudio, C., Di Nardo, P., Manzari, V., Carotenuto, F., and Teodori, L. (2020). 3D Printing Decellularized Extracellular Matrix to Design Biomimetic Scaffolds for Skeletal Muscle Tissue Engineering. *Biomed Res. Int.* 2020.
181. Bencze, M., Negroni, E., Vallese, D., Yacoubyousssef, H., Chaouch, S., Wolff, A., Aamiri, A., Di Santo, J.P., Chazaud, B., Butler-Browne, G., *et al.* (2012). Proinflammatory macrophages enhance the regenerative capacity of human myoblasts by modifying their kinetics of proliferation and differentiation. *Mol. Ther.* 20, 2168–2179.
182. Mozzetta, C., Consalvi, S., Saccone, V., Tierney, M., Diamantini, A., Mitchell, K.J., Marazzi, G., Borsellino, G., Battistini, L., Sassoon, D., *et al.* (2013). Fibroadipogenic progenitors mediate the ability of HDAC inhibitors to promote regeneration in dystrophic muscles of young, but not old Mdx mice. *EMBO Mol. Med.* 5, 626–639. Available at: <https://onlinelibrary.wiley.com/doi/10.1002/emmm.201202096> [Accessed April 20, 2021].
183. Cosgrove, B.D., Gilbert, P.M., Porpiglia, E., Mourkioti, F., Lee, S.P., Corbel, S.Y., Llewellyn, M.E., Delp, S.L., and Blau, H.M. (2014). Rejuvenation of the muscle stem cell population restores strength to injured aged muscles. *Nat. Med.* 20, 255–64. Available at: <http://www.ncbi.nlm.nih.gov/pubmed/24531378>.
184. Bernet, J.D., Doles, J.D., Hall, J.K., Kelly Tanaka, K., Carter, T.A., and Olwin, B.B. (2014). P38 MAPK signaling underlies a cell-autonomous loss of stem cell self-renewal in skeletal muscle of aged mice. *Nat. Med.* 20, 265–271. Available at: <https://www.nature.com/articles/nm.3465> [Accessed April 23, 2021].
185. Bentzinger, C.F., von Maltzahn, J., Dumont, N.A., Stark, D.A., Wang, Y.X., Nhan, K., Frenette, J., Cornelison, D., and Rudnicki, M.A. (2014). Wnt7a stimulates myogenic stem cell motility and engraftment resulting in improved muscle strength. *J. Cell Biol.* 205, 97–111. Available at: <https://rupress.org/jcb/article/205/1/97/37610/Wnt7a-stimulates-myogenic-stem-cell-motility-and> [Accessed April 20, 2021].
186. Parker, M.H., Loretz, C., Tyler, A.E., Duddy, W.J., Hall, J.K., Olwin, B.B., Bernstein, I.D., Storb, R., and Tapscott, S.J. (2012). Activation of notch signaling during ex vivo expansion maintains donor muscle cell engraftment. *Stem Cells* 30, 2212–2220.
187. Takahashi, K., and Yamanaka, S. (2006). Induction of Pluripotent Stem Cells from Mouse Embryonic and Adult Fibroblast Cultures by Defined Factors. *Cell* 126, 663–676.
188. van der Wal, E., Herrero-Hernandez, P., Wan, R., Broeders, M., in 't Groen, S.L.M., van Gestel, T.J.M., van IJcken, W.F.J., Cheung, T.H., van der Ploeg, A.T., Schaaf, G.J., *et al.* (2018). Large-Scale Expansion of Human iPSC-Derived Skeletal Muscle Cells for Disease Modeling and Cell-Based Therapeutic Strategies. *Stem Cell Reports* 10, 1975–1990.
189. Sato, T. (2020). Induction of Skeletal Muscle Progenitors and Stem Cells from human induced Pluripotent Stem Cells. *J. Neuromuscul. Dis.* 7, 395. Available at: </pmc/articles/PMC7592659/> [Accessed July 14, 2021].
190. Gussoni, E., Soneoka, Y., Strickland, C.D., Buzney, E.A., Khan, M.K., Flint, A.F., Kunkel, L.M., and Mulligan, R.C. (1999). Dystrophin expression in the mdx mouse restored by stem cell transplantation. *Nature* 401, 390–394. Available at: www.nature.com [Accessed April 23, 2021].
191. Muskiewicz, K.R., Frank, N.Y., Flint, A.F., and Gussoni, E. (2005). Myogenic potential of muscle side and main population cells after intravenous injection into sub-lethally irradiated mdx mice. *J. Histochem. Cytochem.* 53, 861–873. Available at: <http://journals.sagepub.com/doi/10.1369/jhc.4A6573.2005> [Accessed April 23, 2021].

192. Bachrach, E., Perez, A.L., Choi, Y.-H., Illigens, B.M.W., Jun, S.J., Nido, P. Del, McGowan, F.X., Li, S., Flint, A., Chamberlain, J., *et al.* (2006). Muscle engraftment of myogenic progenitor cells following intraarterial transplantation. *Muscle Nerve* **34**, 44–52. Available at: <http://doi.wiley.com/10.1002/mus.20560> [Accessed April 23, 2021].
193. Motohashi, N., Uezumi, A., Yada, E., Fukada, S.I., Fukushima, K., Imaizumi, K., Miyagoe-Suzuki, Y., and Takeda, S. (2008). Muscle CD31(-) CD45(-) side population cells promote muscle regeneration by stimulating proliferation and migration of myoblasts. *Am. J. Pathol.* **173**, 781–791.
194. Moyle, L.A., Tedesco, F.S., and Benedetti, S. (2019). Pericytes in Muscular Dystrophies. In *Advances in Experimental Medicine and Biology* (Springer New York LLC), pp. 319–344. Available at: https://link.springer.com/chapter/10.1007/978-3-030-16908-4_15 [Accessed April 20, 2021].
195. Cossu, G., Previtali, S.C., Napolitano, S., Cicalese, M.P., Tedesco, F.S., Nicastro, F., Noviello, M., Roostalu, U., Natali Sora, M.G., Scarlato, M., *et al.* (2015). Intra-arterial transplantation of HLA-matched donor mesoangioblasts in Duchenne muscular dystrophy. *EMBO Mol. Med.* **7**, 1513–1528. Available at: <https://onlinelibrary.wiley.com/doi/10.15252/emmm.201505636> [Accessed April 20, 2021].
196. Quinn, L.S., Norwood, T.H., and Nameroff, M. (1988). Myogenic stem cell commitment probability remains constant as a function of organismal and mitotic age. *J. Cell. Physiol.* **134**, 324–36. Available at: <http://www.ncbi.nlm.nih.gov/pubmed/3350858>.
197. Baroffio, A., Bochaton-Piallat, M.L., Gabbiani, G., and Bader, C.R. (1995). Heterogeneity in the progeny of single human muscle satellite cells. *Differentiation* **59**, 259–268. Available at: http://www.ncbi.nlm.nih.gov/entrez/query.fcgi?cmd=Retrieve&db=PubMed&dopt=Citation&list_uids=8575648.
198. Qu, Z., Balkir, L., van Deutekom, J.C., Robbins, P.D., Pruchnic, R., and Huard, J. (1998). Development of approaches to improve cell survival in myoblast transfer therapy. *J. Cell Biol.* **142**, 1257–67. Available at: <http://www.pubmedcentral.nih.gov/articlerender.fcgi?artid=2149359&tool=pmcentrez&rendertype=abstract> [Accessed February 9, 2016].
199. Yoshida, N., Yoshida, S., Koishi, K., Masuda, K., and Nabeshima, Y. (1998). Cell heterogeneity upon myogenic differentiation: down-regulation of MyoD and Myf-5 generates “reserve cells”. *J. Cell Sci.* **111**, 769–779.
200. Kitzmann, M., Carnac, G., Vandromme, M., Primig, M., Lamb, N.J.C., and Fernandez, A. (1998). The Muscle Regulatory Factors MyoD and Myf-5 Undergo Distinct Cell Cycle-specific Expression in Muscle Cells. *J. Cell Biol.* **142**, 1447–1459. Available at: <http://www.ncbi.nlm.nih.gov/pubmed/9744876> [Accessed May 29, 2019].
201. Halevy, O., Piestun, Y., Allouh, M.Z., Rosser, B.W.C., Rinkevich, Y., Reshef, R., Rozenboim, I., Wleklinski-Lee, M., and Yablonka-Reuveni, Z. (2004). Pattern of Pax7 expression during myogenesis in the posthatch chicken establishes a model for satellite cell differentiation and renewal. *Dev. Dyn.* **231**, 489–502.
202. Baroffio, A., Hamann, M., Bernheim, L., Bochaton-Piallat, M.L., Gabbiani, G., and Bader, C.R. (1996). Identification of self-renewing myoblasts in the progeny of single human muscle satellite cells. *Differentiation*. **60**, 47–57. Available at: <http://www.ncbi.nlm.nih.gov/pubmed/8935928>.

203. Laumonier, T., Bermont, F., Hoffmeyer, P., Kindler, V., and Menetrey, J. (2017). Human myogenic reserve cells are quiescent stem cells that contribute to muscle regeneration after intramuscular transplantation in immunodeficient mice. *Sci. Rep.* 7, 3462. Available at: <http://www.ncbi.nlm.nih.gov/pubmed/28615691> [Accessed June 20, 2017].
204. Abou-Khalil, R., Le Grand, F., and Chazaud, B. (2013). Human and Murine Skeletal Muscle Reserve Cells. In *Methods in Molecular Biology* (Humana Press Inc.), pp. 165–177. Available at: http://link.springer.com/10.1007/978-1-62703-508-8_14 [Accessed April 21, 2020].
205. Bar-Nur, O., Gerli, M.F.M., Di Stefano, B., Almada, A.E., Galvin, A., Coffey, A., Huebner, A.J., Feige, P., Verheul, C., Cheung, P., et al. (2018). Direct Reprogramming of Mouse Fibroblasts into Functional Skeletal Muscle Progenitors. *Stem Cell Reports* 10, 1505–1521.
206. Low, S., Barnes, J.L., Zammit, P.S., and Beauchamp, J.R. (2018). Delta-Like 4 Activates Notch 3 to Regulate Self-Renewal in Skeletal Muscle Stem Cells. *Stem Cells* 36, 458–466. Available at: <http://doi.wiley.com/10.1002/stem.2757> [Accessed July 27, 2020].
207. Conboy, I.M., Conboy, M.J., Smythe, G.M., and Rando, T.A. (2003). Notch-mediated restoration of regenerative potential to aged muscle. *Science* 302, 1575–7. Available at: <http://www.sciencemag.org/cgi/doi/10.1126/science.1087573> [Accessed June 10, 2018].
208. Yaffe, D. (1968). Retention of differentiation potentialities during prolonged cultivation of myogenic cells. *Proc. Natl. Acad. Sci. U. S. A.* 61, 477–483. Available at: <https://www.pnas.org/content/61/2/477> [Accessed January 26, 2021].
209. Richler, C., and Yaffe, D. (1970). The in vitro cultivation and differentiation capacities of myogenic cell lines. *Dev. Biol.* 23, 1–22.
210. Rando, T.A., and Blau, H.M. (1994). Primary mouse myoblast purification, characterization, and transplantation for cell-mediated gene therapy. *J. Cell Biol.*
211. Sellathurai, J., Cheedipudi, S., Dhawan, J., and Schröder, H.D. (2013). A Novel In Vitro Model for Studying Quiescence and Activation of Primary Isolated Human Myoblasts. *PLoS One* 8, e64067. Available at: <https://dx.plos.org/10.1371/journal.pone.0064067> [Accessed April 21, 2020].
212. Charaïbeh, B., Lu, A., Tebbets, J., Zheng, B., Feduska, J., Crisan, M., Péault, B., Cummins, J., and Huard, J. (2008). Isolation of a slowly adhering cell fraction containing stem cells from murine skeletal muscle by the preplate technique. *Nat. Protoc.* 3, 1501–1509. Available at: <http://www.nature.com/doi/10.1038/nprot.2008.142> [Accessed September 25, 2017].
213. Qu-Petersen, Z., Deasy, B., Jankowski, R., Ikezawa, M., Cummins, J., Pruchnic, R., Mytinger, J., Cao, B., Gates, C., Wernig, A., et al. (2002). Identification of a novel population of muscle stem cells in mice: potential for muscle regeneration. *J. Cell Biol.* 157, 851–64. Available at: <http://www.ncbi.nlm.nih.gov/pubmed/12021255> [Accessed July 23, 2018].
214. Corti, M., Liberati, C., Smith, B.K., Lawson, L.A., Tuna, I.S., Conlon, T.J., Coleman, K.E., Islam, S., Herzog, R.W., Fuller, D.D., et al. (2017). Safety of Intradiaphragmatic Delivery of Adeno-Associated Virus-Mediated Alpha-glucosidase (rAAV1-CMV-hGAA) Gene Therapy in Children Affected by Pompe Disease. *Hum. Gene Ther. Clin. Dev.* 28, 208–218. Available at: <http://www.ncbi.nlm.nih.gov/pubmed/29160099> [Accessed March 15, 2019].
215. Feige, P., Brun, C.E., Ritso, M., and Rudnicki, M.A. (2018). Orienting Muscle Stem Cells for Regeneration in Homeostasis, Aging, and Disease. *Cell Stem Cell* 23, 653–664. Available at: <https://www.sciencedirect.com/science/article/pii/S1934590918304879?via%3Dihub> [Accessed January 31, 2019].

216. Thornell, L.E., Lindstöm, M., Renault, V., Klein, A., Mouly, V., Ansved, T., Butler-Browne, G., and Furling, D. (2009). Satellite cell dysfunction contributes to the progressive muscle atrophy in myotonic dystrophy type 1. *Neuropathol. Appl. Neurobiol.*
217. Capell, B.C., and Collins, F.S. (2006). Human laminopathies: nuclei gone genetically awry. *Nat. Rev. Genet.* 7, 940.
218. Schaaf, G.J., van Gestel, T.J.M., Brusse, E., Verdijk, R.M., de Coo, I.F.M., van Doorn, P.A., van der Ploeg, A.T., and Pijnappel, W.W.M.P. (2015). Lack of robust satellite cell activation and muscle regeneration during the progression of Pompe disease. *Acta Neuropathol. Commun.* 3, 65. Available at: <http://www.pubmedcentral.nih.gov/articlerender.fcgi?artid=4625612&tool=pmcentrez&rendertype=abstract> [Accessed November 11, 2015].
219. Schaaf, G.J., van Gestel, T.J.M., in 't Groen, S.L.M., de Jong, B., Boomaars, B., Tarallo, A., Cardone, M., Parenti, G., van der Ploeg, A.T., and Pijnappel, W.W.M.P. (2018). Satellite cells maintain regenerative capacity but fail to repair disease-associated muscle damage in mice with Pompe disease. *Acta Neuropathol. Commun.* 6, 119. Available at: <https://actaneurocomms.biomedcentral.com/articles/10.1186/s40478-018-0620-3> [Accessed November 22, 2018].
220. Schaaf, G.J., Canibano-Fraile, R., van Gestel, T.J.M., van der Ploeg, A.T., and Pijnappel, W.W.M.P. (2019). Restoring the regenerative balance in neuromuscular disorders: satellite cell activation as therapeutic target in Pompe disease. *Ann. Transl. Med.* 7, 280. Available at: <http://www.ncbi.nlm.nih.gov/pubmed/31392192> [Accessed August 28, 2019].



Chapter 2

Lysosomal glycogen accumulation in Pompe disease results in disturbed cytoplasmic glycogen metabolism

Rodrigo Canibano-Fraile^{1,2,3}, Laurike Harlaar^{3,4}, Carlos A. dos Santos^{1,2,3}, Marianne Hoogeveen-Westerveld¹, Jeroen A. A. Demmers⁵, Tim Snijders⁶, Philip Lijnzaad⁷, Robert M. Verdijk⁸, Nadine A. M. E. van der Beek^{3,4}, Pieter A. van Doorn^{3,4}, Ans T. van der Ploeg^{2,3}, Esther Brusse^{3,4}, W. W. M. Pim Pijnappel^{1,2,3,*}, Gerben J. Schaaf^{1,2,3,*}

¹Department of Clinical Genetics, Erasmus MC University Medical Center, 3015 GE Rotterdam, Netherlands

²Department of Pediatrics, Erasmus MC University Medical Center, 3015 GE Rotterdam, Netherlands

³Center for Lysosomal and Metabolic Diseases, Erasmus MC University Medical Center, 3015 GE Rotterdam, Netherlands

⁴Department of Neurology, Erasmus MC University Medical Center, 3015 GE Rotterdam, Netherlands

⁵Erasmus Center for Biomics, Erasmus MC University Medical Center, 3000 CA Rotterdam, Netherlands

⁶Department of Human Biology, NUTRIM School of Nutrition and Translational Research in Metabolism, Maastricht University Medical Center+, Maastricht, Netherlands

⁷Princess Máxima Center for Pediatric Oncology, Heidelberglaan 25, 3584 CS, Utrecht, Netherlands

⁸Department of Pathology, Section Neuropathology, Erasmus MC University Medical Center, 3015 GE Rotterdam, Netherlands

*Correspondence: g.schaaf@erasmusmc.nl; w.pijnappel@erasmusmc.nl

Submitted to *Journal of Inherited Metabolic Disease*.

Abstract

Pompe disease is an inherited metabolic myopathy caused by deficiency of acid α -glucosidase (GAA), resulting in lysosomal glycogen accumulation. Residual GAA enzyme activity affects disease onset and severity, although other factors, including dysregulation of cytoplasmic glycogen metabolism, are suspected to modulate the disease course. In this study, performed in mice and patients, we found elevated protein levels of enzymes involved in glucose uptake and cytoplasmic glycogen synthesis in skeletal muscle from mice with Pompe disease, including glycogenin (GYG1), glycogen synthase (GS), glucose transporter 4 (GLUT4), glycogen branching enzyme (GBE1), and UDP-glucose pyrophosphorylase (UGP2). Expression levels were elevated before the loss of muscle mass and function. Quantitative mass spectrometry in skeletal muscle biopsies from five adult patients with Pompe disease showed increased expression of glycogen branching enzyme protein relative to healthy controls at the group level. Paired analysis of individual patients who responded well to treatment with enzyme replacement therapy (ERT) showed reduction of glycogen synthase, glycogenin, and glycogen branching enzyme 1 in all patients after start of ERT compared to baseline. These results indicate that metabolic changes precede muscle wasting in Pompe disease, and imply a positive feedforward loop in Pompe disease, in which lysosomal glycogen accumulation promotes cytoplasmic glycogen synthesis and glucose uptake, resulting in aggravation of the disease phenotype.

Keywords:

Skeletal muscle, lysosomal storage disorder, metabolic myopathy, Pompe disease, glycogen metabolism.

Highlights

- Elevated levels of enzymes involved in glycogen biosynthesis in tissue of Pompe disease mice.
- Expression levels in mice were increased before loss of muscle mass and function.
- GBE1 protein expression was elevated in muscle biopsies from Pompe disease patients compared to healthy controls
- GS, GYG1, and GBE1 protein expression was reduced in muscle biopsies from patients in response to ERT

List of abbreviations:

BR: brain

DP: diaphragm

ERT: enzyme replacement therapy

GAA: acid α -glucosidase

GBE1: glycogen branching enzyme

GLUT4: glucose transporter 4

GMA: glycolmethacrylate

GS: glycogen synthase

GSD: glycogen storage disorder

GYG1: glycogenin

GYS1: glycogen synthase (muscle isoform)

HHD: hand-held dynamometry

HRT: heart

IVS1: c.-32-13T>G disease associated variant

MRC: Medical Research Council

MS: mass spectrometry

QF: *quadriceps femoris*

UGP2: UDP-glucose pyrophosphorylase

Introduction

Glycogen biosynthesis is largely dependent on: 1) glucose entry into the cell, and 2) the action of glycogen biosynthetic and degradative enzymes. While most glycogen is stored in the cytoplasm, part of it is located inside lysosomes. Degradation of glycogen in the cytoplasm takes place via degradative enzymes, while in the lysosomes it is hydrolyzed by GAA under acidic conditions. Glycogen metabolism is therefore the result of a delicate balance between biosynthesis and degradation, which is disturbed in glycogen storage disorders (GSDs).

Pompe disease is a rare metabolic myopathy characterized by acid α -glucosidase deficiency caused by disease-associated variants in the *GAA* gene. As a consequence, glycogen cannot be degraded and accumulates in the lysosomes [1–3]. In the most severe classic infantile form of Pompe disease, *GAA* enzyme activity is virtually absent and symptoms manifest shortly after birth, consisting of generalized skeletal muscle weakness and a hypertrophic cardiomyopathy. In patients with symptom onset at childhood or adulthood (late-onset patients), a more slowly progressive skeletal muscle weakness develops resulting in impaired motor and respiratory function that can lead to wheelchair and ventilator dependency at any age [2,4]. Since 2006 enzyme replacement therapy (ERT) using α -glucosidase alfa (Lumizyme/Myozyme, Sanofi Genzyme) is available for Pompe disease. ERT improves survival of classic infantile patients and largely normalizes hypertrophic cardiomyopathy [8–11] and improves muscle strength and stabilize respiratory function in patients with onset at childhood or adulthood, albeit with considerable inter-individual variability in treatment response [5,6].

Previous studies found a number of enzymes involved in cytoplasmic glycogen metabolism that are dysregulated in a mouse model of Pompe disease. Surprisingly, the effect of this dysregulation suggested increased cytoplasmic glycogen levels in Pompe disease, increasing the availability of substrate for lysosomal glycogen and generating a predicted positive feed forward loop for cellular glycogen accumulation [7,8]. Treatment of mice with ERT resulted in reversal of the levels of these enzymes [8]. A multi-center study found extra-lysosomal glycogen accumulation in muscle biopsies from late-onset patients [9], in agreement with the predicted feed forward loop [8]. Notably, extra-lysosomal glycogen accumulation was not cleared by ERT [9], consistent with the optimal enzymatic activity of recombinant human *GAA* used in ERT to degrade glycogen at an acidic pH that is found in lysosomes but not in the cytoplasm.

In this study, we extended these observations in a mouse model of Pompe disease with a different genetic background. We included skeletal muscles, heart, and brain, and determined the timing of metabolic changes relative to the development of muscle wasting. In addition, we identified additional enzymes involved in glycogen metabolism to be dysregulated in mice with Pompe disease. Disturbances were found mainly in skeletal muscle, although heart or brain were also affected. Interestingly, dysregulated glycogen metabolism was detected before loss of muscle function, suggesting that metabolic changes precede the onset of muscle loss. We analyzed skeletal muscle biopsies from 5 mildly affected patients with symptom onset at adulthood that were treated with ERT. We found large variability between patients in expression of enzymes involved in glycogen metabolism. Comparison of individual patients before and after start of ERT indicated a downregulation of candidate enzymes involved in cytoplasmic glycogen metabolism, suggesting that Pompe disease in humans may disturb cytoplasmic glycogen metabolism, and that ERT could reverse this dysregulation.

Results

Cytoplasmic glycogen metabolism in *Gaa*^{-/-} mice

Glycogenin is encoded by the *Gygl* gene. It participates in the initiation stage of glycogen synthesis acting as a primer to form glycogen (Figure 1A) [10,11]. Western blot analysis indicated a >2-fold upregulation of GYG1 levels in quadriceps and diaphragm, and a slight (1.3-fold) upregulation in brain of 34-week old *Gaa*^{-/-} mice (a time point at which Pompe disease induced muscle weakness is evident as measured with histochemical and functional analyses [18]), whereas no significant difference was detected in heart (Figure 1 B-E).

GYS1 is the isoform of glycogen synthase (GS) expressed in skeletal muscle and other tissues, and takes part in the elongation stage of glycogen biosynthesis (Figure 1A) [12,13]. No significant differences in GS expression were observed in quadriceps, heart, and diaphragm between age-matched WT and *Gaa*^{-/-} animals (Figure 1F-H). GS was not detected in the brain (data not shown).

GLUT4 mediates glucose uptake into skeletal muscle (Figure 1A) [14,15]. GLUT4 levels were found to be upregulated >2 fold in quadriceps of *Gaa*^{-/-} mice compared to WT. There were no differences in GLUT4 levels between *Gaa*^{-/-} and WT mice in heart, diaphragm, and brain tissues (Figure 1I-L).

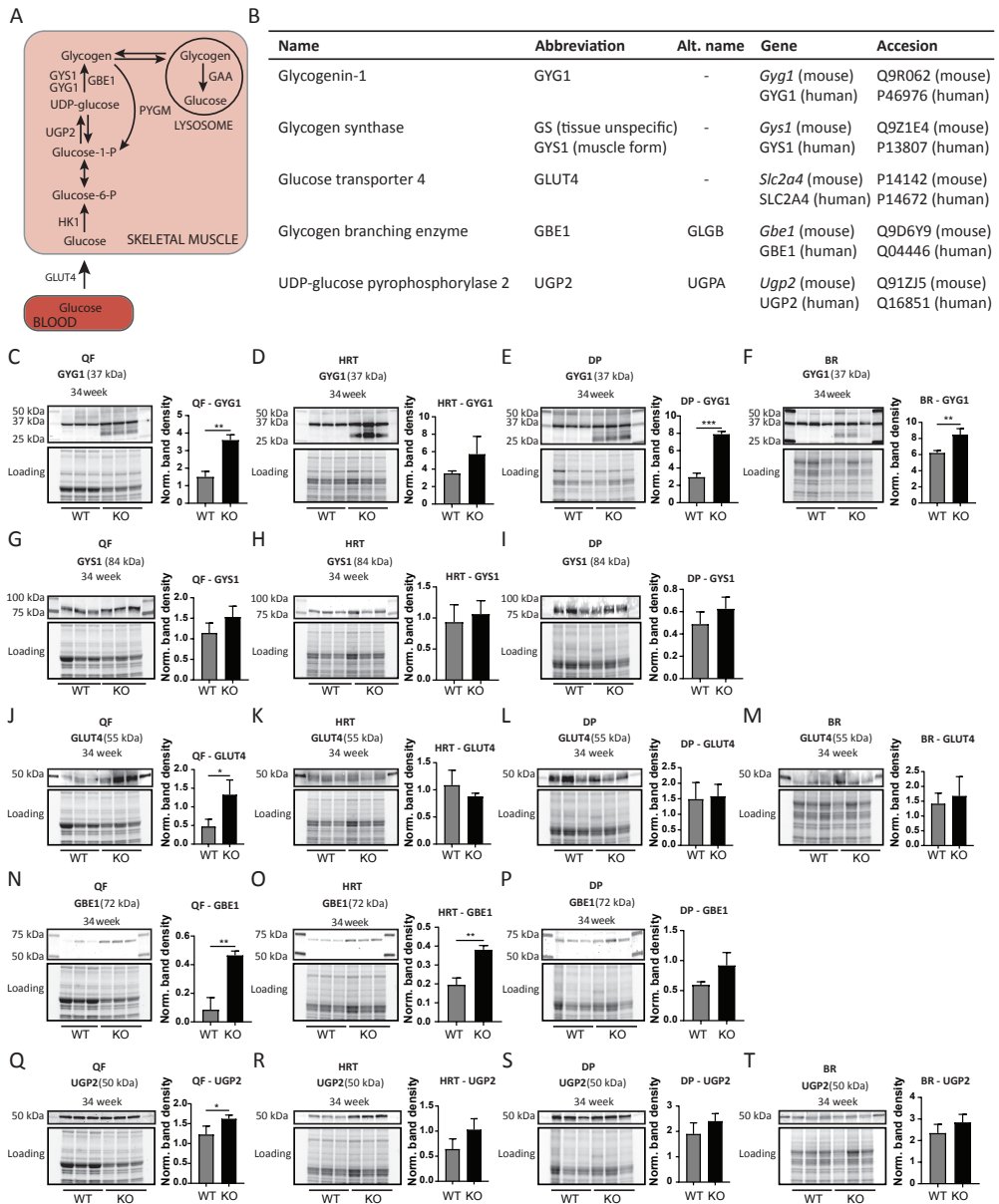


Figure 1. Expression of glycogen metabolizing enzymes in skeletal muscles, heart, and brain of adult *Gaa*^{-/-} mice. (A) Diagram representing metabolic steps and enzymes involved in glycogen biosynthesis in skeletal muscle. (B) Summary of the nomenclature and accession numbers of the enzymes used in this study. (C-F) Western Blot analyses and quantification of GYG1 in WT and *Gaa*^{-/-} mice at 34 weeks in QF, HRT, DP, and BR lysates respectively. To quantify GYG1 levels, all bands between 50 and 30 kDa were used, as GYG1 is known to have a heterogeneous molecular weight due to its association to glycogen [8]. Values from three independent mice were normalized to total protein and averaged. Data are shown as mean \pm SE. *n*=3. ***p*≤0.01; ****p*≤0.001. (G-J) Western Blot analyses and quantification of GS in WT and *Gaa*^{-/-} mice at 34 weeks in QF, HRT, and DP lysates respectively. Values from three independent mice were normalized to total protein and averaged. Data are shown as mean \pm SE. *n*=3. (K-M) Western Blot analyses and quantification of GLUT4 in WT and *Gaa*^{-/-} mice at 34 weeks in QF, HRT, DP, and BR lysates respectively. Values from three independent mice were normalized to total protein and averaged. Data are shown as mean \pm SE. *n*=3. **p*≤0.05. (N-P) Western Blot analyses and quantification of GBE1 in WT and *Gaa*^{-/-} mice at 34 weeks in QF, HRT, and DP lysates respectively. Values from three independent mice were normalized to total protein and averaged. Data are shown as mean \pm SE. *n*=3. ***p*≤0.01. (Q-T) Western Blot analyses and quantification of UGP2 in WT and *Gaa*^{-/-} mice at 34 weeks in QF, HRT, DP, and BR lysates respectively. Values from three independent mice were normalized to total protein and averaged. Data are shown as mean \pm SE. *n*=3. **p*≤0.05

Glycogen-branching enzyme is encoded by the *Gbe1* gene. GBE1 enables the generation of branches during glycogen biosynthesis (Figure 1A) [16]. GBE1 was expressed at significantly increased levels in *Gaa*^{-/-} quadriceps (>4-fold) and heart (~2-fold) compared to WT. Slightly increased GBE1 levels were observed in *Gaa*^{-/-} diaphragm although this was not statistically different (Figure 1M-O). GBE1 was not detected in brain tissue (data not shown). GBE1 enzyme activity was also increased in *Gaa*^{-/-} quadriceps and heart (Supplementary Figure 2). Interestingly, GBE1 activity was also significantly increased in *Gaa*^{-/-} diaphragm compared to WT (Supplementary Figure 2), despite similar GBE1 protein levels between *Gaa*^{-/-} and wild type mice (Figure 1O).

UDP-glucose pyrophosphorylase (UGP2) catalyzes the conversion of glucose-1-phosphate to UDP-glucose (Figure 1A) [17]. UGP2 levels were slightly (~1.3 fold) but significantly upregulated in quadriceps of *Gaa*^{-/-} mice, whereas its levels were unchanged in *Gaa*^{-/-} heart, diaphragm, and brain tissues (Figure 1P-S).

Together, these results indicate that protein expression of enzymes involved in glycogen synthesis/glucose uptake including GYG1, GLUT4, GBE1, and UGP2 but not GS is upregulated in selected skeletal muscles in adult mice with Pompe disease-induced loss of muscle mass and function.

Timing of disturbed cytoplasmic glycogen metabolism in *Gaa*^{-/-} mice

We previously reported that loss of muscle mass and function in *Gaa*^{-/-} mice (FVB/N) start between 15 and 25 weeks of age [18]. To determine the timing of metabolic changes relative to the development of functional changes, we analyzed expression of the above enzymes in quadriceps and heart of mice before onset (at 10 weeks) and during advanced muscle loss (at 60 weeks).

Western blot analysis of GYG1 in quadriceps revealed increased expression in *Gaa*^{-/-} versus WT mice at both 10 (7-fold) and 60 weeks (~4.8 fold) of age. In addition, GYG1 expression increased with age in both wild type and *Gaa*^{-/-} mice (Figure 2A). In the heart, GYG1 expression was elevated in *Gaa*^{-/-} mice at 10 weeks (>5-fold) but not significantly at 60 weeks (Figure 2B). GS levels were unchanged in *Gaa*^{-/-} quadriceps at 10 weeks, but were increased 1.5-fold in *Gaa*^{-/-} quadriceps at 60 weeks (Figure 2C). GS levels were equal in heart of both genotypes and at both ages (Figure 2D). GLUT4 expression was similarly low in quadriceps muscles for both genotypes at 10 weeks, while at 60 weeks the levels were increased 3-fold in *Gaa*^{-/-} mice compared to WT mice (Figure 2E). In heart, there was no difference between *Gaa*^{-/-} and WT mice at any age (Figure 2F). GBE1 levels in *Gaa*^{-/-} quadriceps were upregulated ~4-fold compared to WT at both 10 weeks and 60 weeks (Figure 2G). GBE1 differences in heart were similar at both ages between both genotypes (Figure 2H). UGP2 levels were increased 2-fold at 10 weeks, but not at 60 weeks, in quadriceps of *Gaa*^{-/-} mice compared to age-matched WT counterparts (Figure 2I). In heart, UGP2 levels were similar between WT and *Gaa*^{-/-} mice at both ages (Figure 2J).

Taken together, in *Gaa*^{-/-} quadriceps, UGP2 was strongly upregulated at 10 weeks of age, before onset of loss of muscle function, while this upregulation attenuated with progression of pathology at 34 and 60 weeks; GYS1 and GLUT4 were upregulated at 34 and/or 60 weeks but not at 10 weeks; and GBE1 expression was upregulated at all ages analyzed. Results of this and previous studies were summarized in Table 2.

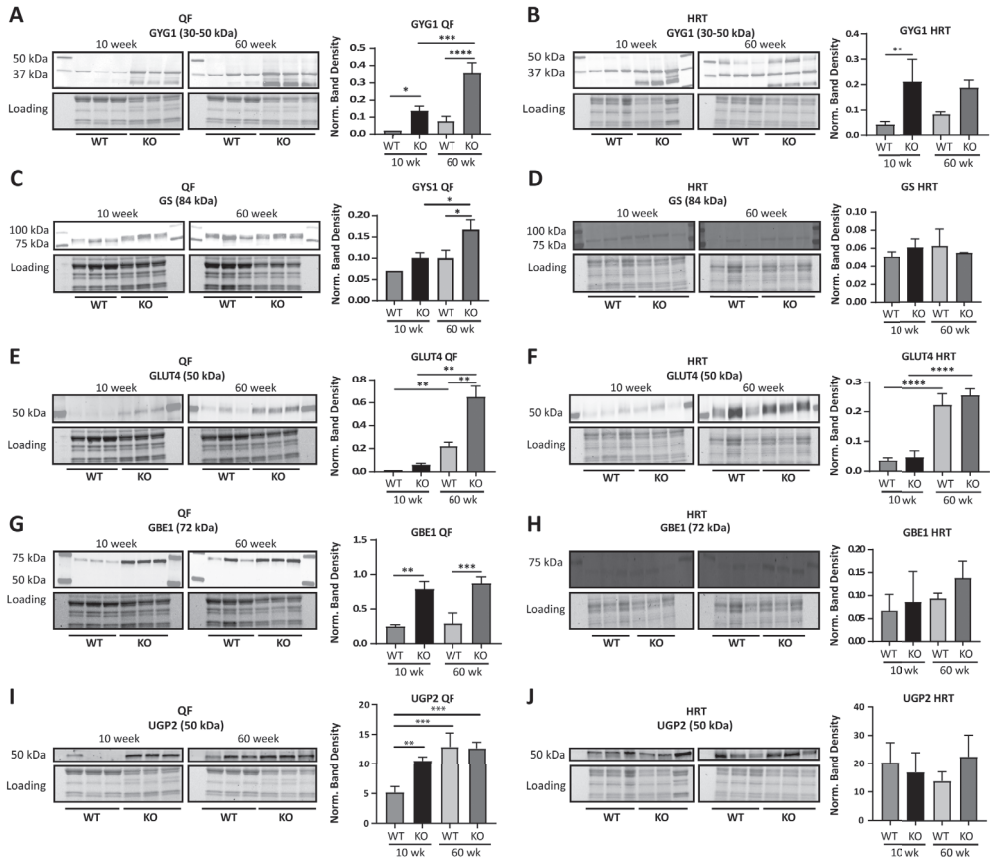


Figure 2. Timing of disturbed expression of glycogen metabolizing enzymes in *Gaa*^{-/-} mice.

(A-B) Western blot analyses and quantification of GYG1 in WT and *Gaa*^{-/-} mice at 10 and 60 weeks in QF and HRT respectively. To quantify GYG1 levels, all bands between 50 and 30 kDa were used. (C-D) Western blot analyses and quantification of GS in WT and *Gaa*^{-/-} mice at 10 and 60 weeks in QF and HRT respectively. (E-F) Western blot analyses and quantification of GLUT4 in WT and *Gaa*^{-/-} mice at 10 and 60 weeks in QF and HRT respectively.

(G-H) Western blot analyses and quantification of GBE1 in WT and *Gaa*^{-/-} mice at 10 and 60 weeks in QF and HRT respectively. (I-J) Western blot analyses and quantification of UGP2 in WT and *Gaa*^{-/-} mice at 10 and 60 weeks in QF and HRT respectively. In all quantifications values from three independent mice were normalized to total protein and averaged. Data are shown as mean \pm SE. $n=3$. * $p \leq 0.05$; ** $p \leq 0.01$; *** $p \leq 0.001$; **** $p \leq 0.0001$.

Study	Species/Tissues	ERT	GYGI	GS	GLUT4	GBE1	UGP2	PYGM	HK1	pGS	G6P
Orth and Mundegar, 2003	Human	Not disclosed	-	-	in Pompe	-	-	-	-	-	-
Douillard-Guilloux et al., 2009	Mouse	Heart	-	Genetic inactivation of Cys7 in a <i>Gaa</i> ^{-/-} mice rescued muscle function	-	-	-	-	-	-	-
	Heart	No	-	-	-	-	-	-	-	-	-
	Gastrocnemius	-	-	-	-	-	-	-	-	-	-
	Tibialis anterior	-	-	-	in <i>Gaa</i> ^{-/-}	-	-	-	-	-	-
	Soleus	-	-	-	Normalized in <i>Cys7</i> ^{+/+} <i>Gaa</i> ^{-/-}	-	-	-	-	-	-
	EDL	-	-	-	-	-	-	-	-	-	-
Taylor et al., 2013	Mouse	Heart	-	in <i>Gaa</i> ^{-/-} Normalized after ERT	-	-	-	-	in <i>Gaa</i> ^{-/-} Normalized after ERT	in <i>Gaa</i> ^{-/-} Normalized after ERT	in <i>Gaa</i> ^{-/-} Normalized after ERT
	Triceps	-	in <i>Gaa</i> ^{-/-} Normalized after ERT	in <i>Gaa</i> ^{-/-} Normalized after ERT	-	-	-	Active form - in <i>Gaa</i> ^{-/-}	in <i>Gaa</i> ^{-/-} Normalized after ERT	in <i>Gaa</i> ^{-/-} Normalized after ERT	in <i>Gaa</i> ^{-/-} Normalized after ERT
	Quadriceps	-	-	in <i>Gaa</i> ^{-/-}	-	-	-	-	-	in <i>Gaa</i> ^{-/-}	-
	Liver	-	-	-	-	-	-	-	-	-	-
Baligand et al., 2017	Mouse	Gastrocnemius	-	-	-	-	-	-	-	-	in <i>Gaa</i> ^{-/-} Normalized after rAAV-GAA (intramuscular)
	Mouse	Gastrocnemius	-	-	in <i>Gaa</i> ^{-/-} Normalized after ERT	-	UDP-glucose, (product of UGP2) in <i>Gaa</i> ^{-/-}	-	-	in <i>Gaa</i> ^{-/-} Normalized after ERT	in <i>Gaa</i> ^{-/-} Normalized after rAAV-GAA
Meena et al., 2020	Mouse	Gastrocnemius	-	-	-	-	-	-	-	-	in <i>Gaa</i> ^{-/-} Normalized after ERT

Study	Species/Tissues	ERT	GYG1	CS	GLUT4	GBE1	UGP2	PYGM	HK1	pCS	G6P
This study	Quadriceps	No	in <i>Gaa</i> ^{-/-}	in <i>Gaa</i> ^{-/-}	in <i>Gaa</i> ^{-/-}	in <i>Gaa</i> ^{-/-}	in <i>Gaa</i> ^{-/-}	-	-	-	-
	Mouse Diaphragm		in <i>Gaa</i> ^{-/-}	= in <i>Gaa</i> ^{-/-} and WT	-	-	-	-			
	Heart		in <i>Gaa</i> ^{-/-}	= in <i>Gaa</i> ^{-/-} and WT	-	-	-	-			
	Brain		in <i>Gaa</i> ^{-/-}	-	= in <i>Gaa</i> ^{-/-} and WT	-	= in <i>Gaa</i> ^{-/-} and WT	-	-	-	-
Human Quadriceps	Yes	Reduced after ERT *	Reduced after ERT *	-	in Pompe Normalized after ERT *	in Pompe Normalized after ERT *	= in Healthy and Pompe	-	-	-	-
							= in Baseline and ERT				

Table 2. Overview of in vivo studies evaluating glycogen metabolism in Pompe disease. * Reduction in protein levels after paired analysis of each patient before and after ERT

Cytoplasmic glycogen metabolism in human patients

To assess whether these findings observed in *Gaa^{-/-}* mice could be extended to human patients with Pompe disease, we analyzed muscle biopsies from patients who were mildly affected at baseline and who showed a positive response to ERT within 2-3 years after start of treatment. The reasons for this selection were 1) that it would most resemble the phenotype in the *Gaa^{-/-}* mice, which develop a muscle phenotype at adulthood; 2) that biopsies with a very strong muscle pathology would have excessive loss of muscle tissue and possibly replacement with fat. Age-matched healthy control biopsies were included in the analysis. To this end, biopsies taken from the vastus lateralis of late-onset compound heterozygous c.-32-13T>G (IVS1) patients (i.e. that carry the IVS1 variant on 1 allele and a disease-associated *GAA* variant on the 2nd allele) were selected (Table 3).

	Pompe	Control
Gender		
Male	20%	50%
Female	80%	50%
Age		
≤49	20%	0%
50-80	80%	83%
≥81	0%	17%
Follow-up (months)		
20-30	60%	N/A
31-36	40%	N/A
Reduced muscle function (MRC score)		
75-80%	40%	N/A
≥81%	60%	N/A

Table 3. Distribution and characteristics of patient and control groups

Histopathological changes were analyzed using HE- and PAS- stained muscle sections from patients at baseline as well as after start of ERT (Figure 3A). This revealed in patients at baseline the presence of vacuolar myopathy, alterations in fiber size and structure, disruption of cross striation, lysosomal enlargement, increased presence of round-shaped glycogen-filled lysosomes, and fat tissue replacement (Supplementary Figure 3). These parameters were scored as described in Table 4. On average all patients scored higher for disruption of cross-striation at baseline (1.5

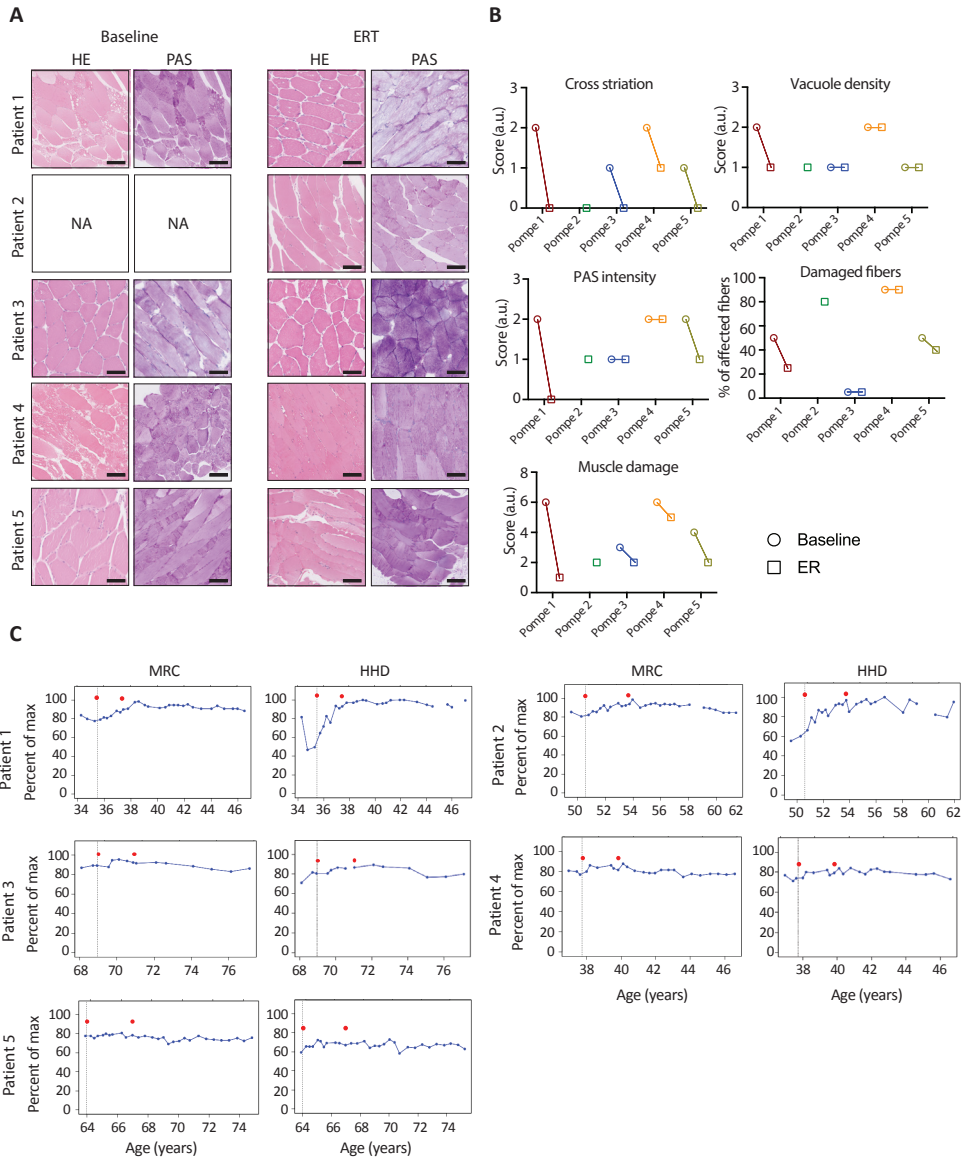


Figure 3. Histopathological and clinical evaluation of patient analyzed in this study.

(A) H&E and PAS staining of biopsies from QF in patients at baseline and after start of ERT treatment. Scale bars 100 μ m. (B) Quantification of histological parameters by 2 independent researchers to assess muscle damage. HE and PAS stainings of patients at baseline and after start of ERT were used. * Baseline image of Patient 2 (Pompe 2) at baseline was not available. (C) MRC and HHD scores of patients. Percentage of maximum force is represented in Y-axis. Age in years is represented in X-axis. Black vertical lines with a red dot indicate the start of ERT. The second red dot indicates the time of the follow-up biopsy.

± 0.6) compared to ERT treatment (0.2 ± 0.4), indicating a recovery of cross-striation after start of ERT treatment (Figure 3B). The intensity of PAS staining was overall reduced after start of ERT compared to that at baseline (1.8 ± 0.5 at baseline vs. 1 ± 0.7 at ERT) (Figure 3B). There were no changes in vacuolar density (1.5 ± 0.6 vs 1.2 ± 0.4) or the percentage of affected fibers before and after start of ERT, except for patient 1, who showed a reduction of damaged fibers after start of ERT treatment (Figure 3B). Muscle damage was calculated as the sum of all scores for each patient at baseline and after start of ERT, with higher scores indicating increased muscle damage. Overall, all patients analyzed scored lower for total muscle damage after treatment with ERT (4.8 ± 1.5 at baseline vs. 2.4 ± 1.5 at ERT) (Figure 3B). All patients showed improvement or stabilization of muscle function. MRC sum-scores at baseline were on average $80.8\% \pm 4.7$, and this value was increased to $86.8\% \pm 6.5$ upon treatment with ERT (Figure 3C). For HHD sum-score baseline values were at $66.8\% \pm 10.5$, which were increased to 84.8 ± 13 after start of ERT (Figure 3C).

Score	Cross striation	PAS intensity	Vacuolization
0	Normal	None	None
1	$\geq 75\%$ normal	Little in most or all	Little in all and/or significant in some
2	25-75% normal	Significant in all and strong in some; significant or strong in most	Significant in all and/or many in some
3	$\leq 25\%$ normal	Very strong in all	Many in all

Table 4. Muscle damage scoring system based on tissue pathology

Expression of metabolic proteins in patient and healthy control biopsies was assessed using quantitative mass spectrometry (MS) employing TMT labelling followed by LC-MS/MS. Out of the 5 human orthologs of the mouse proteins studied here, 4 (GYS1, GBE1, GYG1, and UGP2) reached significant expression levels to be detected by mass spectrometry, leaving GLUT4 undetected. Considerable differences between individual expression levels of these proteins were found in both healthy controls and patients that ranged up to 3-fold (Figure 4). The average expression levels of GYS1, GBE1, GYG1, and UGP2 were not statistically different between patients at baseline and healthy controls. However, paired analysis of baseline vs ERT-treated for each individual patient indicated that all patients downregulated GYS1 (FC 0.78 ± 0.2), GBE1 (FC 0.8 ± 0.05), and GYG1 (0.76 ± 0.29), and all but one patient downregulated UGP2 (FC 0.9 ± 0.21) in response to ERT.

This suggests that expression of human GYS1, GBE1, GYG1, and UGP2, all of which are involved in cytoplasmic glycogen biosynthesis, is responsive to ERT in skeletal muscle of late-onset Pompe disease patients.

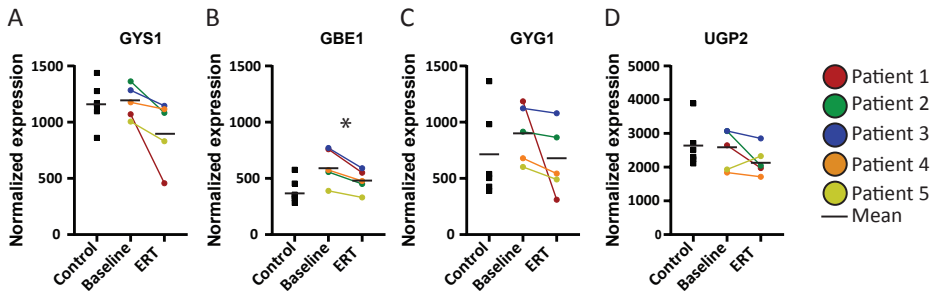


Figure 4. Quantitative mass spectrometry analysis of muscle biopsies from Pompe disease patients.

(A-D) Normalized expression of GYS1, GBE1, GYG1, and UGP2 in Controls, Baseline, and ERT groups. Horizontal bars represent the mean for each group. * $q=0.15$.

Discussion

In the present study, we extended previous observations indicating that cytoplasmic glycogen metabolism is altered in Pompe disease towards increased glycogen biosynthesis in skeletal muscle of *Gaa*^{-/-} mice. These effects were less pronounced in heart and brain of *Gaa*^{-/-} mice. We found differential regulation of glycogen synthesis and glucose transport enzymes depending on the onset of functional changes in the muscle of mice. UGP2 was preferentially upregulated before the loss of muscle mass and function, GYG1, GLUT4, and GBE1 during progression of loss of muscle function, and GS only when muscle loss was already advanced. In human patients that responded well to ERT, 4 enzymes involved in glycogen synthesis (GYS, GBE1, GYG1, and UGP2) were found here to be downregulated upon ERT treatment in skeletal muscle biopsies, suggesting that cytoplasmic glycogen metabolism is sensitive to ERT treatment, similarly to mouse models.

Previous work found dysregulation of enzymes involved in glucose metabolism and/or transport (see Table 2 for an overview). In a publication from Taylor et al, 16-week old mice were used in the Bl6/129 mixed background [8]. The same mouse model has been analyzed more recently by Meena et al. GYS levels were strongly elevated in *Gaa*^{-/-} triceps and quadriceps in Taylor et al., but not in *Gaa*^{-/-} quadriceps in Meena et al., and also not in *Gaa*^{-/-} quadriceps in our study at 10 and 34 weeks, but was elevated in *Gaa*^{-/-} quadriceps in our study at 60 weeks of age [8,19]. This

may indicate that the genetic background may influence the timing by which GS expression is elevated in muscle of *Gaa*^{-/-} mice. GYG1 was strongly elevated in triceps in Taylor's study, as well as in our study in quadriceps femoris at all ages analyzed. Dysregulation of GLUT4 has also been found in tibialis anterior muscle of *Gaa*^{-/-} (B16/129) mice by Douillard-Guilloux et al., and in human skeletal muscle biopsies from late-onset patients by Orth and Mundegar [7,20]. Other evidence for dysregulated cytoplasmic glycogen metabolism in *Gaa*^{-/-} (B16/129) mice includes elevated activity of hexokinase and its activator glucose-6-phosphate in triceps and heart, reduced levels of phosphorylase-b (which degrades cytoplasmic glycogen at high AMP concentrations), and increased levels of UDP-glucose [8,19]. In addition, ERT has been shown to revert dysregulation of GS, hexokinase, and glucose 6-phosphate levels in skeletal muscles of *Gaa*^{-/-} mice [8]. The current study complements these previous observations by establishing that glycogen metabolism is dysregulated early during disease progression predominantly in limb skeletal muscle and to a lesser extent in heart, diaphragm and brain.

In the present study two new enzymes were identified that showed dysregulated expression in skeletal muscle of *Gaa*^{-/-} mice, GBE1 and UGP2. Together with GS and GYG1, GBE1 regulates the last step of glycogen biosynthesis. GYG1 functions as a protein primer that initiates glycogen synthesis, GS elongates the growing chains, and GBE1 inserts side chains to branch the glycogen molecule [16]. All these enzymes were upregulated in skeletal muscle of Pompe disease mice, suggesting enhanced cytoplasmic glycogen build-up, as reported previously [9]. In addition to increasing glycogen levels, GBE1 may affect the structure of glycogen. It is known that reduced levels of GBE1, as observed in glycogen storage disorder IV (Andersen disease), alters the structure of glycogen, affecting its solubility and resulting in accumulation of insoluble glycogen [21,22].

The increased levels of UGP2 would also promote glycogen synthesis. UGP2 is the only enzyme that catalyzes the conversion of glucose-1-phosphate to UDP-glucose [23]. The importance of correct UGP2 expression for the regulation of glycogen metabolism was recently highlighted by study reporting the development of a severe epileptic encephalopathy due to loss of UGP2 in the brain [17]. Insufficient UDP-glucose levels in the brain compromised the synthesis of glycogen in these patients. Furthermore, UDP-glucose is crucial for the synthesis of glycolipids, glycoproteins, and proteoglycans indicating that the dysregulation of UGP2 may affect biological processes other than glycogen metabolism as well [24].

The *Gaa^{-/-}* (FVB/N) mouse model that was used for this study starts to accumulate biochemically detectable glycogen in tibialis anterior at least at 2 weeks of age [18,27]. Previous studies show that the lysosomal muscle phenotype developed between 15 and 25 weeks in GAAKO mice. GYG1, GBE1, and UGP2 were already upregulated in quadriceps muscle at 10 weeks of age in the present study. This indicates that a subset of enzymes involved in cytoplasmic glycogen metabolism is already dysregulated at the onset of loss of muscle mass and function in skeletal muscle of *Gaa^{-/-}* mice. It remains to be determined to what extent cytoplasmic glycogen levels are elevated in *Gaa^{-/-}* mice, and what their possible contribution to the Pompe disease phenotype is. The experiments in the present study indicate that cytoplasmic glycogen metabolism continues to increase during disease progression. This might contribute to the Pompe disease phenotype in two ways: 1) by increasing the availability of glycogen substrate for entry into the lysosomes; 2) by causing cytoplasmic glycogen accumulation. Indeed it has been demonstrated that glycogen synthesized in the cytoplasm can be taken up in the lysosomes by autophagy, in a process termed glyco-phagy [28]. Further support for this mechanism has been obtained by Douillard-Guilloux who showed that inhibition of cytoplasmic glycogen synthesis by knock down or knock out of GYS1 in a mouse model of Pompe disease results in reduced lysosomal glycogen accumulation [7]. Cytoplasmic glycogen accumulation in human muscle biopsies from late-onset patients with Pompe disease has been reported previously [9].

This study has identified for the first time that the cytoplasmic glycogen metabolizing enzymes GYG1, GYS, GBE1, UPG2 are dysregulated in human patients with Pompe disease. The analyses pointed towards large individual variation in gene expression, as noted before. This remains an obstacle for the study of human phenotypes using patient-derived material. Paired analyses, in which samples before and after treatment are compared per patient may help to minimize individual variation caused by differences in genetic backgrounds. In the current study, ERT was able to decrease the expression levels of GYG1, GYS, GBE1, UPG2 in all patients (except patient 5 for UGP2). The patients that were selected for this study had a mild muscle phenotype, and also responded well to ERT treatment within 1-3 years. This suggests that mild changes in cytoplasmic glycogen metabolism in human patients are reversible. We speculate that the effect of ERT on cytoplasmic glycogen metabolism is indirect by decreasing lysosomal glycogen levels, although we did not explore the mechanism involved. It is unlikely that recombinant human GAA used in ERT acts directly on cytoplasmic glycogen, as it is only active at acidic

pH in lysosomes. When muscle pathology has advanced beyond a certain stage, it might be difficult or impossible to revert cytoplasmic build up [9]. This study was limited by the small sample size of patient biopsies. Future studies should investigate a larger cohort of patients, including good and poor responders to ERT. Remaining questions include: how is cytoplasmic glycogen metabolism affected in classic infantile and severely affected late-onset patients, and what is the effect of ERT treatment on glycogen metabolism in these patients?

Methods

Collection of mouse tissue

Mice were sacrificed by cervical dislocation according to institutional regulations. Quadriceps femoris (QF), heart (HRT), diaphragm (DP), and brain (BR) tissue was obtained from wild type FVB/N (Envigo, the Netherlands) and *Gaa*^{-/-} (in the FVB/N background) animals at 10, 34, and 60 weeks [18,27]. Animals were housed at the Erasmus MC Animal Facility under a light-dark cycle of 12 hours and with access to food and water *ad libitum*.

Tissue handling

Mouse tissues were dissected and flash-frozen in liquid nitrogen-cooled isopentane (Honeywell, Germany). All samples were stored at -80°C until analysis. To obtain tissue lysates, dissected tissues were kept at -20°C and cut with a cooled scalpel (Swann-Morton). Tissues were then transferred to 2 mL round-bottom Safe-Lock Eppendorf tubes (Eppendorf AG, Hamburg, Germany) and stored at -80°C until generation of lysates.

Muscle biopsies and patient selection

Muscle biopsies were taken from *vastus lateralis* from patients and controls using a standard open surgery or needle biopsy procedure as described previously [29]. Selected patients were diagnosed with Pompe disease with confirmed GAA enzyme deficiency and had symptom onset at adulthood. All patients carried the c.32-13T>G (IVS1) variant on one allele and a disease-associated variant on the other. Patients showed disease-associated histological changes in muscle biopsies and reduced scores on clinical assessments regarding muscle function and strength at baseline.

Histological features in patients' muscle biopsies – as evaluated (see below) by two researchers, including an experienced neuropathologist – included increased vacuolization, increased PAS-positive staining, cross-striation, and a reduced number of healthy fibers. Skeletal muscle strength was measured using the Medical Research Council (MRC) grading scale and by hand-held dynamometry (HHD, Cytec dynamometer, Groningen, the Netherlands) [30]. The following muscle groups were tested for either method: neck extensors, neck flexors, shoulder abductors, elbow flexors, elbow extensors, hip flexors, hip abductors, knee flexors, and knee extensors. In addition, the MRC grade was determined for shoulder adductors, shoulder exorotators and endorotators, hip extensors, and hip adductors. This was expressed as the percentage of the maximum possible score for MRC sum scores, and as the percentage of the median strength of healthy males and females for HHD sum scores. Selected patients scored <90% on manual muscle testing function using MRC grading and <80% in HHD score at baseline. Patients were selected based on a positive response to ERT within 2-3 years after start of treatment as reflected by stabilization or improvement of histological and functional parameters.

Histology

Hematoxylin and eosin (HE) and periodic acid Schiff (PAS) stainings were performed on muscle sections that were processed into glycolmethacrylate (GMA), as described [31]. The sample from Patient 2 at baseline for HE and PAS stainings was not available.

Histological evaluation of muscle biopsies

Scoring of histological changes in muscle biopsies was previously described [32]. In short, all sections were evaluated by two researchers (RCF and RV) who were blinded to the identity and clinical details of each patient. Vacuole density was assessed in HE and PAS stainings. The changes in cross-striation, PAS intensity, and tissue damage were assessed using PAS stainings. These levels were scored using a scale from 0 to 3 (Table 4). The percentage of damaged fibers was expressed as a percentage of the total number of fibers present in the section. The overall muscle damage score was expressed as the sum of cross-striation, vacuole density, and PAS intensity.

Protein isolation and Western Blot analysis

20 µg of protein was processed for Western Blot analysis as described before [33] (Supplemental Methods). Equal loading was determined by scanning gels using a GelDoc EZ (Bio-Rad Laboratories B.V., Veenendaal, Netherlands) and quantification of the stain-free signal using Image Lab (v.6.0.1.34) software (Bio-Rad Laboratories B.V., Veenendaal, Netherlands). Nitrocellulose membranes were incubated with respective antibodies as delineated in the text. See Table 1 for antibodies and dilutions). Western Blot membranes were read on an Odyssey CLx reader (Li-Cor).

Enzyme activity assay for GBE1

Further detailed in Supplemental Methods

Image acquisition and analysis

Western Blot images were analyzed using Adobe Photoshop CS6 and FIJI (fiji.sc/Fiji). Histological sections were scanned on a Hamamatsu NanoZoomer 2.0 (Hamamatsu Photonics). Images were analyzed using NDP view software (v.2.5.19) (Hamamatsu Photonics).

Antibody	Dilution	Info
Mouse anti-GYG1	1:500	Novus Bio (Cat#: H00002992-M07). RRID: AB_539428
Rabbit anti-GS	1:1000	Cell Signaling (Cat#: 3886S) RRID: AB_2116392
Rabbit anti-GLUT4	1:1000	Abcam (Cat#: ab654) RRID: AB_305554
Rabbit anti-GBE1	1:1000	Atlas Antibodies (Cat#: HPA038074) RRID: AB_10672403
Mouse anti-UGP2	1:250	Santa Cruz (Cat#: sc-514174) RRID: N/A
Goat anti-Rabbit IRDye 800CW	1:5000	Li-Cor (Cat#: 925-32211) RRID: AB_2651127
Goat anti-Mouse IRDye 800CW	1:5000	Li-Cor (Cat#: 925-32210) RRID: AB_2687825
Goat anti-Rabbit IRDye 680RD	1:5000	Li-Cor (Cat#: 925-68071) RRID: AB_2721181
Goat anti-Mouse IRDye 680RD	1:5000	Li-Cor (Cat#: 925-68070) RRID: AB_2651128

Table 1. Antibodies and dyes.

Mass Spectrometry

Details are thoroughly described in Supplemental Methods.

Statistics

Data are expressed as means \pm SE. Data from two independent groups was tested using two-sided t-tests. Data from paired groups was tested using two-sided paired t-tests. Normally distributed data for experiments with three or more independent groups was tested with one-way ANOVA followed by post-hoc Tukey or Games-Howell correction for multiple tests (depending on homogeneity of variance). Non-normally distributed data for experiments with three or more independent groups was tested with Kruskal-Wallis test. A *p*-value of less than 0.05 was considered significant. Data was analyzed using IBM SPSS Statistics (version 26).

For the analysis of quantitative mass spectrometry data, only proteins that registered an expression value for all the individuals were used. Paired t-tests were conducted to analyze Baseline vs ERT samples. Unpaired t-tests were conducted to analyze Healthy vs Baseline. Proteins were then filtered using the GO term "Glycogen metabolic process" (GO:0005977). Multiple testing correction was calculated using the Benjamini-Hochberg method. A q-value of 0.2 was used as cut-off.

Study approval

Animal experiments were approved by the local (Animal Experiments Committee (DEC) and national (Central Committee for Animal Experiments (CCD) animal experiment authorities in compliance with the European Community Council Directive guidelines (EU directive 86/609), regarding the protection of animals used for experimental purposes.

The Ethical Committee of the Erasmus MC University Medical Center approved the use of the biopsies for research purposes (MEC 2007-103). Written informed consent was obtained from all patients and control subjects or their legal guardians. Control biopsies were obtained from healthy subjects for which a progressive neuromuscular disorder was ruled out by medical history.

Author contributions

R.C.F. designed the study, performed experiments, analyzed and interpreted the data, and participated in the preparation of the manuscript. C.d.S., M.H., and J.D. performed experiments. T.S. and P.L. assisted with the statistical analyses. R.V. analyzed and interpreted the data. L.H. and E.B. interpreted the data. N.vd.B., P.v.D, and A.v.d.P. interpreted the data. W.W.M.P. and G.S. designed the study, interpreted the data, and participated in the preparation of the manuscript.

Sources of Funding

The work was funded by Health-Holland, Top Sector Life Sciences & Health and by a research grant from Sanofi Genzyme to the Center of Lysosomal and Metabolic Diseases at Erasmus MC.

Disclosures

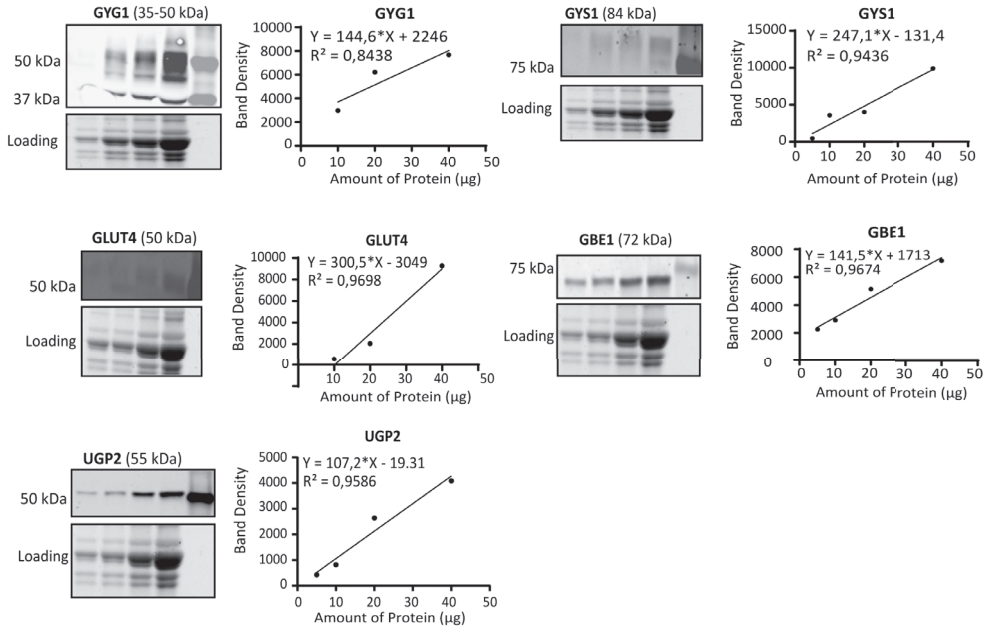
A.T.v.d.P. has provided consulting services for various industries in the field of Pompe disease under an agreement between these industries and Erasmus MC, Rotterdam, the Netherlands. All the other authors declare no conflict of interest.

References

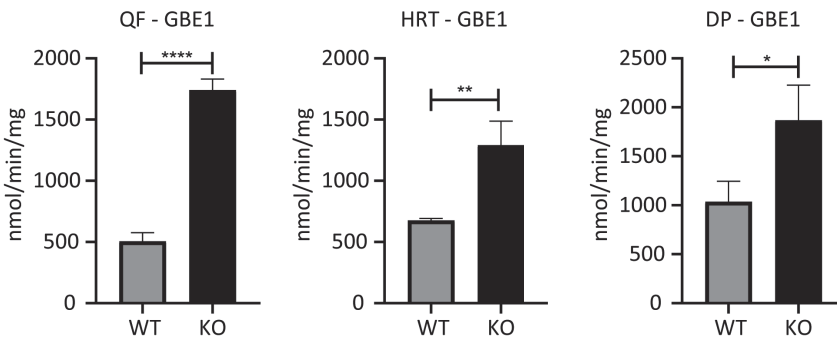
- 1 van der Ploeg AT, Reuser AJ. Pompe's disease. *Lancet* 2008;372:1342–1353.
- 2 Reuser AJJ, Hirschhorn R, Kroos MA. Pompe disease: Glycogen storage disease type II, acid α -glucosidase (acid maltase) deficiency. In: Beaudet AL, Vogelstein B, Kinzler KW, et al., eds. *Online Metab. Mol. Bases Inherit. Dis. Lysosomal Storage Disord.*, New York, NY: The McGraw-Hill Companies, INC, 2018:
- 3 Fukuda T, Ewan L, Bauer M, et al. Dysfunction of endocytic and autophagic pathways in a lysosomal storage disease. *Ann Neurol* 2006.
- 4 Schoser B, Stewart A, Kanters S, et al. Survival and long-term outcomes in late-onset Pompe disease following α -glucosidase treatment: a systematic review and meta-analysis. *J Neurol* 2017;264:621–630.
- 5 Harlaar L, Hogrel J-Y, Perniconi B, et al. Large variation in effects during 10 years of enzyme therapy in adults with Pompe disease. *Neurology* 2019;10.1212/WNL.00000000000008441.
- 6 de Vries JM, van der Beek NA, Hop WC, et al. Effect of enzyme therapy and prognostic factors in 69 adults with Pompe disease: an open-label single-center study. *Orphanet J Rare Dis* 2012;7:73.
- 7 Douillard-Guilloux G, Raben N, Takikita S, et al. Restoration of muscle functionality by genetic suppression of glycogen synthesis in a murine model of Pompe disease. *Hum Mol Genet* 2009;19:684–696.
- 8 Taylor KM, Meyers E, Phipps M, et al. Dysregulation of multiple facets of glycogen metabolism in a murine model of Pompe disease. *PLoS One* 2013;8:e56181.
- 9 van der Ploeg A, Carlier PG, Carlier R-Y, et al. Prospective exploratory muscle biopsy, imaging, and functional assessment in patients with late-onset Pompe disease treated with α -glucosidase: The EMBASSY Study. *Mol Genet Metab* 2016.
- 10 Roach PJ, Depaoli-Roach AA, Hurley TD, et al. Glycogen and its metabolism: some new developments and old themes. *Biochem J* 2012;441:763–787.
- 11 Hurley TD, Stout S, Miner E, et al. Requirements for catalysis in mammalian glycogenin. *J Biol Chem* 2005;280:23892–23899.
- 12 Manchester J, Skurat A V., Roach P, et al. Increased glycogen accumulation in transgenic mice over expressing glycogen synthase in skeletal muscle. *Proc Natl Acad Sci U S A* 1996;93:10707–10711.
- 13 Pederson BA, Chen H, Schroeder JM, et al. Abnormal Cardiac Development in the Absence of Heart Glycogen. *Mol Cell Biol* 2004;24:7179–7187.
- 14 Thorens B, Mueckler M. Glucose transporters in the 21st Century. *Am J Physiol - Endocrinol Metab* 2010;298:141–145.
- 15 Cushman SW, Wardzala LJ. Potential mechanism of insulin action on glucose transport in the isolated rat adipose cell. Apparent translocation of intracellular transport systems to the plasma membrane. *J Biol Chem* 1980;255:4758–4762.
- 16 Sean Froese D, Michaeli A, McCorvie TJ, et al. Structural basis of glycogen branching enzyme deficiency and pharmacologic rescue by rational peptide design. *Hum Mol Genet* 2015;24:5667–5676.
- 17 Perenthaler E, Nikoncuk A, Yousefi S, et al. Loss of UGP2 in brain leads to a severe epileptic encephalopathy, emphasizing that bi-allelic isoform-specific start-loss mutations of essential genes can cause genetic diseases. *Acta Neuropathol* 2020;139:415–442.

- 18 Schaaf GJ, van Gestel TJM, in 't Groen SLM, et al. Satellite cells maintain regenerative capacity but fail to repair disease-associated muscle damage in mice with Pompe disease. *Acta Neuropathol Commun* 2018;6:119.
- 19 Meena NK, Ralston E, Raben N, et al. Enzyme Replacement Therapy Can Reverse Pathogenic Cascade in Pompe Disease. *Mol Ther - Methods Clin Dev* 2020;18:199–214.
- 20 Effect of acid maltase deficiency on the endosomal/lysosomal system and glucose transporter 4. *Neuromuscul Disord* 2003;13:49–54.
- 21 Thon VJ, Khalil M, Cannon JF. Isolation of human glycogen branching enzyme cDNAs by screening complementation in yeast. *J Biol Chem* 1993;268:7509–7513.
- 22 Bruno C, Cassandrini D, Assereto S, et al. Neuromuscular forms of glycogen branching enzyme deficiency. *Acta Myol* 2007;26:75–78.
- 23 Turnquist RL, Turnquist MM, Bachmann RC, et al. Uridine diphosphate glucose pyrophosphorylase: differential heat inactivation and further characterization of human liver enzyme. *BBA - Enzymol* 1974;364:59–67.
- 24 Flores-Díaz M, Alape-Girón A, Persson B, et al. Cellular UDP-glucose deficiency caused by a single point mutation in the UDP-glucose pyrophosphorylase gene. *J Biol Chem* 1997;272:23784–23791.
- 25 Sidman RL, Taksir T, Fidler J, et al. Temporal neuropathologic and behavioral phenotype of 6 neo/6 neo Pompe disease mice. *J Neuropathol Exp Neurol* 2008;67:803–818.
- 26 Byrne BJ, Fuller DD, Smith BK, et al. Pompe disease gene therapy: neural manifestations require consideration of CNS directed therapy. *Ann Transl Med* 2019;7:290–290.
- 27 Bijvoet AGA, van de Kamp EHM, Kroos MA, et al. Generalized glycogen storage and cardiomegaly in a knockout mouse model of Pompe disease. *Hum Mol Genet* 1998;7:53–62.
- 28 Zirin J, Nieuwenhuis J, Perrimon N. Role of Autophagy in Glycogen Breakdown and Its Relevance to Chloroquine Myopathy. *PLoS Biol* 2013;11:1001708.
- 29 Winkel LPF, Kamphoven JHJ, van den Hout HJMP, et al. Morphological changes in muscle tissue of patients with infantile Pompe's disease receiving enzyme replacement therapy. *Muscle Nerve* 2003;27:743–751.
- 30 Van Der Ploeg RJO, Fidler V, Oosterhuis HJGH. Hand-held myometry: Reference values. *J Neurol Neurosurg Psychiatry* 1991;54:244–247.
- 31 Van den Hout JMP, Kamphoven JHJ, Winkel LPF, et al. Long-term intravenous treatment of Pompe disease with recombinant human alpha-glucosidase from milk. *Pediatrics* 2004;113:e448–e457.
- 32 Schaaf GJ, van Gestel TJM, Brusse E, et al. Lack of robust satellite cell activation and muscle regeneration during the progression of Pompe disease. *Acta Neuropathol Commun* 2015;3:65.
- 33 Demirdas S, van Slegtenhorst MA, Verdijk RM, et al. Delayed Diagnosis of Danon Disease in Patients Presenting With Isolated Cardiomyopathy. *Circ Genomic Precis Med* 2019;12:e002395.
- 34 Orth M, Mundegar RR. Effect of acid maltase deficiency on the endosomal/lysosomal system and glucose transporter 4. *Neuromuscul Disord* 2003;13:49–54.
- 35 Baligand C, Todd AG, Lee-McMullen B, et al. 13C/31P MRS Metabolic Biomarkers of Disease Progression and Response to AAV Delivery of hGAA in a Mouse Model of Pompe Disease. *Mol Ther - Methods Clin Dev* 2017;7:42–49.

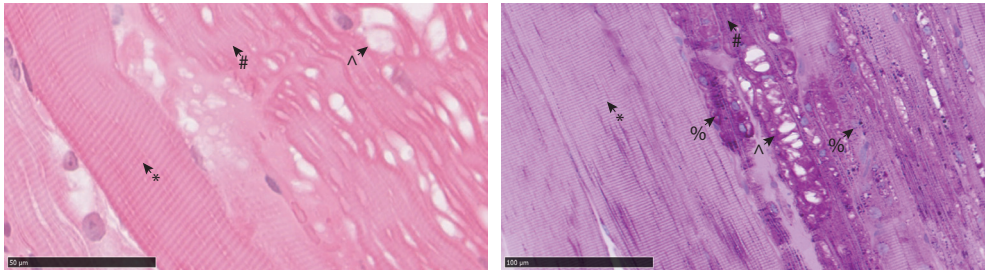
Supplementary Information



Supplementary Figure 1. Western Blot analyses and quantification of GYG1, GS, GLUT4, GBE1, and UGP2 to determine the range of detection of the antibodies. Protein lysates from QF of *Gaa*^{-/-} mice at 40 weeks were used. In order to determine the optimal protein load for quantification of Western Blot data, the linearity of the antibodies was first assessed. 5, 10, 20, and 40 µg of protein from mouse lysate were loaded in gels and blotted. The intensity of the signal was quantified and plotted. 20 µg were taken as the optimal amount of protein.



Supplementary Figure 2. Enzyme activity assay of GBE1 in WT and *Gaa*^{-/-} mice at 34 weeks in QF, HRT, and DP lysates respectively. Values from three independent mice were normalized to total protein and averaged. Data are shown as mean ± SE. n=3. *p<0.05; **p<0.01; ****p<0.0001.



Supplementary Figure 3. Analysis of HE and PAS stainings allows evaluation of total muscle damage.

Representative images are shown. * shows cross striation; # shows fiber myopathy, characterized by disorganized fiber architecture; ^ shows vacuolization; % shows areas of intense PAS positive staining and round-shaped glycogen-filled lysosomes.

Supplementary Methods

Protein isolation and Western Blot analysis

Tissues were lysed in RIPA buffer (50 mM Tris.HCl pH 7.4, 150 mM NaCl, 2 mM EDTA, 1% Triton X-100) supplemented with a phosphatase inhibitor cocktail (10 mM NaF, 60 mM β -glycerolphosphate, 2 mM Na-orthovanadate) and cOmplete™ protease inhibitor cocktail (Sigma-Aldrich). Total protein concentration was determined using Pierce™ BCA Protein Assay Kit according to manufacturer's instructions (Thermo Scientific, Rockford IL, USA).

Enzyme activity assay for GBE1

10% (w/v) muscle homogenates in 50 mM aqueous NaF were prepared using an ultrasonic homogenizer (VCX 130, Sonics, Newtown CT, USA). Samples were centrifuged 10 minutes at 10000 rpm at 4°C. Pellets were discarded. Total protein concentration was determined using Pierce™ BCA Protein Assay Kit according to manufacturer's instructions (Thermo Scientific, Rockford IL, USA). Lysates were diluted in 50 mM NaF to a concentration of 2 mg/ml. 10 μ l of 2x lysate were diluted in 100 μ l of reaction mix (25 μ g/ml glycogen; 18.5 mM glycine buffer (0.2 M glycyglycine/NaOH, pH 6.4); 5 mM AMP; 50 mM 2-mercapto ethanol, 50 mM glucose-1-phosphate (G1P); 0.3 mg/ml phosphorylase B). Samples were incubated at 30°C for 90 minutes. Reactions were stopped by incubation on ice. Free inorganic phosphate was measured in a spectrophotometer (Cary 300, Varian/Agilent Technologies) using MoFe-reagent (144 mM $\text{FeSO}_4 \cdot 7\text{H}_2\text{O}$).

Mass Spectrometry

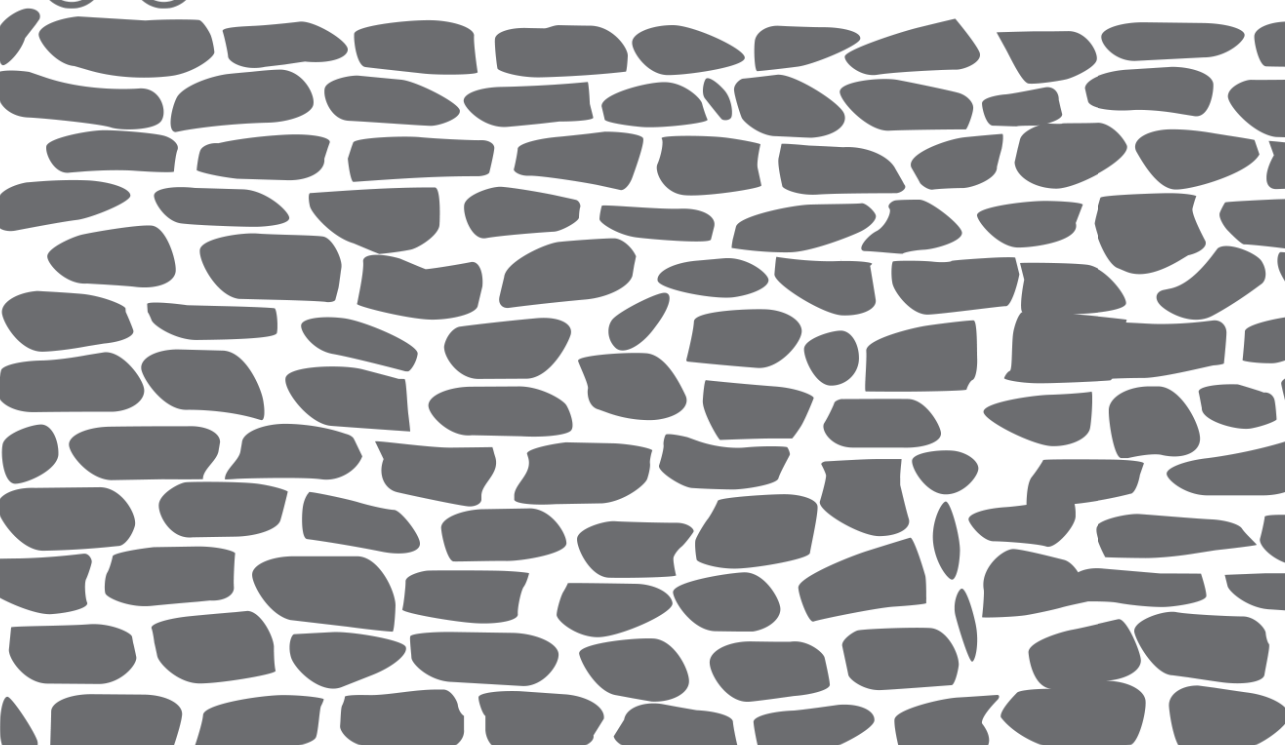
Sample preparation and quantitative mass spectrometry

Human skeletal muscle biopsies were cut and lysed in 1 ml 50 mM Tris/HCl pH 8.2, 0.5 % sodium deoxycholate (SDC) and MS-SAFE™ protease and phosphatase inhibitor using a Bioruptor ultrasonicator (Diagenode). Protein concentrations were measured using the BCA assay (Thermo Scientific). Proteins were reduced with 5 mM DTT and cysteine residues were alkylated with 10 mM iodoacetamide. Protein was extracted by acetone precipitation at -20 °C overnight. Samples were centrifuged at 8,000 g for 10 min at 4 °C. The acetone was removed and the pellet allowed to dry. The protein pellet was dissolved in 1 ml 50 mM Tris/HCl pH 8.2, 0.5 % SDC and proteins were digested with LysC (1:200 enzyme:protein ratio) for 4 h

at 37 °C. Next, trypsin was added (1:100 enzyme:protein ratio) and the digestion proceeded overnight at 30 °C. Digests were acidified with 50 µl 10 % formic acid (FA) and centrifuged at 8,000 g for 10 min at 4 °C to remove the precipitated SDC. The supernatant was transferred to a new centrifuge tube. The digests were purified with C18 solid phase extraction (Sep-Pak, Waters), lyophilized and stored at -20 °C. Proteolytic peptides were labeled with TMT 10-plex labeling reagents (Thermo Scientific) allowing for peptide quantitation. Peptides were mixed at the 10-plex level and further fractionated by HILIC chromatography. Fractions were collected and analyzed by nanoflow LC-MS/MS. nLC-MS/MS was performed on EASY-nLC 1200 coupled to an Orbitrap Lumos Tribid mass spectrometer (Thermo) operating in positive mode and equipped with a nanospray source. Peptides were separated on a ReproSil C18 reversed phase column (Dr Maisch GmbH; column dimensions 15 cm × 50 µm, packed in-house) using a linear gradient from 0 to 80% B (A = 0.1 % formic acid; B = 80% (v/v) acetonitrile, 0.1 % formic acid) in 70 min and at a constant flow rate of 200 nl/min using a splitter. The column eluent was directly sprayed into the ESI source of the mass spectrometer. Mass spectra were acquired in continuum mode; fragmentation of the peptides was performed in data-dependent mode using the multinotch SPS MS3 reporter ion-based quantification method.

Data analysis

Data were analyzed with Proteome Discoverer 2.3. The Mascot search algorithm (version 2.3.2, MatrixScience) was used for searching against the Uniprot database (taxonomy: *Homo sapiens*, release version October 2019). The peptide tolerance was typically set to 10 ppm and the fragment ion tolerance was set to 0.8 Da. A maximum number of 2 missed cleavages by trypsin were allowed and carbamidomethylated cysteine and oxidized methionine were set as fixed and variable modifications, respectively. Typical contaminants were omitted from the output tables.



Chapter 3

Restoring the regenerative balance in neuromuscular disorders: satellite cell activation as therapeutic target in Pompe disease

**Gerben J. Schaaf^{1,3}, Rodrigo Canibano-Fraile^{1,3}, Tom van Gestel^{1,3}, Ans T.
van der Ploeg^{2,3} and WWM Pim Pijnappel^{1,3}**

¹Department of Clinical Genetics, Erasmus MC University Medical Center, Rotterdam, the Netherlands

²Department of Pediatrics, Erasmus MC University Medical Center, Rotterdam, the Netherlands

³Center for Lysosomal and Metabolic Diseases, Erasmus MC University Medical Center, Rotterdam, the Netherlands

Corresponding authors:

Gerben J. Schaaf, Ph. D.: g.schaaf@erasmusmc.nl

W.W.M. Pim Pijnappel, Ph. D.: w.pijnappel@erasmusmc.nl

Ann Transl Med. 2019;7(13):280. doi:10.21037/atm.2019.04.48

Abstract

Skeletal muscle is capable of efficiently regenerating after damage in a process mediated by tissue-resident stem cells called satellite cells. This regenerative potential is often compromised under muscle-degenerative conditions. Consequently, the damage produced during degeneration is not efficiently repaired and the balance between repair and damage is lost. Here we review recent progress on the role of satellite cell-mediated repair in neuromuscular disorders with a focus on Pompe disease, an inherited metabolic myopathy caused by deficiency of the lysosomal enzyme acid alpha glucosidase (GAA). Studies performed in patient biopsies as well as in Pompe disease mouse models demonstrate that muscle regeneration activity is compromised despite progressing muscle damage. We describe disease-specific mechanisms of satellite cell dysfunction to highlight the differences between Pompe disease and muscle dystrophies. The mechanisms involved provide possible targets for therapy, such as modulation of autophagy, muscle exercise, and pharmacological modulation of satellite cell activation. Most of these approaches are still experimental, although promising in animal models, still warrant caution with respect to their safety and efficiency profile.

Keywords: Pompe disease, muscle regeneration, satellite cells, regenerative therapies

Introduction

Pompe disease is an inherited metabolic disorder due to deficiency in the lysosomal enzyme acid alpha glucosidase (GAA). Pompe disease is characterized by progressive degeneration of skeletal muscle in all patients. In classic infantile patients, development of hypertrophic cardiomyopathy [1] and involvement of the central nervous system [2,3] is observed. Enzyme replacement therapy (ERT) extends survival for classic infantile patients and improves motor function, although the heterogeneous response between patients remains challenging [4–6]. Together, with the cost of therapy and the burden of the regular infusions for patients and caretakers it is clear that novel treatment strategies are warranted. Such novel therapeutic opportunities include improved ERT, substrate-reduction strategies, the use of chaperone, antisense oligonucleotides, and gene therapy approaches [7,8].

Pompe disease is one of the almost 900 different conditions associated with a muscle wasting phenotype [9]. Although different muscle disorders are heterogeneous in disease mechanism and in pattern of progression, these conditions often share a defect in muscle regeneration. Muscle-regenerative pathways are common for all patients with neuromuscular disorders and may offer novel therapeutic opportunities to improve the muscle phenotype across the different diseases. Here, we review muscle regeneration defect(s) in neuromuscular diseases, focusing on Pompe disease. We will also discuss advances in the development of regenerative therapies and the feasibility of using these in the treatment of Pompe disease patients.

1. Mechanism of the regenerative defect in Pompe disease

Muscle pathology in Pompe disease

Pompe disease is considered a clinical spectrum indicating that the disease can develop at any age and progress at any rate. The onset and progression of disease is roughly correlated with the genotype [10] with classic infantile patients harbouring severe GAA mutations and showing an aggressive course of disease. Deficiency of GAA causes glycogen accumulation that is particularly damaging to skeletal muscle in all patients [11], and to the heart and central nervous system in classic infantile patients [3,12]. Skeletal muscles from Pompe disease patients are characterized by vacuolization, irregularly shaped myofibers, and loss of cross-striation [1]. During disease progression the lysosomal compartment grows in size and number, replacing healthy cellular content [11]. The numerous glycogen-filled lysosomes rupture and

release glycogen into the cytoplasm. In the final stages cytoplasmic glycogen has replaced most contractile elements of the muscle cell, resulting in loss of myofiber function. Obviously, glycogen accumulation and lysosomal dysfunction affect other processes that contribute to the pathology, including disturbed macroautophagy (herein referred to as autophagy) and calcium homeostasis, oxidative stress, and mitochondrial abnormalities. Autophagy dysfunction, which is common among lysosomal storage disorders [13], contributes to sarcopenia during aging and will be discussed further below in the context of the muscle regenerative response.

Pathological tissue remodeling, where myogenic tissue is replaced by fat or fibrotic tissue, is a frequent feature of neuromuscular disorders. Adipose deposition of certain muscle groups is observed in most Pompe disease patients at the macroscopic level, and is most prominent in axial muscles, scapular girdle muscles, thigh muscles and specifically tongue [14,15]. Pompe disease patients show a typical distribution of affected muscles, with shoulder abductors, abdominal muscles, paraspinal muscles, hip flexors, hip extensors, and hip adductors among the most affected muscles. Hip abductors were affected in more than 80% of all patients [16]. The quadriceps femoris was affected in little over half of the patients, while the hand and feet muscle were found to be relatively spared.

The muscle damage in Pompe disease develops predominantly intracellularly, leaving the sarcolemma and basal lamina largely intact. This is in contrast to the increased sarcolemmal fragility, increased sensitivity for contractile damage, and myofiber rupturing that characterizes dystrophic muscle. Ruptured myofibers recruit immune cells that contribute to pathological deposition of adipose and fibrous tissue in dystrophic muscle. A robust intramuscular immune response to progressing disease is absent in Pompe disease, consistent with maintained sarcolemmal integrity. The ruptured and necrotic myofibers in dystrophic muscle also drive the muscle regenerative response and robustly activate MuSCs. Therefore, the lack of robust sarcolemmal damage in Pompe disease may contribute to satellite cell inactivity, as will be delineated further below. The comparison of Pompe disease and dystrophic muscle illustrates that differences in muscle pathology can have profoundly different effects on muscle regeneration.

The role of satellite cells in muscle regeneration

To understand the clinical consequences of distinct defects in muscle regeneration, we will first discuss the role of skeletal muscle stem cells and muscle regeneration

in healthy skeletal muscle. Skeletal muscle can regenerate damage by recruiting the activity of tissue-resident stem cells. Skeletal muscle stem cells (MuSCs) or muscle satellite cells are located at the myofiber periphery underneath the basal lamina [17]. In homeostasis MuSCs are quiescent, but become rapidly activated after damage and proliferate to generate a large set of progeny that is capable of regenerating damaged myofibers by fusion (**Figure 1**). Quiescent MuSCs express high levels of Pax7, a master regulator of postnatal myogenesis. Upon activation MuSCs downregulate Pax7 and upregulate the determination factor MyoD [18] that drives terminal myogenic differentiation. Part of the activated MuSCs return to quiescence in a process called self-renewal [19] to replenish the stem cell pool and secure long-term regenerative potential. The activated MuSCs proliferate and progress to become a population of myogenic progenitors that eventually start expressing myogenin. Previously, it was demonstrated that, after conditionally depleting MuSCs in a Pax7-dependent manner, skeletal muscle did not or hardly regenerate after damage [20,21]. In the absence of MuSCs, injured muscle became infiltrated with inflammatory cells and muscle tissue was replaced with fat and fibrotic tissue, further emphasizing the important role of MuSCs in mediating a healthy regenerative response. Earlier studies already found that skeletal muscle can still regenerate when MuSC numbers are at least 10% of the levels in healthy young animals [22], indicating a large “regenerative reserve” under healthy conditions.

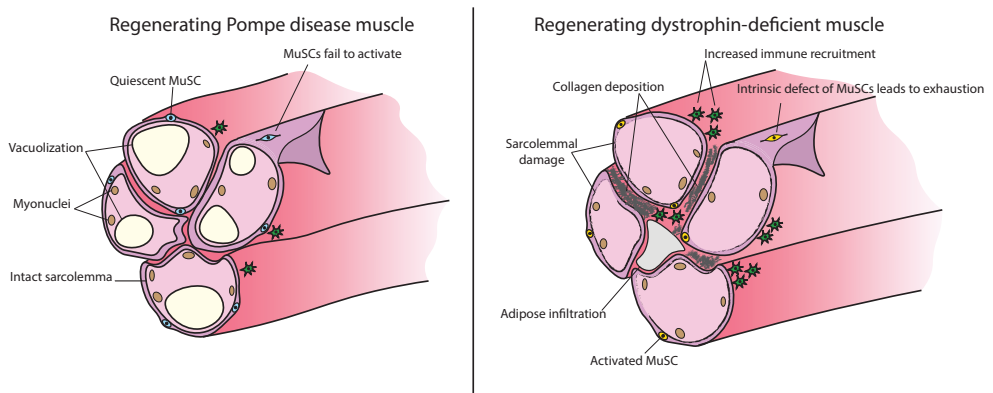


Figure 1: Lack of satellite cell activation in Pompe disease. The figure depicts a cross-sectional view of skeletal muscle in Pompe disease (left panel) and in dystrophic muscle for comparison (right panel). While dystrophin-deficient muscle is characterized by MuSC hyperactivation, chronic inflammation, and severe tissue remodeling, Pompe disease is characterized by a failing regenerative response.

Table 1: MuSC defects in various neuromuscular diseases

Proliferative defect	Disease	Species	Patients age range*	Number of patients	Animal model	Animals age	Muscles analyzed	Type analysis	Result	Mechanism of MuSC loss of function	Reference
	DMD [5], PM [5], MD [5], ALS [5]; healthy [7]	Human	30-60	5	-	-	Deltoid, biceps, QF, GAS, triceps, peroneal	LM and EM	DMD \pm 6 fold increased and MD/PM \pm 3-fold increased over adult control	Abnormal proliferation	[28]
	DMD	Human	2-14	9	-	-	Vastus lateralis, vastus medialis	Ex vivo isolated cells	80% of DMD clones with long doubling times and aberrant morphology (vs 8% normal clones)	Loss of replicative potential	[23]
	DMD	Human	2-7	7	-	-	Vastus lateralis, rectus femoris	IF tissue: Pax7	Increased SC levels	Abnormal proliferation	[29]
	Myotonic dystrophy	Human	46-54	4	-	-	Vastus lateralis, TA	IF tissue: NCAM	Increased SC numbers in distal muscles, reduced regeneration, proliferative defect	Loss of replicative potential	[24]
	Nemaline myopathy	Human	3 wk-72 yr	12 NM, 21 ctrl	-	-	Psoas, diaphragm, quadriceps, abdominal wall, quadriceps, deltoid, TA, intercostal, pectoral, biceps	IF tissue: NCAM/ Pax7	Increased MuSC levels in NM muscle (\pm 10 fold)	Abnormal proliferation	[31]

Table 1 (continued)

Proliferative defect	Disease	Species	Patients age range*	Patients number of patients	Animal model	Animals age	Muscles analyzed	Type analysis	Result	Mechanism of MuSC loss of function	Reference						
Various NMD	Human	16-89	sIBM (39), PM (13), DM (13), MD (10), Ctrl (10)	-	-	Deltoid, biceps brachii, QF, extensor forearm, TA	IF tissue: Pax7	All NMD have increased Pax7-positive cells, MyoD-positive and Myogenin-positive compared to ctrl	Perturbed regeneration/ Excessive MuSC activation	[25]							
							DMD	Mouse	-	-	mdx	6-8 wks	Hindlimb muscles	IF isolated myofibers: Pax7	Initial increase in mdx, decline after 6 m of age	Loss of replicative potential	[35]
							DMD	Mouse	-	-	C57Bl/10ScSn-DMDmdxJ	4 and 8 weeks	GAS	MACS-based isolation of MuSCs	Increased SC levels MDX (early)	Abnormal proliferation	[34]
Limb girdle muscular dystrophy 2A	Human	2-62	13	-	-	Biceps	IF tissue: Pax7	Increased SC count in fibrotic group	Impaired differentiation	[33]							
Pompe disease	Human	2-71	22	-	-	Vastus lateralis	IF tissue: Pax7	Equal number, Impaired MuSC activation	Failing MuSC activation	[32]							
Myasthenia gravis	Human + mouse	-	-	AchR immunization	>10 weeks	TA	IF tissue: Pax7	Increased SC levels; reduced regeneration efficiency	Impaired differentiation	[39]							

Proliferative defect	Disease	Species	Patients age range*	Number of patients	Animal model	Animals age	Muscles analyzed	Type analysis	Result	Mechanism of MuSC loss of function	Reference
	Mdx	Mouse	-	-	Mdx	2-3 mo	EDL	IF Isolated myofibers: Pax7	Increased SC/fiber (1.5 fold); reduced asymmetric division	Self-renewal defect	[38]
	Pompe disease	Mouse	-	-	<i>Cad15^{Neo/15Neo}</i> in FVB/N (42) and <i>Cad6^{Neo/6Neo}</i> (10) in 129Sv/c57/B16	2-60 wks	TA, GAS, hindlimb muscles	IF tissue: Pax7; FACS: MuSC, VCAM	Increased MuSC, impaired MuSC activation; Gaa-deficient MuSC respond to injury and self-renew	Failing MuSC activation	[36]
	Pompe disease	Mouse	-	-	<i>Cad6^{Neo/6Neo}</i> (10)	6-36 wks	TA, Triceps brachii	IF tissue: Pax7	impaired MuSC activation; Gaa-deficient MuSC respond to injury	Failing MuSC activation	[37]

Abbreviations: ALS: amyotrophic lateral sclerosis; DM: DMD; Duchenne muscular dystrophy; EDL: Extensor digitorum longus; GAS: Gastrocnemius; MD: myotonic dystrophy; PM: Polymyositis; sIBM: sporadic inclusion body myositis TA: Tibialis Anterior; QF: Quadriceps Femoris. * Patients age range is expressed in years.

A defect in MuSC activation in Pompe disease

Defects in MuSC activity have been reported for various neuromuscular diseases. These comprise effects on their proliferative potential [23–27], changes in MuSC numbers [25,28–31], and alterations in their potential to properly activate [32] or differentiate [33] (**Table 1**). Animal models for these and other muscle-degenerative diseases were also found to have defects in MuSC activation, proliferation, self-renewal, and differentiation potential [34–39] (**Table 1**). These effects of the failing MuSC population can be irreversible -as in certain dystrophies- or reversible as in Pompe disease.

The current dogma for Duchenne muscular dystrophy (DMD) is that affected muscles undergo continuous rounds of de- and regeneration -as result of contractile myofiber damage - which is thought to eventually exhaust the MuSC pool (see for recent excellent reviews [40,41]). This proliferative/exhaustive phenotype was observed in myogenic progenitors explanted from dystrophic muscle, with the defect more pronounced in cells isolated from older patients [23,43]. Loss of proliferative potential has been attributed to attrition of telomere length [44], which was indeed demonstrated in samples from human DMD subjects [45]. The loss of proliferative potential of MuSCs is not restricted to DMD, but also described for other muscle disorders, including myotonic dystrophy (24) or sporadic body inclusion myopathy [25] (**Table 1**). Another mechanism for loss of MuSC function is through premature differentiation of MuSCs, resulting in depletion of the self-renewing stem cell pool, such as has been reported for Emery-Dreifuss dystrophy [46,47]. In addition, as it was reported for Myasthenia Gravis, the differentiation potential of MuSC progeny may be compromised, so that muscle regeneration cannot be successfully completed [39] (**Table 1**). In these examples, the MuSC defect is cell-intrinsic and is likely to be irreversible.

Our recent results show that the mechanism of MuSC inactivation in Pompe disease is different and, reversible. We previously described that MuSC numbers are stable in biopsies from Pompe disease patients across a large age-range (2 months – 71.7 years) [32] and we and others demonstrated that in mouse models of Pompe disease MuSCs are not exhausted [36,37] (**Table 1**). In fact, MuSC numbers were increased in *Gaa-ko*-mice in two different backgrounds – *fvb/n* and the mixed *c57/b16* and *129sv* background. Muscle biopsies from Pompe disease patients showed considerable muscle damage which is expected to elicit a robust regenerative response, but we found that MuSCs were not activated to repair the damage. Markers of active regeneration, which includes the expression of embryonic

myosin heavy chain, were absent [32]. Similarly, *Gaa*-deficient mice show muscle wasting, as reflected in decreasing muscle wet weight, and show limited MuSC activation and regeneration [36], reminiscent of the observations in human Pompe disease patients. Interestingly, *Gaa*-ko mice, despite completely lacking functional *Gaa* similarly as classic infantile patients, only develop a muscle phenotype from 15 weeks onwards. At this age, an initial mild regenerative response observed in younger animals, reflected by a gradual increase in myofiber central nucleation and low-level MuSC proliferation, is lost. It can be hypothesized that in young *Gaa*-ko mice the mild regenerative response delayed the onset of muscle wasting.

To determine if the observed regenerative defect could be explained by compromised MuSC function, we as well as Lagalice and colleagues, performed muscle-injury experiments. Both these studies showed that *Gaa*-deficient muscle regenerated efficiently after chemical injury (i.e. using BaCl₂ or cardiotoxin), excluding a cell-intrinsic defect of *Gaa*-deficient MuSCs. Moreover, we also showed that *Gaa*-ko muscle regenerated completely after serial injury, indicating that the *Gaa*-deficient MuSCs are also capable of self-renewal [36]. Our current work focuses on explaining this apparent paradox between MuSC inactivity during disease progression, while still capable of responding efficiently to exogenous damage. We hypothesize that the failing MuSC activation in Pompe disease may be explained by an inhibitory environment or by insufficient activation signals.

The role of autophagy in MuSC activation and muscle regeneration

In order to maintain the quiescent state, MuSCs require a basal level of autophagic activity [48,49]. Disruption of autophagy during aging is shown to affect homeostasis of MuSCs and results in reduction of the pool of quiescent MuSCs in aging individuals [49]. In fact, autophagic activity is one of the first processes to be upregulated during MuSC activation. While quiescent cells reside in a low metabolic and energetic state, autophagic activity is rapidly increased after damage to supply the increased demand for ATP, and reducing cofactors and amino acids needed to sustain proliferation [48]. Tang and colleagues identified SIRT1 as critical regulator of autophagic flux in activating MuSCs. Loss of SIRT1 resulted in disturbed autophagic activity and delayed MuSC activation. Blocking autophagy disrupted MuSC activation [48,50]. Paolini and colleagues found in mice that were genetically modified to express reduced levels of autophagic activity - by

ablation of *Atg16l1*, a key component in autophagy - that the muscle regenerative response was delayed [51]. The regenerating muscle of these mice contained increased levels of uncommitted MuSCs (Pax7+/MyoD-) and less activated/committed muscle progenitors that expressed MyoD. The authors concluded that failure to upregulate autophagic activity during the early stages of regeneration blocked full MuSC activation. While autophagic activity needs to be increased during the very early stages of MuSC activation, inhibition of autophagy in MuSC progeny is essential for completing regeneration [52]. These studies indicate that autophagic activity is tightly controlled during different stages of regeneration, and may even be differentially regulated in different states of MuSC activation. The role of autophagy in MuSC activation and muscle regeneration under diseased conditions is still not entirely clear and warrants more studies.

Disruption of autophagic activity contributes to neuromuscular disease

Inhibition as well as excessive activation of autophagy is found to induce muscle atrophy [53,54], suggesting a narrow window of autophagic activity during muscle homeostasis. Genetic inhibition of autophagy was sufficient to induce morphological features of myopathy, including myofiber vacuolization and decreasing fiber diameter [55,56]. Disrupted autophagic flux has been observed in biopsies from DMD patients [57], in X-linked myopathy [58], Danon disease [59] and Pompe disease [60,61]. Studies in animal models of these diseases support a prominent role of autophagic dysfunction in the disease development. Lysosomal dysfunction in Pompe disease results in accumulation of glycogen as well as autophagic debris, that eventually blocks autophagic flux [62] and disrupts endosomal trafficking. Loss of endosomal trafficking has dramatic effects on cellular health and might also adversely impact uptake of recombinant GAA that is used as ERT in Pompe disease. Defective autophagy also affects mitochondrial functioning, as damaged mitochondria are removed through autophagy - in a process called mitophagy [8]. In Pompe disease reduced autophagic activity may contribute to the mitochondrial abnormalities that are frequently observed in muscle biopsies [11,63]. Regulation of autophagy plays a prominent role in Pompe disease progression. More extensive reviews on the topic can be found elsewhere [64,65]. It is hypothesized that normalization of autophagy restores the potential to regenerate muscle damage.

The role of the MuSC niche in muscle regeneration

Under homeostatic conditions the MuSC niche is defined by a) the myofiber that conveys chemical, electrical, and mechanical signals, and b) the basal lamina, which is largely composed of laminin, collagen, and proteoglycans (**Figure 1**). This polarized protective environment is completely remodeled after myofiber damage exposing MuSCs to several environmental factors that include chemical and electrical signals, auxiliary cells (reviewed in [66]) and matrix components. Interfering with the contact to either the myofiber and/or the basal lamina results in MuSC activation.

The damaged myofiber has an important role in engaging repair after injury. The MuSC-activating potential harnessed within myofibers was already demonstrated by Bischoff in 1986 [67]. Bischoff described that exposure to saline extract from crushed myofibers pushed quiescent MuSCs into entering the cell cycle. It is now recognized that disruption of the sarcolemma induces the damaged myofiber to release signals that activate MuSCs, including nitric oxide (NO) [68] and matrix-remodeling proteins MMP-2, MMP-9 and MMP-10 [69,70]. The MMP remodeling proteases release growth factors -such as HGF- that are embedded in the matrix. NO that is released by the damaged fiber or by recruited macrophages that also play an important role in liberating HGF [71]. HGF binds to c-met -the receptor for HGF- that is expressed on quiescent MuSCs. MuSCs also express fibroblast growth factor receptors 1 and 4 [72], and respond to FGF2 that is expressed by the myofiber and accumulates under basal lamina during aging [73]. In fact, purified extracts from aged myofibers compared to those from adult fibers were found to stimulate MuSC proliferation more potently [73], indicating that the changing myofiber niche directly impacts behavior of MuSCs.

The myofiber niche does not solely consist of chemical signals: resident and recruited cells play important roles in mediated muscle homeostasis and regeneration. Among the resident cells are fibro-adipogenic progenitors (FAPs), that are increasingly recognized for their crucial role in regenerative myogenesis [74,75]. The role of the immune response after damage has been known for much longer [76]. As mentioned above, damaged myofibers recruit immune cells, including neutrophils, eosinophils, and monocytes, that are crucial for proper muscle regeneration [77].

The niche is not only important during MuSC activation but also plays a pivotal role in maintaining quiescence under homeostatic conditions. For instance,

heparan sulfate is the glycosaminoglycan component of many proteoglycans in the basal membrane and is dynamically regulated during MuSC activation [78]. During aging 6-O sulfation specifically increased, augmenting FGF2-signaling, MuSC activation and age-dependent loss of MuSC quiescence [78]. These data show that the composition of the niche can determine and mediate the MuSC response and that the niche composition is responsive to changes in the host.

The role of the niche in Pompe disease

Immunofluorescence analyses of patient biopsies as well as those from *Gaa*-deficient mice show that both the sarcolemma and basal lamina remain intact throughout the course of disease, although we did not analyze changes in niche composition. Also, we did not observe changes in recruitment of major immune populations, including macrophages and lymphocytes (*unpublished observations*). These findings suggest that myofiber rupturing and necrotic death do not seem to play a major role in Pompe disease muscle pathology. In light of the observed lack of MuSC activation, concomitant with the absence of cell-intrinsic defects (see above), it can be hypothesized that in Pompe disease the MuSC niche either fails to generate signals that activate MuSCs or that the niche actively suppresses MuSC activation. This may suggest that the niche could be a novel therapeutic target in Pompe disease.

The effect of targeting the niche is illustrated in Merosin-deficiency or congenital muscular dystrophy 1A (CMD1A). CMD1A is caused by mutations in basal lamina protein LAMA2. It has been demonstrated that expression of integrin A7 - that normally binds laminin - restores function and integrity of the basal lamina, and reduces muscle pathology in merosin-deficient mice [79].

2. Muscle-regenerative therapies for Pompe disease

Various experimental approaches have been developed to target specific regenerative defects in animal models of different muscle disorders. As was discussed above, the regenerative defect in Pompe disease is distinct from that observed in DMD, with insufficient MuSC activation vs MuSC hyperactivation, respectively. The observed MuSC inactivity in Pompe disease suggests that focusing on safe and efficient methods to activate MuSCs may have the potential to attenuate muscle pathology in Pompe disease. As possible targets for regenerative therapy we will discuss approaches to activate MuSCs directly – providing signals

that activate MuSCs – or indirectly, such as by restoring autophagic activity. Some of these approaches bypass the contribution of the endogenous niche, such as injecting growth factors, or involve the niche by inducing myofiber damage – as in the exercise approach. The aim of these strategies is not only to improve muscle morphology and function, but also to reduce the lysosomal damage and improve autophagic/endosomal activity. As a bystander effect, improving muscle morphology and function may positively affect the response to the current ERT therapy.

Activating MuSCs by exercise

Activation of MuSCs and increase in MuSC numbers after resistance exercise are well-documented [80–82], and occur even after a single bout of exercise [83–85]. Several factors of the exercise program have been found to affect the MuSC response including mode of exercise -i.e. resistance vs endurance-, exercise intensity, duration of the program, age, and sex of the subjects (see also [86]). Exercise programs are being used and appear well-tolerated for patients with various types of neuromuscular diseases, including DMD [87], Becker muscular dystrophy (BMD) [88], Myasthenia Gravis [89] and myotonic dystrophy [90]. Beneficial effects of exercise have also been observed in patients with metabolic myopathies, including glycogen storage diseases [91,92]. In our center we performed a 12-week exercise programs with Pompe disease patients consisting of 36 sessions of standardized aerobic, resistance, and core stability exercises [93,94]. This study showed that exercise was well-tolerated by patients and improved endurance of patients' muscles -as reflected by increased workload capacity, maximum oxygen uptake capacity and walking distance- and muscle function of hip flexors and shoulder abductors. It will be interesting to determine whether focused and safe exercise programs are capable of sufficiently activating MuSCs to restore the muscle regenerative response in Pompe disease patients.

Concerns exists regarding the safety and potential harmful effects of exercise in patients with increased sensitivity for contractile damage, such as in DMD. Exercise programs for such patients should probably minimize inclusion of lengthening eccentric contractions, which produces greater sarcolemmal disruptions. It should be noted that eccentric, - but not concentric contractions - are associated with an efficient MuSC-mediated response [95]. Such concerns are not as relevant for Pompe disease patients because of the lack of sarcolemmal

fragility. Another concern is immobility of more advanced stage patients that may prevent participation in intensive exercise programs. Interestingly, pathways that were found to be affected by exercise, including AMPKA and PGC1 α , can be activated by small molecule reagents - called exercise mimetics - and would offer the possibility of exercising less-mobile patients "pharmacologically". Narkar and colleagues found that treating sedentary *c57/b16* mice with AICAR and PPAR γ agonist increased running endurance [96]. AMPK signaling as potential target in modulating MuSC activation is supported by observations from Fu *et al.*, who showed that inhibition of AMPK severely impairs satellite cell-mediated muscle regeneration [97].

Exercise programs for neuromuscular patients constitute a minimally invasive therapeutic modality that can be combined with the current state of care or with future therapeutic interventions. As mentioned above, for Pompe disease improving condition of affected muscles may attenuate disease progression and could even positively affect the response to ERT. Obviously, nutrition plays a role in optimizing the response to exercise, although that is beyond the scope of this review.

Activating MuSCs by soluble factor

MuSCs respond to soluble signals that are released into their direct environment following damage, including FGF2, HGF, and NO. Intraperitoneal injection of HGF was found to reverse experimental atrophy in mice and activate MuSCs, as determined by an increase in the fraction of MuSCs that expressed the cell cycle marker Ki67 [98]. Interestingly, mTOR activity was reduced in muscle homogenates of treated animals, suggesting that changes in autophagic activity and protein synthesis may also be involved in the observed effect.

Activating MuSCs by targeting autophagy

Autophagic activity is a major determinant of MuSC activation and successful muscle regeneration, and is often dysregulated in neuromuscular patients, in particular in those with lysosomal storage disorders. The beneficial effects of exercise are also mediated through changes in autophagic activity in the skeletal muscle of mice [99] and humans [100]. Exercise activates autophagy through increases in AMPK activity, which in turn inhibits mTORC1 -an inhibitor of autophagy [101]. The exercise mimetics that were discussed above activate AMPK signaling and function, at least partly, by increasing autophagic activity.

It is thought that glycogen traffics to the lysosome through autophagy [102] and as a result of this process cellular debris is taken up as well. Disrupted autophagy as is observed in Pompe disease results in lysosomal accumulation of waste material that eventually terminates the autophagic flux. Based on this it has been proposed that blocking autophagy would prevent the buildup of autophagic waste material and glycogen in Pompe disease and as such improve the condition of *Gaa*-deficient muscle. Indeed, autophagic buildup and glycogen accumulation were reduced in fast muscle from autophagy-deficient *Gaa*-KO mice, where *Atg7* – a critical member of the autophagy pathway – was depleted. The *Gaa*^{-/-}/*Atg7*^{KO} mice actually appeared healthier compared to, the “regular” *Gaa*-KO mice [103]. Interestingly, the *Gaa*^{-/-}/*Atg7*^{KO} mouse model also showed increased lysosomal glycogen clearing after ERT [103]. A recent study showed different strategies targeting autophagy that resulted in removal of autophagic debris, reactivation of autophagic activity and restoration of the response to ERT in *Gaa*-KO mice [104], demonstrating the potential of autophagy as a therapeutic target.

Increasing autophagy activity was also found to improve the muscle phenotype in the mouse model of DMD [105]. In *mdx* mice autophagic activity is inhibited possibly as a result of enhanced levels of oxidative stress, as determined using a Nox2-specific reactive oxygen species (ROS) biosensor. Oxidative stress was found to induce mTOR activity, which is a potent inhibitor of autophagy [105]. Genetic inhibition of Nox2, which was found to mediate ROS development in *mdx* mice, reduced oxidative stress levels, reversed autophagic activity, and resulted in improvement of muscle morphological abnormalities and muscle function [105]. A similar improvement of the condition of *mdx* mice was observed after a low-protein diet, which was thought to be mediated by attenuation of autophagic dysfunction [57]. Together these and other studies suggested that autophagy may be a novel target in the treatment of DMD and Pompe disease and perhaps also for other neuromuscular diseases.

Cell-based therapies and ex-vivo gene therapy

The strategies described above harness the regenerative potential of endogenous muscle stem cells. Such strategies are feasible for Pompe disease where the endogenous MuSC population is retained and functional. However, activating MuSCs without gene correction will not constitute a permanent cure.

Advances in gene therapy strategies show promise of achieving gene correction. Current strategies are mediated through adeno-associated virus (AAV) and predominantly target the liver. *Gaa* expressed in the liver is excreted into the circulation and is then taken up by affected muscle in a process called cross-correction [106]. Intramuscular injection of AAV into the diaphragm has also been developed. In this regard, clinical trials using AAV-mediated gene therapy are currently ongoing and show a good safety profile, as was recently reported in children [107].

AAV-vectors carrying truncated versions of dystrophin – microdystrophin – were found to be safe and seemed effective in dystrophic mice and dogs [108] and are currently being evaluated in clinical trials. A disadvantage of AAV-vectors is that they do not integrate into the host genome and may be lost on the longer term. Other vector backbones, such as lentiviral vectors [109,110] – that integrate –, are investigated for use in gene therapy strategies, including for Pompe disease and DMD. A more detailed discussion of these strategies is beyond the scope of this review and has been reviewed elsewhere [8,111].

Cell-based therapies offer potential to replenish the MuSC pool with gene-corrected cells via *ex vivo* gene therapy. As during muscle regeneration muscle progenitors fuse to form new myofibers, donor cells share their genetic content with affected fibers. Furthermore, a major advantage of cell-based therapies is the opportunity for long-term improvement of affected muscles. In the 1990s major efforts were undertaken to explore myoblast transfer therapies, based on promising results obtained in the mdx mouse model [112,113]. Unfortunately, for a number of reasons the human trials all turned out negative and little if any efficacy was shown [114]. In more recent studies, transplantation of MuSCs was found to be much more effective compared to myoblast transfer [115–117], at least in mouse studies. This reignited interest in the development of a cell-based therapy for muscle-wasting disorders. The major drawback still is that MuSCs lose most of their regenerative potential when expanded *ex vivo* [118]. The advent of induced pluripotent stem cells (iPSCs) [119] opened novel opportunities of generating tissue-specific progenitor cells without the problems associated with expansion. We have recently described a method to generate skeletal muscle progenitors from Pompe disease patient fibroblasts that retain large expansion potential while maintaining the capacity to differentiate efficiently *in vitro* and engraft *in vivo* [120]. The advantage of iPSC cells as cell source is that these are amenable for *ex vivo* gene correction using CRISPR-Cas9, for example, to generate gene-corrected myogenic progenitors.

Additionally, we used the IPS-derived muscle progenitor model to show the efficacy of an antisense oligonucleotide strategy to increase exon inclusion correcting a frequent splicing mutation found in the Pompe population [121–123]. Splicing-targeted therapies for muscle disorders are a very fruitful and promising field and are recently reviewed elsewhere [124]. The use of IPS-derived muscle progenitors as sources for cell-based therapies is also considered for other muscle-wasting disorders, including DMD, and has much potential. However, it is currently difficult to fully assess the clinical potential using small animal models, and further studies into the safety of the reprogramming and gene-editing strategies are required.

***In vivo* gene editing as a therapy**

The development of current gene editing tools, in particular CRISPR-Cas9 technology, is rapidly moving forward the field of gene-correction strategies. Recently, this technology has been used to explore the efficacy of gene-editing the genetic defect in *mdx* [125–127]. In these studies, the CRISPR-Cas9 components were delivered using AAV vectors, and were delivered either directly intramuscularly or systemically. Long and colleagues showed by using this strategy in *mdx* mice that up to 25.5 % of TA fibers expressed dystrophin after intramuscular delivery as judged by immunofluorescent analysis. Systemic -intraperitoneal administration in this study- was less efficient [126].

Tabebordbar and colleagues isolated MuSCs from the *mdx/ Pax7 zgreen+* compound reporter mouse, and demonstrated truncated DMD transcripts in MuSC-derived myotubes *in vitro* [127], suggesting that the MuSCs had indeed been targeted *in vivo*. Recently, early results -2 months follow-up- from an *in vivo* gene-editing study in a canine model of DMD using CRISPR/Cas9 technology were reported showing improved histology in four dogs. After systemic delivery dystrophin levels up to 90% of WT levels were found depending on the tissue analyzed [128].

A recent study in a DMD model in nonhuman primates also showed effectivity of *in vivo* gene editing [129]. Despite these encouraging early results, caution is warranted. *In vivo* gene-editing is still associated with safety concerns [130] and is still rather inefficient. Further study is required for the development of safe and efficient gene-editing method for future clinical implementation.

Conclusion

In this review we focused on the mechanism of the observed failing regenerative response in Pompe disease and conclude that the failure to efficiently activate MuSCs contributes to ongoing muscle wasting. In the absence of muscle regeneration, muscle damage is not compensated by repair. To restore the regenerative balance, novel therapies may be directed to activate MuSCs directly - through direct administration of MuSC-activating agents - or indirectly, for instance by targeting autophagic activity. In particular, exercise therapy aimed to activate the inactive MuSC population is minimally invasive and has proven to be well-tolerated by patients. Based on the safety profile exercise therapy can be assumed to have clinical feasibility, although studies into their regenerative efficacy are warranted.

References

1. van der Ploeg AT, Reuser AJ. Pompe's disease. *Lancet*. 2008;372(9646):1342-1353. doi:10.1016/S0140-6736(08)61555-X
2. Ebbink BJ, Aarsen FK, Van Gelder CM, et al. Cognitive outcome of patients with classic infantile Pompe disease receiving enzyme therapy. *Neurology*. 2012;78(19):1512-1518. doi:10.1212/WNL.0b013e3182553c11
3. Spiridigliozzi GA, Heller JH, Case LE, et al. Early cognitive development in children with infantile Pompe disease. *Mol Genet Metab*. 2012. doi:10.1016/j.ymgme.2011.10.012
4. van der Ploeg AT, Clemens PR, Corzo D, et al. A randomized study of alglucosidase alfa in late-onset Pompe's disease. *N Engl J Med*. 2010;362(15):1396-1406. doi:10.1056/NEJMoa0909859
5. Van den Hout JMP, Kamphoven JHJ, Winkel LPF, et al. Long-Term Intravenous Treatment of Pompe Disease With Recombinant Human α -Glucosidase From Milk. *Pediatrics*. 2004;113(5):e448-e457. doi:10.1542/peds.113.5.e448
6. Kuperus E, Kruijshaar ME, Wens SCA, et al. Long-term benefit of enzyme replacement therapy in Pompe disease. *Neurology*. 2017;89(23):2365-2373. doi:10.1212/WNL.0000000000004711
7. Bergsma AJ, in 't Groen SL, Verheijen FW, et al. From Cryptic Toward Canonical Pre-mRNA Splicing in Pompe Disease: a Pipeline for the Development of Antisense Oligonucleotides. *Mol Ther - Nucleic Acids*. 2016;5(9):e361. doi:10.1038/mtna.2016.75
8. Kohler L, Puertollano R, Raben N. Pompe Disease: From Basic Science to Therapy. *Neurotherapeutics*. 2018. doi:10.1007/s13311-018-0655-y
9. Bonne G, Rivier F, Hamroun D. The 2019 version of the gene table of neuromuscular disorders (nuclear genome). *Neuromuscular Disorders*. 2018.
10. Raben N, Nagaraju K, Lee E, et al. Targeted disruption of the acid α -glucosidase gene in mice causes an illness with critical features of both infantile and adult human glycogen storage disease type II. *J Biol Chem*. 1998;273(30):19086-19092. doi:10.1074/jbc.273.30.19086
11. Thurberg BL, Lynch Maloney C, Vaccaro C, et al. Characterization of pre- and post-treatment pathology after enzyme replacement therapy for Pompe disease. *Lab Invest*. 2006;86(12):1208-1220. doi:10.1038/labinvest.3700484
12. Ebbink BJ, Poelman E, Plug I, et al. Cognitive decline in classic infantile Pompe disease: An underacknowledged challenge. *Neurology*. 2016;86(13):1260-1261. doi:10.1212/WNL.0000000000002523
13. Seranova E, Connolly KJ, Zatyka M, et al. Dysregulation of autophagy as a common mechanism in lysosomal storage diseases. *Essays Biochem*. 2017. doi:10.1042/EBC20170055
14. Pichiecchio A, Uggetti C, Ravaglia S, et al. Muscle MRI in adult-onset acid maltase deficiency. *Neuromuscul Disord*. 2004. doi:10.1016/j.nmd.2003.08.003
15. Carlier RY, Laforet P, Wary C, et al. Whole-body muscle MRI in 20 patients suffering from late onset Pompe disease: Involvement patterns. *Neuromuscul Disord*. 2011;21:791-799. doi:10.1016/j.nmd.2011.06.748
16. van der Beek N a ME, de Vries JM, Hagemans MLC, et al. Clinical features and predictors for disease natural progression in adults with Pompe disease: a nationwide prospective observational study. *Orphanet J Rare Dis*. 2012;7(1):88. doi:10.1186/1750-1172-7-88

17. MAURO A. Satellite cell of skeletal muscle fibers. *J Biophys Biochem Cytol.* 1961;9:493-495. doi:10.1083/jcb.9.2.493
18. Zammit PS, Golding JP, Nagata Y, et al. Muscle satellite cells adopt divergent fates: A mechanism for self-renewal? *J Cell Biol.* 2004. doi:10.1083/jcb.200312007
19. Shea KL, Xiang W, LaPorta VS, et al. Sprouty1 Regulates Reversible Quiescence of a Self-Renewing Adult Muscle Stem Cell Pool during Regeneration. *Cell Stem Cell.* 2010;6:117-129. doi:10.1016/j.stem.2009.12.015
20. Lepper C, Partridge TA, Fan C-M. An absolute requirement for Pax7-positive satellite cells in acute injury-induced skeletal muscle regeneration. *Development.* 2011;138:3639-3646. doi:10.1242/dev.067595
21. von Maltzahn J, Jones AE, Parks RJ, et al. Pax7 is critical for the normal function of satellite cells in adult skeletal muscle. *Proc Natl Acad Sci U S A.* 2013;110(41). doi:10.1073/pnas.1307680110
22. Gayraud-Morel B, Chrétien F, Flamant P, et al. A role for the myogenic determination gene Myf5 in adult regenerative myogenesis. *Dev Biol.* 2007. doi:10.1016/j.ydbio.2007.08.059
23. Blau HM, Webster C, Pavlath GK. Defective myoblasts identified in Duchenne muscular dystrophy. *Proc Natl Acad Sci U S A.* 1983;80:4856-4860. doi:10.1073/pnas.80.15.4856
24. Thornell LE, Lindstöm M, Renault V, et al. Satellite cell dysfunction contributes to the progressive muscle atrophy in myotonic dystrophy type 1. *Neuropathol Appl Neurobiol.* 2009. doi:10.1111/j.1365-2990.2009.01014.x
25. Wanschitz J V., Dubourg O, Lacene E, et al. Expression of myogenic regulatory factors and myo-endothelial remodeling in sporadic inclusion body myositis. *Neuromuscul Disord.* 2013;23(1):75-83. doi:10.1016/j.nmd.2012.09.003
26. Renault V, Piron-Hamelin G, Forestier C, et al. Skeletal muscle regeneration and the mitotic clock. In: *Experimental Gerontology.* Vol 35. ; 2000:711-719. doi:10.1016/S0531-5565(00)00151-0
27. Decary S, Ben Hamida C, Mouly V, et al. Shorter telomeres in dystrophic muscle consistent with extensive regeneration in young children. *Neuromuscul Disord.* 2000;10:113-120. doi:10.1016/S0960-8966(99)00093-0
28. Ishimoto S, Goto I, Ohta M, et al. A quantitative study of the muscle satellite cells in various neuromuscular disorders. *J Neurol Sci.* 1983;62(1-3):303-314.
29. Kottlors M, Kirschner J. Elevated satellite cell number in Duchenne muscular dystrophy. *Cell Tissue Res.* 2010;340:541-548. doi:10.1007/s00441-010-0976-6
30. Wakayama Y. Electron microscopic study on the satellite cell in the muscle of Duchenne muscular dystrophy. *J Neuropathol Exp Neurol.* 1976;35(5):532-540. <http://www.ncbi.nlm.nih.gov/pubmed/956871>.
31. Sanoudou D, Haslett JN, Kho AT, et al. Expression profiling reveals altered satellite cell numbers and glycolytic enzyme transcription in nemaline myopathy muscle. *Proc Natl Acad Sci.* 2003. doi:10.1073/pnas.0330960100
32. Schaaf GJ, van Gestel TJ, Brusse E, et al. Lack of robust satellite cell activation and muscle regeneration during the progression of Pompe disease. *Acta Neuropathol Commun.* 2015;3:65. doi:10.1186/s40478-015-0243-x
33. Rosales XQ, Malik V, Sneh A, et al. Impaired regeneration in LGMD2A supported by increased PAX7-positive satellite cell content and muscle-specific microRNA dysregulation. *Muscle and Nerve.* 2013. doi:10.1002/mus.23669

34. Iannotti FA, Pagano E, Guardiola O, et al. Genetic and pharmacological regulation of the endocannabinoid CB1 receptor in Duchenne muscular dystrophy. *Nat Commun.* 2018. doi:10.1038/s41467-018-06267-1
35. Jiang C, Wen Y, Kuroda K, et al. Notch signaling deficiency underlies age-dependent depletion of satellite cells in muscular dystrophy. *Anal Quant Cytol Histol.* 2014;36(1):997-1004. doi:10.1242/dmm.015917
36. Schaaf GJ, van Gestel TJM, in 't Groen SLM, et al. Satellite cells maintain regenerative capacity but fail to repair disease-associated muscle damage in mice with Pompe disease. *Acta Neuropathol Commun.* 2018;6(1):119. doi:10.1186/s40478-018-0620-3
37. Lagalice L, Pichon J, Gougeon E, et al. Satellite cells fail to contribute to muscle repair but are functional in Pompe disease (glycogenosis type II). *Acta Neuropathol Commun.* 2018. doi:10.1186/s40478-018-0609-y
38. Dumont NA, Wang YX, von Maltzahn J, et al. Dystrophin expression in muscle stem cells regulates their polarity and asymmetric division. *Nat Med.* 2015;21(12):1455-1463. doi:10.1038/nm.3990
39. Attia M, Maurer M, Robinet M, et al. Muscle satellite cells are functionally impaired in myasthenia gravis: consequences on muscle regeneration. *Acta Neuropathol.* 2017;134(6):869-888. doi:10.1007/s00401-017-1754-2
40. Almada AE, Wagers AJ. Molecular circuitry of stem cell fate in skeletal muscle regeneration, ageing and disease. *Nat Rev Mol Cell Biol.* 2016;17(5):267-279. doi:10.1038/nrm.2016.7
41. Feige P, Brun CE, Ritso M, et al. Orienting Muscle Stem Cells for Regeneration in Homeostasis, Aging, and Disease. *Cell Stem Cell.* 2018. doi:10.1016/j.stem.2018.10.006
42. Bijvoet AGA, Van De Kamp EHM, Kroos MA, et al. Generalized glycogen storage and cardiomegaly in a knockout mouse model of Pompe disease. *Hum Mol Genet.* 1998;7:53-62. doi:10.1093/hmg/7.1.53
43. Webster C, Blau HM. Accelerated age-related decline in replicative life-span of Duchenne muscular dystrophy myoblasts: Implications for cell and gene therapy. *Somat Cell Mol Genet.* 1990;16(6):557-565. doi:10.1007/BF01233096
44. Sacco A, Mourkioti F, Tran R, et al. Short telomeres and stem cell exhaustion model duchenne muscular dystrophy in mdx/mTR mice. *Cell.* 2010;143(7):1059-1071. doi:10.1016/j.cell.2010.11.039
45. Tichy ED, Sidibe DK, Tierney MT, et al. Single Stem Cell Imaging and Analysis Reveals Telomere Length Differences in Diseased Human and Mouse Skeletal Muscles. *Stem Cell Reports.* 2017;9(4):1328-1341. doi:10.1016/j.stemcr.2017.08.003
46. Capell BC, Collins FS. Human laminopathies: nuclei gone genetically awry. *Nat Rev Genet.* 2006;7:940. <https://doi.org/10.1038/nrg1906>.
47. Frock RL, Kudlow B a, Evans AM, et al. Lamin A/C and emerin are critical for skeletal muscle satellite cell differentiation. *Genes Dev.* 2006;20(4):486-500. doi:10.1101/gad.1364906
48. Tang AH, Rando TA. Induction of autophagy supports the bioenergetic demands of quiescent muscle stem cell activation. *EMBO J.* 2014;33(23):2782-2797.
49. Sousa-Victor P, Gutarra S, García-Prat L, et al. Geriatric muscle stem cells switch reversible quiescence into senescence. *Nature.* 2014;506(7488):316-321. doi:10.1038/nature13013
50. Fiacco E, Castagnetti F, Bianconi V, et al. Autophagy regulates satellite cell ability to regenerate normal and dystrophic muscles. *Cell Death Differ.* 2016. doi:10.1038/cdd.2016.70

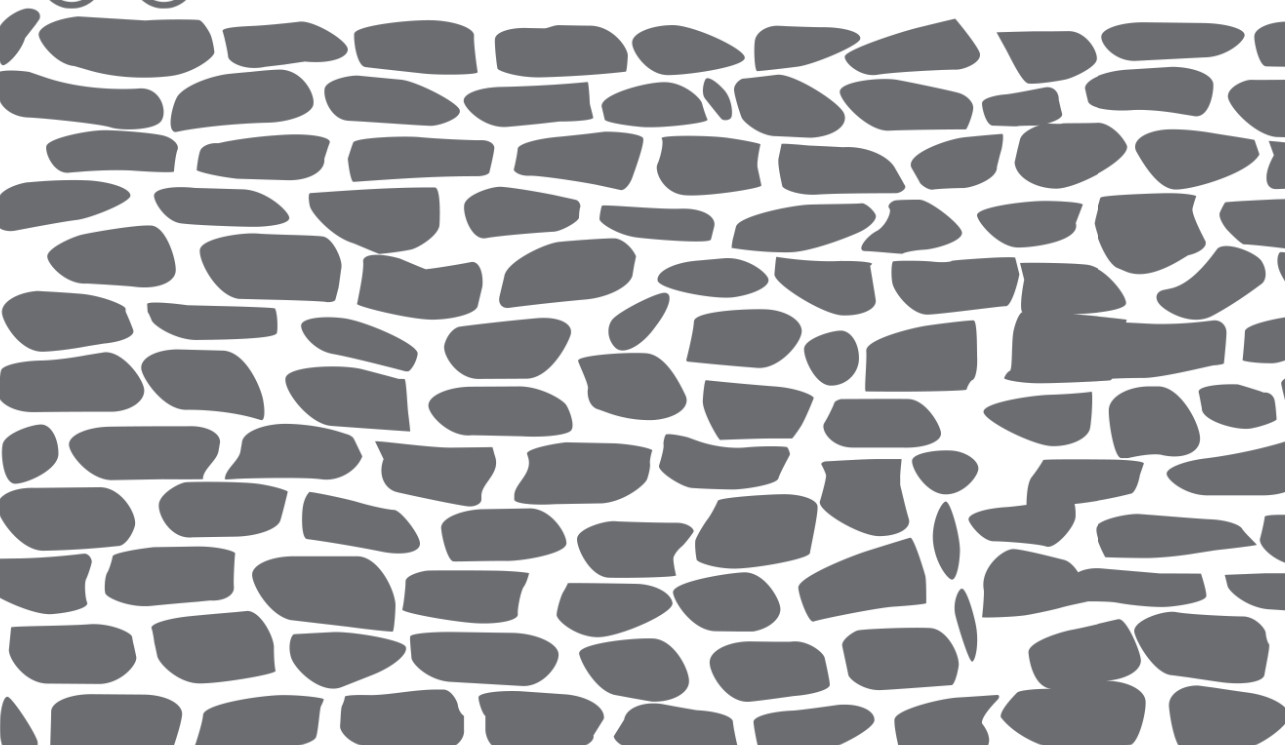
51. Paolini A, Omairi S, Mitchell R, et al. Attenuation of autophagy impacts on muscle fibre development, starvation induced stress and fibre regeneration following acute injury. *Sci Rep*. 2018. doi:10.1038/s41598-018-27429-7
52. Matsumoto A, Pasut A, Matsumoto M, et al. MTORC1 and muscle regeneration are regulated by the LINC00961-encoded SPAR polypeptide. *Nature*. 2017. doi:10.1038/nature21034
53. Sandri M. Autophagy in skeletal muscle. *FEBS Lett*. 2010. doi:10.1016/j.febslet.2010.01.056
54. Mammucari C, Milan G, Romanello V, et al. FoxO3 Controls Autophagy in Skeletal Muscle In Vivo. *Cell Metab*. 2007. doi:10.1016/j.cmet.2007.11.001
55. Masiero E, Agatea L, Mammucari C, et al. Autophagy Is Required to Maintain Muscle Mass. *Cell Metab*. 2009. doi:10.1016/j.cmet.2009.10.008
56. Masiero E, Sandri M. Autophagy inhibition induces atrophy and myopathy in adult skeletal muscles. *Autophagy*. 2010. doi:10.4161/auto.6.2.11137
57. De Palma C, Morisi F, Cheli S, et al. Autophagy as a new therapeutic target in Duchenne muscular dystrophy. *Cell Death Dis*. 2014. doi:10.1038/cddis.2014.312
58. Dowling JJ, Moore SA, Kalimo H, et al. X-linked myopathy with excessive autophagy: a failure of self-eating. *Acta Neuropathol*. 2015. doi:10.1007/s00401-015-1393-4
59. Nascimbeni AC, Fanin M, Angelini C, et al. Autophagy dysregulation in Danon disease. *Cell Death Dis*. 2017;8(1). doi:10.1038/cddis.2016.475
60. Nascimbeni AC, Fanin M, Masiero E, et al. The role of autophagy in the pathogenesis of glycogen storage disease type II (GSDII). *Cell Death Differ*. 2012;19:1698-1708. doi:10.1038/cdd.2012.52
61. Fukuda T, Ewan L, Bauer M, et al. Dysfunction of endocytic and autophagic pathways in a lysosomal storage disease. *Ann Neurol*. 2006. doi:10.1002/ana.20807
62. Raben N, Hill V, Shea L, et al. Suppression of autophagy in skeletal muscle uncovers the accumulation of ubiquitinated proteins and their potential role in muscle damage in Pompe disease. *Hum Mol Genet*. 2008;17(24):3897-3908. doi:10.1093/hmg/ddn292
63. Schoser BGH, Müller-Höcker J, Horvath R, et al. Adult-onset glycogen storage disease type 2: Clinico-pathological phenotype revisited. *Neuropathol Appl Neurobiol*. 2007. doi:10.1111/j.1365-2990.2007.00839.x
64. Rodríguez-Arribas M, Niso-Santano M, C.J. Pinheiro De Castro D, et al. Pompe Disease and Autophagy: Partners in Crime, or Cause and Consequence? *Curr Med Chem*. 2016. doi:10.2174/1567201812666150122131046
65. Lim JA, Zare H, Puertollano R, et al. Atg5flox-Derived Autophagy-Deficient Model of Pompe Disease: Does It Tell the Whole Story? *Mol Ther - Methods Clin Dev*. 2017. doi:10.1016/j.omtm.2017.08.002
66. Mashinchian O, Pisconti A, Le Moal E, et al. The Muscle Stem Cell Niche in Health and Disease. In: *Current Topics in Developmental Biology*.; 2018. doi:10.1016/bs.ctdb.2017.08.003
67. Bischoff R. A satellite cell mitogen from crushed adult muscle. *Dev Biol*. 1986;115:140-147. doi:10.1016/0012-1606(86)90235-6
68. Wozniak AC, Anderson JE. Nitric oxide-dependence of satellite stem cell activation and quiescence on normal skeletal muscle fibers. *Dev Dyn*. 2007. doi:10.1002/dvdy.21012
69. Bobadilla M, Sáinz N, Rodriguez J, et al. MMP-10 is required for efficient muscle regeneration in mouse models of injury and muscular dystrophy. *Stem Cells*. 2014. doi:10.1002/stem.1553

70. Kherif S, Lafuma C, Dehaupas M, et al. Expression of matrix metalloproteinases 2 and 9 in regenerating skeletal muscle: A study in experimentally injured and mdx muscles. *Dev Biol*. 1999. doi:10.1006/dbio.1998.9107
71. Tatsumi R. Release of Hepatocyte Growth Factor from Mechanically Stretched Skeletal Muscle Satellite Cells and Role of pH and Nitric Oxide. *Mol Biol Cell*. 2002. doi:10.1091/mbc.e02-01-0062
72. Pawlikowski B, Orion Vogler T, Gadek K, et al. Regulation of Skeletal Muscle Stem Cells by Fibroblast Growth Factors. *Dev Dyn*. 2017. doi:10.1002/dvdy.24495
73. Chakkalakal J V., Jones KM, Basson MA, et al. The aged niche disrupts muscle stem cell quiescence. *Nature*. 2012. doi:10.1038/nature11438
74. Joe AW, Yi L, Natarajan A, et al. Muscle injury activates resident fibro/adipogenic progenitors that facilitate myogenesis. *Nat Cell Biol*. 2010;12(2):153-163. doi:10.1038/ncb2015
75. Mueller AA, Van Velthoven CT, Fukumoto KD, et al. Intronic polyadenylation of PDGFR α in resident stem cells attenuates muscle fibrosis. *Nature*. 2016;540(7632):276-279. doi:10.1038/nature20160
76. Tidball JG. Regulation of muscle growth and regeneration by the immune system. *Nat Rev Immunol*. 2017;17(3):165-178. doi:10.1038/nri.2016.150
77. Heredia JE, Mukundan L, Chen FM, et al. Type 2 innate signals stimulate fibro/adipogenic progenitors to facilitate muscle regeneration. *Cell*. 2013;153:376-388. doi:10.1016/j.cell.2013.02.053
78. Ghadiali RS, Guimond SE, Turnbull JE, et al. Dynamic changes in heparan sulfate during muscle differentiation and ageing regulate myoblast cell fate and FGF2 signalling. *Matrix Biol*. 2017. doi:10.1016/j.matbio.2016.07.007
79. Doe JA, Allred ET, Elorza M, et al. Transgenic overexpression of the $\alpha 7$ integrin reduces muscle pathology and improves viability in the dyW mouse model of merosin-deficient congenital muscular dystrophy type 1A. *J Cell Sci*. 2011. doi:10.1242/jcs.083311
80. Charifi N, Kadi F, Féasson L, et al. Effects of endurance training on satellite cell frequency in skeletal muscle of old men. *Muscle and Nerve*. 2003. doi:10.1002/mus.10394
81. Kadi F, Eriksson A, Holmner S, et al. Cellular adaptation of the trapezius muscle in strength-trained athletes. *Histochem Cell Biol*. 1999. doi:10.1007/s004180050348
82. Verdijk LB, Snijders T, Drost M, et al. Satellite cells in human skeletal muscle; from birth to old age. *Age (Dordr)*. 2014;36:545-547. doi:10.1007/s11357-013-9583-2
83. Snijders T, Verdijk LB, Beelen M, et al. A single bout of exercise activates skeletal muscle satellite cells during subsequent overnight recovery. *Exp Physiol*. 2012;97:762-773. doi:10.1113/expphysiol.2011.063313
84. Bellamy LM, Joanisse S, Grubb A, et al. The acute satellite cell response and skeletal muscle hypertrophy following resistance training. *PLoS One*. 2014. doi:10.1371/journal.pone.0109739
85. Dreyer HC, Blanco CE, Sattler FR, et al. Satellite cell numbers in young and older men 24 hours after eccentric exercise. *Muscle and Nerve*. 2006. doi:10.1002/mus.20461
86. Bazgir B, Fathi R, Valojerdi MR, et al. Satellite cells contribution to exercise mediated muscle hypertrophy and repair. *Cell J*. 2016.
87. Jansen M, Van Alfen N, Geurts ACH, et al. Assisted bicycle training delays functional deterioration in boys with Duchenne muscular dystrophy: The randomized controlled trial "no use is disuse." *Neurorehabil Neural Repair*. 2013. doi:10.1177/1545968313496326

88. Sveen ML, Jeppesen TD, Hauerslev S, et al. Endurance training improves fitness and strength in patients with Becker muscular dystrophy. *Brain*. 2008. doi:10.1093/brain/awn189
89. Lohi EL, Lindberg C, Andersen O. Physical training effects in myasthenia gravis. *Arch Phys Med Rehabil*. 1993.
90. Tollback A, Eriksson S, Wredenberg A, et al. Effects of high resistance training in patients with myotonic dystrophy. *Scand J Rehabil Med*. 1999.
91. Vissing J. Exercise training in metabolic myopathies. *Rev Neurol (Paris)*. 2016. doi:10.1016/j.neurol.2016.08.005
92. Preisler N, Haller RG, Vissing J. Exercise in muscle glycogen storage diseases. *J Inherit Metab Dis*. 2015. doi:10.1007/s10545-014-9771-y
93. Favejee MM, van den Berg LE, Kruijshaar ME, et al. Exercise training in adults with Pompe disease: the effects on pain, fatigue, and functioning. *Arch Phys Med Rehabil*. 2015;96(5):817-822. doi:S0003-9993(14)01284-2 [pii]10.1016/j.apmr.2014.11.020
94. van den Berg LE, Favejee MM, Wens SC, et al. Safety and efficacy of exercise training in adults with Pompe disease: evaluation of endurance, muscle strength and core stability before and after a 12 week training program. *Orphanet J Rare Dis*. 2015;10(1):87. doi:10.1186/s13023-015-0303-010.1186/s13023-015-0303-0 [pii]
95. Hyldahl RD, Olson T, Welling T, et al. Satellite cell activity is differentially affected by contraction mode in human muscle following a work-matched bout of exercise. *Front Physiol*. 2014. doi:10.3389/fphys.2014.00485
96. Narkar VA, Downes M, Yu RT, et al. AMPK and PPAR Agonists Are Exercise Mimetics. *Cell*. 2008. doi:10.1016/j.cell.2008.06.051
97. Fu X, Zhu M, Zhang S, et al. Obesity Impairs Skeletal Muscle Regeneration Through Inhibition of AMPK. *Diabetes*. 2016;65(1):188-200. doi:10.2337/db15-0647
98. Hauerslev S, Vissing J, Krag TO. Muscle atrophy reversed by growth factor activation of satellite cells in a mouse muscle atrophy model. *PLoS One*. 2014;9. doi:10.1371/journal.pone.0100594
99. Lenhare L, Crisol BM, Silva VRR, et al. Physical exercise increases Sestrin 2 protein levels and induces autophagy in the skeletal muscle of old mice. *Exp Gerontol*. 2017;97:17-21. doi:10.1016/J.EXGER.2017.07.009
100. Schwalm C, Jamart C, Benoit N, et al. Activation of autophagy in human skeletal muscle is dependent on exercise intensity and AMPK activation. *FASEB J*. 2015;29(8):3515-3526. doi:10.1096/fj.14-267187
101. Hardie DG. AMPK and autophagy get connected. *EMBO J*. 2011. doi:10.1038/emboj.2011.12
102. Kotoulas OB, Kalamidas SA, Kondomerkos DJ. Glycogen autophagy in glucose homeostasis. *Pathol Res Pract*. 2006. doi:10.1016/j.prp.2006.04.001
103. Raben N, Schreiner C, Baum R, et al. Suppression of autophagy permits successful enzyme replacement therapy in a lysosomal storage disorder - Murine Pompe disease. *Autophagy*. 2010. doi:10.4161/auto.6.8.13378
104. Lim JA, Sun B, Puertollano R, et al. Therapeutic Benefit of Autophagy Modulation in Pompe Disease. *Mol Ther*. 2018. doi:10.1016/j.ymthe.2018.04.025
105. Pal R, Palmieri M, Loehr JA, et al. Src-dependent impairment of autophagy by oxidative stress in a mouse model of Duchenne muscular dystrophy. *Nat Commun*. 2014. doi:10.1038/ncomms5425

106. Puzzo F, Colella P, Biferi MG, et al. Rescue of Pompe disease in mice by AAV-mediated liver delivery of secretable acid α -glucosidase. *Sci Transl Med*. 2017. doi:10.1126/scitranslmed.aam6375
107. Corti M, Liberati C, Smith BK, et al. Safety of Intradiaphragmatic Delivery of Adeno-Associated Virus-Mediated Alpha α -glucosidase (rAAV1-CMV- hGAA) Gene Therapy in Children Affected by Pompe Disease. *Hum Gene Ther Clin Dev*. 2017. doi:10.1089/humc.2017.146
108. Le Guiner C, Servais L, Montus M, et al. Long-term microdystrophin gene therapy is effective in a canine model of Duchenne muscular dystrophy. *Nat Commun*. 2017. doi:10.1038/ncomms16105
109. Morgan JE, Counsell JR, Ferrer V, et al. Lentiviral vectors can be used for full-length dystrophin gene therapy. *Sci Rep*. 2017. doi:10.1038/s41598-017-00152-5
110. Van Til NP, Stok M, Aerts Kaya FSF, et al. Lentiviral gene therapy of murine hematopoietic stem cells ameliorates the Pompe disease phenotype. *Blood*. 2010;115(26):5329-5337. doi:10.1182/blood-2009-11-252874
111. Chamberlain JR, Chamberlain JS. Progress toward Gene Therapy for Duchenne Muscular Dystrophy. *Mol Ther*. 2017. doi:10.1016/j.yymthe.2017.02.019
112. Partridge TA, Morgan JE, Coulton GR, et al. Conversion of mdx myofibres from dystrophin-negative to -positive by injection of normal myoblasts. *Nature*. 1989. doi:10.1038/337176a0
113. Partridge TA, Grounds M, Sloper JC. Evidence of fusion between host and donor myoblasts in skeletal muscle grafts. *Nature*. 1978. doi:10.1038/273306a0
114. Briggs D, Morgan JE. Recent progress in satellite cell/myoblast engraftment - Relevance for therapy. *FEBS J*. 2013. doi:10.1111/febs.12273
115. Collins CA, Olsen I, Zammit PS, et al. Stem cell function, self-renewal, and behavioral heterogeneity of cells from the adult muscle satellite cell niche. *Cell*. 2005;122:289-301. doi:10.1016/j.cell.2005.05.010
116. Sacco A, Doyonnas R, Kraft P, et al. Self-renewal and expansion of single transplanted muscle stem cells. *Nature*. 2008;456:502-506. doi:10.1038/nature07384
117. Cerletti M, Jurga S, Witczak CA, et al. Highly Efficient, Functional Engraftment of Skeletal Muscle Stem Cells in Dystrophic Muscles. *Cell*. 2008;134:37-47. doi:10.1016/j.cell.2008.05.049
118. Schaaf GJ. Ex-vivo Expansion of Muscle-Regenerative Cells for the Treatment of Muscle Disorders. *J Stem Cell Res Ther*. 2012;01(S11). doi:10.4172/2157-7633.S11-003
119. Takahashi K, Yamanaka S. Induction of Pluripotent Stem Cells from Mouse Embryonic and Adult Fibroblast Cultures by Defined Factors. *Cell*. 2006;126(4):663-676. doi:10.1016/j.cell.2006.07.024
120. van der Wal E, Herrero-Hernandez P, Wan R, et al. Large-Scale Expansion of Human iPSC-Derived Skeletal Muscle Cells for Disease Modeling and Cell-Based Therapeutic Strategies. *Stem Cell Reports*. 2018;10(6):1975-1990. doi:10.1016/j.stemcr.2018.04.002
121. van der Wal E, Herrero-Hernandez P, Wan R, et al. Large-Scale Expansion of Human iPSC-Derived Skeletal Muscle Cells for Disease Modeling and Cell-Based Therapeutic Strategies. *Stem Cell Reports*. 2018;10(6):1975-1990. doi:10.1016/J.STEMCR.2018.04.002
122. van der Wal E, Bergsma AJ, van Gestel TJM, et al. GAA Deficiency in Pompe Disease Is Alleviated by Exon Inclusion in iPSC-Derived Skeletal Muscle Cells. *Mol Ther - Nucleic Acids*. 2017;7:101-115.

123. van der Wal E, Bergsma AJ, Pijnenburg JM, et al. Antisense Oligonucleotides Promote Exon Inclusion and Correct the Common c.-32-13T>G GAA Splicing Variant in Pompe Disease. *Mol Ther - Nucleic Acids*. 2017. doi:10.1016/j.omtn.2017.03.001
124. Bergsma AJ, van der Wal E, Broeders M, et al. Alternative Splicing in Genetic Diseases: Improved Diagnosis and Novel Treatment Options. In: *International Review of Cell and Molecular Biology*. ; 2018;335:85-141. doi:10.1016/bs.ircmb.2017.07.008
125. Nelson CE, Soltys S, Rengo G, et al. In vivo genome editing improves muscle function in a mouse model of Duchenne muscular dystrophy. *Science (80-)*. 2016.
126. Long C, Amoasii L, Mireault AA, et al. Postnatal genome editing partially restores dystrophin expression in a mouse model of muscular dystrophy. *Science (80-)*. 2016. doi:10.1126/science.aad5725
127. Tabebordbar T, Zhu K, Cheng JKW, et al. In vivo gene editing in dystrophic mouse muscle and muscle stem cells. *Science (80-)*. 2016. doi:10.1126/science.aad5177
128. Amoasii L, Hildyard JCW, Li H, et al. Gene editing restores dystrophin expression in a canine model of Duchenne muscular dystrophy. *Science (80-)*. 2018;362(6410):86-91. doi:10.1126/SCIENCE.AAU1549
129. Wang S, Ren S, Bai R, et al. No off-target mutations in functional genome regions of a CRISPR/Cas9-generated monkey model of muscular dystrophy. *J Biol Chem*. 2018;293(30):11654-11658. doi:10.1074/jbc.AC118.004404
130. Kosicki M, Tomberg K, Bradley A. Repair of double-strand breaks induced by CRISPR-Cas9 leads to large deletions and complex rearrangements. *Nat Biotechnol*. 2018. doi:10.1038/nbt.4192



Chapter 4

An *in vitro* assay to quantify satellite cell activation using isolated mouse myofibers

**Rodrigo Canibano-Fraile^{1,2,3}, Emma Boertjes^{1,2,3}, Stela Bozhilova^{1,2,3},
W.W.M. Pim Pijnappel^{1,2,3}, and Gerben J. Schaaf^{1,2,3,4,5*}**

¹Department of Clinical Genetics, Erasmus MC University Medical Center, 3015 GD Rotterdam, the Netherlands.

²Department of Pediatrics, Erasmus MC University Medical Center, 3015 GD Rotterdam, the Netherlands.

³Center for Lysosomal and Metabolic Diseases, Erasmus MC University Medical Center, 3015 GE Rotterdam, the Netherlands.

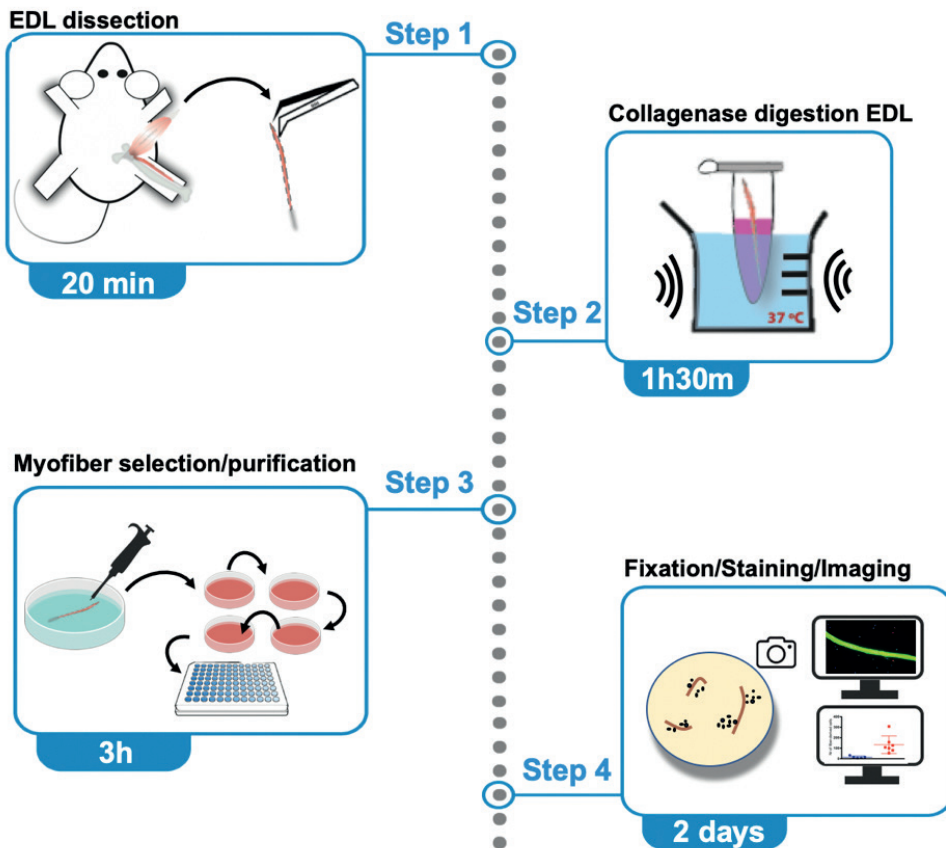
⁴Technical Contact

⁵Lead Contact

*Corresponding Author: g.schaaf@erasmusmc.nl

STAR Protoc. 2021;2(2):100482. doi:10.1016/j.xpro.2021.100482

Graphical abstract



Summary

Isolated myofibers offer the possibility of *in vitro* study of satellite cells in their niche. We describe a mouse myofiber isolation assay to assess satellite cell activation by quantifying myofiber-derived satellite cell progeny. The assay allows isolation of myofibers from mouse using standard equipment and reagents. It can be used to compare satellite cells across different mouse models or to evaluate their response to treatments, offering a valuable complementary tool for *in vitro* experimentation.

Before You Begin

Note: All animal experiments were approved by the local Animal Experiments Committee and national Central Committee for Animal Experiments (animal experiment authorities in compliance with the European Community Council Directive guidelines (EU directive 86/609), regarding the protection of animals used for experimental purposes. All procedures with the animals were performed with the aim of ensuring that discomfort, distress, pain, and injury would be minimal.

Prepare in advance

Timing: 1 – 2 hours (Optional: prepare one day before)

Note: Working under clean conditions is important to reduce the risk of contaminations. If possible work inside a laminar flow cabinet. As indicated below, EDL dissection and fiber selection/purification steps were performed outside the flow cabinet as the setup with the dissection microscope and plate warmer did not fit inside the flow cabinet. All other steps were performed inside a laminar flow cabinet. To allow working outside a laminar flow environment, clean all working surfaces and tools with 70% ethanol (EtOH) and disinfect pipet tips before use, sequentially in 70% EtOH, PBS, and horse serum (HS) (see Optional, below Step-by-step Method Details Step 10c). The media used in this protocol contain antibiotics (10,000 units penicillin and 10 mg streptomycin per mL) to minimize bacterial growth.

1. Prepare digestion solution. Weigh collagenase type II (Col II; 1000 U/ml in dilution medium (see below); aliquot per ml; in our hands it can be stored at -80°C for up to 6 months with negligible loss of yield; 2x 1 ml Col II per mouse) (See Troubleshooting – Problem 1).

Note: The use of collagenase is critical for correct tissue digestion. Other collagenase types have been reported to work (e.g collagenase type I) [1]. This protocol has been optimized using collagenase type II (see Key Resources Table).

Note: Processing fibers from one mouse (i.e. 2 EDLs) takes 7-8 hours per researcher, including plating fibers under experimental conditions.

2. Prepare media (use within 2 weeks after preparation) (See Troubleshooting – Problem 3). See Materials and Equipment for the procedures:
 - a. Fiber selection medium. 100 ml per mouse. Store at 4°C.
 - b. Proliferation medium. 10 ml per 96 well plate. Store at 4°C.
 - c. Experiment base medium. 10 ml per 96 well plate. Store at 4°C.
 - d. Dilution medium. 500 ml. Store at 4°C.
3. Coat 96-well plates with 5% ECM (v/v):
 - a. Cover culture surface with cold ECM (typically 30 µl per well in 96 well format. Incubate at 4°C for 30 min. ECM can be re-used twice if kept cold through the whole process. Keep 5% solution on ice and store at 4°C.
 - b. Remove ECM solution and incubate coated plate(s) at 37°C for 30 min or 12-16 hours at 18-22°C.

Optional: coat for 2nd time: Repeat 3a-b.

Note: Coating for a second time may improve the adherence of fibers. Its use is advised if fibers do not adhere well to the bottom of the plates.

Before the experiment

Timing: 1 hour

4. Incubate 4 x 100 mm cell culture dishes per EDL (8 dishes per mouse) with 100% horse serum (HS) for 30 min at 37°C. This will prevent fibers adhering to the dishes during the purification procedure.
5. Label dishes 1-1, 1-2, 1-3, 1-4 for EDL 1; and 2-1, 2-2, 2-3, 2-4 for EDL 2.
6. Replace HS with 10 mL of fiber selection medium for the first 3 dishes of each EDL (1-1, 1-2, 1-3, and 2-1, 2-2, 2-3).
7. Return the dishes to 37°C until use.
8. Replace HS with 10 mL of experiment base medium for dishes 1-4 and 2-4. This is done to prevent altering the experiment medium composition by mixing it with fiber selection medium (See Step-by-step Methods Details Step 11g-h).

9. Prewarm Col II solution to 37°C in Eppendorf tube heater.
10. Prewarm Slide Warmer.

Note: To calibrate the temperature settings of the slide warmer place a 6-well-plate with medium and adjust temperature setting so that medium temperature remains 37°C. The slide warmer that was used in this protocol was set to 40°C. The slide warmer will be used to keep the dishes warm during fiber selection or during medium changes to avoid fiber contraction. Dishes with fibers should not be kept outside of the incubators for longer than 10 min despite using the slide warmer.

11. Prepare a disinfected working space, work if possible in a laminar flow cabinet.
 - a. Spray surgical area with 70% EtOH.
 - b. Disinfect surgical tools using 70% ethanol: 1 x fine-tip forceps (Extra Fine #5, DBIO), 1x blunt serrated forceps (Standard Forceps, DBIO), 1x scissors (Standard Pattern - Sharp/Blunt, DBIO), 1x fine scissors (Slim iris, DBIO), 1x surgical knife (Disposable Sterile Scalpel 11, Swann-Morton).
 - c. 4x 25G needles (Sterican 100, Braun).
 12. Prepare experiment plates; time spent on this step is largely dependent on the number of plates and treatments (approximately 30-60 minutes for 2 EDL muscles when plating all viable myofibers).
 - a. Coat 96 well plates (Corning 96-well flat-bottom tissue culture plate) or polymer-based 96-well tissue culture plates allowing imaging (Nunc Nunclon 96-well plate with lid, Electron Microscopy Sciences) with 1:20 diluted ECM. We recommend at least 10 wells per treatment/genotype myofiber.
 - b. Dilute experiment additives (i.e. growth factors, inhibitors, agonists, siRNA) in experiment base medium to twice the final concentration ($2 \times [\text{Conc}]_{\text{final}}$) in sterile Eppendorf tubes. The correct concentrations will be achieved after adding the fibers (See Note under Step-by-step Methods Details Step 12c).
 - c. Distribute 50 μ l/well of the prepared experiment media over the appropriate wells. Fill outer wells with PBS to minimize evaporation of medium from treatment wells.
 - d. Keep 96 well plate with pre-prepared experiment medium at 4°C until 15 min before plating (See Step-by-step Methods Details Step 12a).
3. Collect equipment:

- a. Dissecting microscope (Olympus SZX16 was used for this purpose).
- b. 20-200 ml and 100-1000 ml pipettes.
- c. Sterile 200 and 1000 ml unfiltered tips and Eppendorf tubes.
- d. Scissors (to cut tips, clean and EtOH sterilize).
- e. Slidewarmer (Slidewarmer SW85 - Adamas Instruments or equivalent).
- f. Eppendorf tube heater (Eppendorf Thermomixer R for this purpose).

Materials and Equipment

Reagent	Used in text	Final concentration	Solvent	Storage
Phosphate Buffer Saline	PBS	N/A	N/A	4°C; >1 year
DMEM	DMEM	N/A	N/A	4°C; 1 month
Ham's F10	Ham's F10	N/A	N/A	4°C; 1 month
Fetal Calf Serum	FCS	User-defined	User-defined	-20°C; 1-12 months
Horse Serum	HS	User-defined	User-defined	-20°C; 1-12 months
Penicillin-Streptomycin	Pen-Strep	100 U/mL	PBS	-20°C; 1-12 months
Chicken Embryo Extract	CEE	1% (v/v)	User-defined	4°C; 1-6 months
Knockout Serum Replacement	KSR	5% (v/v)	Experiment base medium	-20°C; 1-12 months
Basic FGF	FGF2	20 ng/mL	PBA	-80°C; 1-12 months
Extracellular Matrix	ECM	5%	Dilution medium	4°C; 1 month
Collagenase Type II	Col II	1000 U/mL	Dilution medium	-20°C; 1-12 months
Paraformaldehyde	PFA	8% (w/v), NaOH (to dissolve); pH 7.0	PBS	-20°C; 1-12 months
PBS-BSA	PBA	0.1% BSA (w/v)	PBS	4°C; 1 month
PBS-BSA-Tween 20	PBA-Tw	0.1% BSA (w/v) 0.1% Tw20 (v/v)	PBS	4°C; 1 month
PBS-Tween 20	PBS-Tw	0.1% Tw20 (v/v)	PBS	4°C; 1 month
PBS-Triton X-100	Triton	0.5 Triton X-100 (v/v)	PBS	4°C; 1 month
Hoechst	Hoechst	1 µg/mL	PBS	4°C; >1 year

Fiber selection medium

Store at 4°C for maximum 1 month.

Solution	Volume	Final concentration
DMEM	445 mL	-
FCS	25 mL	5%
HS	25 mL	5%
Penicillin-Streptomycin	5 mL	1%
Total	500 mL	-

4

Proliferation medium

Store at 4°C for maximum 1 month.

Solution	Volume	Final concentration
Ham's F10	390 mL	-
FCS	100 mL	20%
CEE	5 mL	1%
Penicillin-Streptomycin	5 mL	1%
Total	500 mL	-

Experiment base medium

Store at 4°C for maximum 1 month.

Solution	Volume	Final concentration
DMEM	440 mL	-
HS	25 mL	5%
KSR	25 mL	5%
CEE	5 mL	1%
Penicillin-Streptomycin	5 mL	1%
Total	500 mL	-

Dilution medium

Store at 4°C for maximum 1 month.

Solution	Volume	Final concentration
DMEM	470 mL	-
FCS	25 mL	5%
Penicillin-Streptomycin	5 mL	1%
Total	500 mL	-

CRITICAL: Paraformaldehyde (PFA) is toxic after swallowing or inhalation, causes skin irritation, harmful to eyes and respiratory tract; a potential carcinogen. Use in a safety cabinet or with sufficient ventilation. Wear protective measures (gloves, protective eye wear, facemask).

Step-by-Step Method Details

Dissecting extensor digitorum longus

Timing: 20 minutes per mouse

In this step of the protocol EDL muscles from a mouse will be dissected as source of myofibers. This protocol is optimized for muscles that have clear identifiable tendinous insertions at both ends. Recently, a method that allows isolation of fibers from sources without tendinous ends has been published [2]. We have successfully isolated fibers from soleus muscles using this protocol. Others have reported isolating myofibers from flexor digitorum brevis (FDB; [3], but we have not tried this. The surgery is a critical step; therefore, the strategy needs to be optimized for muscles other than EDL. Stretching the target muscles will significantly decrease the yield of viable fibers. In addition, speed is an important factor, since allowing the muscle(s) to cool excessively will also decrease yield. For those starting with this protocol, practice EDL dissections on surplus mice (i.e. mice euthanized in other experiments) prior to the experiment are advised.

Note: These steps can be performed outside the laminar flow cabinet.

1. Euthanize mouse in line with institutional regulations. Here animals were killed by cervical dislocation.
2. Disinfect the hindlimbs with 70% EtOH.
3. Open the skin of one of the hindlegs to expose the lower leg muscles.
4. Remove the fascia covering the TA muscle from knee to ankle using the fine-tip forceps (Figure 1A).

Critical: Remove as much fascia as possible, as remaining fascia will complicate the next step. If fascia are not sufficiently removed it will require more force to liberate the TA and EDL from the underlying bone and from each other. Applying too much force may damage or stretch the muscle and may decrease the yield and viability of isolated fibers .

5. Free the TA/EDL muscles from the bone.
 - a. Insert the fine-tip forceps behind the ankle-tendons of both the EDL and TA (Figure 1B and 1F).
 - b. Liberate the EDL and TA muscles from the underlying tibial bone by moving the forceps behind the EDL/TA up and down from knee to ankle (Figure 1C and 1G).
6. Liberate the TA from the EDL.
 - a. Insert the fine tip forceps between the EDL and TA ankle tendons and lift up the TA and carefully move the forceps up towards the knee (Figure 1H).
 - b. Expose the proximal EDL and fibularis longus tendons by removing tissue around the patella.
 - c. Insert the fine tip forceps behind the proximal EDL and *fibularis longus* tendons.
 - d. Cut the proximal EDL tendon using a scalpel blade (Figure 1D and 1H).
7. Remove TA muscle.
 - a. Cut the TA distal tendon (near the ankle; Figure 1I).
 - b. Lift the TA at the distal tendon.
 - c. Cut TA proximal to the knee to remove it (Figure 1I). The EDL muscle is now exposed.
8. Remove the EDL muscle.
 - a. Carefully lift the EDL at the proximal tendon.

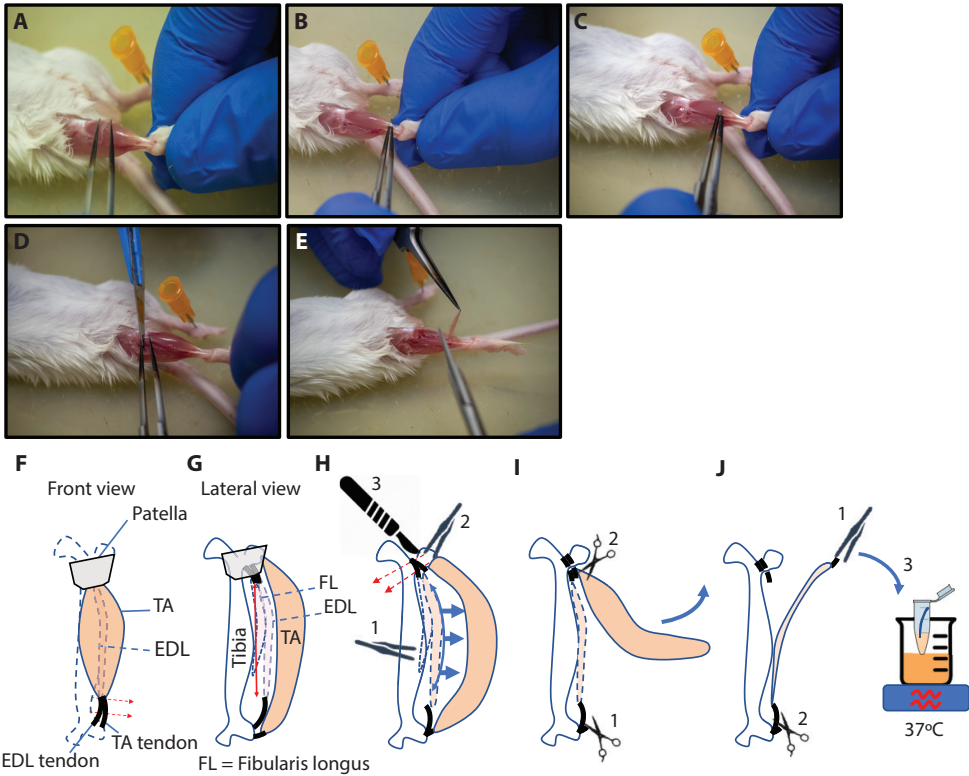


Figure 1: Dissecting the EDL. (A) Removing fascia; (B) Inserting fine-tip forceps between distal tendons; (C) Liberate EDL/TA from tibial bone; (D) Cutting proximal EDL tendon; (E) Removing EDL; (F-J) Schematic representation of the dissection steps. (F) Inserting fine-tip forceps between distal tendons; (G) Liberating EDL/TA from tibial bone; (H) Liberating TA from EDL (1), inserting forceps behind proximal tendons (2), and sectioning cutting proximal EDL tendon with a scalpel (3); (I) Cutting distal part of TA muscle (1), cutting proximal part of TA muscle (2) and removing TA; (J) Transferring EDL to digestion solution. Lift EDL at proximal tendon (1) and cut distal tendon to release EDL (2). The number in the pictures indicate the order of events.

Critical: Prevent stretching the EDL during handling (See Troubleshooting – Problem 1).

- b. Remove the EDL by cutting the distal (ankle) tendon (Figure 1E and J). Make sure to cut as distal as possible to ensure cutting the tendon, not the muscle .
- c. Place the EDL into a 1.5 mL tube with 1 mL of prewarmed Col II solution and shake (500 rpm) at 37°C for 1.5 h. in an Eppendorf Thermomixer (See Troubleshooting – Problem 1).

9. Repeat Step-by-Step Method Details Steps 3-7 for the remaining EDL.

Note: For some steps it may be easier to turn the animal 180° (head facing towards you) for dissecting the contralateral EDL.

Critical To increase the yield of intact myofibers ensure to (See Troubleshooting – Problem 2):

b. Work fast to prevent excessive cooling of EDL

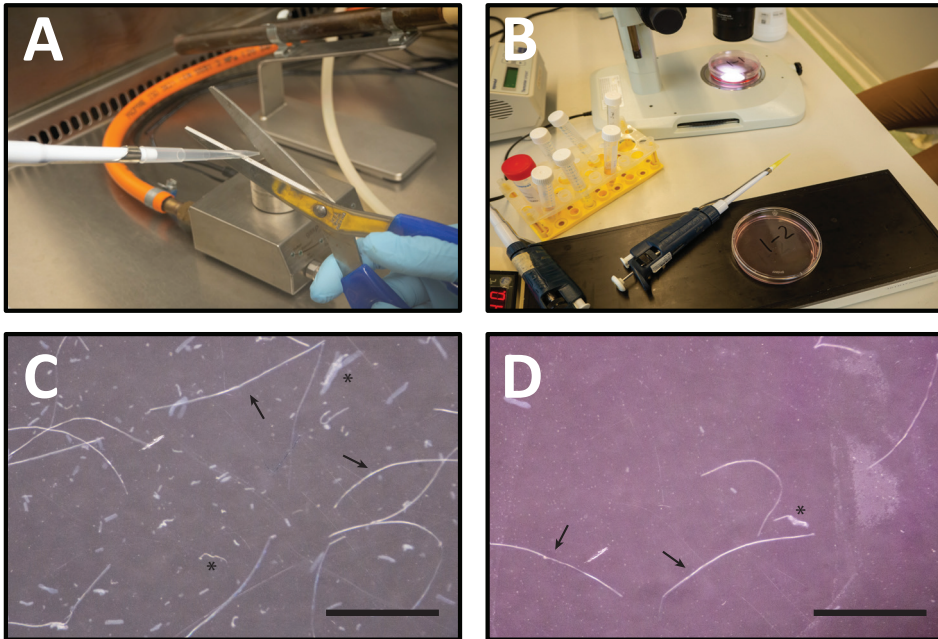


Figure 2: Setup of the material for purification. (A) Cutting and polishing pipet tips; (B) Fiber purification setup with slide warmer (bottom), dissecting microscope and two sequential dishes containing fiber medium; (C) fibers in early dish (dish #1-1) with fiber fragments and debris. Arrows indicate viable fibers. Asterisks indicate non-viable fibers/fiber fragments; (D) purified fibers in late dish (dish #1-3). Arrows indicate viable fibers. Asterisks indicate non-viable fibers/fiber fragments. Scale bars, 2 mm.

- b. Avoid damaging the EDL when liberating the muscles at Step-by-Step Method Details Steps 5-6
- c. Avoid stretching the EDL when removing it from the animal.

Purifying intact myofibers

Note: For adult FVB/N mice we usually get 150-250 fibers per EDL. Nevertheless, the yield of fibers per EDL will vary depending on the mouse model. For example, disease models with muscle damage may yield lower number of fibers compared with healthy mice (see Expected Outcomes).

Timing: 3 hours

In these steps the myofibers are liberated from the digested EDL muscle and subsequently purified by sequential transferring intact myofibers into clean dishes.

Note: These steps were performed outside a laminar flow cabinet. Prepare 3 x 15 mL conical tubes to disinfect and wash the utensils. 1 tube with 70% EtOH, 1 tube with PBS, and 1 tube with HS. For each use the pipet tips were cleansed by sequentially pipetting up/down 3 times in EtOH, PBS and HS. HS is to prevent fibers sticking to the walls of the pipet tips.

10. Liberate fibers from the digested muscles.

- a. Take purification dish #1 (dish 1-1) for the first EDL (EDL1) from incubator and place on slide warmer.
- b. Empty tube with EDL in dish #1-1.
- c. Cut ± 2 mm from the top of a sterile 1 mL plastic pipet tip (Fisher Scientific cat # 22170403) and polish by carefully passing the pipet tip through the flame (Figure 2A) (See Troubleshooting – Problem 1 and 2).

Optional: It may not be possible to fit the dissection microscope and the slide warmer inside the laminar flow cabinet. To work outside the laminar flow cabinet, prepare a clean curtailed/polished 1 mL pipet tip by pipetting up/down, respectively, EtOH, PBS and HS. The pipette is now ready to use. Repeat this step each time you insert the pipette tip in medium again.

- d. Pipet up/down with HS before using a new tip to coat it and prevent adhesion of muscle fibers to the inside of the tip.
- e. Release myofibers by pipetting EDL up/down using a P1000 pipette.

Critical: Aspirate and eject the EDL along the length axis; pipet in a smooth motion (Video S1: Liberating myofibers from digested EDL muscle). Too much force will damage the myofibers and decrease the yield and

viability of the isolated fibers. After the EDL breaks down in smaller parts, move the EDL parts along the length axis through the pipette tip (Video S2: Liberating individual myofibers from digested EDL fragments).

- f. Continue for maximally 10 min., then place dish #1-1 back in the 37 °C incubator. Leave the dish for at least 15 min to recover (See Troubleshooting – Problem 2).
- g. Perform Step-by-step Method Details Steps 10a-f for EDL2 in a new dish (dish 2-1).
- h. While myofibers released from EDL2 are recovering repeat Step-by-step Method Details Steps 10f-g for dish #1-1.

Alternate between dish #1-1 and #2-1 until no more fibers release.

Note: Although isolated viable myofibers can reach up to 5 mm in length, they are typically 1.5-3 mm long, transparent, with smooth sarcolemmal surface when visualized using phase contrast microscopy (Figure 2). However, it is unclear whether isolated fibers are intact fibers or whether they self-seal [4]. Cross-striations and protuberant peripheral nuclei are visible at 200x magnification. Contracting, dying, and damaged fibers are short, opaque and often curved.

11. Sequentially select viable myofibers.
 - a. Place dish #1-1 (with fibers) under the dissection microscope and dish #1-2 (empty dish with warm fiber selection medium) on the slide warmer (Figure 2B).
 - b. Curtail and flame-polish a 200 µL tip (Fisher Scientific cat # 10739254).

Note: The sharp edges left after cutting the tips using scissors may damage the fibers while pipetting up and down. Polishing using a flame will smoothen the edges of the tips for successful isolation of viable myofibers.

Optional: When working outside a laminar flow cabinet clean pipet tip through EtOH, PBS, and HS as described above. Repeat this for each new pipette tip.

- c. Transfer transparent, elongated, straight myofibers from dish #1-1 to dish #1-2 using a P200 pipette (Video S3: Transferring myofibers during purification; and S4: Transferring a single myofiber along the length axis). Avoid contracted and opaque fibers, fragments, and adipose tissue (Figure 2C).

- d. Continue selecting myofibers for maximally 10 min before returning the dishes to 37°C incubator. Leave the dishes for (at least) 15 min to recover.
- e. In the meanwhile, perform Step-by-step Method Details Steps 11a-d for dish #2-1 and #2-2.
- f. When dish #1-1 contains no more intact myofibers, repeat Step-by-step Method Details Steps 11a-d to transfer myofibers from dish #1-2 (under dissecting microscope) to dish #1-3 (on slide warmer). The same applies for EDL2: when dish #2-1 is empty, start transferring myofibers from dish #2-2 to #2-3.
- g. When dishes #1-3 and #2-3 contain no more viable myofibers (Figure 2D), move fibers to the dish with experiment base medium (dishes #1-4 and #2-4, respectively).

Note: Experiment base medium is medium used for the actual experiment but without experiment additives such as growth factors, inhibitors, activators etc. These additives have been added to the respective wells during plate preparation (see Before you begin Step 12).

- h. Continue transferring fibers to dish #1-4 and #2-4 until no more viable myofibers are detected in dish #1-3 and #2-3, respectively.

Note: When the yield is high (>250 myofibers from 2 EDL muscles), dishes #1-4 and #2-4 may still contain debris and fiber fragments. If necessary, add an extra purification step by introducing a fifth dish (dishes #1-5 and #2-5) with experiment base medium and continue purifying intact viable fibers. A highly pure collection of myofibers is necessary to prevent transferring contaminants to experimental wells.

Optional: If proliferation of non-myogenic cells is observed using this culturing strategy, an alternative plating method can be used to ensure formation of pure myogenic fiber-derived cultures, as described in the Optional Step below.

Optional Step: Single fibers can be first cultured for 48 hours in experiment base medium in dishes coated with 20% HS. This promotes contaminating non-myogenic cells to release from the fibers and to adhere to the dish, while at the same time preventing fibers to adhere to the bottom of the well. After this step, single fibers are replated in the experiment dishes and the protocol can continue as described below (*Step-by-step Method Details 12a*).

12. Plating myofibers for assessment of satellite cell activation.

- a. Place the 96-well plate prepared at Before you begin Step 12 in an incubator at 37°C for at least 15 min to warm.
- b. Place the 96-well plate on slide warmer.
- c. Use a freshly cut and polished tip (cleaned with EtOH, PBS and HS as described at the note before Step-by-step Method Details Step 10) to select a single viable myofiber in 50 mL experiment base medium from dish #1-4 (EDL1) or #2-4 (EDL2), and transfer to a 96-well containing 50 mL experiment medium (i.e. medium with 2x concentrated treatment).

Note: As mentioned in Before you begin Step 12b, the respective treatments in the 96-well plates are 2x concentrated and will be diluted to the appropriate concentration automatically by adding the myofiber in medium.

Critical: Avoid transferring any debris with the myofibers, as this may affect the experiment outcome [5].

- d. Pick the next fiber and allocate to a well containing the next treatment (i.e. next row in the plate layout).

Note: We recommend adding a single myofiber to the first well of each treatment before transferring a myofiber to the second well per treatment (first well of next column). This approach allows equal and random distribution of myofibers across all treatments and minimize selection bias (Figure 3).

- e. After 10 min return the 96-well plate and fiber-containing dish to the incubator.
- f. Continue with a second set of dishes or wait 15 min before resuming picking intact myofibers.
- g. Incubate the myofibers in the respective treatments for desired times. Typically, myofiber-derived colonies can be observed within 72 h after start incubation. Treatment time depends on background strain and selected treatments (See Troubleshooting – Problem 3).

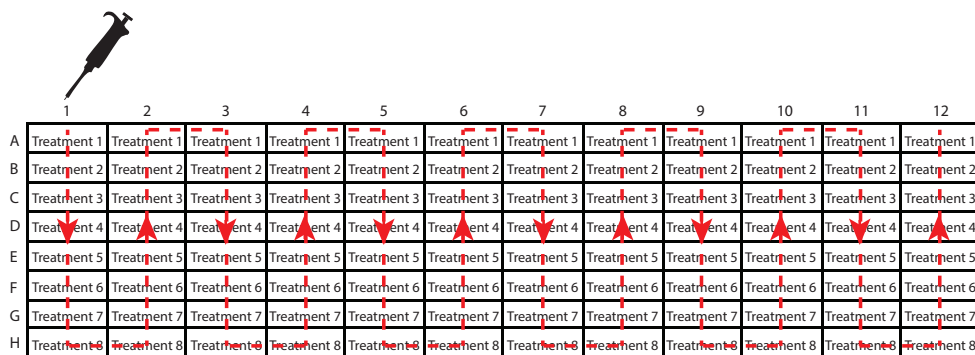


Figure 3: Suggested fiber pipetting scheme. Treatments are arranged in rows. Start adding the first fiber to well A1 (treatment 1), the second to well B1, etc. The dashed red line indicates the order of adding fibers to the respective wells.

Fixation and immunostaining myofibers

Timing: 5 hours

13. Fixing treated myofibers.
 - a. Pre-warm 8% PFA (v/v) at 37°C.
 - b. Place 96-well experiment dish with cultured fibers on slide warmer.
 - c. Add 100 ml of prewarmed 8% PFA (v/v) to each well and incubate for 15 min.

Critical: This step has to be performed inside a chemical safety cabinet to contain toxic fumes.

Note: After incubating 15 min in PFA, plates can be further processed at 18-22°C.

- d. Aspirate PFA solution and replace with PBS.

Note: Fixed fibers can be stored at 4°C up to 2 weeks or stained directly.

Critical: Rinse wells thoroughly with PBS to remove all PFA. This is to prevent over-fixation, as this will compromise subsequent immunostaining and may require antigen retrieval approaches.

14. Immunostaining fiber-derived cells.

Note: Activation of myogenic cells can be measured assess in several manners. Here we describe a PAX7 and KI67 co-staining that allows to assess proliferative, thus activated, myofiber-derived cells. (Figure 4A). Additionally, we describe a PAX7 and MYOD co-staining that allows a complementary method to assess activation of myogenic cells (Figure 4B). Other combinations of antibodies are possible (See Troubleshooting – Problems 4 and 5).

- a. Permeabilize with 0.5% Triton in PBA (see Table Materials and Equipment for abbreviations; v/v) for 30 min at 18-22°C.
- b. Block 30 min with 20% HS (v/v).
- c. Incubate with anti-PAX7 primary antibody (1 in 100 in PBA-Tw) for 1 h at 18-22°C.

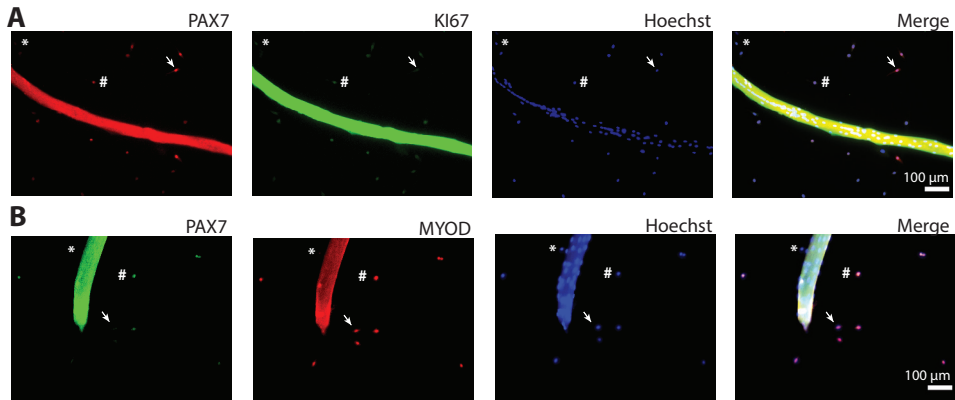


Figure 4: Immunostaining of PAX7/KI67 and PAX7/MYOD in myofibers: (A) Myofibers were isolated from GAAKO donor animals and cultured for 72h in proliferation medium. * indicates a PAX7-low/KI67⁺ cell; # indicates a PAX7⁺/KI67⁺ cell; arrow indicates a PAX7⁺/KI67-low cell. (B) Myofibers were isolated from WT FVB/N donor animals and cultured for 72h in proliferation medium. * indicates a PAX7⁺/MYOD⁻ cell; # indicates a PAX7⁺/MYOD⁺ cell; arrow indicates a PAX7⁺/MYOD⁻ cell. Red indicates MYOD; green indicates PAX7; nuclei were counterstained with Hoechst.

Optional: Previous step may be performed 12-16 hours at 4°C in a humidified chamber.

- d. Rinse once with PBS-Tw.
- e. Incubate with anti-KI67 primary antibody (1 in 100 in PBA-Tw) + biotinylated anti-mouse IgG (1 in 250 in PBA-Tw) for 1 h at 18-22°C .

Note: For PAX7-MYOD co-staining, incubate with anti-MYOD primary antibody (1 in 500 in PBA-Tw) + Biotin Anti-Mouse IgG1 (1 in 250 in PBA-Tw) for 1 h at 18-22°C .

- f. Rinse once with PBA-Tw.
- g. Incubate with Streptavidin-AF647 (1 in 500 in PBA-Tw) + goat anti-rabbit AF488 (1 in 500 in PBA-Tw) 1 hour at 18-22°C .

Note: For PAX7-MYOD co-staining, incubate with Streptavidin-AF647 (1 in 500 in PBA-Tw) + goat anti-mouse IgG2B-Cy3 (1 in 500 in PBA-Tw) 1 hour at 18-22°C .

- h. Rinse once with PBA-Tw.
- i. Incubate with Hoechst (at 1 mg/mL in PBS) for 15 min at 4°C.
- j. Rinse once with PBS-Tw.
- k. Add 100 μ l PBS/well to keep cells moist.
- l. Image immunostained cells as soon as possible for the best results, but at least within one week after finishing immunostaining.

Expected Outcomes

Myofiber yield:

The yield of viable myofibers is dependent on the age, background strain, and genetic makeup of the donor mice. The sex of the donor may affect myofiber yield as well, but we did not test this. Young adult FVB/N animals (8-12 weeks of age) will yield ± 250 intact myofibers and the yield is reduced to <150 myofibers in FVB/N mice of ≥ 30 weeks. Myofibers from wild type FVB/N mice can be kept for a week in culture under the conditions described in this protocol. Maximum culture times should be tested for other genetic backgrounds and disease models.

Isolating myofibers from animals with a muscle-degenerative condition will affect the number and quality. We have wide experience with animals that are knockout for acid alpha glucosidase (GAA), i.e. the mouse model for Pompe disease that was generated in our laboratory [6]. GAAKO mice, which are on a FVB/N background, develop a muscle phenotype after 15 weeks of age [7]. Myofiber yield from young FVB/N and GAAKO animals is similar, but myofiber yield from GAAKO donor mice of 15 weeks and older is reduced compared to age-matched wildtype FVB/N donor mice. GAA-deficient myofibers have a fragile morphology and show accumulation of debris in the core of the fibers as result of distorted autophagy in GAA-deficient myofibers [8].

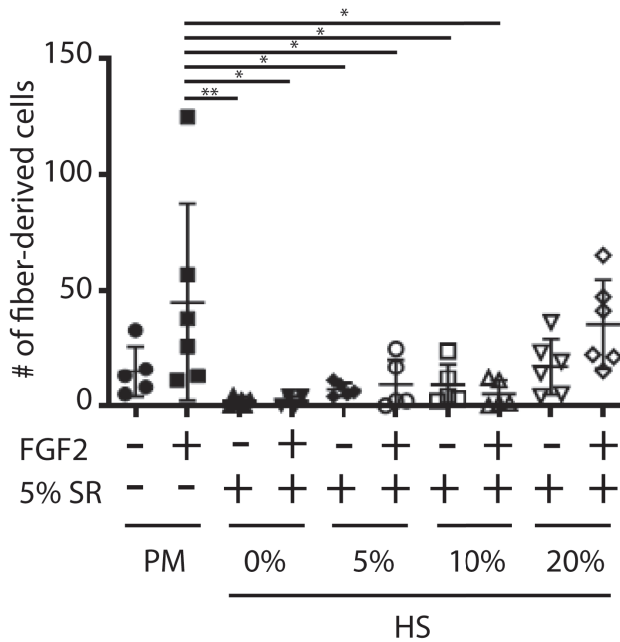


Figure 5: Identifying conditions that activate satellite cells from specific donor backgrounds. Myofibers were isolated from WT FVB/N donor animals and cultured for 72h under indicated conditions. PM: proliferation medium (Ham's F10/20% FCS); SR: knockout serum replacement. Data is indicated as mean \pm SE. Statistics by one-way ANOVA followed by Tukey correction for multiple testing. * $p < 0.05$; ** $p < 0.01$. $n = 4-6$.

Size of colonies of myofiber-derived cells:

The formation of colonies from myofiber-derived cells is dependent on host factors, such as age and genetic makeup of the donor, as well as on culture conditions that are used. The satellite cell response assessed with this assay is a relative measure, i.e. is compared to the colony size under basal conditions. Basal conditions are defined experimentally to use media formulations (i.e. experiment base medium) that limit colony formation (i.e. that keeps satellite cells quiescent), but that allow expansion of myofiber-derived cells after adding supplements that stimulate proliferation, such as high concentrations of serum, FGF2 or HGF. Figure 5 shows the results from such an experiment defining the experiment base medium for myofibers isolated from FVB/N donors. Using defined conditions, the relative potential of satellite cells from different disease models or treatments can be determined.

Myogenic profile of myofiber-derived cells

All myofiber-derived cells are progeny of satellite cells and should express PAX7 and/or the myogenic regulatory factors MYOD or MYOG in the first week of culture. Immunostaining of the colonies is then used to verify the myogenic identity of the cells and is valuable as a quality control of the purity of myofiber selection and plating. In order to ensure best results wells containing >10% non-myogenic cells should be excluded from analysis. Nevertheless, we can not rule out that this will be different in disease models. In our experience four rounds of purification are sufficient to ensure >90% pure myogenic cultures (Figure 4B). However, if necessary, additional purification steps can be added. In addition, as suggested as an optional step in *Step-by-step Method Details 12*, pre-culturing fibers in non-adhering conditions may increase the purity of myogenic colonies during the experiment.

Quantification and Statistical Analysis

Quantifying myofiber-derived cells: After fixation, the immunostained myofibers/cells are imaged. Exclude wells that contain short myofiber fragments, contracted or damaged fibers as these may affect the outcome through release of satellite cell activation signals [5]. The expression of myogenic markers is used to quantify colonies containing satellite cell progeny. The Hoechst (blue) signal is used to identify and count all nuclei. Our analyses indicate a purity >90% of myogenic colonies when the purification steps are followed as described in this text. It is advised to check contamination with non-myogenic cell types in the initial experiments, for instance, by immunostaining. Different markers can be used and are commonly described in the literature to detect fibroadipogenic cells (FAPS), endothelial cells, and pericytes. However, in order to reduce the possibility of including non-myogenic cells in the analysis, we typically include only those cells that are growing adjacent to the myofiber and exclude cells present at a distance farther of 200 μm from the fiber. As a rule of thumb, this is facilitated by including part of the myofiber in each image when using a 10x objective. Image the direct perimeter around the myofiber by taking sequential images. In this protocol a Nikon Eclipse Ti with a 10x objective was used, but equivalent setups may be used. Typically, 5-6 images per myofiber are taken to cover the whole length of the myofibers. For each condition myofiber-derived cells from at least 5 different intact myofibers are counted manually. Colony size is expressed as the number of myofiber-derived cells per myofiber.

Alternatives: Image analysis software such as FIJI or Adobe Photoshop can be used to automate quantification.

Limitations

The protocol described here is suitable to identify fiber-derived myogenic cells and to assess their state of activation. However, this method is not suitable to determine the origin of the colonies. For such purpose, a lineage tracing strategy would be more adequate.

Other strains or mice from other ages: we have used this protocol mainly for isolating myofibers from adult mice aged between 8 and 40 weeks. We obtained reproducible yields of myofibers also from 40 weeks GAAKO donor animals, which have already developed a considerable muscle phenotype at that age. Using the protocol for other strains, including transgenic lines, older/younger mice should be verified and may require optimization of digestions parameters (collagenase type II concentration, digestion time, plating media).

Other muscles: we did apply this protocol successfully to isolate myofibers from soleus and diaphragm muscle (not shown), but cannot exclude that using the protocol to obtain myofibers from other muscles require optimization. Most likely, it requires developing a dissection approach for the muscle of interest. The dissection strategy in this protocol is designed for muscles with easy identifiable tendons, such as the EDL. The EDL is then dissected at/through its tendons without damaging the myofibers. Damaging myofibers reduces the yield and viability of the isolated fibers.

Troubleshooting

Problem 1:

Few viable (transparent) myofibers obtained (Step-by-step Method Details Step 11).

Potential Solution:

Solution 1: Improve dissection technique: swift but careful dissection of the EDL muscles is key to the success of myofiber isolation and takes practice to master and produce consistent yields. Prevent stretching and damaging the muscles. Ensure cutting the tendons to release the EDL and not to damage the myogenic part of the muscle. Limit cooling the muscles by prewarming the digestion solution.

Solution 2: Check digestion solution. The quality of collagenase type II batches may vary. Ensure to make sufficiently large stock solutions to finish the experiments dedicated to specific projects. Stock solutions can be stored at -80°C up to 6 months in our hands with negligible loss of yield. We advise to try collagenase everytime a new stock is made in order to adjust calculations if myofiber yield was lower than expected.

Solution 3: Check digestion time: over/under digestion will result in variable myofiber yield and quality. The optimal time may differ slightly per collagenase type II stock solution.

Solution 4: Handle myofibers more carefully: make sure all pipet tips are polished properly, avoid forcing the fibers through the tips or bending fibers during handling.

Solution 5: If possible, preferentially select longer myofibers (>1.5 mm), as short myofibers are usually damaged and will not survive.

Problem 2:

Many contracted myofibers (Step-by-step Method Details Step 11).

Potential Solution:

Solution 1: Practice to improve dissection technique. Success of myofiber yield (number and quality fibers) is largely determined during dissection.

Solution 2: Prevent cooling the myofibers by returning the dishes to the incubator within 10 min and allow to recover for at least 15 min between myofiber selection sessions.

Solution 3: Handle myofibers more carefully: make sure all pipet tips are polished properly, avoid forcing the fibers through the tips or bending fibers during handling.

Problem 3:

Few myofiber-derived cells (Step-by-step Method Details Step 12).

Potential Solution:

Solution 1: Optimize culture conditions, predominantly the media composition as described in Materials and Equipment. Define media conditions to obtain a maximal increase in the number of myofiber-derived cells after adding 20 ng/mL FGF2 for at least 72h.

Solution 2: Verify that viable myofibers have been obtained. One could consider to add viability dyes such as trypan blue, but verify that these do not interfere with the experiment's objective. A retrospective method entails staining myofibers after PFA fixation for Hoechst. Lack of nuclei staining indicates loss of myofiber viability somewhere along the process. Optimize myofiber isolation technique before planning a new experiment.

Solution 3: Extend culture time as satellite cells from some donor strains or genetic backgrounds, including wild type FVB/N, display slow/delayed activation response.

Problem 4:

Lack of staining for selected markers (Step-by-step Method Details Step 14).

Potential Solution:

Solution 1: Verify critical steps of staining protocol: proper permeabilization (over/under permeabilization negatively affect staining of nuclear proteins); (primary and secondary) antibody concentration. Optimize staining protocol on primary satellite cell-derived cultures.

Solution 2: Ensure using high-resolution optics to allow imaging low signals. This includes use of imaging-compatible culture plates (e.g. Nunc Nunclon 96-well plate) (see Key Resources).

Problem 5:

Weak PAX7 signal in immunostaining (Step-by-step Method Details Step 14).

Potential Solution:

Solution 1: Fix fibers as described for 15 minutes and not longer than this. Overfixation could lead to increased background in the immunostaining or even mask the antigens.

Solution 2: Incubate with primary antibody anti-PAX7 8-12 hours at 4°C. in a humidified chamber. Proceed with the rest of the immunostaining as described.

Solution 3: Culture fibers during different time points (e.g. 24, 48, 72, 96, and 120 hours), fix, and stain in order to calculate the time window during which PAX7 is expressed and to prevent loss of PAX7 expression due to satellite cells transitioning into a myoblast state (PAX7/MYOD⁺).

Solution 4: Culture fibers under different quiescence/activation conditions (e.g. varying the concentration of serum) to determine the most optimal for your desired experiment.

Resource Availability

Lead Contact

Further information and requests for resources and reagents should be directed to the lead contact Dr. Gerben Schaaf at g.schaaf@erasmusmc.nl

Materials Availability

This study did not generate new unique reagents.

Data and Code Availability

This study did not generate/analyze any datasets/code.

Acknowledgments

1. Funding: The work is funded through the Center for Lysosomal and Metabolic Diseases at Erasmus MC, and the Prinses Beatrix Spierfonds/Stichting Spieren voor Spieren (Project number W.OR13–21).
2. Core facilities contributing to the work: Imaging was performed at the Erasmus MC Optical Imaging Center.

Author Contributions

Conceptualization: RCF, PP and GS; Investigation: RCF, EB, SB and GS; Writing and editing: RCF, PP and GS; Funding Acquisition: PP and GS.

Declaration of Interests

The authors declare no competing interests.

References

1. Brun, C.E., Wang, Y.X., and Rudnicki, M.A. (2018). Single EDL myofiber isolation for analyses of quiescent and activated muscle stem Cells. In *Methods in Molecular Biology* (Humana Press Inc.), pp. 149–159. Available at: https://link.springer.com/protocol/10.1007/978-1-4939-7371-2_11 [Accessed October 9, 2020].
2. Feige, P., Tsai, E.C., and Rudnicki, M.A. (2021). Analysis of human satellite cell dynamics on cultured adult skeletal muscle myofibers. *Skelet. Muscle* *11*, 1. Available at: <https://skeletalmusclejournal.biomedcentral.com/articles/10.1186/s13395-020-00256-z> [Accessed February 16, 2021].
3. Garcia-Pelagio, K.P., Pratt, S.J., and Lovering, R.M. (2020). Effects of myofiber isolation technique on sarcolemma biomechanics. *Biotechniques*.
4. Järvinen, T.A.H., Kääriäinen, M., Äärimaa, V., Järvinen, M., and Kalimo, H. (2008). Skeletal Muscle Repair After Exercise-Induced Injury. In *Skeletal Muscle Repair and Regeneration* (Springer Netherlands), pp. 217–242. Available at: https://link.springer.com/chapter/10.1007/978-1-4020-6768-6_11 [Accessed February 12, 2021].
5. Tsuchiya, Y., Kitajima, Y., Masumoto, H., and Ono, Y. (2020). Damaged Myofiber-Derived Metabolic Enzymes Act as Activators of Muscle Satellite Cells. *Stem Cell Reports* *15*, 926–940. Available at: <https://doi.org/10.1016/j.stemcr.2020.08.002> [Accessed November 3, 2020].
6. Bijvoet, A.G.A., Van De Kamp, E.H.M., Kroos, M.A., Ding, J.H., Yang, B.Z., Visser, P., Bakker, C.E., Verbeet, M.P., Oostra, B.A., Reuser, A.J.J., *et al.* (1998). Generalized glycogen storage and cardiomegaly in a knockout mouse model of Pompe disease. *Hum. Mol. Genet.* *7*, 53–62.
7. Schaaf, G.J., van Gestel, T.J.M., in 't Groen, S.L.M., de Jong, B., Boomaars, B., Tarallo, A., Cardone, M., Parenti, G., van der Ploeg, A.T., and Pijnappel, W.W.M.P. (2018). Satellite cells maintain regenerative capacity but fail to repair disease-associated muscle damage in mice with Pompe disease. *Acta Neuropathol. Commun.* *6*, 119.
8. Lim, J.A., Li, L., Kakhlon, O., Myerowitz, R., and Raben, N. (2015). Defects in calcium homeostasis and mitochondria can be reversed in Pompe disease. *Autophagy* *11*, 385–402.

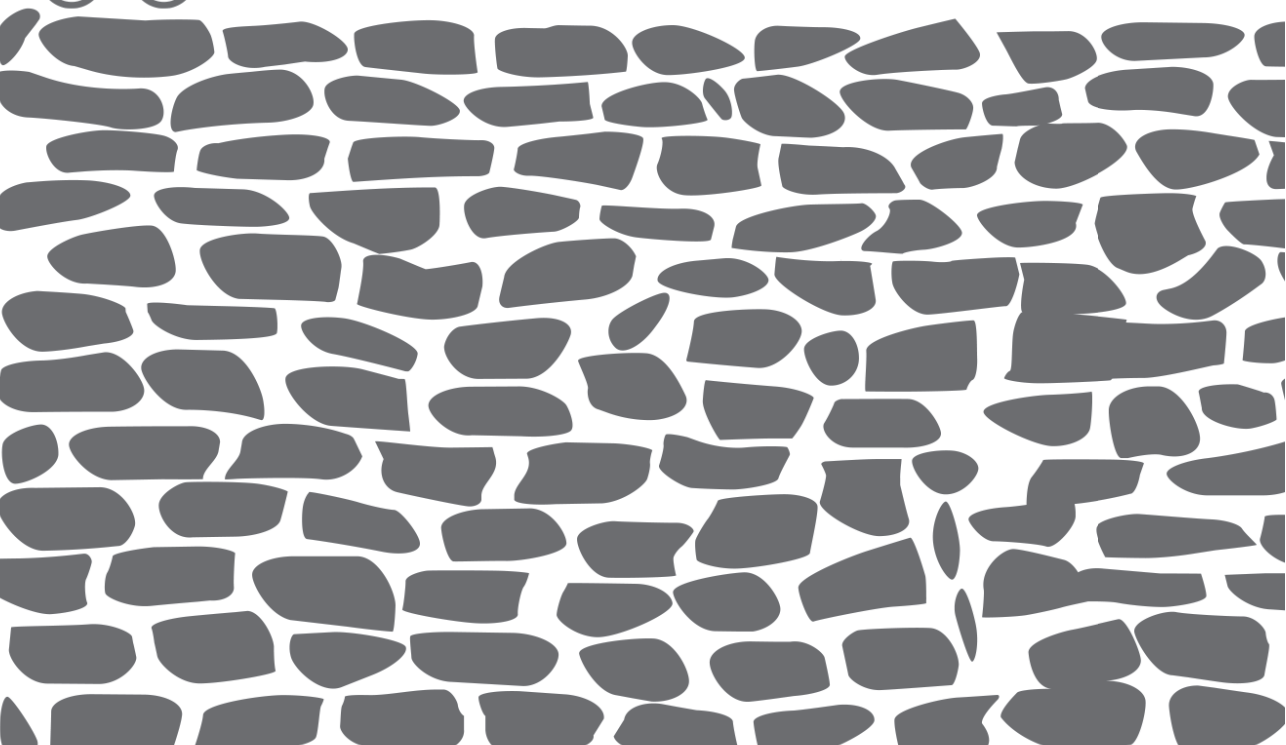
Supplementary information

Video S1: Liberating myofibers from digested EDL muscle. Related to Step-by-step Method Details Step 10. The video shows the first aspirating and releasing steps with the digested EDL. This step is performed with the dish on the slide warmer.

Video S2: Liberating individual myofibers from digested EDL fragments. Related to Step-by-step Method Details Step 10. The EDL has been broken down into smaller parts and fibers are released from the individual parts. This step is performed with the dish on the slide warmer.

Video S3: Transferring myofibers during purification. Related to Step-by-step Method Details Step 11. Transferring myofibers from the source dish (e.g. dish 1-1) to the next purification dish (e.g. dish 1-2). The source plate is under the dissecting microscope at the top of the video, the next purification dish is on the slide warmer at the bottom of the video.

Video S4: Transferring a single myofiber along the length axis. Related to Step-by-step Method Details Step 11.



Chapter 5

Provoked muscle regeneration transiently rescues the Pompe disease phenotype: the role of autophagy

Gerben J. Schaaf^{1,2,3}, Rodrigo-Canibano Fraile^{1,2,3}, Tom J.M. van Gestel^{1,2,3},
Emma Boertjes^{1,2,3}, Bart de Jong^{1,2,3}, Björn Boomaars^{1,2,3}, Stella Bozhilova^{1,2,3},
Thomas Hartjes⁴, Martin van Royen⁴, Ans T. van der Ploeg^{2,3} & W.W.M. Pim
Pijnappel^{1,2,3,*}

¹Department of Clinical Genetics, Erasmus MC University Medical Center, 3015 GE Rotterdam, Netherlands

²Department of Pediatrics, Erasmus MC University Medical Center, 3015 GE Rotterdam, Netherlands

³Center for Lysosomal and Metabolic Diseases, Erasmus MC University Medical Center, 3015 GE Rotterdam, Netherlands

⁴Department of Pathology, Section Neuropathology, Erasmus MC University Medical Center, 3015 GE Rotterdam, Netherlands

*Correspondence: w.pijnappel@erasmusmc.nl

Manuscript in preparation

Abstract

Pompe disease is an inherited metabolic myopathy caused by deficiency of acid α -glucosidase (GAA). GAA deficiency results in lysosomal glycogen accumulation, an increase in lysosomal size and number, impaired autophagy, accumulation of autophagic debris, and muscle wasting. We previously found that in Pompe disease, muscle stem cells – termed satellite cells – are dormant but capable of efficient muscle regeneration when provoked experimentally. Here, we investigated the relationship between murine satellite cell activation, muscle regeneration, and autophagy in Pompe disease. We found that cultured isolated myofibers from GAAKO mice accumulated autophagic debris and displayed enhanced satellite cell activation in response to FGF2 treatment compared to wild type myofibers. Treatment of cultured GAAKO myofibers with rapamycin stimulated autophagic flux, normalized satellite cell activation to wild type levels, and improved myofiber morphology; although it failed to remove autophagic debris. Surprisingly, treatment of cultured myofibers with chloroquine, which further inhibited autophagic flux, worsened myofiber morphology; though it also normalized satellite cell activation to normal levels. We hypothesize that in Pompe disease, a critical level of autophagic flux is required for satellite cell activation. Experimentally induced muscle injury *in vivo* transiently reduced lysosomal size and restored muscle function in Pompe GAAKO mice, suggesting that provoked muscle regeneration could overcome the autophagic block in Pompe disease.

Introduction

Pompe disease is a metabolic myopathy caused by deficiency of acid alpha glucosidase (GAA), a lysosomal enzyme responsible for the degradation of glycogen [1]. Pompe disease patients develop progressive skeletal muscle weakness, followed by lysosomal disruption and myofiber death. Affected muscles include those involved in mobility and respiration. As a result, Pompe disease patients become wheelchair- and ventilator-dependent [2]. In its most severe form, the classic infantile, GAA is completely absent, and results in death within the first year of life if left untreated [3]. In milder forms of Pompe disease, residual GAA activity exists, and patients develop symptoms later in life [4,5]. A treatment for Pompe disease is available in the form of enzyme replacement therapy (ERT). Although ERT improves muscle function and prolongs survival, the heterogeneous response among patients has urged the development of alternative treatment options [6–15].

Skeletal muscle has an enormous capacity to repair damage, a process that relies on muscle stem cells, called satellite cells [16,17]. This has stimulated researchers to develop regenerative therapies for muscle disorders through modulation of satellite cell activity. However, under muscle-degenerative conditions muscle regeneration activity is often compromised [18]. This defect not only hampers the development of novel treatment strategies, but also contributes to the progression of muscle wasting, as the disease-mediated damage cannot be repaired. We and others have shown that satellite cell activation is compromised in Pompe disease, and that the regenerative response to the accumulating glycogen damage is lacking [19–21]. Notably, GAA-deficient satellite cells are activated in response to BaCl_2 -induced muscle damage, indicating that GAA-deficient satellite cells are functional stem cells [20]. These findings suggest that activating signals are not generated or cannot reach muscle stem cells during disease progression. However, the mechanisms behind the satellite cell activation defects have not been yet identified.

The primary defect in Pompe disease is deficiency to degrade lysosomal glycogen. Glycogen accumulation induces a progressive increase of the lysosomal compartment that eventually results in dysregulated autophagy [22–24]. Macroautophagy, hereafter referred to as autophagy, is a catabolic process to provide nutrients for the cell under stress situations, as well as to protect cells by removing damaged or potentially toxic cellular components and excreting cytoplasmic material [25]. Autophagy is dysregulated in several human pathologies, and its

critical role in satellite cell quiescence and activation and in muscle regeneration is becoming increasingly appreciated [26–28]. The importance of autophagy for cellular homeostasis has been demonstrated using autophagy-deficient satellite cells, which resulted in reduced regenerative capacity and satellite cell numbers [27]. In addition, satellite cells from geriatric mice showed impaired autophagic flux, resulting in loss of quiescence and induction of stem cell senescence [27]. Interestingly, rapamycin-treatment – which induces autophagy – restored regenerative capacity in both autophagy-impaired as well as in geriatric satellite cells, and prevented induction of senescence in the latter [27].

Based on these observations we investigated whether dysfunctional autophagy in Pompe disease contributes to the failing satellite cell response. We found that autophagy was dysregulated in limb muscle of GAA-knockout (GAAKO) mice before loss of muscle function was observed. Further inhibition of autophagic flux expanded the size of autophagic vacuoles in isolated GAAKO myofibers, accelerated myofiber death, and reduced FGF-2-mediated stimulation of satellite cell activation to wild type levels. Activation of autophagy improved autophagic flux but failed to resolve the autophagic vacuoles. Surprisingly it also restored the satellite cell response to wild type levels. *Ex vivo* FGF-2 treatment or BaCl₂-induced muscle injury efficiently activated GAAKO satellite cells and mediated muscle regeneration in line with in previous results obtained *in vivo* [20]. The forced regenerative response transiently improved the lysosomal phenotype, reduced glycogen accumulation, and restored muscle function *in vivo* in GAAKO mice. Taken together, our results suggest that autophagy is dysregulated early during Pompe disease progression, which may contribute to the attenuated satellite cell response to the progressing muscle damage. However, the level of autophagic flux seems to remain sufficient to support forced satellite cell-dependent muscle regeneration. The observed improvement of the lysosomal phenotype and muscle function in regenerated GAAKO muscle justify further studies aimed at finding safe and efficient strategies to stimulate satellite cells activation.

Results

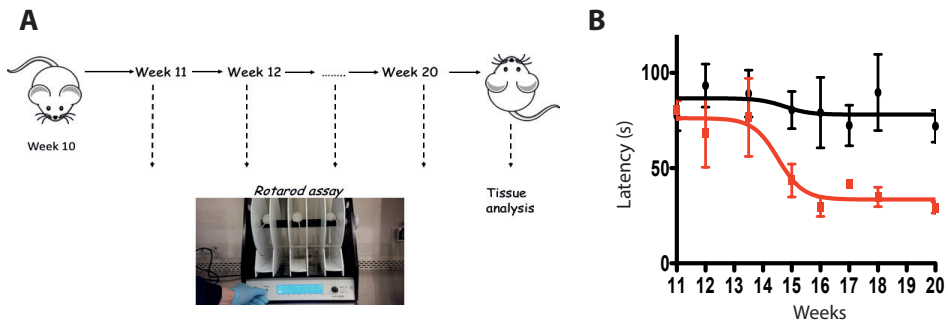
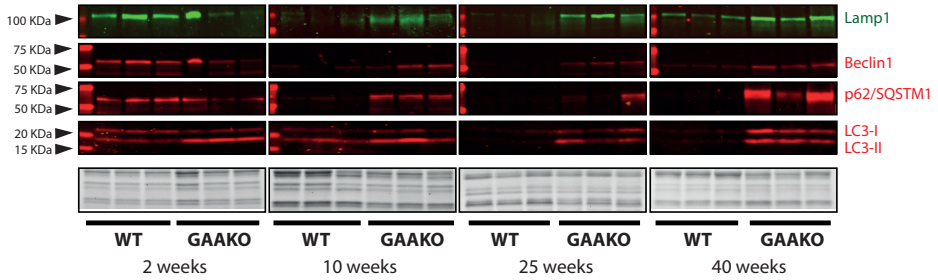


Figure 1. The onset of muscle wasting in GAAKO mice starts at 15 weeks. (A) Experimental layout. (B) Loss of muscle function in GAAKO mice of 15 weeks and older as determined by the rotarod assay. Latency (s) of FVB wild-type (WT) (black line/symbols) and GAAKO (red line/symbols) mice was plotted (average \pm SD). $N=3$ per genotype per timepoint.

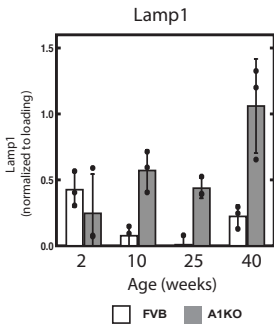
Previous findings indicated that in GAAKO mice the muscle regenerative response to the progressive glycogen accumulation and lysosomal dysfunction in adult animals was lost between 11 and 25 weeks of age, which coincided with the development of muscle damage [19–21]. To better characterize the onset of functional muscle loss, we performed weekly muscle function tests in FVB wild-type (WT) and GAAKO animals between the age of 11 and 20 weeks (Figure 1A-B). Rotarod performance was similar between WT and GAAKO mice up to 14 weeks. From 15 weeks and beyond, rotarod performance was sharply reduced in GAAKO animals compared to that in age-matched WT mice (latency at 15 weeks of $43,5 \pm 19,3$ s in GAAKO vs $81,4 \pm 21,2$ s in WT) (Figure 1B) and remained reduced at an average of 50,8% of baseline levels with increasing age. The average rotarod latency was 64,95 s in GAAKO animals from 10 to 14 weeks and 33,9 s from 15 to 20 weeks. These data indicate that muscle function in GAAKO animals starts to decline at 15 weeks of age.

We and others found that glycogen accumulation develops early in the Pompe disease mouse model, starting already from birth [20,29,30]. It has been demonstrated both in Pompe disease patients and mouse model that glycogen accumulation affects autophagic function [23,31], but it has not been established when during disease progression autophagy becomes defective. To document this, we first determined the expression of key autophagy-related enzymes Lamp1, Beclin1, P62, and LC3 during the natural course of disease *in tibialis anterior* (TA) muscles of WT and GAAKO mice.

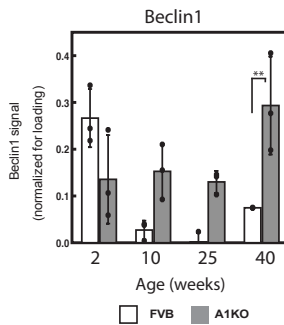
A



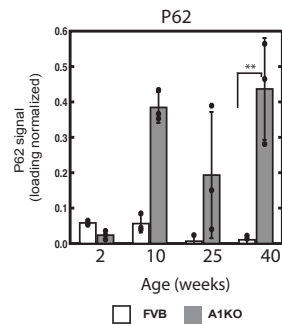
B



C



D



E

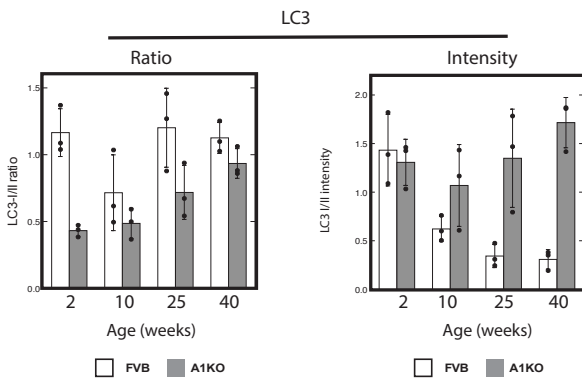


Figure 2. Autophagy is disrupted in GAAKO muscle before disease onset. (A) Western blot analysis of Lamp1, Beclin1, P62, and LC3 in WT and GAAKO tibialis anterior (TA) muscle at different ages during disease progression. The lower panel shows a representative image for equal protein loading. *N*=3 animals per genotype/timepoint. (B-E) Quantification of Lamp1 signal (B), Beclin1 (C), P62 (D) and LC3 (E) signals, as shown in (A).

Western Blot analysis showed that Lamp1 – a lysosomal membrane protein as indicator of the size of the lysosomal compartment - was expressed at 2 weeks

at elevated levels in WT animals, while at 10, 25 and 40 weeks Lamp1 levels were increased in GAAKO TA muscle (Fig 2A-B).

Beclin1, the mammalian orthologue of yeast Atg6, forms a core complex through interaction with other proteins including HMGB1, PINK and others, and initiates autophagy [32]. The expression pattern of Beclin1 in TA muscle during disease progression was similar to that of Lamp1, with slightly elevated expression in WT muscle at 2 weeks, while at 10, 25 and 40 weeks the levels of Beclin1 were increased in GAAKO TA muscle compared to that in WT TA, although the differences were not statistically significant (Fig. 2A and C).

P62 or sequestome1 (SQTM1) is a ubiquitin-binding scaffold protein that targets specific cargo for degradation through autophagy [33]. P62 itself is degraded through autophagy, so that P62 accumulation suggests disturbed autophagic flux [34]. P62 levels were similar between the genotypes at 2 weeks. In WT muscle P62 levels decreased and were barely detectable at 25 and 40 weeks. In GAAKO TA muscle P62 levels were increased at 10, 25 and 40 weeks compared to those in age-matched WT counterparts, suggesting P62 was accumulating (Figure 2D). This may suggest that autophagic flux is decreasing in aging GAAKO.

To further characterize autophagic flux we assessed the levels of LC3. Microtubule-associated protein 1A/1B-light chain 3 (LC3-I) is a soluble protein that becomes engulfed during autophagy and is integrated in the membrane of autophagosomes following lipidation into LC3-II. LC3-II is subsequently degraded in the lysosomes [35]. The levels of LC3-II are thought to reflect increased autophagosome formation [34], while a change in the ratio of LC3-I and -II, in combination with P62 accumulation, may suggest changes in autophagic flux [36]. Our results show that the levels of LC3-I and -II were elevated in TA muscles from 2 weeks WT and GAAKO animals compared to those in the older WT animals. The levels of LC3 steadily decreased in WT TA muscle, but remained high in GAAKO TA muscle of animals at 10, 25, and 40 weeks. In WT TA muscle both LC3-I and -II decreased simultaneously, while in GAAKO muscle the ratio of LC3-I/II increased to almost one at 40 weeks TA muscle, which was caused by a relative increase of LC3-I with ageing (Figure 2E). In conclusion, autophagic flux seems to be reduced already in GAAKO TA muscle at 10 weeks, before the onset of functional muscle loss at 15 weeks as was determined in Figure 1.

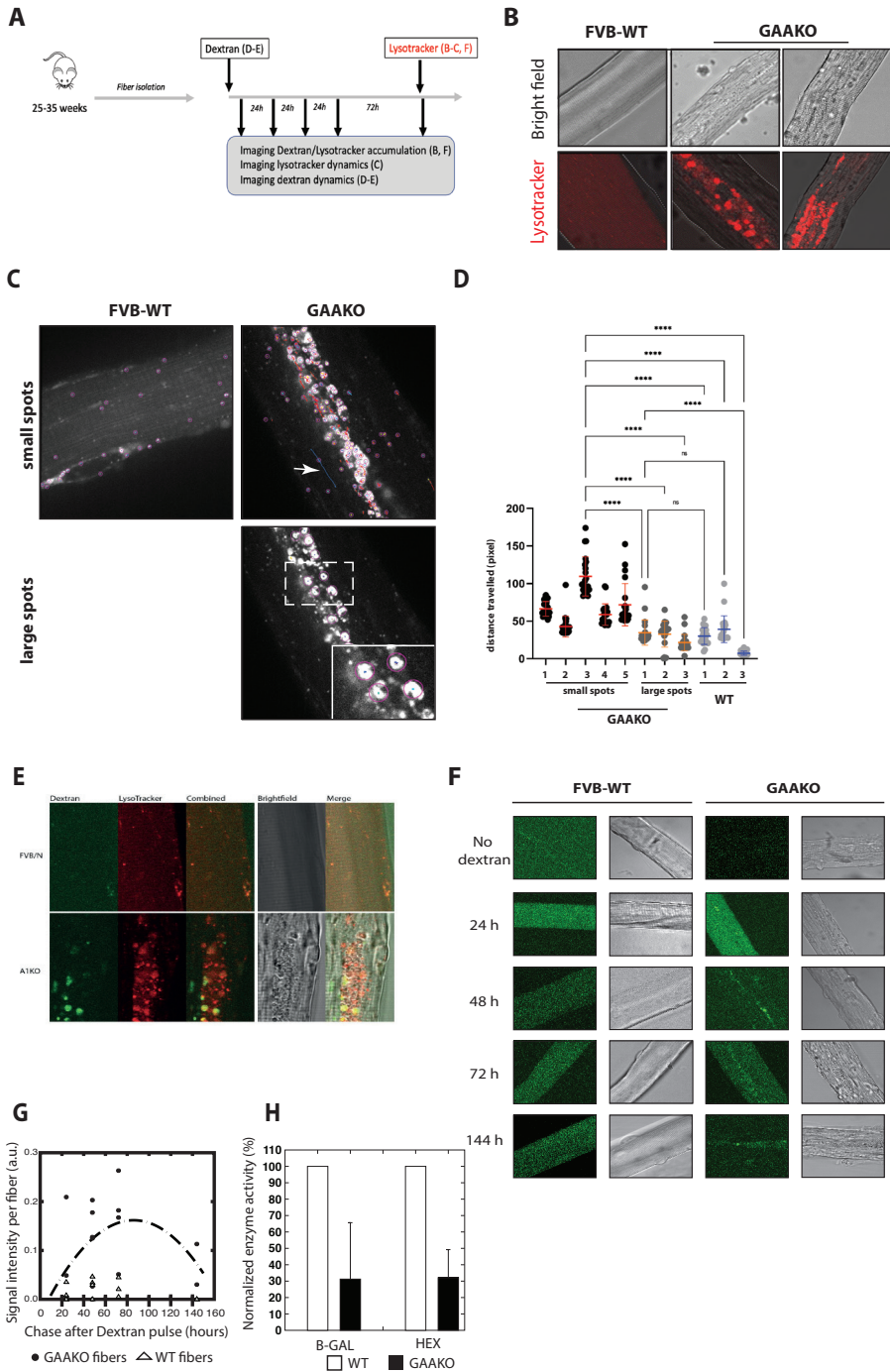


Figure 3. Lysosomal defects in isolated GAAKO myofibers. (A) Experimental layout. (B) Confocal images of isolated WT and GAAKO myofibers stained with lysotracker. Upper panels: bright field confocal images of WT and GAAKO myofibers. Lower panels: lysotracker (in red) confocal images of WT and GAAKO myofibers. (C) Representative still images from spinning disc video files of lysotracker-positive particles in isolated myofibers of WT and GAAKO mice. The figure depicts confocal still-images with track-overlay. Tracks are colorized (white arrow). Spots are detected based on preset maximum spot size (indicated with purple circles, see zoom in lower image). The boxed area in the lower upper image is depicted as inset representing 4 selected spots. (D) Quantification of the maximum distance travelled by the top 23 spots per sample (in pixels). For each genotype at least 2 different fibers were imaged and/or at 2 locations along the length of the fiber. **** $p < 0,0001$; ns= not significant. (E) Dextran (in green) lysosomal localization was determined by co-staining fibers with lysotracker (in red). The picture shows confocal images of WT and GAAKO myofibers from animal at ± 25 weeks 72h after isolation. (F) Determination of endosomal pathway activity by dextran pulse-chase experiments in isolated myofibers of WT and GAAKO mice. Dextran (in green) signal at indicated time-points after dextran-pulse. (G) Quantification of D. The figures depict dextran signal in particles with size exceeding size threshold (> 10 pixels). (H) Myofiber exocytosis was determined by measuring the activity of lysosomal B-GAL and HEX in the medium. ($n = 3$ fibers from at least 2 independent experiments. Enzyme activity is expressed relative to activity in medium of WT myofibers. Enzyme activity was measured as nmol/h and normalized from protein content.

To further characterize the lysosomal phenotype and autophagy defect, we isolated single myofibers from 25-35 weeks WT and GAAKO mice, an age at which the muscle phenotype in GAAKO mice is well-developed. We first imaged the lysosomal compartment by staining isolated myofibers with lysotracker, a fluorescent agent that accumulates in acidic vesicles such as lysosomes (Figure 3A-B). GAAKO myofibers accumulated lysotracker in large vesicles at the fibers' central core (Figure 3B). In addition, most of the lysotracker signal concentrated to the center-core of GAAKO fibers, in line with previous reports of autophagic debris in the center core of myofibers isolated from GAAKO mice kept on a different (mixed BL6/129Sv) background [37,38]. These data are in line with dramatic expansion of the lysosomal compartment [24]. The striated pattern seemed disrupted in regions with expanded lysosomal compartment, although short stretches with intact striation were still observed (Figure 3B; Supplemental Figure 1).

Large aggregates containing undegraded storage material have also been observed in other lysosomal storage disorders (LSDs), such as neuronal ceroid lipofuscinosis type 3 (CLN3) and mucopolipidosis type IV (ML-IV) [39]. These aggregates were reported to form when lysosomes containing non-degraded material became mispositioned and/or changed motility, which eventually affected autophagic activity and flux [40]. To determine if the motility of lysosomes was also affected, we performed live-tracking experiments of lysotracker positive vesicles (Figure 3C). Many more lysotracker-positive spots were detected in the GAAKO myofibers compared to those in WT fibers, in line with expansion of the lysosome

compartment. Large vesicle-aggregates in GAAKO myofibers (average spot size $24, 8 \pm 0,78$ pixels) moved significantly less within the imaged time-frame, (Figure 3C and Supplemental Video 1) compared to small lysotracker-positive vesicles (average spot size 8.89 ± 1.44 pixels), some of which were located at the periphery of GAAKO fibers. Lysosomes are known to move along microtubule tracks [41]. In skeletal muscle fibers microtubules are arranged along the longitudinal fiber axis [42]. Interestingly, the highly motile lysosome-like spots primarily moved along the longitudinal axis (Supplemental video 1). The small lysotracker-positive vesicles in GAAKO myofibers were also significantly more mobile than lysotracker-positive vesicles in WT myofibers (average spots size $7.55 \pm 0,19$). As the majority of the spots were hardly or not moving, the difference in lysosome motility was best visualized by plotting the track distances of the most-moving spots for each sample (Figure 3C). The lysotracker-positive vesicles in WT myofibers were barely visible, although detected by the tracking software. The WT lysosome-like vesicles were homogeneous in size and distribution.

Glycogen is thought to reach the lysosome through autophagy in a process called glycophagy [43]. Glycophagy is dependent on adequate functioning of the endosomal and autophagic pathways. To characterize the early steps of the endosomal pathways we used fluorescently-labelled dextran (AlexaFluor488-dextran; AF488-dextran) and performed dextran pulse-chase experiments (Figure 3A and 3D-F). Dextran is first taken up in cells by mannose receptor-dependent endocytosis – a pathway with a critical role in myoblast fusion –, enters the endosomal pathway, and reaches the lysosome [44,45]. AF488-dextran accumulated in isolated myofibers in a dose- and time-dependent manner (data not shown). Competition experiments by co-incubation of fibers with AF488-dextran and increasing concentrations of mannose reduced accumulation of dextran, indicating that dextran was endocytosed in a mannose receptor-dependent manner (Supplemental Figure 2). To establish if dextran reached the lysosomes dextran-pulsed fibers were co-stained with lysotracker and imaged. AF488-dextran signal partially overlapped with lysotracker, indicating that dextran reached acidic vesicles, suggesting these represented lysosomes (Figure 3D). In GAAKO fibers some dextran-positive vesicles did not co-stain with lysotracker, which could indicate localization outside the lysosome or localization in less acidic lysosomes. It is known that peripheral lysosomes have increased pH [46].

To determine differential endosomal activity isolated WT and GAAKO myofibers were pulsed with AF488-labelled dextran and its distribution across

the myofiber was chased by confocal imaging for 144h. Dextran pulse-chase experiments showed that dextran reached the highest concentration in both WT and GAAKO myofibers within 40-60 hr and decreased afterwards, suggesting further distribution of dextran (Figure 3E-G). In addition, WT myofibers showed equal distribution of dextran in small vesicles across the fiber (Supplemental Figure 3), in a pattern reminiscent of lysotracker stained myofibers (Fig. 3B). GAAKO fibers initially accumulated dextran in both small and large vesicles, while at later time points dextran was primarily detected in larger vesicles, which suggests reduced autophagic flux in larger vesicles (Figure 3E-G).

Apart from its role in degrading cellular waste material the endosomal and autophagic pathways play a role in extracellular release pathways [47,48]. Waste material reaching the lysosome is either degraded by lysosomal hydrolases or processed for excretion through exocytosis. To determine if the excretory function of the lysosome was still functional in GAAKO myofibers, we determined the exocytosis of lysosomal enzymes β -galactosidase (B-GAL) and hexaminidase (HEX). Figure 3H shows that exocytosis of these enzymes was significantly reduced, indicating that autophagic flux is blocked and the last step of the autophagic pathway compromised in GAAKO fibers.

These findings show that mannose receptor-mediated endocytosis and intracellular routing to the lysosomes are still functional in GAAKO myofibers, but that extracellular release pathway (i.e. routing out) seem to be compromised.

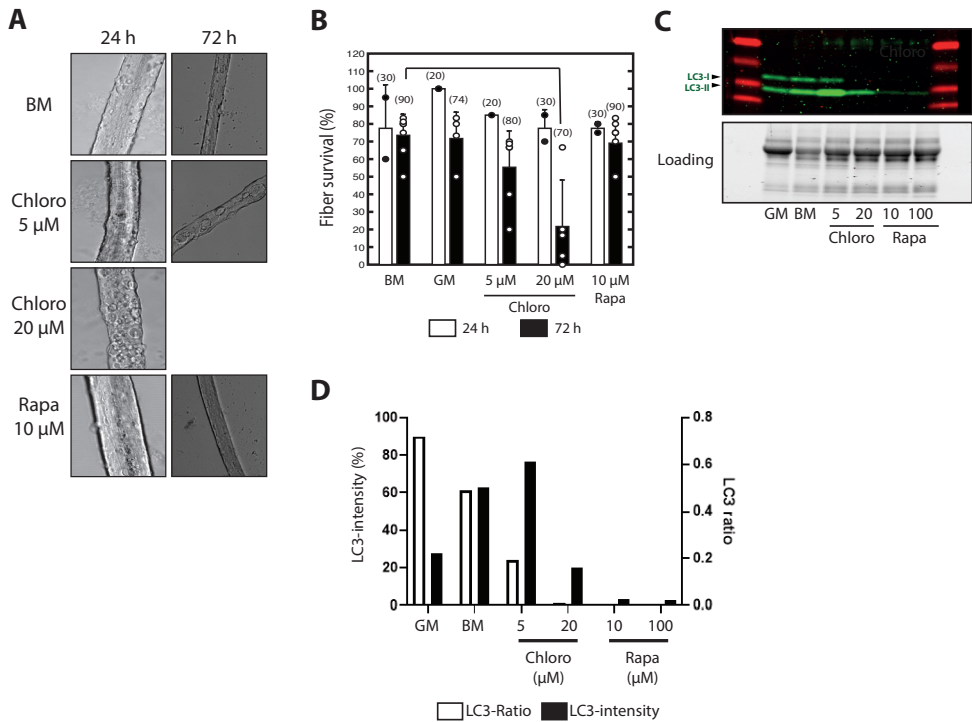


Figure 4. Modulation of autophagy does not contribute to clearance of autophagic buildup. (A) Effect of modulation of autophagic activity on myofiber structure and viability. Brightfield confocal images from fibers exposed to chloroquine or rapamycin for 24h (left panels) or 72h (right panels). (B) Quantification of fiber survival after 24h and 72h of treatment. Intact fibers were counted and plotted as the percentage of total fibers plated and treated. $N=1-5$. (C) Upper panel: Western blot analysis of LC3 in chloroquine- and rapamycin-treated GAAKO myofibers. Lower panel: image for equal protein loading. (D) Quantification of LC3 I/II ratio. $N=1$.

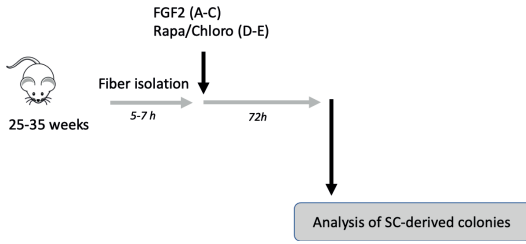
We asked if the disturbed autophagic flux in GAA-deficient myofibers described here and reported by others [23,31] could have contributed to the failing satellite cell response that we described previously [20,21]. To explore this, we modulated autophagic activity in isolated myofibers and assessed the effects on satellite cell activation using a recently described *ex vivo* assay [49]. We either blocked or activated autophagy using chloroquine or rapamycin, respectively (Figure 4A). Chloroquine, which inhibits autophagy by increasing the pH of lysosomes, induced the formation of higher number and larger vacuole-like vesicles in GAAKO myofibers within the first 24h of treatment (Figure 4A-B), and caused a dose-dependent loss of fiber viability (Figure 4C). Chloroquine-treated fibers showed reduced lysotracker

signal, in line with neutralization of lysosomal pH (Supplemental Figure. 4) [50]. At 5 μ M, chloroquine treatment decreased the LC3-I/II ratio, indicating that phagosome formation was further inhibited by treatment [51]. This also seems to indicate that isolated GAAKO myofibers displayed a residual level of autophagic flux that was reduced further by chloroquine treatment. At higher concentrations chloroquine was toxic and fibers hypercontracted rapidly after exposure (Figure 4D).

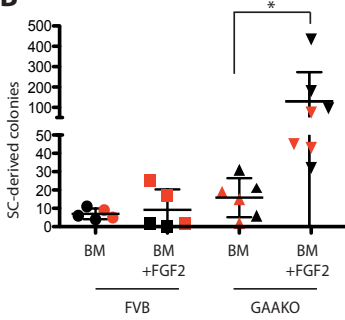
Rapamycin, a well-established inducer of autophagy through inhibition of mTOR, showed a decrease in both LC3-I and II levels consistent with active autophagy. (Figure 4D) [52]. Rapamycin-treatment did not reduce or remove the autophagic buildup observed in the fiber center core (Supplemental Figure 4) or increase fiber survival (Figure 4B). These data suggest that autophagic build up could be aggravated by inhibiting autophagy, but that once formed, it could not be removed following stimulation of autophagy.

To investigate the effect of modulating autophagic activity on the satellite cell response, we assessed satellite cell activation. First, we determined if the assay reflected the differential satellite cell response observed *in vivo* (GAAKO satellite cells did not respond to disease-induced damage, while they rapidly responded to acute injury induced experimentally) (Figure 5A) [20]. To test this, we cultured WT and GAAKO-myofibers under satellite cell activation- limiting conditions by culturing myofibers with basal medium (BM), which was defined previously [49]. The formation of fiber-derived cells was used as a parameter to measure satellite cell activation. Under BM conditions, fiber-derived cell formation was limited, without differences between FVB and GAAKO myofiber cultures (Figure 5B). To mimic satellite cell activation, myofibers were treated with FGF-2, a potent satellite cell mitogenic ligand both *in vitro* and *in vivo* [53]. Exposing the isolated fibers to FGF-2 for 72h resulted in a robust response in GAAKO fiber cultures compared to GAAKO under BM conditions, as well as compared to FVB fiber cultures exposed to FGF2 (Figure 5B), reminiscent of the rapid increase in Ki67-positive satellite cells *in vivo* after induction of acute muscle injury [20]. The formation of fiber-derived cells from FGF-2 stimulated WT myofibers was more modest (Figure 5B), also in line with the reduced increase in Ki67-positive satellite cells during injury-induced muscle regeneration *in vivo* [20]. We characterized the profile of expanding fiber-derived cells by staining with Pax7 and Ki67 (Figure 5C). 67% of cells were proliferative (Ki67-positive) Pax7 cells, 25% were Ki67-negative Pax7 cells, while 3 % and 5% were negative for PAX7-only or for both markers (Figure 5C). This showed that the satellite cell response in GAAKO muscle could be assessed *in vitro* and was in agreement with the results obtained *in vivo*.

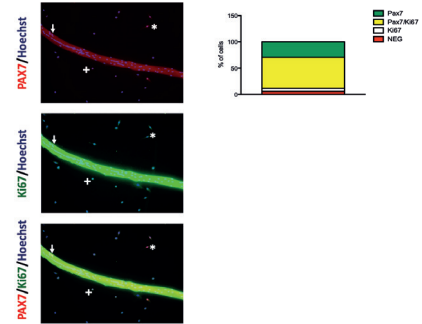
A



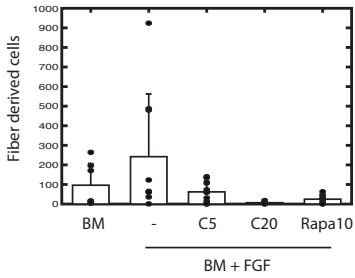
B



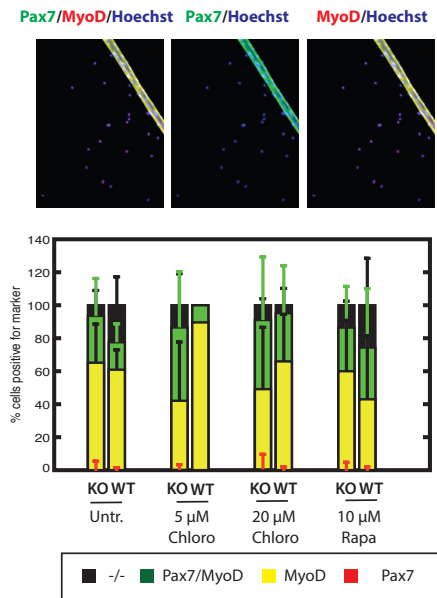
C



D



E

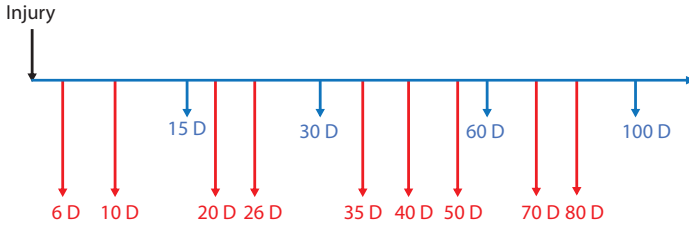


◀Figure 5. Ex vivo modulation of autophagy does not restore satellite cell activation. (A) Experimental layout. (B) Ex vivo satellite cell activation response to FGF-2 exposure. Isolated WT and GAAKO myofibers were maintained under basal activation conditions (basal medium, BM) with and without FGF-2. Satellite cell-derived colonies were plotted. $N=2-4$. * $p<0.05$. (C) Left panels: immunostaining of fiber-derived cells for PAX7 (red) and KI67 (green) 72h after fiber isolation and culture; nuclei counterstained with Hoechst (blue). Right graph: quantification of left panels. $N>3$ fibers/condition. (D) Quantification of the number of fiber derived cells after exposure of GAAKO myofibers to chloroquine or rapamycin for 72h. Data was not significantly different by Kruskal-Wallis test and after correction for multiple testing. (E) Upper panels: immunostaining of fiber-derived cells for PAX7 (green) and MYOD (red) 72h after fiber isolation and culture; nuclei counterstained with Hoechst (blue). Lower panels: quantification.

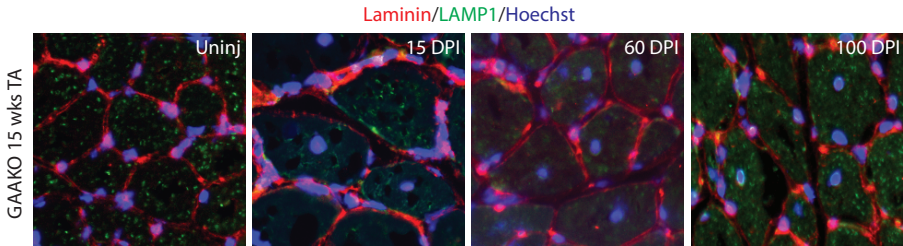
We then used chloroquine and rapamycin to modulate autophagic activity and assessed the effect on the size of fiber-derived mononuclear cell colonies. Inhibiting autophagic flux by treating fibers with a low dose of chloroquine (5 μM) – that was found to increase the LC3-II/I ratio but not affect fiber survival – reduced the numbers of colonies – (Figure 5D). This result suggested that a minimum level of autophagic flux was required for satellite cell activation and expansion in GAAKO fibers. A higher dose of chloroquine (20 μM) induced excessive formation of vacuoles and rapid myofiber death (Figure 5D and data not shown). The reduced formation of fiber-derived cells after treatment with 20 μM chloroquine ($p=0.071$) may be due to chloroquine toxicity. Treating fibers with the mTor-inhibitor rapamycin – which improved LC3 processing but did not remove the autophagic buildup in the center core – also reduced the colony-size of fiber-derived cells to levels similar to those obtained in in WT fibers (compare Fig 5D and 5B). We hypothesize that satellite cell activation is critically affected by a tight window of autophagic flux, and that this process is independent of the autophagic built up observed in GAAKO fibers.

We then assessed the myogenic state of fiber-derived cells by co-staining for PAX7 and MYOD. The myogenic profile of fiber-derived cells from WT or GAAKO donors was similar (Figure 5E). Treatment with chloroquine or rapamycin did not change the myogenic profile (i.e. percentages of cells expressing PAX7 and/or MYOD did not change) of fiber-derived cells, suggesting that the myogenic profile of fiber-derived cells is independent of these treatments (Figure 5E).

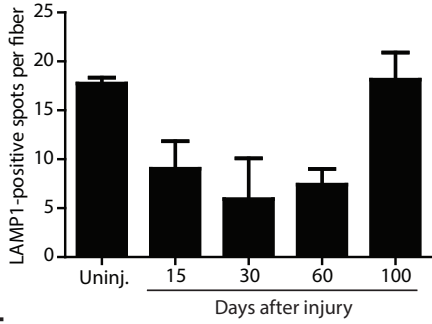
A



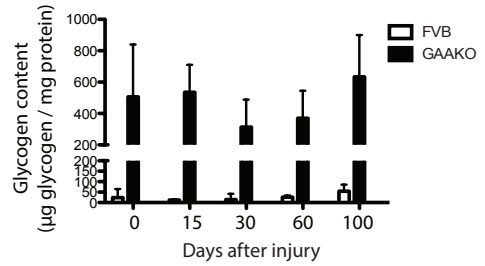
B



C



D



E

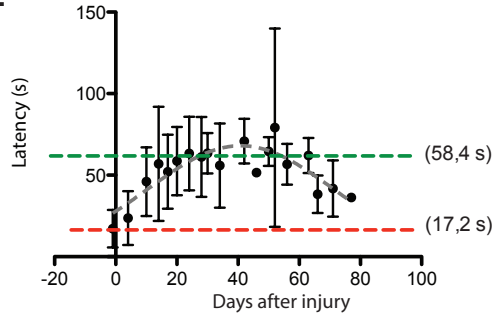


Figure 6. Inducing satellite cell-dependent regeneration through muscle injury improved lysosomal phenotype and muscle function. (A) Schematic layout of the experiment. (B) Immunostaining in cryosections of regenerated tibialis anterior (TA) muscle for Lamp1 (green) at the indicated time points after induction of injury. Laminin (red) indicates fiber perimeter, nuclei were counterstained with Hoechst (blue). (C) Quantification of B. Bars depict the average number of Lamp1-positive spots per myofiber plotted as average \pm SD. N=3 per genotype. (D) Glycogen levels during muscle regeneration. Glycogen levels were determined at indicated timepoints after inducing injury and plotted as average \pm SD. N=3 per genotype. (E) Effect of injury-induced muscle regeneration on muscle function determined by rotarod assay. The figure depicts the latency plotted as average \pm SD. The green dotted line depicts the average latency of non-injured WT animals. The red dotted line depicts the average latency of non-injured GAAKO animals. N \geq 3 per genotype and time point.

The effect of modulating autophagy on the satellite cell response *in vitro* was not conclusive. We proceeded to test if direct satellite cell activation would “overrule” the autophagic block and reverse lysosomal pathology. To this end, we designed a muscle-injury experiment to induce traumatic muscle injury by injecting BaCl₂ – an approach that induces massive myofiber degeneration while efficiently activates satellite cells – (Figure 6A) [54]. We analyzed the lysosomal phenotype by assessing the number of LAMP1-positive vesicles during the regenerative phase (i.e. in the first 30 days after inducing injury) and after regeneration (from day 30 after injury) (Figure 6B). These data showed a decrease of LAMP1-positive lysosomes during the regenerative phase, indicating improvement of the lysosomal phenotype. After completion of regeneration, the number of LAMP1-positive spots progressively increased until returning to similar levels from uninjured muscle, indicating the improvement of the lysosomal phenotype was transient (Figure 6C). Similarly, muscle glycogen levels first decreased up to 30 days after injury, and progressively returned to pre-injury levels between day 30 and 100 after injury (Figure 6D). Together, these findings suggest a transient improvement of the disease phenotype, with a decreased lysosomal compartment and reduced glycogen levels.

Finally, we assessed if the phenotypic improvement also translated to a functional muscle improvement. In parallel with the histological data, muscle function in GAAKO mice first improved to WT levels up to 40-50 days after injury. Similarly, as the morphological parameters, it decreased towards preinjury levels from 50 days after injury onwards (Figure 6E). Taken together, these data indicate that a single induction of muscle regeneration through acute injury transiently improved the Pompe phenotype in GAAKO mice, both at the morphological and functional level, for a period of 40-60 days.

Discussion

During Pompe disease progression satellite cells fail to activate and regenerate the progressive muscle damage. We have shown previously that GAA-deficient satellite cells are fully functional and capable of completing muscle repair, suggesting that the regenerative defect may be originated from the lack of signals from the satellite cell environment or from active inhibition [20]. Our data show that the autophagic flux becomes reduced- but not completely blocked- before the onset of functional muscle loss. Further Inhibition of autophagy in isolated myofibers blocked satellite cell activation and accelerated the myofiber pathology with rapidly expanding vesicles and rapid fiber death suggesting that a minimal level of autophagic flux in GAAKO muscle is needed to support an efficient satellite cell response. Our data with FGF-2-stimulated myofibers *in vitro* and muscle injury *in vivo* suggest that during Pompe disease progression the residual autophagic flux is sufficient for robust for satellite cell activation. Forcing muscle regeneration improved the lysosomal phenotype, decreased glycogen accumulation, and restored muscle function to that of WT counterparts. These data underscore the potential benefit of muscle regenerative therapies for patients with Pompe disease.

Autophagy is dysregulated before onset of muscle wasting

We observed increased levels of Lamp1, Beclin1 and LC3 in TA muscle at 2 weeks compared to the levels of these proteins in TA muscle of older WT animals. Moreover, the low levels of p62 suggest that autophagy is active in both WT and GAAKO neonatal TA muscle, in line with an important role for autophagy in neonatal myogenesis [55]. However, the situation changed with increasing age, as the expression of these autophagy-related proteins was reduced in WT TA muscle, while in GAAKO muscle their levels increased or remained high. LC3-I and BECLIN1 levels were increased already at 10 weeks in GAAKO mice, suggesting increased autophagic activity, while elevated levels of LAMP1 indicate increased lysosome biogenesis [25,56,57]. However, the accumulation of p62 – which is degraded in the lysosome – is indicative of reduced autophagic flux, in line with previous observations [23,31]. The increase in LC3-I/II ratio suggests that lipidation of LC3 was reduced resulting in a relative increase in LC3-I levels. These changes were already observed in animals of 10 weeks of age, 5 weeks before we could detect an effect on muscle performance (see Figure 1).

Chloroquine treatment of myofibers isolated from ± 30 week GAAKO animals further reduced autophagic flux – as indicated by the increase in LC3-II – and expanded the size of autophagic vacuoles with profound effects on myofiber survival and satellite cell activation. This indicated that the autophagic flux – at least based on the isolated myofiber model – was not completely blocked, even in mice that already developed a disease phenotype. The limitation of our approach includes the use of one agent to inhibit autophagy. The use of models with (inducible) genetic inactivation of key autophagy genes, such as Atg5 or Atg7, would help in further exploring the role of autophagy in satellite cell activation in Pompe disease.

Increasing autophagy with the mTor inhibitor rapamycin improved autophagic flux (visualized by increased processing of LC3), although it failed to resolve the autophagic vacuoles under the conditions tested. In Niemann-Pick disease decreasing disease-specific lysosomal cholesterol-load resolved the accumulation of the autophagic vacuoles and improved survival of NPC1^{-/-} cells [58]. A similar strategy for Pompe disease – using ERT treatment to decrease lysosomal glycogen accumulation – failed to reduce vacuoles and autophagic buildup [31]. Therefore, strategies that reverse autophagic buildup may be insufficient to restore regenerative activity in GAA-deficient muscle, although additional strategies should be explored.

Chronic and repeated mTor inhibition studies resulted in stem cell depletion, also in skeletal muscle; providing a possible explanation for the lack of effect of rapamycin treatment in the experiments conducted in our study [59]. Considering the importance of mTor signaling for muscle regeneration, strategies aimed to reverse autophagic buildup might need to be mTor-independent to avoid undesired interference with the regenerative process [60]. A good candidate for mTor-independent activation of autophagy is AMPK. Pharmacological stimulation of AMPK using AICAR was found to increase muscle regeneration as an exercise mimetic, as well as in a myopathy mouse model [61,62].

Satellite cell activation requires a minimal level of autophagic flux

The early occurrence of autophagy defects observed already in myofibers from 10-week-GAAKO mice, weeks before we detected reduced satellite cell activation [20,21] and loss of muscle function (Figure 1), raised the question whether reduced

autophagic flux and buildup of autophagic vacuoles contribute to the failing regenerative response. Satellite cell activation is dependent on signals from the niche as well as on paracrine signals derived from the associated myofiber [63–65]. The latter implies properly functioning endosomal pathways [66] that allow release of matrix remodeling enzymes such as MMP-2 and MMP-9, that mediate release of ligands that are embedded in the satellite cell niche [53,67]. Our data suggest that the inward endosome trafficking – i.e. uptake of extracellular material into the lysosome – is functional in GAAKO myofibers. However, our data suggests reduced excretion of lysosomal content – i.e. reduced outward signaling – that may affect the release of satellite cell activating signals. With respect to reduced autophagic flux, the increased motility of small-sized lysosomes in GAAKO myofibers that we observed was unexpected, and may be regulated by dysregulated Ca^{2+} homeostasis reported for Pompe disease muscle [68]. Lysosome motility has been suggested to be regulated by intracellular Ca^{2+} levels [69].

Not only are functioning autophagic pathways in the fiber important, but also those in the satellite cells. Autophagy was found to be upregulated by satellite cells to supply the bioenergetic demands for satellite cell activation [26]. Although we did not assess autophagic activity and flux in satellite cells, the robust response after FGF-2-stimulation *ex vivo* (Figure 5B) or following injury [20,21] suggest that autophagic flux remained sufficient to mediate satellite cell activation, even after the onset of muscle wasting.

Improving the lysosomal phenotype and the autophagy defect by inducing muscle regeneration

We demonstrated that stimulating satellite cell activation directly *in vivo* through induction of muscle injury improved the lysosomal phenotype and muscle regeneration. Moreover, *in vitro* we found that treatment of isolated myofibers with satellite cell ligand FGF-2 overruled the autophagic defect and stimulated satellite cell proliferation. This could indicate that satellite cells depend on either signaling from the damaged niche or from the associated fiber, as discussed above, to become fully activated. In contrast to dystrophic muscle, myofiber integrity is not affected in Pompe disease, and the pathology in develops mainly inside myofibers by the expansion of glycogen-filled vacuoles [24,70,71]. Analysis of Evans blue staining during disease progression in GAAKO animals revealed no increase in sarcolemmal damage (data not shown). Thus, probably the satellite cell

niche remains intact during disease progression. As discussed above, autophagic defects inside myofibers prevent myofiber-induced satellite cell activation, explaining the lack of satellite cell activation during Pompe disease progression. Our findings suggest that exogenous signals are needed (and may be sufficient) to induce satellite cell activation and muscle regeneration. Once induced beyond the “autophagic block” activated satellite cells are effective in regenerating damage in the context of Pompe disease. From a clinical perspective this may be achieved through pharmacological approaches (by activation satellite cells using mitogens) or by developing exercise programs that are safe for patients with neuromuscular disorders aimed to enhance satellite cell activation [72,73]. A past study showed that the widely described positive effects of exercise on satellite cell activation and muscle regeneration may also be achieved by pharmacological strategies (using exercise mimetics) by targeting AMPK signaling [61].

Overruling the blocked satellite cell response by inducing muscle regeneration directly improved the lysosomal phenotype and muscle function, although the beneficial effect was only transient. Therefore, a satellite cell-dependent regenerative therapy is only clinically relevant for the longer term when combined with current ERT or future therapies that are aimed at correcting the genetic defect, such as gene therapy, that are in development for Pompe disease.

In this report we have shown that autophagic defects are correlated to the regenerative defects that prevent repair of the progressive disease-mediated damage. Our data show that the satellite cell response may be restored by signals that do not depend on autophagic pathways but that activate satellite cells directly. The beneficial effects of the resulting regenerative response warrant further study to find approaches that can target the satellite cell compartment in a safe and efficient manner.

Material and methods

Mice and animal procedures

In vivo studies were performed in 10-30-week-old wild-type FVB/N (FVB) (Envigo, the Netherlands) and GAAKO (in the FVB/N background; generated in-house [29]) mice. Mice were housed at the Erasmus MC Animal Facility according to institutionally approved protocols. Through all experiments, mice were housed under a light-dark cycle of 12 hours and with access to food and water *ad libitum*.

Muscle regeneration was induced by i.m. injection of 50 μ l 1.2% w/v BaCl₂

(Sigma-Aldrich) into *tibialis anterior* (TA) muscles. Mice were pre-anesthetized with 4% isofluorane with a vaporizer (Pharmachemie B.V., Haarlem, Netherlands). Mice were sacrificed by cervical dislocation according to institutional regulations. TA muscle tissue was obtained from WT and *Gaa*^{-/-} mice at the specified time points.

Motor muscle tasks were performed with the accelerating rotarod (from 4 to 40 rpm in 5 minutes; model 7650, Ugo Basile Biologic Research apparatus). Mice were given 2 trials of 3 runs per time-point with a 15-minute break. Time to fall was recorded as measure of performance.

All animal experiments were approved by the local Animal Experiments Committee (DEC) and national Central Committee for Animal Experiments (CCD), animal experiment authorities in compliance with the European Community Council Directive guidelines (EU directive 86/609), regarding the protection of animals used for experimental purposes. All procedures with the animals were performed with the aim of ensuring that discomfort, distress, pain, and injury would be minimal.

Western Blot analysis

TA muscle resected from WT and GAAKO animals sacrificed at indicated age was snap-frozen in liquid nitrogen. Frozen tissue was homogenized using a tissue sonicator [brand] in precooled RIPA buffer (50 mM TrisHCl pH 7.4, 150 mM NaCl, 2 mM EDTA, 1% Triton X-100) supplemented with a phosphatase inhibitor cocktail (10 mM NaF, 60 mM β -glycerolphosphate, 2 mM Na-orthovanadate) and cComplete™ protease inhibitor cocktail (Sigma-Aldrich). Total protein concentration was determined using Pierce™ BCA Protein Assay Kit according to manufacturer's instructions (Thermo Scientific, Rockford IL, USA).

Samples were electrophoreses and blotted to nitrocellulose membranes as described before [74]. Membranes were developed with specific antibodies against LC3 (Sigma), Lamp1 (Abcam), P62 (Santa Cruz) and Beclin1. Membranes were read on an Odyssey reader (Li-Cor).

Myofiber analysis and *in vitro* satellite cell activation

Individual myofibers were isolated from 20-30-week WT and GAAKO mice as recently outlined [49]. Isolated myofibers were cultured in basal medium (DMEM supplemented with penicillin-streptomycin (50 U/ml), 5% horse serum (v/v; Lonza), 5% FCS (v/v, Lonza), chicken embryo extract (US Biologicals; 1 mg/ml) or activation

medium (Hams F10 (Lonza) supplemented with penicillin-streptomycin (50 U/ml), 20% FCS (v/v, Lonza) and FGF-2 (20 ng/ml, PeproTech). For confocal imaging single fibers were plated in 96-well optical bottom plates (Thermo Scientific). For analysis of *in vitro* satellite cell activation, single fibers were plated on ECM-coated (50 µg/ml Sigma) 96-well plates (Gibco) and treated as indicated. Fibers and fiber-derived cells were fixed with 4% (w/v) paraformaldehyde and stained as indicated in the figures. Fiber-derived cells were counted using Fiji software.

Imaging experiments

For lysotracker staining myofibers were treated as described and exposed to 70 nM lysotracker (Lysotracker-Red; Molecular Probes) for 15 min at 37 C and then fixed in 4% (w/v) paraformaldehyde. Lysotracker-staining was imaged on a Leica SP5 confocal laser scanning microscope or by wide-field microscopy. Dynamic imaging of lysotracker-positive vesicles was performed by superresolution imaging using a spinning disc confocal microscope (Leica SD AF). For dextran pulse-chase experiments myofibers were exposed to 0.5 mg/mL AF488-dextran for 1h or 3h. After wash-out of dextran myofibers were cultured in proliferation medium and imaged at indicated timepoints on a Zeiss LSM 510 Meta confocal microscope equipped with a climate chamber supporting 37C and 5% CO₂.

Immunostaining analyses

In vitro cultured myofibers were fixed in 4% paraformaldehyde (PFA) and permeabilized with 0.5% Triton X-100%; 3% BSA in PBS for 30 minutes at room temperature (RT). Blocking was performed using 20% horse serum (Lonza) for 1 hour at RT. Antibodies were diluted in 0.1% BSA; 0.1% Tween 20 in PBS and incubated for 30 minutes at RT. Nuclei were counter-stained with Hoechst 33258 (H3569; Life Technologies; 1:15000) for 10 minutes at RT in the dark. Stained samples were imaged on a Nikon Eclipse Ti-E Wide Field inverted microscope (Nikon Instruments Europe B.V. Amsterdam, Netherlands). Images were analyzed using Adobe Photoshop CS6 and FIJI (fiji.sc/Fiji).

Immunostaining in murine muscle sections

Immunostainings on mouse muscle tissue was performed as described previously [20]. In short, fresh sections were cut, immediately fixed in 4% EM-grade PFA (Electron Microscopy Sciences, Hatfield, PA) at RT for 5 minutes. Tissue sections

were permeabilized using 0.5% Triton X-100 in 20% goat serum 3% BSA in PBS for 1 hour at RT. Primary antibodies were diluted in the permeabilization/blocking solution and incubated at RT for 2 hours. Sections were washed with 0.1% Tween20 in PBS and secondary antibodies incubated in permeabilization/blocking solution for 1h at RT. Nuclei were counterstained with Hoechst. The slides were then mounted using Mowiol® (475904; Calbiochem) mounting solution and imaged on a Zeiss LSM700 microscope (Carl Zeiss B. V. Sliedrecht, The Netherlands) using tile-scan modality with a 20x objective lens using Zen 2009 imaging software (Carl Zeiss B. V.). The respective fields were digitally stitched to obtain whole-section images. Image analysis and processing was performed using FIJI (fiji.sc/Fiji) and Adobe Photoshop CS6.

Enzymatic assays

All tissues were homogenized in water by sonication (MSE sonifier) on ice until completely lysed (medium level, amplitude 5 m). Glycogen content was determined as described [75] The resulting glucose was measured after conversion by glucose-oxidase and reaction with 2,2-azino-di-(ethyl-benzthiazolinsulfonate).

Statistical Analysis

Data are expressed as means \pm SD. For all experiments normality of data was estimated based on calculated residuals. Normally distributed data from two independent groups was tested using two-sided t-tests. Normally distributed data for experiments with three or more independent groups was tested with one-way ANOVA followed by post-hoc Tukey or Games-Howell correction for multiple tests (depending on homogeneity of variance). Non-normally distributed data for experiments with three or more independent groups was tested with Kruskal-Wallis test. *p*-values were adjusted by the Bonferroni correction for multiple tests. A *p*-value of less than 0.05 was considered significant. Data was analyzed using IBM SPSS Statistics (version 26). Plots were generated in Graphpad prism (v9) or in Publishplot 9.

Author contributions

G.J.S. designed the study, performed experiments, analyzed and interpreted the data, and participated in the preparation of the manuscript. R.C.F. performed experiments, interpreted the data, and participated in the preparation of the manuscript. T.J.M.v.G., E.B, B.d.J., B.B., and S.B, TH and M.v.R. performed experiments and interpreted the data. A.v.d.P. interpreted the data. W.W.M.P. designed the study, interpreted the data, and participated in the preparation of the manuscript.

Sources of Funding

This work was funded through the Erasmus MC.

Disclosures

A.T.v.d.P. has provided consulting services for various industries in the field of Pompe disease under an agreement between these industries and Erasmus MC, Rotterdam, the Netherlands. All the other authors declare no conflict of interest.

References

1. Reuser, A., Hirschhorn, R., and Kroos, M.A. (2018). Pompe Disease: Glycogen Storage Disease Type II, Acid α -Glucosidase (Acid Maltase) Deficiency. In *The online Metabolic and Molecular Bases of Inherited Disease*. David Valle, MD, Editor-in-Chief, Arthur L. Beaudet, MD, Editor, Bert Vogelstein, MD, Editor, Kenneth W. Kinzler, Ph.D., Editor, Stylianos E. Antonarakis, MD, D.Sc., Editor, Andrea Ballabio, M, pp. 1-72.
2. van der Ploeg, A.T., and Reuser, A.J. (2008). Pompe's disease. *Lancet* 372, 1342-1353. Available at: <http://www.thelancet.com/article/S014067360861555X/fulltext> [Accessed October 12, 2015].
3. van den Hout, H.M., Hop, W., van Diggelen, O.P., Smeitink, J.A., Smit, G.P., Poll-The, B.T., Bakker, H.D., Loonen, M.C., de Klerk, J.B., Reuser, A.J., *et al.* (2003). The natural course of infantile Pompe's disease: 20 original cases compared with 133 cases from the literature. *Pediatrics* 112, 332-340.
4. Hagemans, M.L.C., Hop, W.J.C., Van Doom, P.A., Reuser, A.J.J., and Van Der Ploeg, A.T. (2006). Course of disability and respiratory function in untreated late-onset Pompe disease. *Neurology* 66, 581-3.
5. van der Beek, N. a M.E., de Vries, J.M., Hagemans, M.L.C., Hop, W.C.J., Kroos, M. a, Wokke, J.H.J., de Visser, M., van Engelen, B.G.M., Kuks, J.B.M., van der Kooij, A.J., *et al.* (2012). Clinical features and predictors for disease natural progression in adults with Pompe disease: a nationwide prospective observational study. *Orphanet J. Rare Dis.* 7, 88.
6. Van den Hout, H., Reuser, A.J., Vulto, A.G., Loonen, M.C., Cromme-Dijkhuis, A., and Van der Ploeg, A.T. (2000). Recombinant human α -glucosidase from rabbit milk in Pompe patients. *Lancet* 356, 397-398.
7. Kishnani, P.S., Corzo, D., Nicolino, M., Byrne, B., Mandel, H., Hwu, W.L., Leslie, N., Levine, J., Spencer, C., McDonald, M., *et al.* (2007). Recombinant human acid α -glucosidase: Major clinical benefits in infantile-onset Pompe disease. *Neurology* 68, 99-109. Available at: www.neurology.com [Accessed April 19, 2021].
8. van der Ploeg, A.T., Clemens, P.R., Corzo, D., Escolar, D.M., Florence, J., Groeneveld, G.J., Herson, S., Kishnani, P.S., Laforet, P., Lake, S.L., *et al.* (2010). A randomized study of alglucosidase alfa in late-onset Pompe's disease. *N. Engl. J. Med.* 362, 1396-1406.
9. Raben, N., Takikita, S., Pittis, M.G., Bembi, B., Marie, S.K.N., Roberts, A., Page, L., Kishnani, P.S., Schoser, B.G.H., Chien, Y.H., *et al.* (2007). Deconstructing pompe disease by analyzing single muscle fibers: To see a world in a grain of sand... *Autophagy* 3, 546-52.
10. Bembi, B., Pisa, F.E., Confalonieri, M., Ciana, G., Fiumara, A., Parini, R., Rigoldi, M., Moglia, A., Costa, A., Carlucci, A., *et al.* (2010). Long-term observational, non-randomized study of enzyme replacement therapy in late-onset glycogenosis type II. *J. Inherit. Metab. Dis.* 33, 727-35.
11. Regnery, C., Kornblum, C., Hanisch, F., Vielhaber, S., Strigl-Pill, N., Grunert, B., Müller-Felber, W., Glocker, F.X., Spranger, M., Deschauer, M., *et al.* (2012). 36 months observational clinical study of 38 adult Pompe disease patients under alglucosidase alfa enzyme replacement therapy. *J. Inherit. Metab. Dis.* 35, 837-845.
12. Papadopoulos, C., Orlikowski, D., Prigent, H., Lacour, A., Tard, C., Furby, A., Praline, J., Sole, G., Hogrel, J.-Y., De Antonio, M., *et al.* (2017). Effect of enzyme replacement therapy with alglucosidase alfa (Myozyme(R)) in 12 patients with advanced late-onset Pompe disease. *Mol. Genet. Metab.* 22, 80-85.

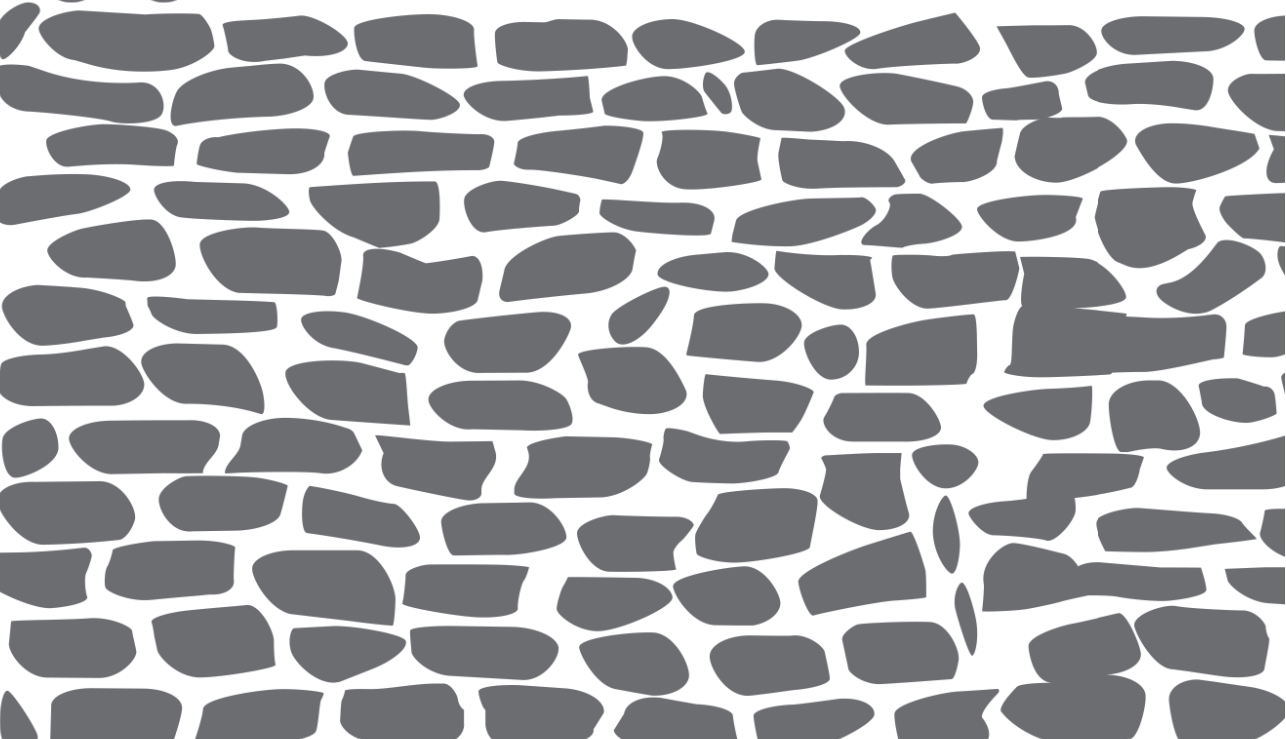
13. Angelini, C., Semplicini, C., Ravaglia, S., Bembi, B., Servidei, S., Pegoraro, E., Moggio, M., Filosto, M., Sette, E., Crescimanno, G., *et al.* (2012). Observational clinical study in juvenile-adult glycogenosis type 2 patients undergoing enzyme replacement therapy for up to 4 years. *J. Neurol.* 259, 952–8.
14. Kuperus, E., Kruijshaar, M.E., Wens, S.C.A., de Vries, J.M., Favejee, M.M., van der Meijden, J.C., Rizopoulos, D., Brusse, E., van Doorn, P.A., van der Ploeg, A.T., *et al.* (2017). Long-term benefit of enzyme replacement therapy in Pompe disease. *Neurology* 89, 2365–2373.
15. Bergsma, A.J., van der Wal, E., Broeders, M., van der Ploeg, A.T., and Pim Pijnappel, W.W.M. (2018). Alternative Splicing in Genetic Diseases: Improved Diagnosis and Novel Treatment Options. In *International Review of Cell and Molecular Biology*, pp. 335:85–141.
16. Lepper, C., Partridge, T. a, and Fan, C.-M. (2011). An absolute requirement for Pax7-positive satellite cells in acute injury-induced skeletal muscle regeneration. *Development* 138, 3639–3646.
17. Sambasivan, R., Yao, R., Kissenpfennig, A., van Wittenberghe, L., Paldi, A., Gayraud-Morel, B., Guenou, H., Malissen, B., Tajbakhsh, S., and Galy, A. (2011). Pax7-expressing satellite cells are indispensable for adult skeletal muscle regeneration. *Development* 138, 3647–3656.
18. Schaaf, G.J., Canibano-Fraile, R., van Gestel, T.J.M., van der Ploeg, A.T., and Pijnappel, W.W.M.P. (2019). Restoring the regenerative balance in neuromuscular disorders: satellite cell activation as therapeutic target in Pompe disease. *Ann. Transl. Med.* 7, 280. Available at: <http://www.ncbi.nlm.nih.gov/pubmed/31392192> [Accessed August 28, 2019].
19. Schaaf, G.J., van Gestel, T.J.M., Brusse, E., Verdijk, R.M., de Coo, I.F.M., van Doorn, P.A., van der Ploeg, A.T., and Pijnappel, W.W.M.P. (2015). Lack of robust satellite cell activation and muscle regeneration during the progression of Pompe disease. *Acta Neuropathol. Commun.* 3, 65. Available at: <http://www.pubmedcentral.nih.gov/articlerender.fcgi?artid=4625612&tool=pmcentrez&rendertype=abstract> [Accessed November 11, 2015].
20. Schaaf, G.J., van Gestel, T.J.M., in 't Groen, S.L.M., de Jong, B., Boomaars, B., Tarallo, A., Cardone, M., Parenti, G., van der Ploeg, A.T., and Pijnappel, W.W.M.P. (2018). Satellite cells maintain regenerative capacity but fail to repair disease-associated muscle damage in mice with Pompe disease. *Acta Neuropathol. Commun.* 6, 119.
21. Lagalice, L., Pichon, J., Gougeon, E., Soussi, S., Deniaud, J., Ledevin, M., Maurier, V., Leroux, I., Durand, S., Ciron, C., *et al.* (2018). Satellite cells fail to contribute to muscle repair but are functional in Pompe disease (glycogenosis type II). *Acta Neuropathol. Commun.* 6, 116. Available at: <https://actaneurocomms.biomedcentral.com/articles/10.1186/s40478-018-0609-y> [Accessed February 7, 2019].
22. Raben, N., Takikita, S., Pittis, M.G., Bembi, B., Marie, S.K.N., Roberts, A., Page, L., Kishnani, P.S., Schoser, B.G.H., Chien, Y.H., *et al.* (2007). Deconstructing pompe disease by analyzing single muscle fibers: To see a world in a grain of sand... *Autophagy*.
23. Nascimbeni, A.C., Fanin, M., Masiero, E., Angelini, C., and Sandri, M. (2012). The role of autophagy in the pathogenesis of glycogen storage disease type II (GSDII). *Cell Death Differ.* 19, 1698–1708. Available at: www.nature.com/cdd [Accessed April 21, 2021].
24. Thurberg, B.L., Lynch Maloney, C., Vaccaro, C., Afonso, K., Tsai, A.C.-H., Bossen, E., Kishnani, P.S., and O'Callaghan, M. (2006). Characterization of pre- and post-treatment pathology after enzyme replacement therapy for pompe disease. *Lab. Invest.* 86, 1208–1220. Available at: <http://www.nature.com/doi/10.1038/labinvest.3700484> [Accessed September 13, 2016].

25. Dikic, I., and Elazar, Z. (2018). Mechanism and medical implications of mammalian autophagy. *Nat. Rev. Mol. Cell Biol.* 19, 349–364.
26. Tang, A.H., and Rando, T.A. (2014). Induction of autophagy supports the bioenergetic demands of quiescent muscle stem cell activation. *EMBO J* 33, 2782–97.
27. García-Prat, L., Martínez-Vicente, M., Perdiguero, E., Ortet, L., Rodríguez-Ubrea, J., Rebollo, E., Ruiz-Bonilla, V., Gutarra, S., Ballestar, E., Serrano, A.L., et al. (2016). Autophagy maintains stemness by preventing senescence. *Nature* 529, 37–42. Available at: <http://www.nature.com/doi/10.1038/nature16187>.
28. Fiacco, E., Castagnetti, F., Bianconi, V., Madaro, L., De Bardi, M., Nazio, F., D'Amico, A., Bertini, E., Cecconi, F., Puri, P.L., et al. (2016). Autophagy regulates satellite cell ability to regenerate normal and dystrophic muscles. *Cell Death Differ.*
29. Bijvoet, A.G.A., van de Kamp, E.H.M., Kroos, M.A., Ding, J.-H., Yang, B.Z., Visser, P., Bakker, C.E., Verbeet, M.P., Oostra, B.A., Reuser, A.J.J., et al. (1998). Generalized glycogen storage and cardiomegaly in a knockout mouse model of Pompe disease. *Hum. Mol. Genet.* 7, 53–62. Available at: <https://academic.oup.com/hmg/article-lookup/doi/10.1093/hmg/7.1.53> [Accessed July 16, 2019].
30. Raben, N., Nagaraju, K., Lee, E., Kessler, P., Byrne, B., Lee, L., LaMarca, M., King, C., Ward, J., Sauer, B., et al. (1998). Targeted disruption of the acid α -glucosidase gene in mice causes an illness with critical features of both infantile and adult human glycogen storage disease type II. *J. Biol. Chem.* 273, 19086–92. Available at: <http://www.ncbi.nlm.nih.gov/pubmed/9668092> [Accessed October 14, 2016].
31. Fukuda, T., Ewan, L., Bauer, M., Mattaliano, R.J., Zaal, K., Ralston, E., Plotz, P.H., and Raben, N. (2006). Dysfunction of endocytic and autophagic pathways in a lysosomal storage disease. *Ann. Neurol.*
32. Kang, R., Zeh, H.J., Lotze, M.T., and Tang, D. (2011). The Beclin 1 network regulates autophagy and apoptosis. *Cell Death Differ.* 18, 571.
33. Rusten, T.E., and Stenmark, H. (2010). p62, an autophagy hero or culprit? *Nat. Cell Biol.* 2010 123 12, 207–209.
34. Mizushima, N., and Yoshimori, T. (2007). How to Interpret LC3 Immunoblotting. *Autophagy* 542.
35. Tanida, I., Ueno, T., and Kominami, E. (2008). LC3 and Autophagy. *Methods Mol. Biol.* 445, 77–88.
36. González-Rodríguez, Á., Mayoral, R., Agra, N., Valdecantos, M.P., Pardo, V., Miquilena-Colina, M.E., Vargas-Castrillón, J., Lo Iacono, O., Corazzari, M., Fimia, G.M., et al. (2014). Impaired autophagic flux is associated with increased endoplasmic reticulum stress during the development of NAFLD. *Cell Death Dis.* 2014 54 5, e1179–e1179.
37. Raben, N., Schreiner, C., Baum, R., Takikita, S., Xu, S., Xie, T., Myerowitz, R., Komatsu, M., Van Der Meulen, J.H., Nagaraju, K., et al. (2010). Suppression of autophagy permits successful enzyme replacement therapy in a lysosomal storage disorder - Murine Pompe disease. *Autophagy*.
38. Raben, N., Roberts, A., and Plotz, P. (2007). Role of autophagy in the pathogenesis of Pompe Disease. *Acta Myol* 26, 45–48.
39. J, P., CM, G., T, K.-K., and JS, B. (2016). Mechanisms and functions of lysosome positioning. *J. Cell Sci.* 129, 4329–4339.

40. Oyarzún, J.E., Lagos, J., Vázquez, M.C., Valls, C., De la Fuente, C., Yuseff, M.I., Alvarez, A.R., and Zanlungo, S. (2019). Lysosome motility and distribution: Relevance in health and disease. *Biochim. Biophys. Acta - Mol. Basis Dis.* 1865, 1076–1087.
41. Matteoni, R., and Kreis, T.E. (1987). Translocation and clustering of endosomes and lysosomes depends on microtubules. *J. Cell Biol.* 105, 1253–1265.
42. S, B., M, V., CH, C., and PA, R. (1993). Cytoskeletal structure of skeletal muscle: identification of an intricate exosarcomeric microtubule lattice in slow- and fast-twitch muscle fibers. *J. Histochem. Cytochem.* 41, 1013–1021.
43. Zirin, J., Nieuwenhuis, J., and Perrimon, N. (2013). Role of Autophagy in Glycogen Breakdown and Its Relevance to Chloroquine Myopathy. *PLoS Biol.* 11, 1001708. Available at: www.plosbiology.org [Accessed May 6, 2021].
44. Anguille, S., Smits, E.L.J.M., Cools, N., Goossens, H., Berneman, Z.N., and Van Tendeloo, V.F.I. (2009). Short-term cultured, interleukin-15 differentiated dendritic cells have potent immunostimulatory properties. *J. Transl. Med.* 7.
45. Jansen, K.M., and Pavlath, G.K. (2006). Mannose receptor regulates myoblast motility and muscle growth. *J. Cell Biol.* 174, 403–413.
46. Johnson, D.E., Ostrowski, P., Jaumouillé, V., and Grinstein, S. (2016). The position of lysosomes within the cell determines their luminal pH. *J. Cell Biol.* 212, 677–692.
47. Buratta, S., Tancini, B., Sagini, K., Delo, F., Chiaradia, E., Urbanelli, L., and Emiliani, C. (2020). Lysosomal Exocytosis, Exosome Release and Secretory Autophagy: The Autophagic- and Endo-Lysosomal Systems Go Extracellular. *Int. J. Mol. Sci.* 21, 2576.
48. Dikic, I., and Elazar, Z. (2018). Mechanism and medical implications of mammalian autophagy. *Nat. Rev. Mol. Cell Biol.* 19, 349–364.
49. Canibano-Fraile, R., Boertjes, E., Bozhilova, S., Pijnappel, W.W.M.P., and Schaaf, G.J. (2021). An in vitro assay to quantify satellite cell activation using isolated mouse myofibers. *STAR Protoc.* 2, 100482.
50. Al-Bari, M. (2015). Chloroquine analogues in drug discovery: new directions of uses, mechanisms of actions and toxic manifestations from malaria to multifarious diseases. *J. Antimicrob. Chemother.* 70, 1608–1621.
51. Nath, S., Dancourt, J., Shteyn, V., Puente, G., Fong, W.M., Nag, S., Bewersdorf, J., Yamamoto, A., Antony, B., and Melia, T.J. (2014). Lipidation of the LC3/GABARAP family of autophagy proteins relies upon a membrane curvature-sensing domain in Atg3. *Nat. Cell Biol.* 16, 415.
52. Noda, T., and Ohsumi, Y. (1998). Tor, a phosphatidylinositol kinase homologue, controls autophagy in yeast. *J. Biol. Chem.* 273, 3963–3966.
53. Pawlikowski, B., Vogler, T.O., Gadek, K., and Olwin, B.B. (2017). Regulation of skeletal muscle stem cells by fibroblast growth factors. *Dev. Dyn.* 246, 359–367. Available at: <http://doi.wiley.com/10.1002/dvdy.24495> [Accessed April 6, 2021].
54. Hardy, D., Besnard, A., Latil, M., Jouvion, G., Briand, D., Thépenier, C., Pascal, Q., Guguin, A., Gayraud-Morel, B., Cavaillon, J.-M., *et al.* (2016). Comparative Study of Injury Models for Studying Muscle Regeneration in Mice. *PLoS One* 11, e0147198. Available at: <http://dx.plos.org/10.1371/journal.pone.0147198> [Accessed April 26, 2017].
55. Zecchini, S., Giovarelli, M., Perrotta, C., Morisi, F., Touvier, T., Di Renzo, I., Moscheni, C., Bassi, M.T., Cervia, D., Sandri, M., *et al.* (2019). Autophagy controls neonatal myogenesis by regulating the GH-IGF1 system through a NFE2L2- and DDIT3-mediated mechanism. *Autophagy* 15, 58–77.

56. Ma, X., Godar, R.J., Liu, H., and Diwan, A. (2012). Enhancing lysosome biogenesis attenuates BNIP3-induced cardiomyocyte death. *Autophagy* 8, 297. Available at: [/pmc/articles/PMC3337840/](https://pubmed.ncbi.nlm.nih.gov/22711111/) [Accessed July 30, 2021].
57. Cheng, X.T., Xie, Y.X., Zhou, B., Huang, N., Farfel-Becker, T., and Sheng, Z.H. (2018). Revisiting LAMP1 as a marker for degradative autophagy-lysosomal organelles in the nervous system. *Autophagy* 14, 1472–1474.
58. Meske, V., Erz, J., Priesnitz, T., and Ohm, T.G. (2014). The autophagic defect in Niemann-Pick disease type C neurons differs from somatic cells and reduces neuronal viability. *Neurobiol. Dis.* 64, 88–97.
59. Haller, S., Kapuria, S., Riley, R.R., O'Leary, M.N., Schreiber, K.H., Andersen, J.K., Melov, S., Que, J., Rando, T.A., Rock, J., et al. (2017). mTORC1 Activation during Repeated Regeneration Impairs Somatic Stem Cell Maintenance. *Cell Stem Cell*.
60. Zhang, P., Liang, X., Shan, T., Jiang, Q., Deng, C., Zheng, R., and Kuang, S. (2015). mTOR is necessary for proper satellite cell activity and skeletal muscle regeneration. *Biochem. Biophys. Res. Commun.* 463, 102–8. Available at: <http://www.sciencedirect.com/science/article/pii/S0006291X15009468> [Accessed October 30, 2015].
61. Narkar, V.A., Downes, M., Yu, R.T., Embler, E., Wang, Y.-X., Banayo, E., Mihaylova, M.M., Nelson, M.C., Zou, Y., Juguilon, H., et al. (2008). AMPK and PPARdelta agonists are exercise mimetics. *Cell* 134, 405–15.
62. Peralta, S., Garcia, S., Yin, H.Y., Arguello, T., Diaz, F., and Moraes, C.T. (2016). Sustained AMPK activation improves muscle function in a mitochondrial myopathy mouse model by promoting muscle fiber regeneration. *Hum. Mol. Genet.*
63. Yin, H., Price, F., and Rudnicki, M.A. (2013). Satellite cells and the muscle stem cell niche. *Physiol. Rev.* 93, 23–67. Available at: <http://www.ncbi.nlm.nih.gov/pubmed/23303905> [Accessed July 1, 2016].
64. Guerci, A., Lahoute, C., Hébrard, S., Collard, L., Graindorge, D., Favier, M., Cagnard, N., Batonnet-Pichon, S., Précigout, G., Garcia, L., et al. (2012). Srf-dependent paracrine signals produced by myofibers control satellite cell-mediated skeletal muscle hypertrophy. *Cell Metab.* 15, 25–37.
65. Hesselink, R.P., Van Kranenburg, G., Wagenmakers, A.J.M., Van Der Vusse, G.J., and Drost, M.R. (2005). Age-related decline in muscle strength and power output in acid 1-4 α -glucosidase knockout mice. *Muscle and Nerve* 31, 374–381.
66. Sorkin, A., and Von Zastrow, M. (2009). Endocytosis and signalling: Intertwining molecular networks. *Nat. Rev. Mol. Cell Biol.* 10, 609–622.
67. Sbai, O., Ould-Yahoui, A., Ferhat, L., Gueye, Y., Bernard, A., Charrat, E., Mehanna, A., Risso, J.-J., Chauvin, J.-P., Fenouillet, E., et al. (2010). Differential vesicular distribution and trafficking of MMP-2, MMP-9, and their inhibitors in astrocytes. *Glia* 58, 344–366. Available at: <https://onlinelibrary.wiley.com/doi/full/10.1002/glia.20927> [Accessed July 30, 2021].
68. Lim, J.A., Li, L., Kakhlon, O., Myerowitz, R., and Raben, N. (2015). Defects in calcium homeostasis and mitochondria can be reversed in Pompe disease. *Autophagy* 11, 385–402.
69. Li, X., Rydzewski, N., Hider, A., Zhang, X., Yang, J., Wang, W., Gao, Q., Cheng, X., and Xu, H. (2016). A molecular mechanism to regulate lysosome motility for lysosome positioning and tubulation. *Nat. Cell Biol.* 2016 184 18, 404–417.

70. Griffin, J.L. (1984). Infantile acid maltase deficiency. I. Muscle fiber destruction after lysosomal rupture. *Virchows Arch. B. Cell Pathol. Incl. Mol. Pathol.* 45, 23–36.
71. Petrof, B.J., Shrager, J.B., Stedman, H.H., Kelly, A.M., and Sweeney, H.L. (1993). Dystrophin protects the sarcolemma from stresses developed during muscle contraction. *Proc. Natl. Acad. Sci. U. S. A.* 90, 3710–3714.
72. Masschelein, E., D'Hulst, G., Zvick, J., Hinte, L., Soro-Arnaiz, I., Gorski, T., Meyenn, F. von, Bar-Nur, O., and Bock, K. De (2020). Exercise promotes satellite cell contribution to myofibers in a load-dependent manner. *Skelet. Muscle* 2020 101 10, 1–15.
73. Hauerslev, S., Vissing, J., and Krag, T.O. (2014). Muscle atrophy reversed by growth factor activation of satellite cells in a mouse muscle atrophy model. *PLoS One* 9.
74. Demirdas, S., van Slegtenhorst, M.A., Verdijk, R.M., Lee, M., van den Hout, H.M.P., Wessels, M.W., Frohn-Mulder, I.M.E., Gardeitchik, T., van der Ploeg, A.T., and Schaaf, G.J. (2019). Delayed Diagnosis of Danon Disease in Patients Presenting With Isolated Cardiomyopathy. *Circ. Genomic Precis. Med.* 12, e002395. Available at: <http://ahajournals.org> [Accessed April 26, 2021].
75. Bijvoet, A.G.A., Van Hirtum, H., Kroos, M.A., Van de Kamp, E.H.M., Schoneveld, O., Visser, P., Brakenhoff, J.P.J., Weggeman, M., van Corven, E.J., Van der Ploeg, A.T., *et al.* (1999). Human Acid α -Glucosidase from Rabbit Milk Has Therapeutic Effect in Mice with Glycogen Storage Disease Type II. *Hum. Mol. Genet.* 8, 2145–2153.



Chapter 6

Ex vivo generation of reserve cell populations with enhanced muscle regenerative properties

Rodrigo Canibano-Fraile,^{1,2,3} Wesley Huisman,^{1,2,3} Jip Zonderland,^{1,2,3} Faidra Karkala,^{1,2,3} Claudia Milazzo,^{1,2,3} Tom J.M. van Gestel,^{1,2,3} Wilfred van IJcken,⁴ Ans T. van der Ploeg,^{2,3} W. W. M. Pim Pijnappel,^{1,2,3} Gerben J. Schaaf^{1,2,3,*}

¹Department of Clinical Genetics, Erasmus MC University Medical Center, 3015 GE Rotterdam, Netherlands

²Department of Pediatrics, Erasmus MC University Medical Center, 3015 GE Rotterdam, Netherlands

³Center for Lysosomal and Metabolic Diseases, Erasmus MC University Medical Center, 3015 GE Rotterdam, Netherlands

⁴Erasmus Center for Biomimetics, Erasmus MC University Medical Center, 3000 CA Rotterdam, Netherlands

*Correspondence: g.schaaf@erasmusmc.nl

Submitted. *Stem Cell Reports*.

Abstract

Loss of regenerative capacity during *ex vivo* expansion of muscle stem cells hampers the development of cell-based therapies for skeletal muscle disorders. During myogenic differentiation *in vitro*, reserve cells are formed that remain as mononuclear cells. However, their *in vivo* properties remain poorly understood. Here, we developed a method to isolate regenerative reserve cell fractions from expanded murine primary myoblasts using differential adhesion and sequential cycles of proliferation and myogenic differentiation. Fast-adhering reserve cells (FRCs) were enriched for cells expressing myogenin and contributed efficiently to muscle regeneration following transplantation to immunodeficient hosts. Slow-adhering reserve cells (SRCs) generated higher number of PAX7⁺ cells under differentiating conditions and predominantly regenerated muscle after a secondary injury, suggesting engraftment as muscle stem cells. Transcriptome analysis revealed that FRCs were enriched for myogenic differentiation genes, while SRCs showed increased expression of genes involved in cell migration and growth factor binding and decreased expression of genes involved in cell adhesion and cAMP phosphodiesterases. These results show that reserve cells display enhanced muscle regenerative capacity *in vivo* and provide insight in the molecular pathways involved.

Introduction

More than 1000 conditions affecting skeletal muscle have been described, while only few therapies exist [1]. Currently, the available treatments are expensive, often not curative, and require life-long medication. The highly efficient regenerative capacity of healthy skeletal muscle mediated by stem cells has urged researchers to investigate the development of cell-based therapies to treat muscle disorders [2]. Initial trials using muscle progenitors (myoblast transfer therapy) largely failed due to immunogenic responses, the lack of functional improvement associated with poor survival and negligible migration of transplanted cells, and low engraftment efficiency [3–10]. More recent studies in mouse models suggested that freshly isolated satellite cells – muscle-resident stem cells located under the basal lamina [11,12] – are a better source for transplantation than myoblasts due to satellite cells' greater capacity for self-renewal. Importantly, satellite cells allow for the replenishment of the stem cell pool to ensure continuous contribution to successive rounds of regeneration [13,14,15].

The success of clinically-proven stem cell therapies, including bone marrow transplantation and the use of *ex vivo* expanded limbal stem cells in the treatment of corneal burns highlights the importance of including self-renewing stem cells among the grafted cells [16,17]. However, satellite cells are rare, accounting only for 2-4 % of all myonuclei. Consequently, extensive expansion of muscle stem cells is required to obtain clinically-relevant numbers for therapy. Unfortunately, *ex vivo* expansion of satellite cells was found to induce rapid loss of regenerative potential presenting a major challenge in the development of cell-based therapies [15,18].

A novel perspective was offered by an observation from previous *in vitro* studies using muscle cultures, which showed that under differentiating conditions a population of cells, termed reserve cells, escape from differentiation, self-renew, and express features of stem cells. [19–22]. As such, reserve cells can be defined as the progeny of satellite cells that escape differentiation and express stem cell-like features. The formation of muscle reserve stem cells has been identified in cultures from different species including chick, mouse and human [19,23,24] as well as in studies using isolated myofibers [25–28]. Reserve cells are characterized by increased expression of PAX7, decreased MYOD levels, and slow proliferation rates *in vitro*; properties that resemble those of muscle stem cells [29,30]. Despite reports on the *in vitro* characterization of reserve cells, limited information is available on their *in vivo* properties. Recently, Laumonier and colleagues transplanted the total

reserve cell population from human muscle cultures and found higher contribution to muscle regeneration, compared with transplantation of human myoblasts [24], suggesting that human reserve cells could possess enhanced regenerative properties *in vivo*.

Stem cell populations, including satellite cells are highly heterogenous [31–33]. Previous studies showed that a subpopulation of satellite cells with increased levels of PAX7 displayed enhanced self-renewal potential *in vivo* [34]. Here, we developed a method to enrich for subpopulations of murine reserve cells based on their differential adhesive properties. Analysis of *in vivo* muscle regenerative capacity revealed the identification of reserve cells fractions that either contributed primarily to direct muscle differentiation and/or to the muscle stem cell population. Genome-wide mRNA expression analysis identified cAMP signaling, cell adhesion, and growth factor binding to be associated with enhanced engraftment of fractionated reserve cells as muscle stem cells. These results demonstrate that the regenerative properties of myoblasts can be enhanced by reserve cell generation combined with fractionation, and provide insight in the underlying transcriptional mechanisms.

Material and methods

Establishment of pure myogenic lines

Primary myoblasts were generated from 20 weeks-old adult wild type (WT) FVB/N or C57/BL6 mice using the pre-plating technique, reported elsewhere [35–37]. Myoblasts at passage 32 were used as parental populations to generate reserve cells.

Cell culture

Myoblasts were cultured on dishes coated with 40 $\mu\text{g/ml}$ extracellular matrix (ECM) in proliferation medium (GM) (Ham's F10, 20% fetal calf serum (FCS), 100 U/ml penicillin/streptomycin (PS), and 20 ng/ml fibroblast growth factor 2 (FGF2)). For differentiation, confluent cultures were switched to differentiation medium (DM) (Dulbecco's Modified Eagle Medium (DMEM); 2% horse serum (HS) and 100 U/ml PS).

Reserve cell isolation protocol

Myoblasts were grown to confluency and differentiated for 5 days. Cells were trypsinized, strained through a 40 μm pore-sized filter, and resuspended through a 21G needle. Filtered cells were plated on an ECM-coated culture dish in GM. After one hour the non-attached cells were transferred onto a second ECM-coated dish and allowed to adhere during three hours. The adhered fraction was annotated as fast-adhering reserve cells; FRCs). The non-adherent cells from the second dish were transferred to a third ECM-coated dish and the attached cells on the second dish were discarded. After incubation of the third dish overnight (16h), non-attached cell-containing medium was discarded, and the attached cells continued in culture, annotated as slow-adhering reserve cells (SRCs). FRCs and SRCs were cultured in GM and were passed twice after isolation before their use for experiments.

Mice and animal procedures

All animal experiments were approved by the local (Animal Experiments Committee (DEC)) and national (Central Committee for Animal Experiments (CCD)) animal experiment authorities in compliance with the European Community Council Directive guidelines (EU directive 86/609), regarding the protection of animals used for experimental purposes. 2-6 months old NOD.CB17-*Prkdc*^{SCID}/NcrCrl mice (NOD-SCID) (Charles River Laboratory) were used as hosts for transplantation experiments. Mice were housed at the Erasmus MC Animal Facility under a light-dark cycle of 12 hours and with access to food and water *ad libitum*.

Transplantation of reserve cells

One day prior to cell transplantation *tibialis anterior* (TA) muscles of recipient NOD-SCID mice were preinjured by intramuscular injection of 50 μl 1.2% w/v BaCl₂ (Sigma-Aldrich). The next day 20000 cells were suspended in 20 μl PBS supplemented with 10% mouse serum (NOD-SCID derived) and injected directly into the preinjured TA muscles of host mice. Mice were anesthetized with isoflurane before each procedure and sacrificed by cervical dislocation during daytime 3 or 6 weeks after transplantation

Analysis of transplanted muscles

Transplanted TA muscles and *quadriceps femoris* (QF) (non-transplanted) were dissected and processed for cryosectioning as described previously [38]. Cryosectioned material not used for image analysis was processed for Western Blot analysis.

Immunostaining analyses

Cells were fixed in 4% PFA and permeabilized with 0.5% (v/v) Triton X-100%; 3% BSA in PBS for 30 minutes at room temperature (RT). Blocking using 20% horse serum (Lonza) for 1 hour at RT. Antibodies were diluted in 0.1% BSA; 0.1% Tween 20 in PBS and incubated for 30 minutes at RT. Nuclei were counter-stained with Hoechst 33258 (H3569; Life Technologies). Immunostainings on mouse muscle tissue was performed as described previously [39].

Image acquisition and analysis

Engraftment efficiency was determined by imaging GFP directly in sections of (unstained) transplanted muscles. Samples were imaged on a Zeiss LSM700 microscope (Carl Zeiss B. V. Sliedrecht, The Netherlands) using Zen 2009 imaging software (Carl Zeiss B. V.). Image analysis and processing was performed using FIJI (fiji.sc/Fiji) and Adobe Photoshop CS6. Percentage of engraftment was calculated as the area occupied by GFP⁺ fibers relative to the total area of each muscle section.

Protein isolation and Western Blot analysis

Muscle transversal sections were homogenized using a tissue homogenizer and lysed in RIPA. Cell and tissue lysates were processed for Western Blot as described previously [39].

RNA Isolation and RNA-Seq

RNA was extracted using the RNeasy minikit with DNase treatment (QIAGEN). RNA-Seq libraries were prepared according to the Illumina TruSeq stranded mRNA protocol (www.illumina.com). Sequencing-by-synthesis was performed using the HiSeq 2500 with a single read 50-cycle protocol. Sequences were mapped against the GRCm38 mouse reference using HiSat2 (version 2.1.0) [40]. Gene expression

values were called using htseq-count (version 0.9.1) [41] and Ensembl release 91 gene and transcript annotation. Normalization and expression value generation was done using DESeq2 (rlog). Visualization and analyses of RNA-Seq data and GO analysis were performed using R2: Genomics Analysis and Visualization Platform (<http://r2.amc.nl>).

Accession numbers

RNA-Seq fastq files are accessible at GEO under GEO accession GSE161075.

RT-qPCR

cDNA was generated using the iScript cDNA synthesis kit (Bio-Rad) using 600 ng of input per reaction. Amplification was performed using iTaq universal SYBR Green Supermix (Bio-Rad) with a CFX96 RT-system (Bio-Rad). RT-qPCR data were normalized to *Rps18* and *Ppia*. Intron-spanning primers were used to avoid gDNA amplification. PCR primers are listed in Supplementary Table 2.

Gene ontology analyses

The differentially up- and down-regulated genes (DEGs) (≥ 1.5 fold-change; FDR ≤ 0.05) were analyzed separately for gene ontology (GO) enrichment using the web-tool PANTHER [42]. Statistical overrepresentation tests for PANTHER GO-Slim or GO Complete categories were performed. A cutoff of ≥ 5 input genes was used.

Statistical Analysis

Data are expressed as means \pm SE. Statistical tests were performed with two-sided t-tests, one-way ANOVA followed by post-hoc Tukey or Games-Howell correction, and Kruskal-Wallis test followed by the Bonferroni correction. A *p*-value of less than 0.05 was considered significant. Data was analyzed using IBM SPSS Statistics (version 26).

Supplemental Methods

Additional information on all procedures are described in the Supplemental information.

Results

Isolation of reserve cell fractions with differential adhesion properties

Historically, reserve cells have been defined as those cells that, under differentiation conditions *in vitro*, escape terminal differentiation, self-renew, and remain mononuclear, expressing stem cell markers including PAX7 possibly in combination with MYOD [21,43]. Cells that enter the myogenic differentiation program are characterized by expression of MYOD in the absence of PAX7, and later, by expression of MyHC and fusion into multinucleated muscle fibers. To exclude presence of non-myogenic cells, the purity of the original parental population of myoblasts obtained from an adult FVB/N mouse was confirmed. All cells were positive for MYOD and/or PAX7 when cultured in proliferation medium (Figure 1A). To induce reserve cell formation, myoblasts were differentiated *in vitro* and characterized by immunostaining for PAX7, MYOD, and MyHC (Figure 1B). The FVB/N myoblast cultures differentiated into MyHC-positive multinucleated myotubes, and generated $21.6\% \pm 2.7$ reserve cells ($3.8\% \text{ PAX7}^+/\text{MYOD}^-$ plus $17.8\% \text{ PAX7}^+/\text{MYOD}^+$ (Figure 1C). $70.3\% \pm 4.3$ of all nuclei were $\text{PAX7}^+/\text{MYOD}^+$, and $8\% \pm 2$ were $\text{PAX7}^+/\text{MYOD}^-$ (Figure 1C). These data confirm formation of reserve cells in our cultures and indicate phenotypic heterogeneity in the reserve cell population.

Previous studies have shown that the satellite cell population *in vivo* is heterogeneous [44], and that myoblasts with stem cell phenotypic features adhere more slowly than more committed cells [22,45,78,79]. Based on these findings and on the observed heterogeneity of reserve cells (Figure 1C), we hypothesized that differential adhesion could be used to separate phenotypically and functionally distinct reserve cells populations from differentiated primary muscle cultures. To test this, proliferating primary muscle cultures (parental (PAR) cultures) were grown to confluency and differentiated for 5 days. The reserve cell isolation protocol was then applied to the differentiated cultures (Figure 1D). As a result, we isolated fast-adhering reserve cells (FRCs) – which adhered in the first hour after plating –, and slow-adhering reserve cells (SRCs) – which attached between 3 and 24 hours after plating (Figure 1D). FRCs and SRCs were expanded for two passages and maintained a PAX7/MYOD profile similar to PAR cells, indicating they were pure and myogenic (Figure 1E).

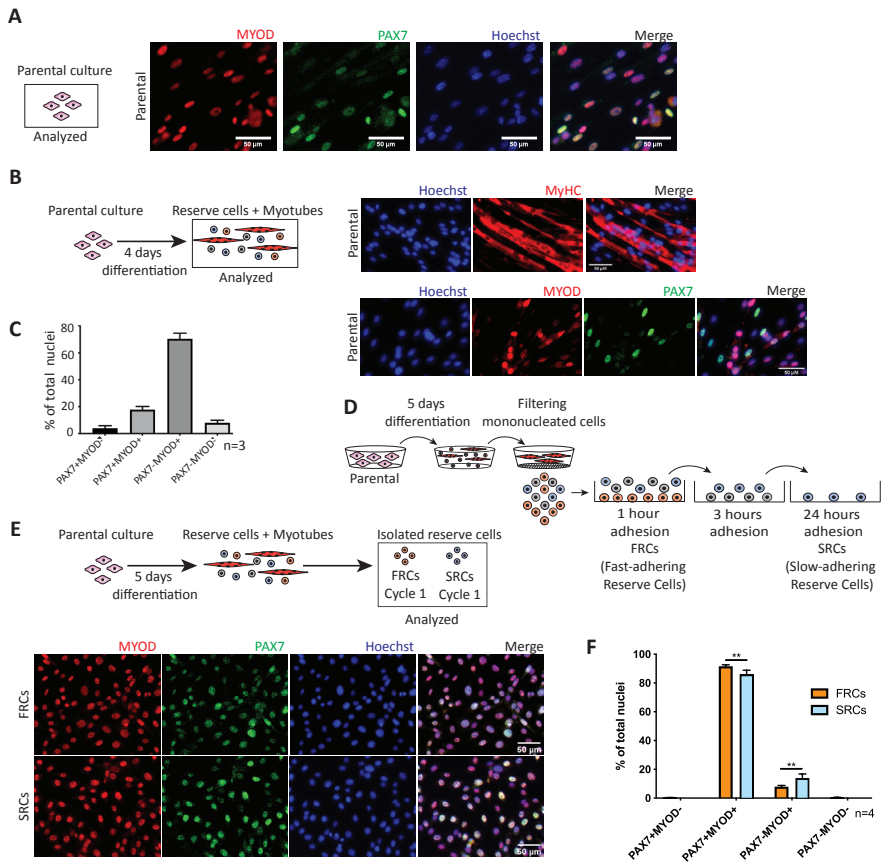


Figure 1. Isolation of reserve cell fractions from primary myoblasts based on differential adhesion properties. (A) Left panel, schematic representation of the experimental setup. Right panels, immunostaining of FVB/N parental (PAR) myoblasts for MYOD (red); PAX7 (green) in proliferation medium; nuclei counterstained with Hoechst (blue). Scale bars, 50 μ m. Representative images are shown. (B) Upper left panel, schematic representation of the experimental setup. Upper right panels, immunostaining of FVB/N parental myoblasts that had been differentiated for 4 days for MyHC (red); nuclei counterstained with Hoechst (blue). Scale bars, 50 μ m. Lower right panels, immunostaining of FVB/N parental myoblasts that had been differentiated for 4 days for MYOD (red); PAX7 (green); nuclei counterstained with Hoechst (blue). Scale bars, 50 μ m. Representative images are shown. (C) Bar graph depicting the quantification of the PAX7/MYOD profile of (B). 3 independent experiments per group were performed ($n=3$). Data are expressed as mean \pm SE. (D) Schematic representation of the reserve cell isolation protocol. Parental cells are differentiated for 5 days. Multinucleated fibers are removed by straining. Mononucleated cells are plated on new dishes sequentially after indicated adhesion times. Fast-adhering Reserve Cells (FRCs) adhere after 1 hour. Slow-adhering Reserve Cells (SRCs) adhere within 24 hours after plating. (E) Upper panel, schematic representation of the experimental setup. Lower panels, immunostaining of MYOD (red); PAX7 (green) in FVB/N reserve cells (FRCs and SRCs) cultured in proliferation medium; nuclei were counterstained with Hoechst (blue). Scale bars, 50 μ m. Representative images are shown. (F) Bar graph depicting the quantification of (E). 3 independent experiments per group were performed ($n=3$). Data are expressed as mean \pm SE.

Sequential cycles of reserve cell isolation result in enrichment of PAX7⁺ cells

Previous studies using a sequential subculturing approach showed that reserve cells could generate new reserve cells *in vitro* [19,43]; i.e. reserve cells can be expanded and redifferentiated to generate new reserve cells. To test this and to characterize the myogenic properties of newly *in vitro* generated reserve cells, we differentiated reserve cells (FRCs and SRCs) for 4 days and performed immunostaining for PAX7 and MYOG, a marker of myogenic differentiation. PAR cells that were differentiated for 4 days were used as control (Figure 2A). Interestingly, reserve cells showed increased percentage of PAX7⁺ (14.2% ± 0.8 for FRCs and 17.9% ± 1 for SRCs) cells compared to PAR (7.5% ± 0.5) (Figure 2B). In addition, the percentage of MYOG⁺ cells was reduced in SRCs (69.5% ± 2.7) compared to PAR (82.9% ± 2.8) (Figure 2B). These results indicated that reserve cells can generate new reserve cells, and that SRCs have higher expression of PAX7 and lower expression of MYOG compared to FRCs. We next asked whether we could further enrich for reserve cells by combining sequential reserve cell isolation cycle and differential adhesion of reserve cells *in vitro*. To test this, FRCs and SRCs obtained after the first reserve cell cycle were expanded and differentiated again. The fast-adhering cells resulting from this differentiation were termed FRCs Cycle 2 and the slow-adhering cells isolated from this differentiated culture were termed SRCs Cycle 2. This process was repeated once more to obtain FRCs and SRCs Cycle 3 (Figure 2C).

To characterize the myogenic properties of reserve cell after 3 cycles of isolation, we differentiated FRCs Cycle 3 and SRCs Cycle 3 for 4 days, followed by immunostaining for PAX7 and MYOG (Figure 2D). FRCs Cycle 3 showed an average percentage of PAX7⁺ cells of 29.5% ± 2.7, which was higher compared to FRCs Cycle 1 (14.2% ± 0.8) (Figure 2B/E). SRCs Cycle 3 were also enriched for PAX7⁺ cells (40.9% ± 3.2) compared to SRCs Cycle 1 (17.9% ± 1.1) (Figure 2B/E). Furthermore, similarly as observed for FRCs and SRCs at Cycle 1, SRCs Cycle 3 were also significantly enriched for PAX7⁺ cells compared to FRCs at Cycle 3 (Figure 2E). These results indicated a reserve cell fraction- and cycle-dependent shift in the percentage of PAX7⁺ and MYOG⁺ cells, with the lowest percentage of PAX7⁺ cells and the highest percentage of MYOG⁺ cells in FRCs Cycle 1, and the highest percentage of PAX7⁺ and the lowest percentage of MYOG⁺ cells in SRCs Cycle 3 (Figure 2B/E).

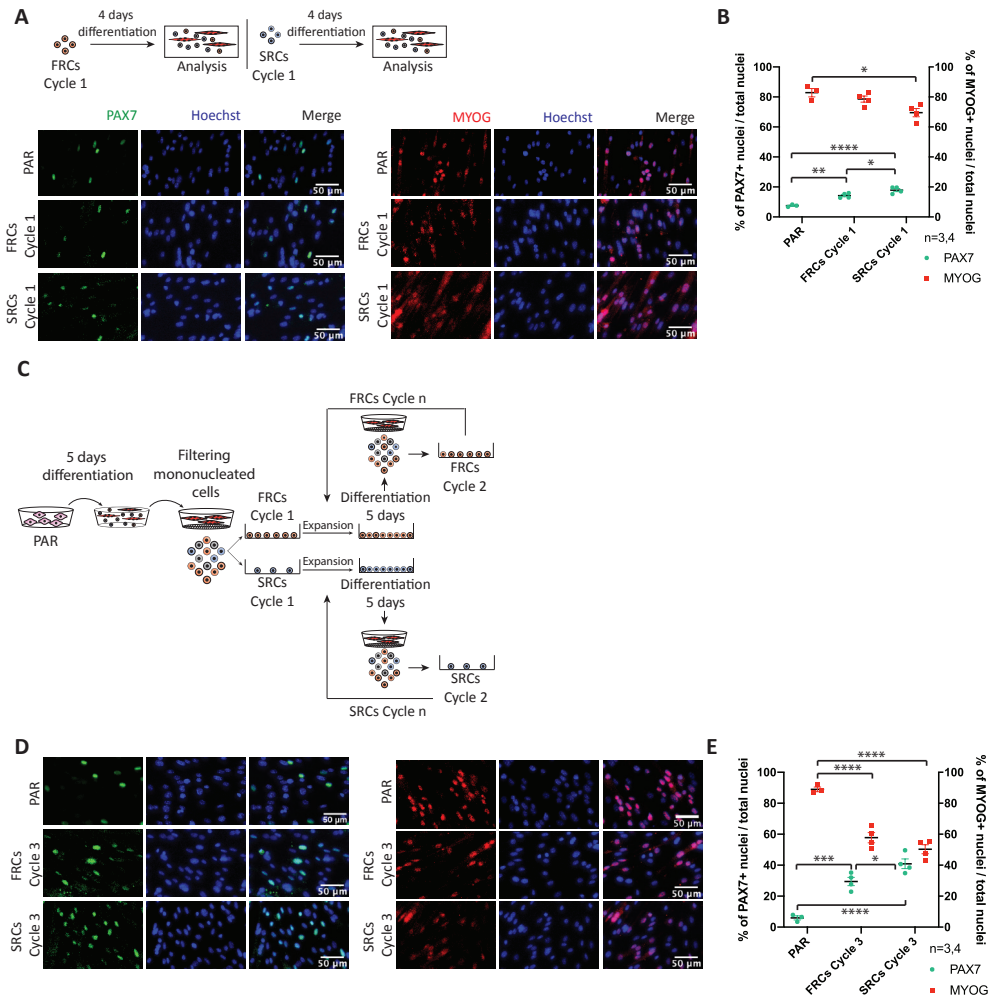


Figure 2. Sequential isolation of slow-adhering reserve cells in vitro enriches for Pax7+ reserve cells. (A) Upper panel, schematic representation of the experimental setup. FRCs and SRCs are first expanded in proliferation medium to confluence and then differentiated for 4 days. Lower panels, immunostaining of FVB/N FRCs Cycle 1 and SRCs Cycle 1 for PAX7 (green); MYOG (red); nuclei were counterstained with Hoechst (blue). Scale bars, 50 μ m. Representative images are shown. (B) Quantification of (A). 3-4 independent culture experiments per group were performed ($n=3-4$). Data are expressed as mean \pm SE ($n=3-5$). n indicates independent experiments. * $p \leq 0.05$; ** $p \leq 0.01$; **** $p \leq 0.0001$. (C) Schematic representation of reserve cell cycling. After the first cycle of reserve cell isolation (Cycle 1), FRCs and SRCs are expanded in ECM-coated dishes and differentiated again to isolate new reserve cells in a second cycle. Mononucleated cells are plated in a similar manner as described in Figure 1E in order to obtain FRCs Cycle 2. The process is repeated once more to obtain FRCs Cycle 3. SRCs Cycle 2 and Cycle 3 are obtained in a similar approach. (D) Immunostaining of FVB/N FRCs Cycle 3 and SRCs Cycle 3, first expanded and then differentiated for 4 days, for PAX7 (green); MYOG (red); nuclei were counterstained with Hoechst (blue). Scale bars, 50 μ m. Representative images are shown. (E) Quantification of (D). 3-4 independent culture experiments per group were performed ($n=3-4$). Data are expressed as mean \pm SE ($n=3-5$). n indicates independent experiments. * $p \leq 0.05$; *** $p \leq 0.001$; **** $p \leq 0.0001$

Direct engraftment capacity of reserve cell fractions

To test if reserve cells could engraft *in vivo* and contribute to muscle regeneration, we performed transplantation experiments. FVB myogenic PAR cells were transduced with a lentiviral vector carrying eGFP to allow tracking their fate *in vivo*. The GFP⁺ PAR cells were used to generate fast and slow-adhering RC fractions undergoing a single cycle or three cycles as described in Figure 2. These fractions – FRCs Cycles 1 and 3 and SRCs Cycles 1 and 3 – were passaged twice in proliferation medium after isolation to allow recovery after the reserve cell isolation process and to verify that they remained as mononuclear cells. Cells were transplanted via intramuscular injection in *tibialis anterior* (TA) muscle of NOD-SCID hosts that had been preinjured using BaCl₂ (Figure 3A). Primary cells that were normally expanded and not subjected to RC isolation, referred to as PAR, were used as controls. Analysis of cryosections from transplanted muscles 3 weeks after transplantation using direct imaging of GFP fluorescence showed that PAR cells had no or very limited contribution to muscle regeneration ($0.72\% \pm 0.3$ GFP⁺ cross-sectional area (CSA), in line with previous findings [15,18] (Figure 3B, left panel). In contrast, FRCs Cycles 1 and 3 significantly contributed to regeneration, forming $9\% \pm 3.2$ and $8.6\% \pm 2.2$ GFP⁺ CSA, respectively (Fig 3B-C). SRCs Cycle 1 formed $7.3\% \pm 3.7$ GFP⁺ fibers. Interestingly, SRCs Cycle 3, while having the highest number of PAX7⁺ cells (Figure 2E), did not contribute much to muscle regeneration ($1.6\% \pm 0.6$ GFP⁺ CSA; Figure 3B-C). Importantly, central nucleation was observed in GFP⁺ fibers, confirming that they had been formed by regeneration (Figure 4F).

To further quantify engraftment and contribution to muscle regeneration, we determined GFP protein levels in lysates of transplanted muscles by immunoblotting. This confirmed the fluorescence imaging in cryosections of transplanted muscles, showing low GFP levels after transplanting PAR, increased levels of GFP (compared to PAR) after transplanting FRCs Cycles 1 and 3 and SRCs Cycle 1, and low GFP levels in muscle engrafted with SRCs Cycle 3 (Figure 3D-E). These data indicate that reserve cells generated *in vitro* have enhanced capacity to engraft *in vivo* and directly contribute to muscle regeneration compared to the parental cells used for their generation.

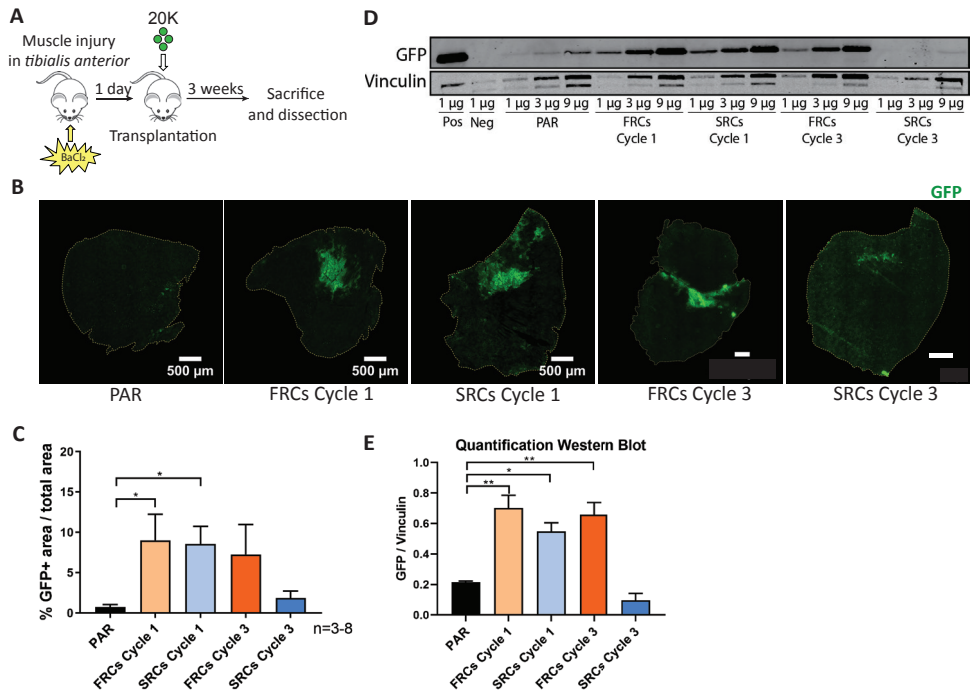


Figure 3. Reserve cell fractions engraft in vivo. (A) Scheme of the experimental design. 24 hours before transplantation the TAs of NOD-SCID mice were injured with intramuscular injection of BaCl₂. FVB/N PAR and reserve cells were transplanted by intramuscular injection of 2 X 10⁴ cells. Three weeks after transplantation engraftment was quantified. (B) Wide field fluorescence microscopy tile scan images of TA sections transplanted with PAR, FRCs and SRCs Cycles 1 and 3. GFP (green). The outline of the sections was drawn. Representative images for each group are shown. Scale bars, 500 μm. (C) Quantification of (B). n=3-8. n indicates the number of mice per transplantation group. Data are shown as mean ± SE *p<0.05. (D) Western Blot analysis of GFP in whole muscle lysates of PAR, FRCs and SRCs at Cycles 1 and 3. Lysates of muscles whose engraftment levels were closest to the mean for each group were used. An antibody to GFP was used. Vinculin was used as a loading control. Lysate from FVB-GFP PAR cells was used as positive control (Pos); lysate from non-transplanted quadriceps femoris was used as negative control (Neg). Lysates of one mouse per group was used (n=1). Three different amounts of the same lysate were loaded per group. (E) Quantification of (D). Values from the three different amounts of protein for each group were normalized to vinculin. These replicates were averaged per group and depicted as mean ± SE. *p<0.05, **p<0.005.

Engraftment capacity of reserve cell fractions after reinjury

To test the capacity of reserve cell fractions to engraft as stem cells, we performed re-injury experiments. We compared the reserve cells fractions that were most distinct *in vitro* with respect to expression of PAX7 and MYOG: FRCs Cycle 1 and

SRCs Cycle 3. PAR cells were used as negative controls. FRCs Cycle 1 and SRCs Cycle 3 were expanded for two passages after isolation and then transplanted by intramuscular injection in TA muscle of NOD-SCID mice that were injured with BaCl₂ 24 hours in advance. The transplanted muscles were re-injured three weeks after transplantation to test whether transplanted reserve cells had engrafted as stem cells capable of regenerating muscle (Figure 4A). Analysis of GFP fluorescence in cryosections confirmed that contribution to regeneration by PAR cells, transplanted as controls, was very limited or non-existent both after transplantation and after the secondary injury, in line with findings presented by others [15,18,46]. Transplanted FRCs Cycle 1 contributed to muscle regeneration at similar levels at 3 weeks after transplantation compared to 3 weeks after re-injury ($9\% \pm 3.2$ and $6.1\% \pm 2.6$ GFP⁺ CSA, respectively). In contrast, SRCs Cycle 3 contributed very modestly at 3 weeks after transplantation ($1.6\% \pm 0.6$ GFP⁺ CSA), but strongly contributed to muscle regeneration after re-injury, increasing donor-mediated contribution ≈ 10 -fold ($16\% \pm 5.5$ GFP⁺ CSA) (Figure 4B-C).

To confirm these results, GFP levels in lysates of transplanted muscles were analyzed by Western Blot (Figure 4D). GFP levels were at or below the detection level in PAR-transplanted muscle both at 3 weeks after transplantation and at 3 weeks after re-injury. The level of GFP in FRCs Cycle 1-transplanted muscle was increased compared to PAR-transplanted muscle at 3 weeks after transplantation, and was not significantly different at 3 weeks after re-injury, as observed in the image analysis. SRCs Cycle 3-transplanted muscle showed slightly, not significantly increased levels of GFP versus PAR-transplanted muscle at 3 weeks after transplantation. In contrast, at 3 weeks after re-injury SRC Cycle 3-transplanted muscle showed a strong and significant increase in GFP levels compared to PAR-transplanted muscle (Figure 4E).

To determine if engrafted reserve cells effectively contributed to myofiber formation, we performed costaining in cryosections of transplanted muscles for GFP, the myogenic differentiation marker MyHC, and laminin. This showed that GFP⁺ regions overlapped with MyHC⁺ areas, confirming that the transplanted RC fractions formed myofibers *in vivo* in both single- and re-injury experiments (Figure 4F-G). In healthy mice, adult skeletal muscle fibers are known to harbor PAX7⁺ satellite cells in between the basal lamina and the sarcolemma [33]. To test whether the regenerated (GFP⁺) areas hosted satellite cells, we performed costaining of transplanted muscles for GFP and PAX7 (Supplementary Figure 2). This showed that both FRCs Cycle 1 and SRCs Cycle 3 formed myofibers that

contained PAX7⁺ satellite cells that were located at the typical sublaminar position. At this point it was unclear whether the satellite cells were host or donor-derived. Nevertheless, these results validated that reserve cells contributed to the formation of intact myofibers.

Taken together, these results indicate that FRCs Cycle 1 preferentially contributed to myofiber formation during muscle regeneration with limited capacity to engraft as stem cells, while SRCs Cycle 3 predominantly engrafted as stem cells that efficiently generated myofibers upon a secondary injury.

To confirm these results using a primary myogenic line from a different genetic background, a myoblast culture from C57/BL6 mice was established and transduced with a lentiviral vector carrying eGFP (BL6-GFP). The regenerative capacity of BL6-GFP PAR, FRCs Cycle 1 and SRCs Cycle 3 *in vivo* was then tested in a re-injury experiment (Supplementary Figure 1A). Imaging of GFP fluorescence in cryosections revealed that BL6-GFP PAR cells had a limited engraftment capacity at 3 weeks after transplantation as well as after re-injury, generating $1\% \pm 0.3$ and $1.4\% \pm 0.8$ GFP⁺ CSA, respectively. Transplantation of BL6-GFP FRCs Cycle 1 cells resulted in increased contribution to muscle regeneration at 3 weeks after transplantation ($3.5\% \pm 1.75$ GFP⁺ CSA), which was reduced to $1.2\% \pm 0.6$ GFP⁺ myofibers 3 weeks after re-injury. BL6-GFP SRCs Cycle 3 showed inefficient contribution to muscle regeneration at 3 weeks after transplantation ($0.5\% \pm 0.4$ GFP⁺ CSA). In contrast, at 3 weeks after re-injury BL6-GFP SRC Cycle 3-transplanted muscle showed ≈ 20 -fold increased contribution to muscle regeneration to $11.3\% \pm 2.2$ GFP⁺ CSA (Supplementary Figure 1B-C). Taken together, these results are in agreement with the results obtained with reserve cells in the FVB background, ruling out genetic background-specific reserve cell properties.

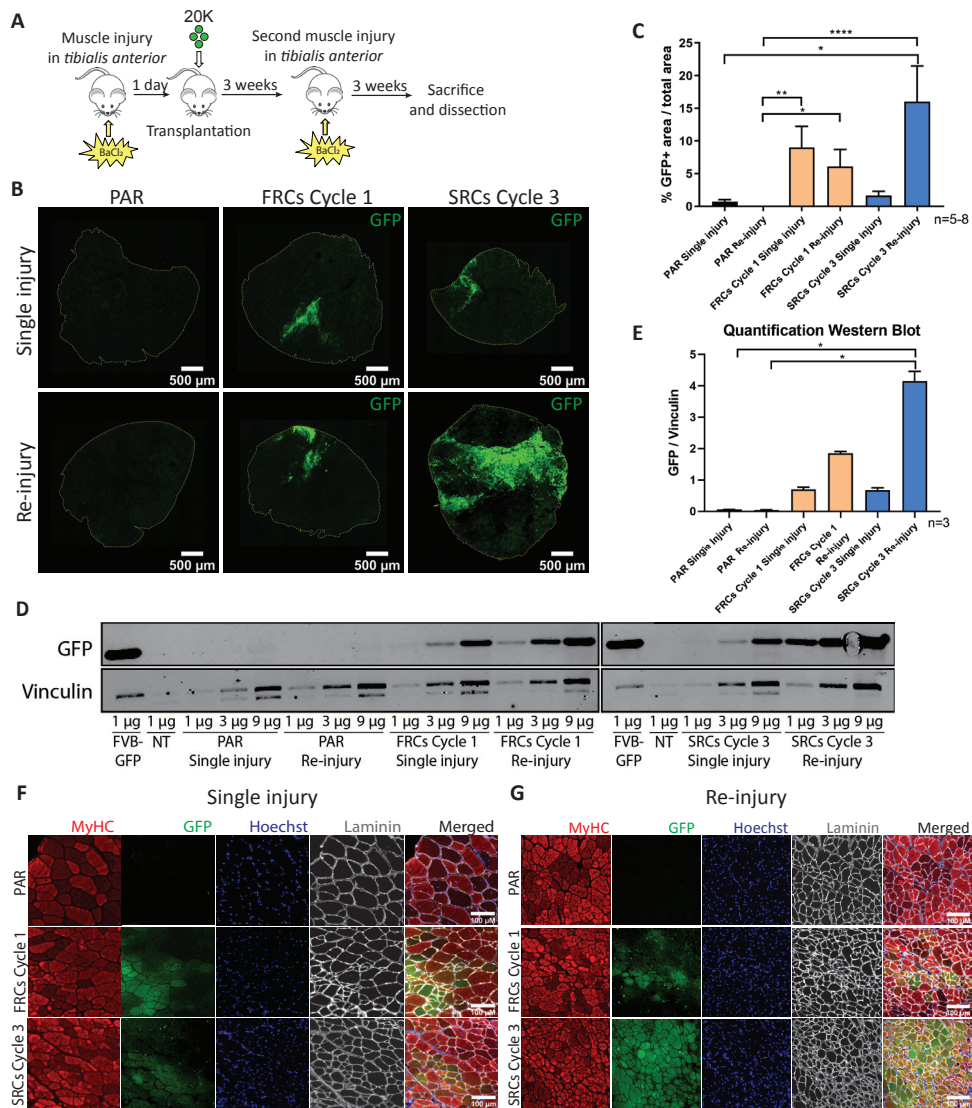
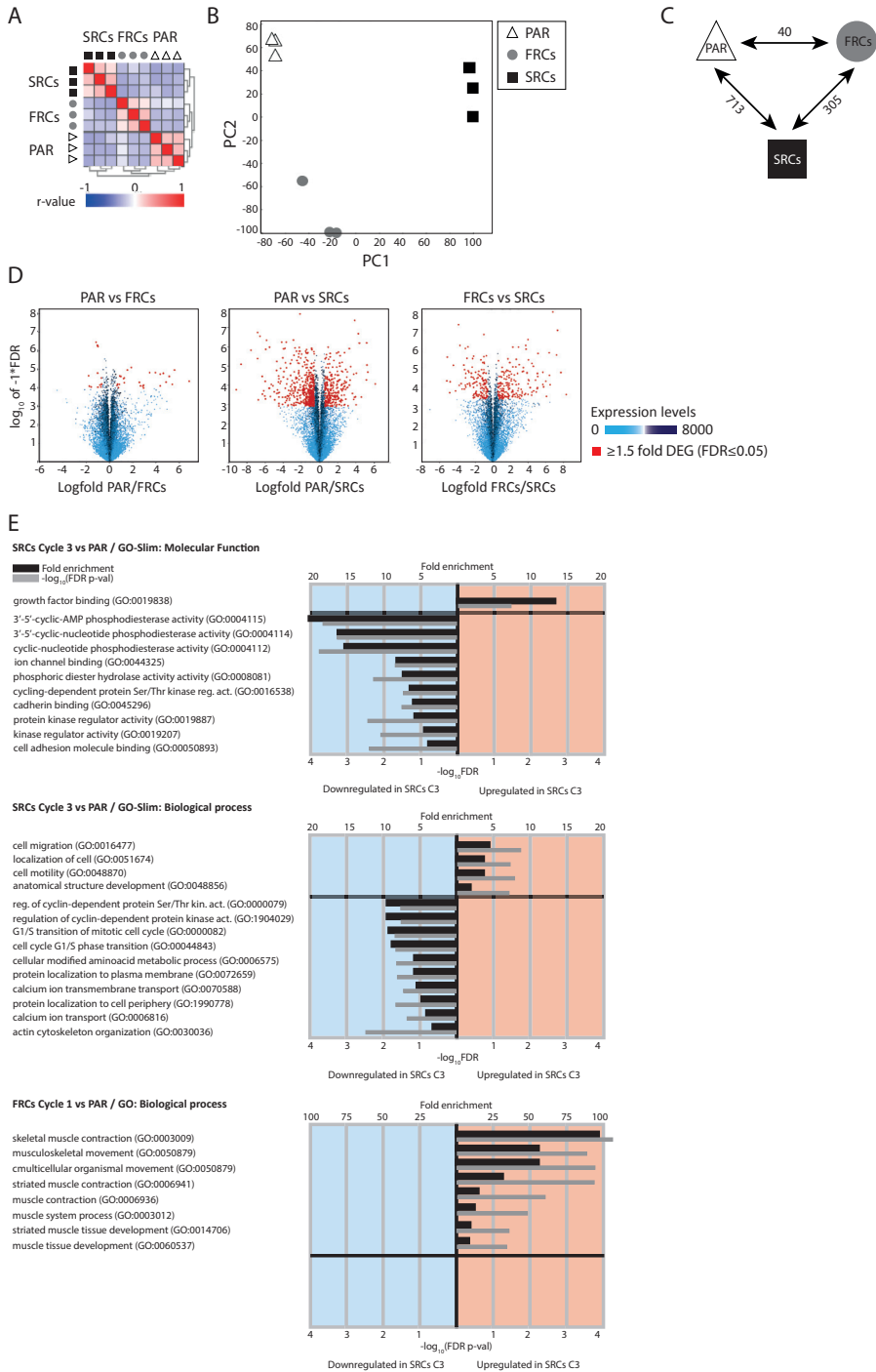


Figure 4. Cycled SRCs preferentially engraft as stem cells and strongly contribute to muscle regeneration after a second round of injury. (A) Scheme of the experimental design. 24 hours before transplantation, the TAs of NOD-SCID mice were injured with intramuscular injection of $BaCl_2$. Reserve cells were transplanted by intramuscular injection of 2×10^4 cells. 3 weeks after transplantation, a new injury was performed. Three weeks after the second injury, engraftment was quantified. (B) Wide field fluorescence microscopy tile scan images of TA cross sections of NOD-SCID mice from single and re-injury experiments upon transplantation of FVB/N PAR, FRCs Cycle 1, and SRCs Cycle 3. GFP (green). The outline of the sections is drawn. Representative images for each group are shown. (C) Quantification of (B). $n=5-8$. n indicates the number of mice per transplantation group. Data are shown as means \pm SE. * $p \leq 0.05$, ** $p \leq 0.005$; **** $p \leq 0.0001$. Data for reserve cells Cycle 1 at 3 weeks after transplantation were taken from Figure 3 to allow comparison to engraftment after second injury. (D) Western Blot analysis of GFP in whole muscle lysates of FVB/N PAR, FRCs Cycle 1, and SRCs Cycle 3 from single- and re-injury experiments. Lysates of muscles whose engraftment levels were closest to the mean for each of the groups were used. An antibody to GFP was used. Vinculin was used as a loading control. Lysates of one mouse per group was used ($n=1$). Three different amounts of the same lysate were loaded per group. (E) Quantification of (D). Values from the three different amounts of protein per group were normalized to vinculin. These replicates were averaged per sample group and depicted as mean \pm SE. * $p \leq 0.05$. (F) Immunostaining for MyHC/laminin in TA cross sections of NOD-SCID mice after transplantation of FVB/N PAR, FRCs Cycle 1, and SRCs Cycle 3 in single injury experiments. MyHC (red); GFP (green); laminin (grey); nuclei counterstained with Hoechst (blue). Scale bars, 100 μ m. $n=3$. n indicates the number of mice analyzed per transplantation group. Representative images are shown. (G) Immunofluorescence for MyHC/laminin in TA cross sections of NOD-SCID mice after transplantation of FVB/N PAR, FRCs Cycle 1, and SRCs Cycle 3 in re-injury experiments. MyHC (red); GFP (green); laminin (grey); nuclei counterstained with Hoechst (blue). Scale bars, 100 μ m. $n=3$. n indicates the number of mice analyzed per transplantation group. Representative images are shown.

RNA-seq analysis indicates distinct transcriptional profiles of reserve cells

To determine the transcriptional signature of reserve cells we performed RNA-sequence analyses of reserve cell populations in proliferation (two passages after isolation), at the same conditions as when they were transplanted, and PAR. Unsupervised hierarchical clustering indicated that FRCs Cycle 1, SRCs Cycle 3, and PAR formed distinct clusters and showed that the biological replicates grouped closely together within each population (Figure 5A). Principal component analysis (PCA) confirmed the clustering pattern (Figure 5B). RT-qPCR analysis of several transcripts specific for each fraction validated the RNA-Seq results (Supplementary Figure 3). In addition, independent reserve cell isolations confirmed gene expression profiles (Supplementary Figure 4). To further investigate changes in the transcriptional signature of reserve cell fractions, we performed pairwise supervised analyses to identify differentially expressed genes (DEGs) between groups. Pairwise supervised comparison of transcriptomes (≥ 1.5 fold-change; FDR ≤ 0.05) revealed 40 DEGs between PAR and FRCs Cycle 1, 305 between FRCs Cycle 1 and SRCs Cycle 3, and 713 between PAR and SRCs Cycle 3 (Figure 5C-D). Gene



◀Figure 5 – Reserve cell populations have distinct transcriptional profiles. (A) Unsupervised hierarchical cluster analysis of FVB/N PAR, FRCs Cycle 1, and SRCs Cycle 3 based on pairwise comparison of all samples. (B) Principal component analysis (PCA) of FVB/N PAR, FRCs Cycle 1, and SRCs Cycle 3. Each dot represents an independent biological replicate. Data were transformed to z-scores. (C) Upper panel, pairwise differential gene expression profile analyses ($FDR \leq 0.05$; fold-change ≥ 1.5 up/down) between sample groups. The number of differential expressed genes (DEGs) is indicated for each pairwise comparison. (D) Volcano plots of the three pairwise comparisons. X-axis represents logfold change. Y-axis represents \log_{10} of $-1 * FDR$. Each dot represents a gene. DEGs ($FDR \leq 0.05$; fold-change ≥ 1.5 up/down) are depicted as red dots. Data were \log_2 transformed. Statistics were performed by one-way ANOVA and FDR multiple testing correction. (E) Gene ontology (GO) analyses of DEGs ($FDR \leq 0.05$; fold-change ≥ 1.5) that were up and downregulated in SRCs Cycle 3 compared to PAR for the categories Molecular function (upper panel) and Biological processes (middle panel), and upregulated in FRCs Cycle 1 compared to PAR for the category Biological function (lower panel). The top list of GO terms are plotted based on fold enrichment. Upper x-axis (black bars) represents fold enrichment; lower x-axis (grey bars) represents $-\log_{10}$ of FDR.

ontology (GO) analyses were performed for up- and down-regulated DEGs between SRCs Cycle 3 and PAR and between FRCs Cycle 1 and PAR for the terms *Molecular function* and *Biological process* (Figure 5E). The most enriched terms upregulated in SRCs Cycle 3 were *growth factor binding* (GO:0019838) and *cell migration* (GO:0016477) in the categories *Molecular function* and *Biological process*, respectively (Figure 5E). The most enriched terms downregulated in SRCs Cycle 3 were *3'-5'-cyclic-AMP phosphodiesterase activity* (GO:0004115) and *regulation of cyclin-dependent protein serine/threonine kinase activity* (GO:0000079) in the categories *Molecular function* and *Biological process* respectively (Figure 5E). The most enriched term upregulated in FRCs Cycle 1 was *skeletal muscle contraction* (GO:0003009) (Figure 5E).

Next, we analyzed the gene expression profiles of both up and downregulated DEGs present in the most enriched GO terms. In the category *cell migration* and *growth factor binding*, members of the integrin family of proteins (*Itgb5*, *Itgb7*), FGFs and FGF-binding proteins (*Fgf2*, *Fgf5*, *Fgfbp1*), plexin/semaphorin members (*Plxnb1*, *Plxna4*, *Sema5a*), and IGF binding proteins (*Igfbp3/4/6*) were found overexpressed in SRCs Cycle 3 relative to PAR. Only some of these genes (*Fgf2*, *Fgf5* and *Plxnb1*) were also overexpressed in FRCs Cycle 1. (Figure 6A-B). *cAMP phosphodiesterase activity* genes *Pde1a/1c/4d/8a/4b/3b/10a* were downregulated in both FRCs Cycle 1 and SRCs Cycle 3 compared to PAR, although this was much more prominent in SRCs Cycle 3 (Figure 6C). Analysis of *cyclin-dependent kinase activity* genes (also present in the terms related to *G1/S transition of mitotic cycle*) showed downregulation of genes in SRCs Cycle 3, and to a lesser extent in FRCs Cycle 1 compared to PAR (Figure 6D). DEGs in *cell adhesion molecule binding* and *cadherin binding* were strongly downregulated in SRCs Cycle 3 compared to PAR,

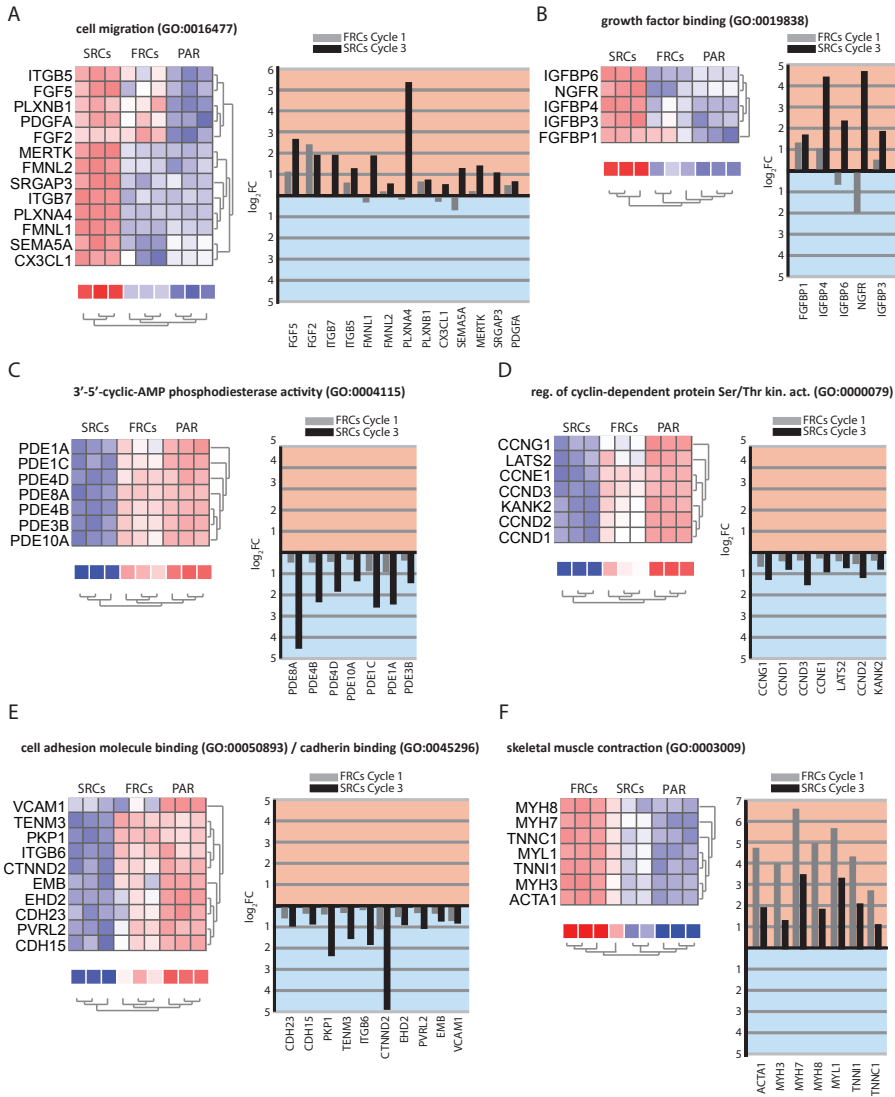


Figure 6 – Gene expression profiles of most enriched GO terms up and downregulated in SRCs Cycle 3. (A-F) Gene expression profiles for the GO terms cell migration (A), growth factor binding (B), 3',5'-cyclic-AMP phosphodiesterase activity (C), regulation of cyclin-dependent protein Ser/Thr kinase activity (D), cell adhesion molecule binding and cadherin binding (E), and skeletal muscle contraction (F). Left, clustered heatmaps of DEGs. Data were transformed to z-score. Each column represents a biological replicate. Each row represents a gene. The color indicates the z-score of transcripts levels. Blue color indicates relative low expression. Red color indicates relative high expression. Right, bar graph for individual genes showing fold change of FRCs Cycle 1 (grey bars) and SRCs Cycle 3 (black bars) relative to PAR. Mean transcription values of three biological replicates per group were used. Y-axis indicates log₂ fold change (log₂FC). X-axis indicates DEGs.

consistent with the selection of SRCs based on their decreased adhesive properties (Figure 6E). Analysis of the term *skeletal muscle contraction* showed upregulation of genes involved in skeletal muscle specific function *Acta1*, *Myh7*, *Myh3*, *Myh8*, *Myf11*, *Tnni1*, and *Tnni3* in FRCs Cycle 1, and to a lesser degree in SRCs Cycle 3, compared to PAR (Figure 6F).

Overall, these data show that reserve cells have markedly distinct transcriptional signatures: cycling and selection based on adhesive properties yields fast-adhering reserve cells, which have increased expression of myogenic differentiation genes, and slowly adhering reserve cells, which have increased expression of growth factor and cell migration genes and decreased expression of cell adhesion, cAMP signaling, and G1/S transition genes.

Discussion

In this study, we isolated reserve cells following repeated cycles of myogenic differentiation of primary myoblasts and fractionated reserve cell fractions based on their adhesive properties. Reserve cells maintained their myogenic properties *in vitro*, and upon increased cycling and selection of fractions for slow adhesion, the slow-adhering cells expressed the stem cell marker PAX7 more frequently at the expense of the differentiation marker MYOG. *In vivo*, reserve cells but not parental cells engrafted and regenerated muscle. Interestingly, fast-adhering reserve cells after one cycle of reserve cell isolation (FRCs Cycle 1) mainly contributed to muscle regeneration directly after transplantation, while slow-adhering reserve cells after 3 cycles of reserve cell isolation (SRCs Cycle 3) preferentially engrafted as stem cells and contributed more efficiently to muscle regeneration after a second injury. Gene expression analysis showed that SRCs Cycle 3 displayed increased expression of genes involved in cell migration and growth factor binding, and decreased expression of genes involved in cell adhesion, cAMP signaling, and G1/S transition. These results identify reserve cells with distinct transcriptional signatures and enhanced muscle regenerative capacities to either contribute to myofiber formation or to the muscle stem cell population.

Expansion of functional adult stem cells *ex vivo* remains a challenge for several tissues [47]. In skeletal muscle, freshly isolated satellite cells lose their regenerative capacity shortly after cell culture *in vitro* [15,18,48]. Available protocols for expansion do not allow long-term *ex vivo* maintenance of primary muscle cells with regenerative and stem cell capacity *in vivo*. It has been proposed that these protocols generated either stem cells with limited myogenic capacity or highly

myogenic post-mitotic cells with limited capacity to repopulate the stem cell niche *in vivo* [49,50]. The demonstration in the present study that reserve cell fractions that were generated from expanded myoblasts have enhanced regenerative capacity is therefore relevant for the development of muscle regenerative therapy [51,52].

The heterogeneity of reserve cell fractions *in vitro* and *in vivo* has remained largely unexplored. *In vivo*, satellite cells are heterogeneous [13,32,33,53,54]. A subset of satellite cells has been shown to be capable of self-renewal to maintain and replenish the stem cell pool to ensure long-term regeneration, while others become more committed progenitors and contribute to proliferation and differentiation, mediating direct repair of damaged tissue [26,28,55]. These properties are reminiscent of the muscle regenerative properties of SRCs Cycle 3 and FRC Cycle 1, respectively.

Cell adhesion has previously been shown to play a role in fate determination in satellite cells [56]. In this study, we introduced the concept of performing sequential reserve cell isolation “cycles” and showed that the percentage of PAX7⁺ reserve cells progressively increased with each cycle; i.e., there was a gradual enrichment for reserve cells with stem cell properties both *in vitro* and *in vivo*. Interestingly, the increase in PAX7⁺ reserve cells per cycle was also observed for the fast-adhering populations (FRCs), suggesting that the enrichment of reserve cells is not only dependent on differences in adhesion but is acquired by the cells going through cycles of expansion and differentiation. This finding suggests the possibility that interaction of reserve cells with myotubes could be a factor in the establishment of reserve cell phenotypes, which has been proposed before for other myogenic cell types [50,57,58]. Further studies are however required to identify the signals involved in reserve cell formation.

Genes overexpressed in SRCs Cycle 3 compared to PAR included several members of the FGF family including *Fgf2*, *Fgf5*, and *Fgfbp1*. In skeletal muscle, FGFs are essential for self-renewal of MuSCs and necessary for skeletal muscle regeneration [59]. This process is facilitated via FGFs by repressing terminal myogenic differentiation and enabling satellite cell proliferation [60,61]. FGF2 expression is increased during muscle regeneration in mice, and enhanced FGF2 sensitivity has been linked with improved muscle regeneration [62,63]. Increased FGF2 sensitivity was also reported during aging due to increased FGF2 levels and loss of *Spry1* expression, and was associated with loss of quiescence and reduced self-renewal capacity. However, overexpression of *Spry1* rescued the phenotype

and allowed preservation of stem cell features [64]. In line with this, *Spry1* was elevated in SRCs Cycle 3, which may allow maintenance of stem cell properties in response to increased FGF2 signalling (data not shown). In addition, FGF2 regulates satellite cell function through activation of myogenic pathways – ERK/MAPK and Akt, among others – [63,65]. It is therefore possible that increased FGF signalling contributes to the regenerative properties of SRCs Cycle 3.

Integrins function as adhesion receptors involved in ECM-cell signaling [66]. Stem cell fate choices in skeletal muscle are determined by the interaction between cell surface proteins and niche signals, among them, integrins [26,63]. In SRCs Cycle 3, ITGB5 and ITGB7 were upregulated. Although its role in skeletal muscle has not been elucidated, ITGB7 was overexpressed in muscle cells during cell cycle arrest *in vitro* [67]. Similarly, ITGB5 – also overexpressed in SRCs Cycle 3 – has previously been proposed as a molecular marker for mononuclear skeletal muscle cells *in vitro* [68]. It will be interesting to investigate the possible role of ITGB5 and ITGB7 in muscle regeneration and to assess whether they contribute to the stem cell regenerative properties of SRCs Cycle 3.

IGF binding proteins (IGFBPs) were upregulated in SRCs Cycle 3 and are known to act as modulators of the IGF-1 pathway [69]. IGF-1 signaling promotes muscle regeneration by supporting proliferation and differentiation of satellite cells [70]. In addition, upregulation of *Ngfr* was observed. *Ngfr* was recently identified [71,72] as a cell surface molecule expressed by iPSC-derived human muscle progenitor cells, and was previously found to be functionally relevant for the survival and maintenance of stemness of murine satellite cells during regeneration [73,74]. Enrichment of the muscle progenitors based on NGFR resulted in increased engraftment following transplantation to immunodeficient hosts [72]. Thus, although further research is necessary, increased activity of pathways mediated by IGFBPs or NGFR could contribute to the regenerative properties of SRCs Cycle 3.

Seven genes in the cAMP/cyclic nucleotide phosphodiesterase pathway were downregulated in SRCs Cycle 3. The superfamily of phosphodiesterase enzymes (PDEs) modulates the strength and duration of cAMP activity by degrading it. PDEs act therefore as drains of cAMP activity [75]. Previous work showed that inhibition of phosphodiesterase activity resulted in increased muscle stem cell marker expression in myoblasts *in vitro* and led to more efficient regeneration and increased engraftment as satellite cells after transplantation in a dystrophic mouse model [76]. Furthermore, stimulation of cAMP levels has been shown to promote direct engraftment of cultured satellite cells upon transplantation [77].

The decreased expression of PDE activity is therefore consistent with the stem cell regenerative properties of SRCs Cycle 3.

Cell adhesion participates in stem cell behavior. In myoblasts, slow cell adhesion has been associated with increased stem cell properties [22,45,78,79]. As expected, several cell adhesion genes were downregulated in SRCs Cycle 3. These included *Vcam1* and *Cdh15* (M-cadherin), which are also expressed in satellite cells, but are not required for skeletal muscle regeneration [80,81]. The downregulation of *Vcam1* and *Cdh15* in SRCs C3 therefore suggested that these genes are also not essential for the stem cell regenerative properties of reserve cells.

Genes involved in skeletal muscle function were overexpressed in FRCs Cycle 1 reserve cells. These genes included *Myh7* (type I adult fibers) and *Myh8* (fetal fibers) and titin, which are hallmarks of developing and mature muscle. This shows that FRCs Cycle 1 already has increased expression of genes that are expressed in differentiating muscle, even when these are cultured in proliferation medium. In agreement, expression of these genes has been observed previously in proliferating myoblasts [82]. Overall, our data indicate that pathways involved in regulation of myogenic fate and niche interactions are differentially regulated in reserve cells, and may contribute to their enhanced regenerative properties *in vivo*.

Conclusion

Using a protocol to generate reserve cells *in vitro* from myoblasts, combined with fractionation based on adhesive properties, we generated reserve cell fractions with enhanced regenerative capacities *in vivo*. We characterized their transcriptional profile and identified molecular pathways in reserve cells that engraft as stem cells involving enhanced expression of cell migration and growth factor binding genes, and decreased expression of cell adhesion and cAMP phosphodiesterase genes.

References

- 1 Benarroch L, Bonne G, Rivier F, et al. The 2021 version of the gene table of neuromuscular disorders (nuclear genome). *Neuromuscul Disord* 2020;30:1008–1048.
- 2 Biressi S, Filareto A, Rando TA. Stem cell therapy for muscular dystrophies. *J Clin Invest* 2020.
- 3 Law PK, Bertorini TE, Goodwin TG, et al. Dystrophin production induced by myoblast transfer therapy in Duchenne muscular dystrophy. *Lancet (London, England)* 1990;336:114–115.
- 4 Huard J, Bouchard JP, Roy R, et al. Human myoblast transplantation: preliminary results of 4 cases. *Muscle Nerve* 1992;15:550–560.
- 5 Miller RG, Sharma KR, Pavlath GK, et al. Myoblast implantation in Duchenne muscular dystrophy: the San Francisco study. *Muscle Nerve* 1997;20:469–478.
- 6 Law PK, Goodwin TG, Fang Q, et al. Cell transplantation as an experimental treatment for Duchenne muscular dystrophy. *Cell Transplant* 1993;2:485–505.
- 7 Tremblay JP, Malouin F, Roy R, et al. Results of a triple blind clinical study of myoblast transplantations without immunosuppressive treatment in young boys with Duchenne muscular dystrophy. *Cell Transplant* 1993;2:99–112.
- 8 Karpati G, Ajdukovic D, Arnold D, et al. Myoblast transfer in Duchenne muscular dystrophy. *Ann Neurol* 1993;34:8–17.
- 9 Tremblay JP, Bouchard JP, Malouin F, et al. Myoblast transplantation between monozygotic twin girl carriers of Duchenne muscular dystrophy. *Neuromuscul Disord* 1993;3:583–592.
- 10 Mendell JR, Kissel JT, Amato AA, et al. Myoblast transfer in the treatment of Duchenne's muscular dystrophy. *N Engl J Med* 1995;333:832–838.
- 11 Mauro A. Satellite cell of skeletal muscle fibers. *J Biophys Biochem Cytol* 1961;9:493–495.
- 12 Seale P, Sabourin LA, Girgis-Gabardo A, et al. Pax7 is required for the specification of myogenic satellite cells. *Cell* 2000;102:777–786.
- 13 Collins CA, Olsen I, Zammit PS, et al. Stem cell function, self-renewal, and behavioral heterogeneity of cells from the adult muscle satellite cell niche. *Cell* 2005;122:289–301.
- 14 Cerletti M, Jurga S, Witczak CA, et al. Highly Efficient, Functional Engraftment of Skeletal Muscle Stem Cells in Dystrophic Muscles. *Cell* 2008;134:37–47.
- 15 Sacco A, Doyonnas R, Kraft P, et al. Self-renewal and expansion of single transplanted muscle stem cells. *Nature* 2008;456:502–506.
- 16 Rama P, Matuska S, Paganoni G, et al. Limbal Stem-Cell Therapy and Long-Term Corneal Regeneration. *N Engl J Med* 2010;363:147–155.
- 17 Kondo M, Wagers AJ, Manz MG, et al. Biology of hematopoietic stem cells and progenitors: Implications for clinical application. *Annu Rev Immunol* 2003.
- 18 Montarras D, Morgan J, Collins C, et al. Direct isolation of satellite cells for skeletal muscle regeneration. *Science* 2005;309:2064–2067.
- 19 Quinn LS, Norwood TH, Nameroff M. Myogenic stem cell commitment probability remains constant as a function of organismal and mitotic age. *J Cell Physiol* 1988;134:324–336.

- 20 Baroffio A, Bochaton-Piallat ML, Gabbiani G, et al. Heterogeneity in the progeny of single human muscle satellite cells. *Differentiation* 1995;59:259–268.
- 21 Yoshida N, Yoshida S, Koishi K, et al. Cell heterogeneity upon myogenic differentiation: down-regulation of MyoD and Myf-5 generates “reserve cells”. *J Cell Sci* 1998;111 (Pt 6:769–779.
- 22 Qu Z, Balkir L, van Deutekom JC, et al. Development of approaches to improve cell survival in myoblast transfer therapy. *J Cell Biol* 1998;142:1257–1267.
- 23 Abou-Khalil R, Le Grand F, Pallafacchina G, et al. Autocrine and Paracrine Angiopoietin 1/Tie-2 Signaling Promotes Muscle Satellite Cell Self-Renewal. *Cell Stem Cell* 2009;5:298–309.
- 24 Laumonier T, Bermont F, Hoffmeyer P, et al. Human myogenic reserve cells are quiescent stem cells that contribute to muscle regeneration after intramuscular transplantation in immunodeficient mice. *Sci Rep* 2017;7:3462.
- 25 Conboy IM, Conboy MJ, Smythe GM, et al. Notch-mediated restoration of regenerative potential to aged muscle. *Science* 2003;302:1575–1577.
- 26 Kuang S, Kuroda K, Le Grand F, et al. Asymmetric self-renewal and commitment of satellite stem cells in muscle. *Cell* 2007;129:999–1010.
- 27 Zammit PS, Golding JP, Nagata Y, et al. Muscle satellite cells adopt divergent fates: A mechanism for self-renewal? *J Cell Biol* 2004.
- 28 Shinin V, Gayraud-Morel B, Gomès D, et al. Asymmetric division and cosegregation of template DNA strands in adult muscle satellite cells. *Nat Cell Biol* 2006;8:677–682.
- 29 Kitzmann M, Carnac G, Vandromme M, et al. The muscle regulatory factors MyoD and myf-5 undergo distinct cell cycle-specific expression in muscle cells. *J Cell Biol* 1998;142:1447–1459.
- 30 Beauchamp JR, Morgan JE, Pagel CN, et al. Dynamics of myoblast transplantation reveal a discrete minority of precursors with stem cell-like properties as the myogenic source. *J Cell Biol* 1999;144:1113–1121.
- 31 Tierney MT, Sacco A. Satellite Cell Heterogeneity in Skeletal Muscle Homeostasis. *Trends Cell Biol* 2016.
- 32 Scaramozza A, Park D, Kollu S, et al. Lineage Tracing Reveals a Subset of Reserve Muscle Stem Cells Capable of Clonal Expansion under Stress. *Cell Stem Cell* 2019.
- 33 Biressi S, Rando TA. Heterogeneity in the muscle satellite cell population. *Semin Cell Dev Biol* 2010.
- 34 Rocheteau P, Gayraud-Morel B, Siegl-Cachedenier I, et al. A subpopulation of adult skeletal muscle stem cells retains all template DNA strands after cell division. *Cell* 2012;148:112–125.
- 35 Yaffe D. Retention of differentiation potentialities during prolonged cultivation of myogenic cells. *Proc Natl Acad Sci U S A* 1968;61:477–483.
- 36 Richler C, Yaffe D. The in vitro cultivation and differentiation capacities of myogenic cell lines. *Dev Biol* 1970.
- 37 Rando TA, Blau HM. Primary mouse myoblast purification, characterization, and transplantation for cell-mediated gene therapy. *J Cell Biol* 1994.
- 38 Schaaf GJ, van Gestel TJM, Brusse E, et al. Lack of robust satellite cell activation and muscle regeneration during the progression of Pompe disease. *Acta Neuropathol Commun* 2015;3:65.

- 39 Schaaf GJ, van Gestel TJM, In 't Groen SLM, et al. Satellite cells maintain regenerative capacity but fail to repair disease-associated muscle damage in mice with Pompe disease. *Acta Neuropathol Commun* 2018;6:119.
- 40 Kim D, Langmead B, Salzberg SL. HISAT: A fast spliced aligner with low memory requirements. *Nat Methods* 2015;12:357–360.
- 41 Anders S, Pyl PT, Huber W. HTSeq-A Python framework to work with high-throughput sequencing data. *Bioinformatics* 2015;31:166–169.
- 42 Mi H, Ebert D, Muruganujan A, et al. PANTHER version 16: A revised family classification, tree-based classification tool, enhancer regions and extensive API. *Nucleic Acids Res* 2021;49:D394–D403.
- 43 Baroffio a, Hamann M, Bernheim L, et al. Identification of self-renewing myoblasts in the progeny of single human muscle satellite cells. *Differentiation* 1996;60:47–57.
- 44 Cho DS, Doles JD. Single cell transcriptome analysis of muscle satellite cells reveals widespread transcriptional heterogeneity. *Gene* 2017.
- 45 Jankowski RJ, Deasy BM, Cao B, et al. The role of CD34 expression and cellular fusion in the regeneration capacity of myogenic progenitor cells. *J Cell Sci* 2002;115:4361–4374.
- 46 Fu X, Xiao J, Wei Y, et al. Combination of inflammation-related cytokines promotes long-term muscle stem cell expansion. *Cell Res* 2015.
- 47 Wilkinson AC, Ishida R, Kikuchi M, et al. Long-term ex vivo haematopoietic-stem-cell expansion allows nonconditioned transplantation. *Nature* 2019;571:117–121.
- 48 Charville GW, Cheung TH, Yoo B, et al. Ex Vivo Expansion and In Vivo Self-Renewal of Human Muscle Stem Cells. *Stem Cell Reports* 2015.
- 49 Kimura E, Han JJ, Li S, et al. Cell-lineage regulated myogenesis for dystrophin replacement: A novel therapeutic approach for treatment of muscular dystrophy. *Hum Mol Genet* 2008.
- 50 Bar-Nur O, Gerli MFM, Di Stefano B, et al. Direct Reprogramming of Mouse Fibroblasts into Functional Skeletal Muscle Progenitors. *Stem Cell Reports* 2018.
- 51 Negroni E, Gidaro T, Bigot A, et al. Invited review: Stem cells and muscle diseases: advances in cell therapy strategies. *Neuropathol Appl Neurobiol* 2015;41:270–287.
- 52 Judson RN, Rossi FMV. Towards stem cell therapies for skeletal muscle repair. *Npj Regen Med* 2020;5:1–6.
- 53 Dell'Orso S, Juan AH, Ko K-D, et al. Single-cell analysis of adult skeletal muscle stem cells in homeostatic and regenerative conditions. *Development* 2019;dev.174177.
- 54 Barruet E, Garcia SM, Striedinger K, et al. Functionally heterogeneous human satellite cells identified by single cell RNA sequencing. *Elife* 2020.
- 55 Gurevich DB, Nguyen PD, Siegel AL, et al. Asymmetric division of clonal muscle stem cells coordinates muscle regeneration in vivo. *Science* 2016.
- 56 Yennek S, Burute M, Théry M, et al. Cell adhesion geometry regulates non-random DNA segregation and asymmetric cell fates in mouse skeletal muscle stem cells. *Cell Rep* 2014;7:961–970.
- 57 Quarta M, Brett JO, DiMarco R, et al. An artificial niche preserves the quiescence of muscle stem cells and enhances their therapeutic efficacy. *Nat Biotechnol* 2016;34:752–759.
- 58 Low S, Barnes JL, Zammit PS, et al. Delta-Like 4 Activates Notch 3 to Regulate Self-Renewal in Skeletal Muscle Stem Cells. *Stem Cells* 2018;36:458–466.

- 59 Pawlikowski B, Orion Vogler T, Gadek K, et al. Regulation of Skeletal Muscle Stem Cells by Fibroblast Growth Factors. *Dev Dyn* 2017.
- 60 Yablonka-Reuveni Z, Danoviz ME, Phelps M, et al. Myogenic-specific ablation of Fgfr1 impairs FGF2-mediated proliferation of satellite cells at the myofiber niche but does not abolish the capacity for muscle regeneration. *Front Aging Neurosci* 2015;7.
- 61 Clegg CH, Linkhart TA, Olwin BB, et al. Growth factor control of skeletal muscle differentiation: Commitment to terminal differentiation occurs in G1 phase and is repressed by fibroblast growth factor. *J Cell Biol* 1987;105:949–956.
- 62 Anderson JE, Mitchell CM, McGeachie JK, et al. The time course of basic fibroblast growth factor expression in crush-injured skeletal muscles of SJL/J BALB/c mice. *Exp Cell Res* 1995;216:325–334.
- 63 Rozo M, Li L, Fan CM. Targeting β 1-integrin signaling enhances regeneration in aged and dystrophic muscle in mice. *Nat Med* 2016;22:889–896.
- 64 Chakkalakal J V., Jones KM, Basson MA, et al. The aged niche disrupts muscle stem cell quiescence. *Nature* 2012.
- 65 Kastner S, Elias MC, Rivera AJ, et al. Gene expression patterns of the fibroblast growth factors and their receptors during myogenesis of rat satellite cells. *J Histochem Cytochem* 2000;48:1079–1096.
- 66 Hynes RO. Integrins: Bidirectional, allosteric signaling machines. *Cell* 2002;110:673–687.
- 67 Sellathurai J, Cheedipudi S, Dhawan J, et al. A Novel In Vitro Model for Studying Quiescence and Activation of Primary Isolated Human Myoblasts. *PLoS One* 2013;8:e64067.
- 68 Sinanan ACM, Machell JRA, Wynne-Hughes GT, et al. α v β 3 and α v β 5 integrins and their role in muscle precursor cell adhesion. *Biol Cell* 2008;100:465–477.
- 69 Swiderski K, Martins KJB, Chee A, et al. Skeletal muscle-specific overexpression of IGFBP-2 promotes a slower muscle phenotype in healthy but not dystrophic mdx mice and does not affect the dystrophic pathology. *Growth Horm IGF Res* 2016;30–31:1–10.
- 70 Allen RE, Boxhorn LK. Regulation of skeletal muscle satellite cell proliferation and differentiation by transforming growth factor-beta, insulin-like growth factor I, and fibroblast growth factor. *J Cell Physiol* 1989;138:311–315.
- 71 van der Wal E, Herrero-Hernandez P, Wan R, et al. Large-Scale Expansion of Human iPSC-Derived Skeletal Muscle Cells for Disease Modeling and Cell-Based Therapeutic Strategies. *Stem Cell Reports* 2018;10:1975–1990.
- 72 Hicks MR, Hiserodt J, Paras K, et al. ERBB3 and NGFR mark a distinct skeletal muscle progenitor cell in human development and hPSCs. *Nat Cell Biol* 2018.
- 73 Deponti D, Buono R, Catanzaro G, et al. The low-affinity receptor for neurotrophins p75 NTR plays a key role for satellite cell function in muscle repair acting via RhoA. *Mol Biol Cell* 2009.
- 74 Clow C, Jasmin BJ. Brain-derived neurotrophic factor regulates satellite cell differentiation and skeletal muscle regeneration. *Mol Biol Cell* 2010.
- 75 Baillie GS. Compartmentalized signalling: spatial regulation of cAMP by the action of compartmentalized phosphodiesterases. *FEBS J* 2009;276:1790–1799.
- 76 Lala-Tabbert N, Fu D, Wiper-Bergeron N. Induction of CCAAT/Enhancer-Binding Protein β Expression With the Phosphodiesterase Inhibitor Isobutylmethylxanthine Improves Myoblast Engraftment Into Dystrophic Muscle. *Stem Cells Transl Med* 2016;5:500–510.

- 77 Xu C, Tabebordbar M, Iovino S, et al. XA zebrafish embryo culture system defines factors that promote vertebrate myogenesis across species. *Cell* 2013;155:909.
- 78 Qu-Petersen Z, Deasy B, Jankowski R, et al. Identification of a novel population of muscle stem cells in mice: potential for muscle regeneration. *J Cell Biol* 2002.
- 79 Gharaibeh B, Lu A, Tebbets J, et al. Isolation of a slowly adhering cell fraction containing stem cells from murine skeletal muscle by the preplate technique. *Nat Protoc* 2008.
- 80 Hollnagel A, Grund C, Franke WW, et al. The Cell Adhesion Molecule M-Cadherin Is Not Essential for Muscle Development and Regeneration. *Mol Cell Biol* 2002;22:4760–4770.
- 81 Choo H-J, Canner JP, Vest KE, et al. A tale of two niches: differential functions for VCAM-1 in satellite cells under basal and injured conditions. *Am J Physiol Physiol* 2017;313:C392–C404.
- 82 Wang J hua, Wang Q jing, Wang C, et al. Heterogeneous activation of a slow myosin gene in proliferating myoblasts and differentiated single myofibers. *Dev Biol* 2015;402:72–80.

Data availability statement

The data that support the findings of this study are available on request from the corresponding author.

Acknowledgments

We wish to thank Dimitris Rizopoulos (Erasmus MC, Department of Biostatistics) for advise on statistical analysis of the data; R. Volckmann (University of Amsterdam Medical Center, Department of Oncogenomics) for his help with R2 for analysis of RNA-SEQ data.

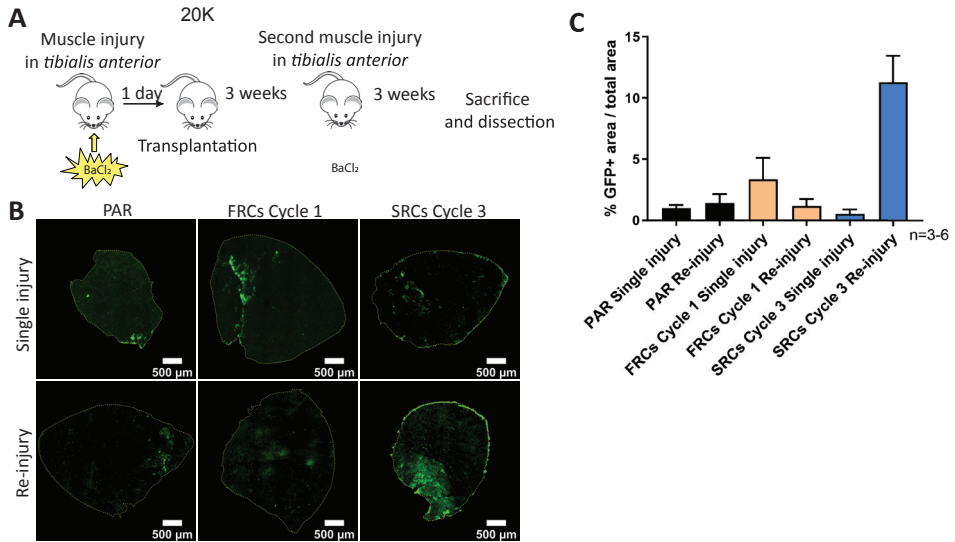
Sources of Funding

The work was funded through the Center of Lysosomal and Metabolic Diseases at Erasmus MC.

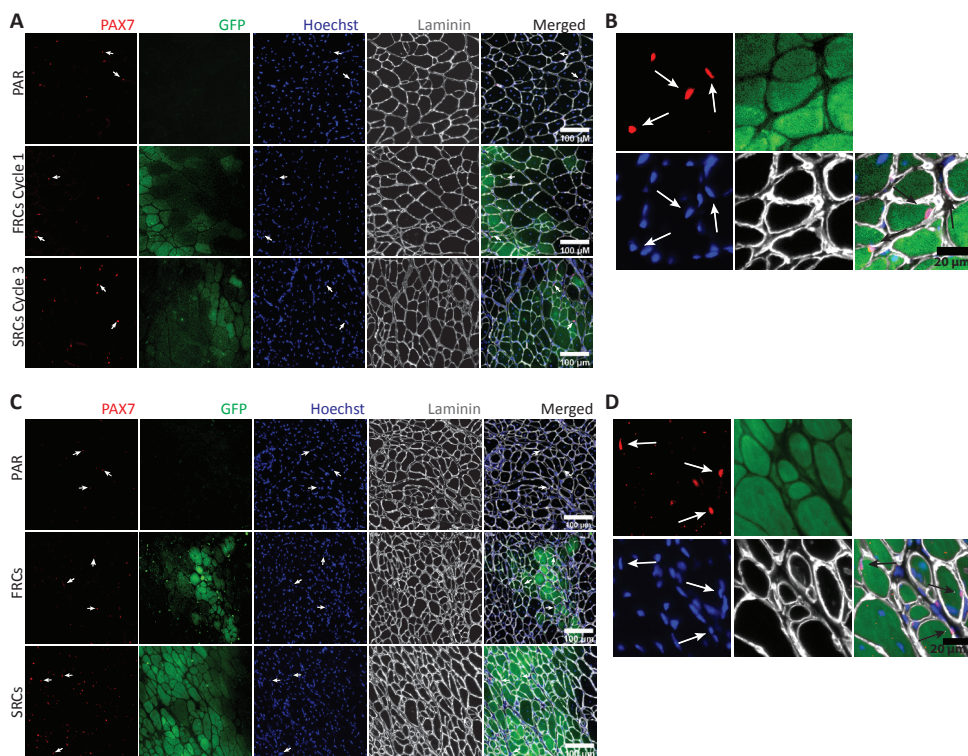
Disclosures

A.T.v.d.P. has provided consulting services for various industries in the field of Pompe disease under an agreement between these industries and Erasmus MC, Rotterdam, the Netherlands. All the other authors declare no conflict of interest.

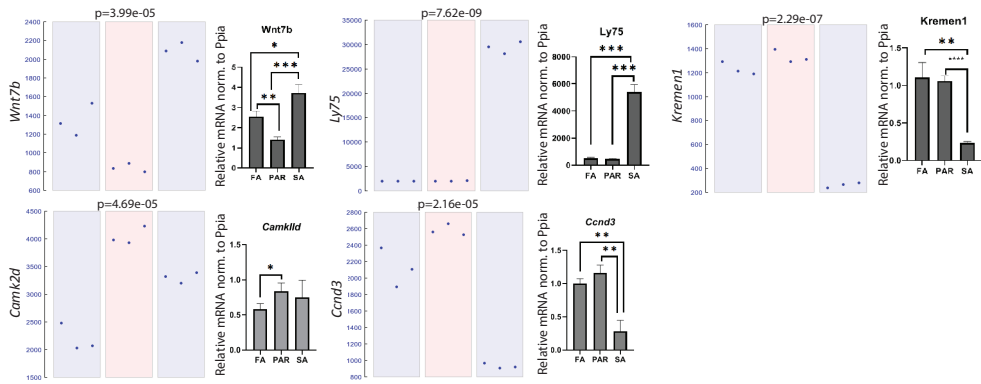
Supplementary information



Supplementary Figure 1. Engraftment of C57BL/6 reserve cells upon injury and re-injury. (A) Scheme of the experimental design. (B) Wide field fluorescence microscopy tile scan images of TA cross sections from injury and re-injury experiments after transplantation of C57/BL6 PAR, FRCs Cycle 1, and SRCs Cycle 3. Green, GFP. The outline of the sections was drawn. Representative images of mean engraftment for each group are shown. (C) Quantification of the engraftment levels from (A). $n=3-6$. n indicates the number of mice per transplantation group. Data are shown as means \pm SE.

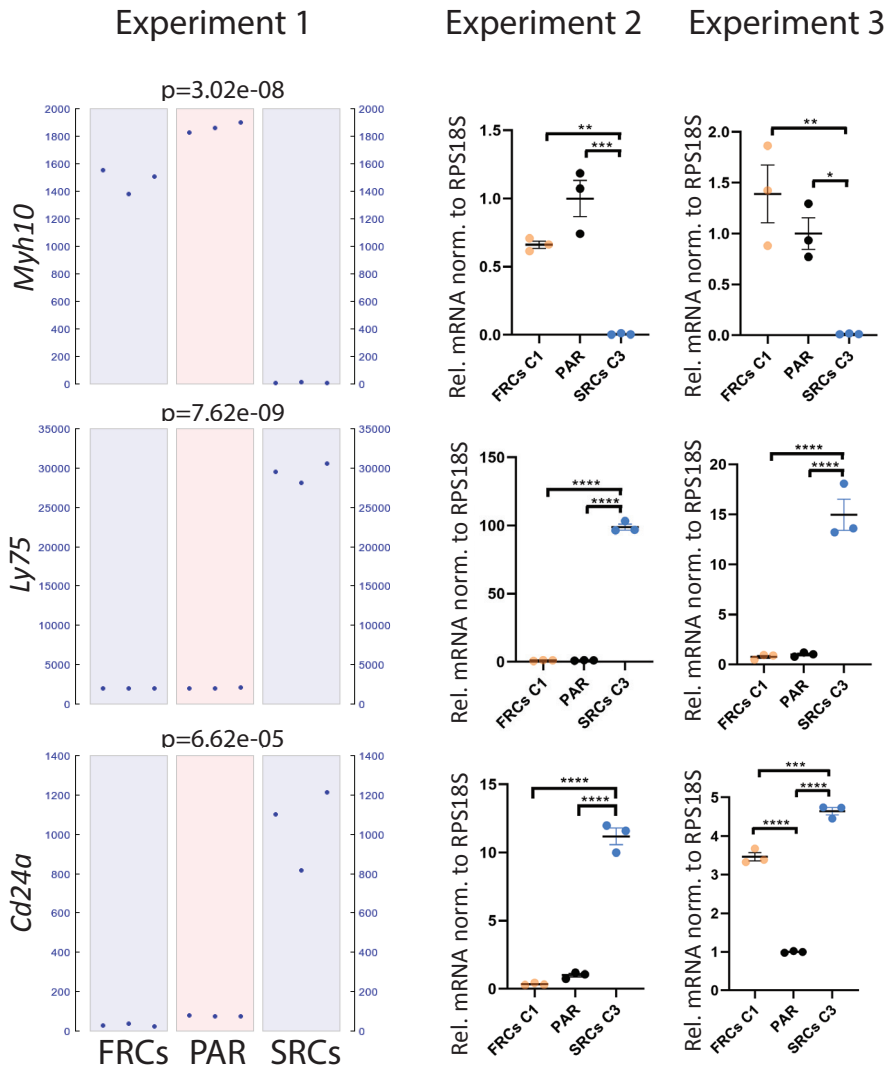


Supplementary Figure 2. Muscle regenerated by reserve cells hosted stem cells *in vivo*. (A) Immunostaining for PAX7/laminin in TA cross sections of NOD-SCID mice after transplantation of FVB/N PAR, FRCs Cycle 1, and SRCs Cycle 3 in single injury experiments. PAX7 (red); GFP (green); laminin (grey); nuclei counterstained with Hoechst (blue). White arrows indicate the location of sublamellar PAX7⁺ nuclei. Scale bars, 100 μ m. $n=3$. n indicates the number of mice analyzed per transplantation group. Representative images are shown. (B) Zoom in image of immunostaining for PAX7/laminin in TA cross sections of NOD-SCID mice after transplantation of FVB/N SRCs Cycle 3 in single injury experiments. PAX7 (red); GFP (green); laminin (grey); nuclei counterstained with Hoechst (blue). Arrows indicate the location of sublamellar PAX7⁺ nuclei. Representative images were used. Scale bars, 20 μ m. (C) Immunostaining for PAX7/laminin in TA cross sections of NOD-SCID mice after transplantation of FVB/N PAR, FRCs Cycle 1, and SRCs Cycle 3 in re-injury experiments. PAX7 (red); GFP (green); laminin (grey); nuclei counterstained with Hoechst (blue). White arrows indicate the location of sublamellar PAX7⁺ nuclei. Scale bars, 100 μ m. $n=3$. n indicates the number of mice analyzed per transplantation group. Representative images are shown. (D) Zoom in image of immunostaining for PAX7/laminin in TA cross sections of NOD-SCID mice after transplantation of FVB/N SRCs Cycle 3 in re-injury experiments. PAX7 (red); GFP (green); laminin (grey); nuclei counterstained with Hoechst (blue). Arrows indicate the location of sublamellar PAX7⁺ nuclei. Representative images were used. Scale bars, 20 μ m



Supplementary Figure 3. Validation of RNaseq by RT-qPCR analysis

mRNA expression levels of *Wnt7b*, *Ly75*, *Kremen1*, *Camk2d*, and *Ccnd3* in FVB/N PAR, FRCs Cycle 1, and SRCs Cycle 3 populations. Coloured panels show total read count from RNA-Seq data. Each dot represents an independent replicate. *P* values of the RNaseq analysis are indicated above each gene. Black and white graphs show RT-qPCR analysis of the same markers. Data were normalized to *Ppia* and expressed as means \pm SE. *n*=3. *N* indicates independent replicates. **p*≤0.05, ***p*≤0.005; ****p*≤0.0005.



Supplementary Figure 4. RNAseq and mRNA expression of DEGs in independently generated reserve cell and PAR fractions

mRNA expression levels of Myh10, Ly75, and Cd24a in PAR, FRCs Cycle 1, and SRCs Cycle 3 populations. Left panels show total read count from RNA-Seq data. Middle and right panels show RT-qPCR transcript levels from alternative, independent experiments. Each dot represents an independent replicate. Data are expressed as means \pm SE. * $p \leq 0.05$; ** $p \leq 0.01$; *** $p \leq 0.001$; **** $p \leq 0.0001$.

Supplementary Table 1

Antibody	Dilution	Info
Mouse anti-PAX7	1:20; 1:100	Bioceros B.V. (3.1 mg/ml)
Rabbit anti-MYOD	1:500	Santa Cruz (sc-304)
Mouse anti-MYOD	1:100	Santa Cruz (sc-377460)
Rabbit anti-MYOG	1:500	Santa Cruz (sc-576)
Rabbit anti-Laminin	1:100	Sigma (L9393)
Rabbit anti-MYF5	1:500	Santa Cruz (sc-302)
Horse Biotin anti-mouse	1:250	Vector Laboratories (BA-2000)
Biotin anti-mouse IgG2B	1:250	BD Biosciences (#553393)
AlexaFluor-488 [®] Goat anti-mouse	1:500	Life Technologies
AlexaFluor-488 [®] Goat anti-rabbit	1:500	Life Technologies (A11307)
AlexaFluor-594 [®] Goat anti-mouse	1:500	Life Technologies
Streptavidin, Alexa Fluor 647 conjugate	1:500	Thermo Fisher (S21374)
AlexaFluor-647 [®] Goat anti-chicken	1:500	Life Technologies (A21449)
Goat anti-mouse IgG2B Cy3	1:500	Jackson ImmunoResearch (115-165-207)
Goat anti-mouse IgG1 Cy3	1:500	Jackson ImmunoResearch (115-165-205)

Supplementary Table 1. List of antibodies used for immunofluorescence staining

Supplementary Table 2

Gene	Forward (5'-3')	Reverse (5'-3')	Amplification product (bp)
<i>Myh10</i>	CATTCAGTACCTTGCCACG	AAAGCTGCCGTTCAAGTTCC	83
<i>Ly75</i>	TGAAATGCAAAGCCTTCGGT	AACTCCGTTCCGTCCGAC	167
<i>Cd24a</i>	AACATCTAGAGAGTCGCGCC	CCTCTGGTGGTAGCGTTACT	197
<i>Wnt7b</i>	TCCGAGTAGGGAGTCGAGAG	CCTCCGCCTGGTTGTAGTA	148
<i>Kremen1</i>	CCGAGTGCAATAGTGTCTGC	TCAGGGAAGTCAGGGGAGTA	145
<i>Camk2d</i>	CAGTGACACCTGAAGCCAAA	GCATCATGGAGGCAACAGTA	129
<i>Ccnd3</i>	CGAGCCTCCTACTTCCAGTG	AGCCAGAGGGAAGACATCCT	123
<i>Ppia</i>	TGCACTGCCAAGACTGAATG	GCTTCCACAATGTTTCATGCC	80
<i>Rps18</i>	TCAACACGGGAAACCTCAC	ACCAGACAAATCGCTCCAC	201

Supplementary Table 2. List of primers

Supplementary Methods

Cell culture

Myoblasts were cultured on culture dishes coated with 40 µg/ml extracellular matrix (ECM) (Sigma-Aldrich, Missouri, USA) in proliferation medium (GM; Ham's F10 (Lonza, Basel, Switzerland) supplemented with 20% fetal calf serum (FCS) (Lonza), 100 U/ml penicillin/streptomycin (PS) (Lonza), and 20 ng/ml fibroblast growth factor 2 (FGF2) (PeproTech, New Jersey, USA)). For differentiation, myoblasts or reserve cells were grown to 90-100 % confluency, after which the medium was switched to differentiation medium (DM), Dulbecco's Modified Eagle Medium (DMEM) (Lonza) supplemented with 2% horse serum (Lonza) and 100 U/ml PS. During differentiation, medium was not refreshed. As is known in the field, the efficiency of myogenic differentiation can vary between experiments, likely due to technical differences related to the exact cell density and medium composition. To minimize this experimental variation, the plating and differentiation conditions within experiments were identical for all biological replicates, making a direct comparison possible.

FVB-GFP murine primary muscle cells (FVB-GFP) were obtained after transduction of myoblasts obtained from a FVB/N mouse with a lentiviral vector carrying an eGFP lentiviral construct under the control of the ubiquitous SF promoter (pRRL.cppt.SFFV.eGFP.WPRE4*.SIN) (Van Til et al. 2010). After transduction close to hundred percent of cells were GFP positive, as judged by microscopic examination of GFP fluorescence. The FVB-GFP murine muscle primary cell line was used for all *in vitro* experiments as well as for transplantations *in vivo*. BL6-GFP murine primary muscle cells (BL6-GFP) were obtained after transduction of primary myoblasts established from a C57/BL6 mouse donor with the same lentiviral vector as used for FVB/N myoblasts.

Reserve cell isolation protocol

Murine primary myoblasts at passage 32 were grown to 90-100% confluency. After 48 hours, differentiation was induced replacing GM with DM. Cultures were left in DM for 5 days at 37° in a humidified air incubator containing 5% CO₂. After 5 days of differentiation, DM containing detached cells was kept and cells were trypsinized as described previously. Cell-containing medium was then filtered through a 40 µm pore-sized filter to remove large myotubes (Falcon cell strainer 40 µm nylon).

The filtered cell-containing solution was resuspended through a 21G needle in order to disaggregate small myotubes that were able to pass through the filter in the previous step. Next, filtered cells were centrifuged at 1000 rpm for 5 minutes. The remaining pellet was resuspended in proliferation medium and plated on a ECM-coated culture dish during one hour at 37°C, 5% CO₂. After adhesion of the fraction 1 (annotated as fast-adhering reserve cells; FRCs) (cells that attached within one-hour), non-attached cells were transferred onto a new ECM-coated dish and allowed to adhere during three hours at 37°C, 5% CO₂. The non-adherent cells were transferred to a third ECM-coated dish and the attached cells (Fraction 2) were discarded. After incubation overnight (16h), non-attached cell-containing medium was discarded, and the attached cells (Fraction 3) continued in culture, annotated slow-adhering reserve cells (SRCs). FRCs and SRCs received fresh GM + 20 ng/mL FGF and were incubated at 37°C in a humidified air incubator containing 5% CO₂. In order to eliminate the possibility of including residual small myotubes and differentiated mononuclear cells, reserve cell cultures were passaged twice in growth conditions before their use for experiments.

6

Transplantation of reserve cells

After isolation, reserve cells were passaged twice before transplantation. One day prior to cell transplantation *tibialis anterior* (TA) muscles of recipient NOD-SCID mice were preinjured by intramuscular injection of 50 µl 1.2% w/v BaCl₂ (Sigma-Aldrich). Mice were pre-anesthetized with 4% isoflurane with a vaporizer (Pharmachemie B.V., Haarlem, Netherlands). The next day cells were harvested by trypsinization and suspended in 20 µl PBS supplemented with 10% mouse serum (NOD-SCID derived). Cell suspensions for transplantations were kept on ice and transplanted within 30 minutes. Cells were injected in pre-anesthetized mice through intra-muscular injection into the pre-injured TA muscle. After each animal procedure – i.e. inducing injury and transplantation – mice were injected subcutaneously with 10 mg/kg enrofloxacin (Baytril®, Bayer, Germany) and 0.1 mg/kg buprenorphine (Temgesic®). Both male and female recipient mice were used for the experiments. Mice were anesthetized with isoflurane and sacrificed by cervical dislocation during daytime 3 or 6 weeks after transplantation.

Immunostaining analyses

In vitro cultured cells were fixed in 4% paraformaldehyde (PFA) and permeabilized

with 0.5% Triton X-100%; 3% BSA in PBS for 30 minutes at room temperature (RT). Blocking was performed using 20% horse serum (Lonza) for 1 hour at RT. Antibodies were diluted in 0.1% BSA; 0.1% Tween 20 in PBS and incubated for 30 minutes at RT. Nuclei were counter-stained with Hoechst 33258 (H3569; Life Technologies; 1:15000) for 10 minutes at RT in the dark. Antibodies are listed in Supplementary Table 1. Stained samples were stored in PBS at 4°C in the dark until imaging. Fluorescence imaging of immunostained cultured cells was performed on an Olympus IX70 fluorescence microscope (Olympus Nederland B.V., Zoeterwoude, Netherlands) or Nikon Eclipse Ti-E Wide Field inverted microscope (Nikon Instruments Europe B.V., Amsterdam, Netherlands). Images were analyzed using Adobe Photoshop CS6 and FIJI (fiji.sc/Fiji).

Immunostaining in murine muscle sections

Immunostainings on mouse muscle tissue was performed as described previously (Schaaf et al. 2018). In short, fresh sections were cut, immediately fixated in 2% EM-PFA (Electron Microscopy Sciences, Hatfield, PA) at RT for 5 minutes. Tissue sections were permeabilized using 0.5% Triton X-100 in 20% goat serum 3% BSA in PBS for 1 hour at RT. Primary antibodies were diluted in the permeabilization/blocking solution and incubated at RT for 2 hours. Sections were washed with 0.1% Tween20 in PBS and secondary antibodies incubated in permeabilization/blocking solution for 1h at RT. Nuclei were counterstained with Hoechst. The slides were then mounted using Mowiol® (475904; Calbiochem) mounting solution and imaged immediately.

Protein isolation and Western Blot analysis

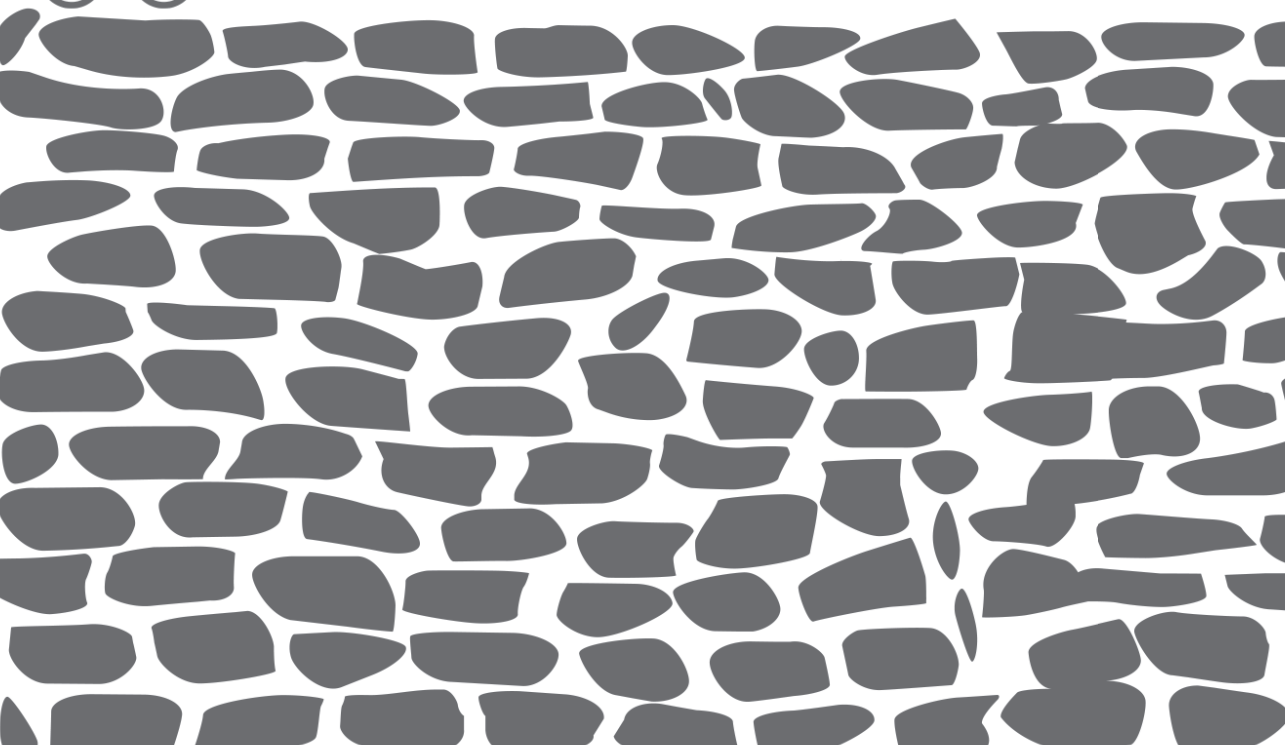
Cultured cells were harvested and lysed in RIPA buffer (50 mM TrisHCl pH 7.4, 150 mM NaCl, 2 mM EDTA, 1% Triton X-100) supplemented with a phosphatase inhibitor cocktail (10 mM NaF, 60 mM β -glycerolphosphate, 2 mM Na-orthovanadate) and cOmplete™ protease inhibitor cocktail (Sigma-Aldrich) for 30 minutes on ice. Muscle transversal sections were homogenized using a tissue homogenizer and lysed in RIPA buffer as described above. Lysates were then centrifuged for 15 minutes at 13000 rpm. Total protein-containing supernatant was used for protein analysis studies. Total protein concentration was determined using Pierce™ BCA Protein Assay Kit according to manufacturer's instructions (Thermo Scientific, Rockford IL, USA).

Samples were diluted in sample buffer (31.25 mM Tris-HCl pH 6.8, 0.5% SDS, 12.5% glycerol, 0.005% bromophenol blue, 2.5% β -mercaptoethanol), denatured at 95°C for 5 minutes, and loaded in 4-15% Criterion™ TGX™ precast gels (BioRad Laboratories B.V., Veenendaal, Netherlands) immersed in Tris/glycine/SDS buffer (25 mM Tris, 192 mM glycine, 0.1% SDS, pH 8.3). Samples went through electrophoresis for 15 minutes at 100 V 80 mA and 45 minutes at 150 V 45 mA. Gels were transferred to nitrocellulose membranes for 30 minutes at 100V in a cassette immersed in Towbin buffer (25 mM Tris-HCl, 192 mM glycine, 20% (v/v) methanol, pH 8.3). Nitrocellulose membranes were blocked in 5% milk diluted in TBST, 5% bovine serum albumin (BSA) or 50% Odyssey® Blocking Buffer (PBS) (Li-Cor) diluted in PBS. Upon blocking, membranes were incubated in primary antibody, washed extensively in TBST, and incubated in secondary antibody. Membranes were read in an Odyssey reader (Li-Cor).

RNA Isolation and RNA-Seq

Freshly isolated reserve cell populations were passaged twice under proliferation conditions before harvesting. Samples were harvested using RLT buffer (QIAGEN, Germantown, MD). RNA was extracted using the RNeasy minikit with DNase treatment (QIAGEN, Germantown, MD). Total RNA for triplicates of PAR, FRCs Cycle 1, and SRCs Cycle 3 were checked for quality on an Agilent Technologies 2100 Bioanalyzer using a RNA nano assay. All samples had RIN value of 10. Triplicate RNA-Seq libraries were prepared according to the Illumina TruSeq stranded mRNA protocol (www.illumina.com). Briefly, 200 ng of total RNA was purified using poly-T oligo-attached magnetic beads to end up with poly-A containing mRNA. The poly-A tailed mRNA was fragmented and cDNA was synthesized using SuperScript II and random primers in the presence of Actinomycin D. cDNA fragments were end repaired, purified with AMPure XP beads, A-tailed using Klenow exo-enzyme in the presence of dATP. Paired end adapters with dual index (Illumina) were ligated to the A-tailed cDNA fragments and purified using AMPure XP beads. The resulting adapter-modified cDNA fragments were enriched by PCR using Phusion polymerase as followed: 30 s at 98°C, 15 cycles of (10 s at 98°C, 30 s at 60°C, 30 s at 72°C), 5 min at 72°C. PCR products were purified using AMPure XP beads and eluted in 30 μ l of resuspension buffer. One microliter was loaded on an Agilent Technologies 2100 Bioanalyzer using a DNA 1000 assay to determine the library concentration and for quality check. Cluster generation was performed according to the Illumina TruSeq SR

Rapid Cluster kit v2 (cBot) Reagents Preparation Guide (www.illumina.com). Briefly, 9 RNA-Seq libraries were pooled together to get a stock of 10 nM. One microliter of the 10 nM stock was denatured with NaOH, diluted to 6 pM and hybridized onto the flowcell. The hybridized products were sequentially amplified, linearized and end-blocked according to the Illumina Single Read Multiplex Sequencing user guide. After hybridization of the sequencing primer, sequencing-by-synthesis was performed using the HiSeq 2500 with a single read 50-cycle protocol followed by dual index sequencing. Illumina adapter sequences have been trimmed off the reads, which were subsequently mapped against the GRCm38 mouse reference using HISat2 (version 2.1.0) (Kim, Langmead, and Salzberg 2015). Gene expression values were called using htseq-count (version 0.9.1) (Anders, Pyl, and Huber 2015) and Ensembl release 91 gene and transcript annotation. Normalization and expression value generation was done using DESeq2 (rlog). Visualization and analyses of RNA-Seq data and GO analysis were performed using R2: Genomics Analysis and Visualization Platform (<http://r2.amc.nl>).



Chapter 7

Discussion

Discussion

The work presented in this thesis aims to explore the molecular mechanisms that drive Pompe disease, and to provide novel insight on *ex vivo* expanded muscle regenerative cells. In the preceding chapters we provided evidence on dysregulation of glycogen metabolism in Pompe disease in mice and patients and shed light in the role of autophagy for satellite cell activation in Pompe disease. Furthermore, we isolated and characterized murine muscle reserve cells, identified populations with differential regenerative properties, and investigated their transcriptional signatures. We developed a protocol to assess muscle stem cell activation through isolation of single muscle fibers, and reviewed muscle regeneration defects in neuromuscular disorders. Multiple approaches are currently being developed in these fields to provide solutions to the same questions that this thesis aimed to answer. Below, we discussed some of our findings in the context of the state-of-the-art, as well as future perspectives and challenges that this research faces towards a clinical outcome.

1. Pompe disease: remaining questions

Pompe disease is characterized by a wide spectrum of clinical heterogeneity in patients with adult onset Pompe disease, even for those who share identical disease-associated variants in the *GAA* gene. This suggests that disease modifying factors affect the clinical spectrum in Pompe disease. Disease modifying factors can have a genetic origin, such as the c.510C>T variant, a genetic modifier in IVS1 patients [1]; or may be determined by environmental or epigenetics factors. Other GSDs are also characterized by a heterogeneous spectrum of disease symptoms. An example is GSDIa, caused by deficiency of G6Pase, where symptom heterogeneity has been associated to the severity of the genetic variants in *G6PC1*, an enzyme involved in glycogen metabolism, which act as a disease modifying factor [2,3]. In Pompe disease, glycogen metabolism and autophagy have been proposed in the past as potential modifying factors [4,5]. Confirmation of the involvement of disease modifying factors in disease onset, progression, or response to therapy could offer novel targets for treatment and open the door for the application of personalized therapies.

1.1. How does dysregulation of glycogen affect Pompe disease, and why does it matter?

Glycogen metabolism depends on a fine balance between biosynthesis and degradation, which is controlled by a set of cytoplasmic and lysosomal enzymes in muscle cells. Studies in mice showed that glycogen metabolism is altered in Pompe disease – suggesting accumulation of cytoplasmic glycogen –, and that ERT treatment normalized enzyme levels [4,6,7]. Similarly, evidence in human skeletal muscle biopsies showed upregulation of GLUT4, involved in glucose uptake, and of deposition of extra-lysosomal glycogen that was not cleared after ERT treatment, indications that glycogen metabolism may also be altered in Pompe disease patients [8,9]. The results reported in chapter 2 are in line with previous findings in human and mouse, and provide further evidence regarding the existence of dysregulation in the metabolism of glycogen in Pompe disease. However, the limited availability of suitable biopsies together with a relatively high variability between individuals limited the power of this study. Further research should aim to analyze glycogen metabolism in a larger cohort of patients in order to determine the significance of the changes. In addition, in our study we used biopsies of mildly affected adult onset patients. A possibility would be that glycogen metabolism was more strongly dysregulated in severely affected patients. Analyzing other patient groups, such as severely affected adults or classic infantile patients, would allow to assess the degree to which disturbances in glycogen metabolism affect patients. Such analysis would allow to determine whether there is any relationship between dysregulation of glycogen metabolism and disease progression, and to indicate whether it could be considered a disease modifying factor, as it has been proposed in the past [4].

Understanding if dysregulation of glycogen metabolism occurs before the onset of muscle pathology, as it is the case in mice, would have a relevant clinical impact, since therapeutic strategies could consider targeting glycogen build-up from an early stage, similarly to what some forms of SRT propose. However, manipulation of glycogen biosynthesis is a very delicate step, as shown by alteration of muscle functionality after depleting GYG1 in mice and the high lethality rate (90%) of GYS1^{-/-} mice [10,11]. Furthermore, deficiency of GYS1 represents a skeletal muscle disease on its own [12]. Lastly, determining whether the response to ERT is affected by the status of glycogen metabolism would be relevant for its use as a potential marker for monitoring the response to treatment.

1.2. Why is the metabolism of glycogen altered in Pompe disease?

In Pompe disease, GAA deficiency causes intra-lysosomal glycogen accumulation. As a result, glycogen cannot be broken down in the lysosome upon need. In homeostatic conditions, cells have compensatory mechanisms, such as negative feedback loops (see next paragraph), that ensure a process does not become overactivated. Under pathological conditions, metabolic stress may unleash a physiological response, or adaptation, that may have adverse consequences and eventually damages cells and tissues, such as it is the case in autoimmune disease or chronic inflammation episodes [13]. In Pompe disease, the excess of glycogen in the lysosomes seems not to be adequately interpreted by muscle cells, which in turn react by increasing glycogen biosynthesis in the cytoplasm. A hypothesis would be the prevalence of a state in which accumulation of glycogen in the lysosomes results in a shortage of free glucose available to the cell, to which the cell reacts by increasing glucose uptake (or alternative glucose synthesis pathways, such as gluconeogenesis) and enhancing glycogen biosynthesis. As mentioned above, this could occur as a response to metabolic stress, ultimately resulting in tissue damage. Nevertheless, this hypothesis has not formally been tested, and future research should aim to elucidate such question.

1.3. Dysregulation of glycogen metabolism in Pompe disease. A unique case?

Metabolic imbalance in glycogen biosynthesis and degradation is not exclusive for Pompe disease (for an overview of glycogen metabolism in GSD, see [14]). An increase in enzymes involved in glycogen biosynthesis in cardiac tissue was reported in a study performed in fasting women, reinforcing the hypothesis that dysregulation of glycogen metabolism could be an adaptation to metabolic stress [15]. In McArdle disease (GSDV), caused by deficiency of PYGM, analysis of transcripts and protein levels in patients revealed downregulation of GYS1 [16]. Interestingly, the overall effect was to prevent further glycogen storage – as would be expected from a compensatory mechanism –, opposite to what occurs in Pompe disease. Another example of a compensatory mechanism related to glycogen metabolism in a GSD is found in a study by Testoni *et al.*, in which glycogen accumulation was reported in skeletal muscle of *Cygt*^{-/-} mice, also opposite to what we and others reported for Pompe disease [10]. Analysis of carbohydrate metabolism in patients

with GYG1 deficiency also revealed exercise-induced impaired glycogenolysis [17]. These examples suggest that glycogen metabolism is a tightly controlled complex mechanism, and that its outcome depends on where in the pathway the interference occurs. Additionally, it seems plausible that additional metabolic abnormalities in glycogen synthesis and degradation could be a common feature in GSDs.

1.4. The impact of metabolic abnormalities in the pathology of GSDs

Dysregulated metabolic activities seem to be relatively common in GSDs, including Pompe disease. As mentioned throughout this thesis, autophagy is one of the most studied metabolic parameters in Pompe disease as a target for therapy. Autophagy is also altered and studied as a candidate for therapy in GSDI, as induction of autophagy improved hepatic lipid metabolism and lipid clearance in several human and animal disease models [18]. Another relevant metabolic feature known to be dysregulated both in GSDI and Pompe disease is oxidative stress. Recent research showed that correction of oxidative stress in Pompe disease improved response to ERT [19,20].

The role of metabolism in GSDs and its potential impact in their pathology seems to be coming to light. Metabolic profiling in GSDI and GSDIII revealed distinct metabolic signatures that allowed clustering of these diseases into several subtypes [21]. It would be interesting to determine whether metabolic signature-based subtypes can also be established in Pompe disease, and whether such subtypes are associated to certain clinical manifestations. If it were the case, the metabolic signature of Pompe disease could be used with therapeutic purposes.

It is manifest that a range of metabolic alterations occur in GSDs, and that they could be relevant for clinical parameters such as response to treatment. Investigation of these abnormalities and their impact on disease progression or treatment response are of importance to improve the current knowledge in GSDs and for the development of new therapeutic avenues.

2. Reserve cells and skeletal muscle regeneration

2.1. Towards the development of cell therapies for muscle disorders: achievements and challenges.

Although satellite cells have capacity to efficiently regenerate skeletal muscle, they are present at low numbers and need expansion in order to be utilized for regenerative purposes [22]. However, satellite cells, also termed muscle stem cells (MuSCs), lose regenerative properties soon after culture *in vitro* [23,24], hence the necessity to develop methods to expand regenerative cells. The lack of suitable culture systems for expanding muscle regenerative cells – whether these are satellite cells or other myogenic cell types – is a long-standing limiting factor for the development of cell-based therapies for skeletal muscle [25,26].

To solve this problem, research strategies aim to maintain or restore regenerative properties in myogenic cells through a series of techniques *in vitro*, such as recapitulation of the muscle microenvironment by mimicking the properties of substrates [27–30], stimulating signalling between MuSCs and other cell types [31,32], and re-inducing regeneration via pharmacological treatment with small molecules [33,34]. Often, these methods require complex or lengthy culture procedures, which are suboptimal for the development of cell-based therapies.

Loss of stem cell properties upon *ex vivo* culture is also a challenge in other fields, such as for several types of hematopoietic cells [35], and for basal bronchial cells for cell therapy in cystic fibrosis [36]. In those fields, the efforts to find solutions for this challenge are similar to those for skeletal muscle: formulation of drug cocktails to enhance stem cell activity and recapitulation of the stem cell microenvironment [37–39].

2.2. Reserve cells: a source for cell-based therapies?

In chapter 6 we described a method to isolate murine reserve cell fractions with regenerative capacity. Myoblasts used for the generation of reserve cells could be expanded for more than 90 population doublings, allowing to obtain large numbers of regenerative cells. Generation of reserve cells was relatively simple and did not require expensive culture additives, making it a cost-effective technique for culturing muscle regenerative cells. In addition, cells could be frozen with maintenance of regenerative potential, which enabled these to be stored in large quantities. Freezing capacity for storage is necessary for cell sources to be used for

future cell-based therapies, as it allows to generate large batches of regenerative cells.

Are reserve cells safe for use in clinical trials?

An important challenge for the development of cell therapies is safety, which is especially relevant when cells are genetically modified. Previous studies in mice used knockdown of *Myod* and overexpression of IL-1RA in myoblasts in order to increase engraftment efficiency and survival after transplantation, respectively [40,41]. To consider these cells for therapy would require a thorough analysis of safety, mostly regarding the methods employed for genetic manipulation; i.e. evaluation of insertion sites, copy numbers, and potential development of variants in delicate genomic regions such as oncogenes or tumor suppressor genes. In contrast, generation of reserve cells did not require genetic manipulation or artificial expression of myogenic factors.

Reserve cells showed properties *in vitro* and *in vivo* that resembled those of adult muscle stem cells. In this regard, advantages of adult stem cells for application in therapy versus other cell types, such as embryonic stem cells (ESCs) or induced pluripotent stem cells (iPSCs), are reduced risk of tumorigenesis arising from undifferentiated cells, and a lower risk for the accumulation of genetic aberrations (e.g. induction of pluripotency in iPSCs increases the possibility for the acquisition of disease-associated variants) [42].

Although the application of adult stem cells for therapy poses a lower risk for the factors mentioned above compared to other stem cell types, there are still risks that need to be assessed. The acquisition of variants that lead to clonal expansion by proliferating stem cells, and their relationship with the development of malignancies has been widely documented [43,44]. For example, attention has been drawn to the accumulation of p53 mutations, which hamper the development of cell-based therapies [45,46]. For this reason, special attention to this matter is necessary when considering cell sources for therapy. The parental populations from which regenerative reserve cells were derived could be expanded for up to 90 population doublings, increasing the risk of acquisition of genomic aberrations. To reduce the impact of expansion-associated variant acquisition, limiting the expansion of regenerative cells to the minimum necessary numbers for therapy would be recommended. In addition, a genomic analysis would still be necessary to evaluate safety, for example to rule out adverse genetic variations or karyotype abnormalities. Further characterization should also evaluate abnormal

differentiation and transformation, since reserve cells have partial resemblance to satellite cells, which are known to have capacity to differentiate into non-muscle cells *in vitro* [47]. It is important to note that several cell types other than satellite cells and their derived progenitors have myogenic capacity, and that the studies that showed multipotent capacity of MuSCs are few and lacked lineage-tracing approaches, which leaves an open possibility for these results to be derived from the expansion of subsets of non-canonical myogenic cells.

2.3. Transplantation methods: autologous vs allogeneic

The capacity to obtain reserve cells from primary myogenic cultures and the relative simplicity of the isolation method would, in principle, make reserve cells suitable candidates for autologous transplantation. An important advantage of autologous transplantation over allogeneic transplantation is a lower immunogenicity, and therefore the ability to avoid immune suppression before transplantation. A number of clinical trials using myogenic cells for cell-based therapy have been performed in the past and in recent times using both autologous and allogeneic transplantation strategies. Autologous approaches reported none or very mild immune reactions [48,49], while allogeneic strategies required the use of immunosuppressants [50]. In combination with major histocompatibility complex (MHC) matching between donors and hosts, immune suppressive treatment limited immunogenicity issues in allogeneic transplantation strategies [51–56]. In addition, the establishment of human leukocyte antigens (HLA) haplotype banks to match hosts and donors could also contribute to diminish tissue incompatibilities for allogeneic transplantation. At the moment, this is widely used for hematopoietic stem cell transplantation and efforts are being made to establish banks for PSCs [57,58].

Reserve cells can be isolated from a patient's muscle biopsy and thus be suitable for autologous transplantation. Considering the low immunogenicity reported in autologous transplantations of myoblasts (the cells from which reserve cells are derived and to which they resemble the closest), a low immunogenic response could be expected. However, taking into consideration the importance of assessing the immune reaction for the success of a cell-based therapy, future experiments should determine the degree of immunogenicity upon transplantation of reserve cells. Autologous strategies for muscle diseases would require gene correction, which would increase the risk of adverse genetic events. The alternative, an allogeneic source, would increase the risk of an unfavourable

immune response. Although not without risk, considering the rapidly progressing array of techniques for a safer genetic manipulation, autologous transplantation of gene corrected cells seems, *a priori*, the most feasible strategy for a future reserve cell-based therapy for muscle disorders.

2.4. Reserve cells towards therapy: translation to human

In this thesis we showed that this reserve cell murine model allows to study the full regenerative process, including regeneration and stem cell engraftment. In addition, this method can be compared with the regeneration dynamics of endogenous muscle stem cells, providing a valuable tool to study muscle stem cells *in vitro*. Human reserve cells have been reported previously, which supports the possibility of a future reserve cell-based therapy for muscle disorders. However, proof-of-concept studies in human are still necessary before considering reserve cells for therapy. To date, murine reserve cells have mostly been characterized *in vitro*, while only one study besides our own work analyzed reserve cells' *in vivo* regenerative potential [59]. The situation is more limited for human reserve cells, where two studies reported the existence of reserve cells in human cultures and another analyzed their *in vitro* and *in vivo* properties [60–62]. Laumonier *et al.* used primary human myoblasts to isolate human myogenic reserve cells [62]. Although the study showed that human reserve cells had regenerative capacity *in vivo*, it did not show stem cell engraftment and regeneration. It would be interesting to determine whether reserve cell fractions with distinct myogenic properties can also be obtained from human cultures, and whether they possess both direct regeneration and stem cell engraftment properties, similarly as murine reserve cells. Previous work in our laboratory generated reserve cells from human iPSC-derived myogenic progenitors (data not shown). However, transplantation of the fast-adhering fraction showed limited capacity to efficiently regenerate muscle when transplanted in pre-injured mouse hosts; while the slow adhering fraction was not transplanted. It is unknown whether iPSC-derived myogenic reserve cells hold sufficient regenerative potential to be considered candidates for therapy. However, cell cycle differences between transplanted human cells and the endogenous satellite cells of the mouse hosts (and the impact that this could have in the regenerative process) make the comparison of engraftment and regeneration upon transplantation in mice very difficult.

2.5 What are the possibilities for the delivery of myogenic cells for regenerative purposes? Local vs systemic delivery

Cell-based therapy trials using myoblasts failed, among other reasons, due to myoblasts' poor migration capabilities. Although satellite cells have a higher regenerative capacity compared to myoblasts, they still have a poor migration potential (for a review, see [26]). Both myoblasts and satellite cells need to be administered locally (intramuscular injection) for efficient regeneration. This limits their clinical efficacy to a relatively reduced region surrounding the area of administration. In practice this means cells need to be injected in every muscle that is affected for a given disease, which is particularly difficult for disorders that affect a large number of muscles or for those diseases that affect delicate muscles, like the diaphragm. Interestingly, alternative cell types with myogenic potential, such as mesoangioblasts and muscle side population cells (SPs), showed capacity to be systemically administered through the blood stream, engraft, and regenerate skeletal muscle [63,64], although this issue remains controversial. Such capacity would eliminate the need to perform multiple intramuscular injections, and would facilitate administration of a future cell therapy, similarly as hematopoietic stem cell transplantations are currently performed. Capacity to permeate blood vessels has not been reported in myoblasts or satellite cells. Since reserve cells are derived from myoblasts and all studies involving transplantation of reserve cells relied on intramuscular delivery, it seems unlikely they would be suitable for systemic delivery.

2.6. Are there other options? Alternative cell types for skeletal muscle regeneration

Although currently the main focus for regenerative approaches for skeletal muscle is attributed to satellite cells, other cells have demonstrated myogenic capacities that resemble those of muscle stem cells [25]. iPSCs are promising candidates for cell-based therapies for a broad range of disorders, among them, skeletal muscle disorders [65]. To date, besides preliminary work performed in our lab (discussed above) there are no studies reporting the use of iPSC-derived myogenic reserve cells. One of the main advantages of iPSCs is their capacity to be expanded virtually unlimitedly. If cells with sufficient regenerative potential, such as reserve cells, would be generated from iPSC-derived myogenic cells, the current limitation to expand regenerative myogenic cells could be solved. Challenges regarding

tumorigenicity and heterogeneity, discussed above, would need, however, to be addressed before consideration for therapy.

Other cell types with capacity to differentiate into several lineages demonstrated potential application for muscle regeneration. *In vivo*, murine muscle SPs were proven capable of permeating the blood vessels, regenerating skeletal muscle, and give rise to MuSCs [66,67]. However, SPs have not been characterized in humans. In addition, doubts regarding their myogenic potential (SPs only formed myotubes when co-cultured with myoblasts *in vitro*) and a limited capacity to regenerate skeletal muscle *in vivo* hampered further studies and applications of muscle SPs [66]. Mesoangioblasts were proven promising in mice and are characterized in human. Intra-arterial transplantation studies using mesoangioblasts reported capacity to regenerate skeletal muscle and populate the stem cell niche, although clinical trials using these cells were largely negative [63,64,68]. Although reserve cells are unlikely to permeate blood vessels, they solely differentiate into skeletal muscle, and have high regenerative capacity. Therefore, reserve cells have a higher *in vivo* resemblance to satellite cells/myoblasts, than to alternative multipotent stem cells with myogenic capacity.

2.7. The long road to therapy: clinical trials

Successful development of a cell-based therapy for skeletal muscle ultimately aims to ensure improvement of muscle function, which has proven a challenge in the past. Although MuSCs are considered the ideal cells for therapy regarding their regenerative properties and functional improvement in mice, the impossibility to expand regenerative MuSCs has prevented their application in clinical trials to date [23,69]. Studies with myoblasts (myoblast transfer therapy studies) showed a limited degree of efficacy in terms of regeneration (dystrophin production); however, no functional improvement was achieved, and these trials were eventually discontinued [49,50,52–56,70]. Reserve cells seem promising in terms of regenerative capacity in mice; however, their effect on muscle function was not evaluated in our study. It is therefore essential to assess whether reserve cells have capacity to improve muscle function before determining if they would be eligible for trials.

Other cell types have been proposed as candidates for therapy and utilized in phase I/II trials. The use of mesoangioblasts in clinical trials for DMD turned unsuccessful due to risks associated to multipotency and the low production of

dystrophin in regenerated fibers [68,71]. Considering their increased regenerative properties, and despite the necessity to be administered locally, it seems more likely that an expandable, canonical myogenic cell type, like satellite cells, would become more suitable candidate for therapy in the future.

2.8. What type of cells are reserve cells? Similarities and differences with satellite cells

Reserve cells efficiently contributed to muscle regeneration both directly after transplantation and in a stem cell-like manner, as shown through re-injury experiments. These two properties resemble the capacities that satellite cells have *in vivo*. Reserve cells, however, share other similarities with MuSCs.

Recent studies showed that MuSCs are a heterogeneous myogenic stem cell population with different properties *in vitro*, such as differential expression of transcription factors, surface markers, or metabolic activity, as well as *in vivo* for their differential capacity to regenerate upon transplantation (for a comprehensive review, see [72]). Stem cell heterogeneity is a common feature for other cell types too, such as hematopoietic, gut, and neural stem cells [73,74]. In a similar manner, the findings reported in chapter 6 suggest certain degree of heterogeneity in the reserve cell population. We described two populations (fast- and slow-adhering cells) that had heterogeneous properties and distinct transcriptional profiles *in vitro* and markedly distinct regenerative activity *in vivo*. The importance of heterogeneity in myogenic cells is given by the need of: 1) cells with capacity to differentiate directly into muscle; 2) cells that repopulate the stem cell niche through self-renewal to ensure regeneration after successive rounds of injury. These two factors are essential to ensure restoration of muscle homeostasis after injury.

Clonal analyses in MuSCs revealed variability in gene expression, time to first division, and rate of division [29,75,76]. More recent studies supported these findings and showed MuSC heterogeneity through single-cell RNA sequencing (scRNA-seq) [77,78]. Similarly, we observed differences in the proliferative capacities between reserve cell fractions, with a delayed start of proliferation in SRCs Cycle 3 after isolation compared to PAR or FRCs Cycle 1. This delay in proliferation was promptly equalized after 1-2 passages (data not shown). This was likely caused by differences in cell density at plating (data not shown). It is widely accepted that myogenic cells with slow proliferation capacity better resemble muscle stem cells,

since they lie in a quiescent state in their niche, under the basal lamina [79,80]. Although we did not explore this in depth, a higher percentage of PAX7-expressing reserve cells and the lower expression of cyclin genes by SRCs Cycle 3 would be in line with a more “stem cell-like” state that could be related with the differences in proliferation between reserve cell fractions. Furthermore, reduced cell adhesion of myogenic cells, such as those of SRCs Cycle 3, has been previously linked with increased stem cell properties [41,81,82], which also correlates with increased stem cell engraftment observed in this fraction.

Functional repopulation assays also showed differential self-renewal capacity *in vivo* by MuSCs subpopulations after several rounds of regeneration, as well as distinct regeneration efficiency depending on the subpopulation of MuSCs employed [83]. Differences between these MuSCs populations were PAX7 expression levels, metabolic activity, and asymmetric DNA segregation. We also observed distinct expression of myogenic factors between reserve cell fractions, among them, PAX7. It is unknown if asymmetric divisions occurred in reserve cells, but this could also be linked to the formation of different reserve cell fractions as well as to their functional differences. Exploring these mechanisms and establishing similarities with MuSCs could provide hints regarding the patterns that regulate establishment of reserve cell fractions. Overall, identifying heterogeneous populations of regenerative cells and understanding the factors that drive heterogeneity are important for the general understanding of the muscle regeneration and the development of cell-based therapies for skeletal muscle.

2.9. Have reserve cells been isolated before? Are all reserve cells the same?

The most distinctive characteristic of the reserve cell isolation protocol described here is the combination of subsequent cycles of reserve cell isolation and selection of fractions based on adhesion properties. By utilizing this method, we obtained reserve cell populations with markedly distinct *in vitro* and *in vivo* properties. However, reserve cells had been characterized *in vitro* and isolation methods had been described in the past. Previous isolation protocols relied on separating the non-differentiated fraction of mononuclear cells from differentiated myotubes, similarly to the method we described. However, there were other differences between protocols that could have an impact on the yield and properties of reserve cells, mainly regarding the time of differentiation and the method to separate the

undifferentiated fraction of cells from myotubes. Previous reserve cell isolation methods were based on differentiation of cells ranging from 3 days to 7 days, although the latter was used to isolate human reserve cells [61,84]. In our protocol, murine myoblasts were differentiated for 5 days. Since reserve cells seem to acquire their fate during differentiation, the time that they are kept in differentiation conditions appears critical for the establishment of regenerative properties. In fact, preliminary experiments in our group showed that the potential of reserve cells to regenerate skeletal muscle was not achieved after 2 days of differentiation, and that 4-5 days were optimal (data not shown). There was also variability between different methods to separate reserve cells from differentiated cells. Kitzmann et al. used a short trypsinization step to detach myotubes and to leave reserve cells attached in the plate [84]. Yoshida et al. trypsinized all cells (differentiated and non-differentiated) and plated them in a new dish for 30 minutes [85]. After this time, floating myotubes were removed. Baroffio et al. used a decantation procedure by which myotubes would deposit on the bottom of a tube, while reserve cells remained floating [61]. Other isolation methods, including more recent ones, were based on modifications of the protocol described by Kitzmann et al. [86,87]. In the method described in this thesis, all reserve cells were trypsinized and re-plated in new culture dishes, which allowed to separate reserve cell fractions based on their adhesion properties. Moreover, cell suspensions were first filtered through a strain to eliminate large myotubes and the filtered solution was then disaggregated using a 21G needle and a syringe. Although we did not compare the efficacy between methods to obtain reserve cells, the isolation protocol described by us included two sequential filtering steps, *a priori* reducing the possibility to include myotubes when compared with decantation or short trypsinization protocols. In addition, reserve cells were always passaged twice in proliferative conditions before transplantation. This was done in order to ensure re-entry in the cell cycle and to enrich for proliferative cells at the cost of residual post-mitotic cells that may permeate the isolation protocol.

In chapter 6, we further explored the existence of heterogeneity within the reserve cell populations by separating and analyzing these in fast- and slow-adhering populations. Our method explored, for first time, the fractionation of the reserve cell population into several subpopulations. In addition, we adapted the concept of performing “cycles” of isolation in order to obtain populations of reserve cells with different *in vitro* and *in vivo* properties. A similar concept, termed subculturing was used by Baroffio et al. to characterize the cytoskeletal

protein α -SR actin and analyze the proliferative capacity of human reserve cells [61]. Interestingly, in that study reserve cells progressively lost proliferation capacity and eventually stopped proliferating after 4 steps of subculturing, which was not the case in our study. The human origin of reserve cells in that study together with the differential culture conditions are possibly attributable for the differences in proliferative potential compared to our study.

2.10. What molecular mechanisms are involved in reserve cell-mediated engraftment?

Although significant progress has been done in the past, there are still many questions regarding the mechanisms involved in muscle regeneration. Current research efforts aim to find molecular and biological processes to stimulate and enhance regeneration. Of particular relevance is the research being performed in salamanders, given the capacity that several species of this organism have to regenerate whole complex body parts, such as limbs [88]. However, its translation to mammals still poses a large obstacle for a hypothetical application for regenerative purposes. Studies performed in skeletal muscle of mammals highlighted the relevance of IGF1-Akt, TGF β , Wnt, and p38 MAPK as some of the most relevant pathways for myogenesis [89–91]. The transcriptional profile of reserve cells allowed us to hypothesize about mechanisms involved in engraftment. Gene ontology analysis revealed enrichment in the transcripts of IGF-binding proteins in SRCs Cycle 3. IGF-binding proteins are known activators of the IGF1-Akt pathway, whose stimulation promotes muscle regeneration, and that have shown evidence to improve dystrophic muscle function upon administration [92–94]. Similarly, SRCs Cycle 3 (the fraction that showed highest stem cell engraftment) showed reduced transcription of phosphodiesterase genes. This was in line with previous findings that showed that pharmacological inhibition of phosphodiesterases resulted in increased satellite cell engraftment and more efficient regeneration [95,96]. These pathways can be targeted through the use of small molecules, which could open interesting avenues regarding the stimulation of muscle regeneration using druggable targets, which has been explored before (for a review, see [97]). This highlights the relevance of discovering new molecular processes involved in skeletal muscle regeneration, and the capacity to modulate these. However, these results are correlative, and functional assessment of candidate pathways in reserve cells is necessary in order to determine the degree of involvement in re-induction

of regenerative properties in cultured muscle cells. This is important, since there are a number of differentially expressed pathways and cellular processes between reserve cell fractions, and there is a possibility that not one but instead a combination of pathways is responsible for the differences in engraftment and regeneration observed in reserve cells.

Conclusion

The work in this thesis provided new insight on the dysregulation of glycogen metabolism in Pompe disease, and suggested that glycogen biosynthesis is sensitive to treatment with ERT in Pompe disease patients. Altogether, our results shed more light on the pathology of Pompe disease, and bring new questions regarding the possibility of glycogen metabolism to be used as a marker for disease progression and response to treatment, or represent a potential target for improved future therapy.

Cell therapy for skeletal muscle represents a promising therapy to treat neuromuscular disorders. Nevertheless, there are still important challenges that need to be overcome. One of them is expansion of regenerative cells. Through the generation of reserve cells and the work described in this thesis, we have shown that reserve cells meet requirements necessary to obtain a suitable candidate for cell therapy. However, further research is necessary in order to determine whether reserve cells could be utilized in the future for such purpose. In addition, reserve cells represent an interesting tool to study the molecular signature of engraftment.

References

1. Bergsma, A.J., in 't Groen, S.L.M., van den Dorpel, J.J.A., van den Hout, H.J.M.P., van der Beek, N.A.M.E., Schoser, B., Toscano, A., Musumeci, O., Bembi, B., Dardis, A., *et al.* (2019). A genetic modifier of symptom onset in Pompe disease. *EBioMedicine* 43, 553–561.
2. Peeks, F., Steunenberg, T.A.H., Boer, F. de, Rubio-Gozalbo, M.E., Williams, M., Burghard, R., Rajas, F., Oosterveer, M.H., Weinstein, D.A., and Derks, T.G.J. (2017). Clinical and biochemical heterogeneity between patients with glycogen storage disease type IA: the added value of CUSUM for metabolic control. *J. Inherit. Metab. Dis.* 40, 695–702. Available at: <https://onlinelibrary.wiley.com/doi/full/10.1007/s10545-017-0039-1> [Accessed November 2, 2021].
3. Rutten, M.G.S., Derks, T.G.J., Huijkman, N.C.A., Bos, T., Kloosterhuis, N.J., Kolk, K.C.W.A. van de, Wolters, J.C., Koster, M.H., Bongiovanni, L., Thomas, R.E., *et al.* (2021). Modeling Phenotypic Heterogeneity of Glycogen Storage Disease Type 1a Liver Disease in Mice by Somatic CRISPR/CRISPR-associated protein 9–Mediated Gene Editing. *Hepatology* 74, 2491–2507. Available at: <https://onlinelibrary.wiley.com/doi/full/10.1002/hep.32022> [Accessed November 1, 2021].
4. Taylor, K.M., Meyers, E., Phipps, M., Kishnani, P.S., Cheng, S.H., Scheule, R.K., and Moreland, R.J. (2013). Dysregulation of multiple facets of glycogen metabolism in a murine model of Pompe disease. *PLoS One* 8, e56181. Available at: <http://www.ncbi.nlm.nih.gov/pubmed/23457523> [Accessed October 14, 2016].
5. Napolitano, F., Bruno, G., Terracciano, C., Franzese, G., Palomba, N.P., Scotto Di Carlo, F., Signoriello, E., De Blasiis, P., Navarro, S., Gialluisi, A., *et al.* (2021). Rare variants in autophagy and non-autophagy genes in late-onset pompe disease: Suggestions of their disease-modifying role in two Italian families. *Int. J. Mol. Sci.* 22, 3625. Available at: <https://doi.org/10.3390/ijms22073625> [Accessed May 18, 2021].
6. Douillard-Guilloux, G., Raben, N., Takikita, S., Ferry, A., Vignaud, A., Guillet-Deniau, I., Favier, M., Thurberg, B.L., Roach, P.J., Caillaud, C., *et al.* (2009). Restoration of muscle functionality by genetic suppression of glycogen synthesis in a murine model of Pompe disease. *Hum. Mol. Genet.* 19, 684–696. Available at: <https://academic.oup.com/hmg/article/19/4/684/609722> [Accessed September 4, 2020].
7. Meena, N.K., Ralston, E., Raben, N., and Puertollano, R. (2020). Enzyme Replacement Therapy Can Reverse Pathogenic Cascade in Pompe Disease. *Mol. Ther. - Methods Clin. Dev.* 18, 199–214. Available at: <https://doi.org/10.1016/j.omtm.2020.05.026>. [Accessed December 2, 2020].
8. van der Ploeg, A., Carlier, P.G., Carlier, R.-Y., Kissel, J.T., Schoser, B., Wenninger, S., Pestronk, A., Barohn, R.J., Dimachkie, M.M., Goker-Alpan, O., *et al.* (2016). Prospective exploratory muscle biopsy, imaging, and functional assessment in patients with late-onset Pompe disease treated with alglucosidase alfa: The EMBASSY Study. *Mol. Genet. Metab.* Available at: <http://www.ncbi.nlm.nih.gov/pubmed/27473031> [Accessed September 13, 2016].
9. Orth, M., and Mundegar, R.R. (2003). Effect of acid maltase deficiency on the endosomal/lysosomal system and glucose transporter 4. *Neuromuscul. Disord.* 13, 49–54. Available at: <http://www.nmd-journal.com/article/S0960896602001864/fulltext> [Accessed September 4, 2020].
10. Testoni, G., Duran, J., García-Rocha, M., Vilaplana, F., Serrano, A.L., Sebastián, D., López-Soldado, I., Sullivan, M.A., Slebe, F., Vilaseca, M., *et al.* (2017). Lack of Glycogenin Causes Glycogen Accumulation and Muscle Function Impairment. *Cell Metab.* 26, 256–266.e4. Available at: <http://www.ncbi.nlm.nih.gov/pubmed/28683291> [Accessed November 28, 2017].

11. Pederson, B.A., Chen, H., Schroeder, J.M., Shou, W., DePaoli-Roach, A.A., and Roach, P.J. (2004). Abnormal Cardiac Development in the Absence of Heart Glycogen. *Mol. Cell. Biol.* 24, 7179–7187. Available at: <http://mcb.asm.org/> [Accessed November 16, 2020].
12. Kollberg, G., Tulinius, M., Gilljam, T., Östman-Smith, I., Forsander, G., Jotorp, P., Oldfors, A., and Holme, E. (2007). Cardiomyopathy and Exercise Intolerance in Muscle Glycogen Storage Disease O. *N. Engl. J. Med.* 357, 1507–1514. Available at: www.nejm.org [Accessed December 9, 2020].
13. Huang, N., and Perl, A. (2018). Metabolism as a Target for Modulation in Autoimmune Diseases. *Trends Immunol.* 39, 562–576. Available at: <http://www.cell.com/article/S1471490618300838/fulltext> [Accessed August 31, 2021].
14. Kanungo, S., Wells, K., Tribett, T., and El-Gharbawy, A. (2018). Glycogen metabolism and glycogen storage disorders. *Ann. Transl. Med.* 6, 474–474. Available at: <https://pubmed.ncbi.nlm.nih.gov/30740405/> [Accessed November 2, 2021].
15. Reichelt, M.E., Mellor, K.M., Curl, C.L., Stapleton, D., and Delbridge, L.M.D. (2013). Myocardial glycophagy - A specific glycogen handling response to metabolic stress is accentuated in the female heart. *J. Mol. Cell. Cardiol.* 65, 67–75.
16. Nogales-Gadea, G., Consuegra-García, I., Rubio, J.C., Arenas, J., Cuadros, M., Camara, Y., Torres-Torronteras, J., Fiuza-Luces, C., Lucia, A., Martín, M.A., *et al.* (2012). A transcriptomic approach to search for novel phenotypic regulators in McArdle disease. *PLoS One* 7, 31718. Available at: www.hgvs.org/mutnomen [Accessed May 19, 2021].
17. Stemmerik, M.G., Madsen, K.L., Laforêt, P., Buch, A.E., and Vissing, J. (2017). Muscle glycogen synthesis and breakdown are both impaired in glycogenin-1 deficiency. *Neurology* 89, 2491–2494. Available at: <https://n.neurology.org/content/89/24/2491> [Accessed December 9, 2020].
18. Farah, B.L., Landau, D.J., Sinha, R.A., Brooks, E.D., Wu, Y., Fung, S.Y.S., Tanaka, T., Hirayama, M., Bay, B.H., Koeberl, D.D., *et al.* (2016). Induction of autophagy improves hepatic lipid metabolism in glucose-6-phosphatase deficiency. *J. Hepatol.* 64, 370–379. Available at: <http://www.journal-of-hepatology.eu/article/S0168827815006790/fulltext> [Accessed November 12, 2021].
19. Yiu, W.H., Mead, P.A., Jun, H.S., Mansfield, B.C., and Chou, J.Y. (2010). Oxidative stress mediates nephropathy in type Ia glycogen storage disease. *Lab. Investig.* 2010 904 90, 620–629. Available at: <https://www.nature.com/articles/labinvest201038> [Accessed November 2, 2021].
20. Tarallo, A., Damiano, C., Strollo, S., Minopoli, N., Indrieri, A., Polishchuk, E., Zappa, F., Nusco, E., Fecarotta, S., Porto, C., *et al.* (2021). Correction of oxidative stress enhances enzyme replacement therapy in Pompe disease. *EMBO Mol. Med.* 13, e14434. Available at: <https://onlinelibrary.wiley.com/doi/full/10.15252/emmm.202114434> [Accessed November 9, 2021].
21. Hannibal, L., Theimer, J., Wingert, V., Klotz, K., Bierschenk, I., Nitschke, R., Spiekerkoetter, U., and Grünert, S.C. (2020). Metabolic Profiling in Human Fibroblasts Enables Subtype Clustering in Glycogen Storage Disease. *Front. Endocrinol. (Lausanne)*. 11. Available at: <https://pubmed.ncbi.nlm.nih.gov/33329388/> [Accessed November 13, 2021].
22. Skuk, D., and Tremblay, J.P. (2017). Cell Therapy in Myology: Dynamics of Muscle Precursor Cell Death after Intramuscular Administration in Non-human Primates. *Mol. Ther. - Methods Clin. Dev.* 5, 232–240. Available at: <http://dx.doi.org/10.1016/j.omtm.2017.05.002>. [Accessed April 23, 2021].

23. Sacco, A., Doyonnas, R., Kraft, P., Vitorovic, S., and Blau, H.M. (2008). Self-renewal and expansion of single transplanted muscle stem cells. *Nature* 456, 502–506.
24. Montarras, D., Morgan, J., Collins, C., Relaix, F., Zaffran, S., Cumano, A., Partridge, T., and Buckingham, M. (2005). Direct isolation of satellite cells for skeletal muscle regeneration. *Science* 309, 2064–7. Available at: <http://www.ncbi.nlm.nih.gov/pubmed/16141372> [Accessed August 12, 2015].
25. Negroni, E., Gidaro, T., Bigot, A., Butler-Browne, G.S., Mouly, V., and Trollet, C. (2015). Invited review: Stem cells and muscle diseases: advances in cell therapy strategies. *Neuropathol. Appl. Neurobiol.* 41, 270–87. Available at: <http://www.ncbi.nlm.nih.gov/pubmed/25405809> [Accessed July 9, 2016].
26. Schaaf, G.J. (2012). Ex-vivo Expansion of Muscle-Regenerative Cells for the Treatment of Muscle Disorders. *J. Stem Cell Res. Ther.* 01. Available at: http://www.researchgate.net/publication/270011806_Ex-vivo_Expansion_of_Muscle-Regenerative_Cells_for_the_Treatment_of_Muscle_Disorders [Accessed November 12, 2015].
27. Rayagiri, S.S., Ranaldi, D., Raven, A., Mohamad Azhar, N.I.F., Lefebvre, O., Zammit, P.S., and Borycki, A.-G. (2018). Basal lamina remodeling at the skeletal muscle stem cell niche mediates stem cell self-renewal. *Nat. Commun.* 9, 1075. Available at: <http://www.nature.com/articles/s41467-018-03425-3> [Accessed April 4, 2018].
28. Ishii, K., Sakurai, H., Suzuki, N., Mabuchi, Y., Sekiya, I., Sekiguchi, K., and Akazawa, C. (2018). Recapitulation of Extracellular LAMININ Environment Maintains Stemness of Satellite Cells In Vitro. *Stem Cell Reports*. Available at: <http://www.sciencedirect.com/science/article/pii/S2213671117305611?via%3Dihub> [Accessed January 23, 2018].
29. Gilbert, P.M., Havenstrite, K.L., Magnusson, K.E.G., Sacco, a, Leonardi, N. a, Kraft, P., Nguyen, N.K., Thrun, S., Lutolf, M.P., and Blau, H.M. (2010). Substrate elasticity regulates skeletal muscle stem cell self-renewal in culture. *Science* 329, 1078–1081.
30. Quarta, M., Brett, J.O., DiMarco, R., De Morree, A., Boutet, S.C., Chacon, R., Gibbons, M.C., Garcia, V.A., Su, J., Shrager, J.B., et al. (2016). An artificial niche preserves the quiescence of muscle stem cells and enhances their therapeutic efficacy. *Nat. Biotechnol.* 34, 752–759.
31. Bencze, M., Negroni, E., Vallese, D., Yacoubyousssef, H., Chaouch, S., Wolff, A., Aamiri, A., Di Santo, J.P., Chazaud, B., Butler-Browne, G., et al. (2012). Proinflammatory macrophages enhance the regenerative capacity of human myoblasts by modifying their kinetics of proliferation and differentiation. *Mol. Ther.* 20, 2168–2179.
32. Mozzetta, C., Consalvi, S., Saccone, V., Tierney, M., Diamantini, A., Mitchell, K.J., Marazzi, G., Borsellino, G., Battistini, L., Sassoon, D., et al. (2013). Fibroadipogenic progenitors mediate the ability of HDAC inhibitors to promote regeneration in dystrophic muscles of young, but not old Mdx mice. *EMBO Mol. Med.* 5, 626–639. Available at: <https://onlinelibrary.wiley.com/doi/10.1002/emmm.201202096> [Accessed April 20, 2021].
33. Charville, G.W., Cheung, T.H., Yoo, B., Santos, P.J., Lee, G.K., Shrager, J.B., and Rando, T.A. (2015). Ex Vivo Expansion and In Vivo Self-Renewal of Human Muscle Stem Cells. *Stem cell reports*. Available at: <http://www.sciencedirect.com/science/article/pii/S2213671115002386> [Accessed September 9, 2015].
34. Cosgrove, B.D., Gilbert, P.M., Porpiglia, E., Mourkioti, F., Lee, S.P., Corbel, S.Y., Llewellyn, M.E., Delp, S.L., and Blau, H.M. (2014). Rejuvenation of the muscle stem cell population restores strength to injured aged muscles. *Nat. Med.* 20, 255–64. Available at: <http://www.ncbi.nlm.nih.gov/pubmed/24531378>.

35. Wilkinson, A.C., Ishida, R., Kikuchi, M., Sudo, K., Morita, M., Crisostomo, R.V., Yamamoto, R., Loh, K.M., Nakamura, Y., Watanabe, M., *et al.* (2019). Long-term ex vivo haematopoietic-stem-cell expansion allows nonconditioned transplantation. *Nature* 571, 117–121.
36. Allan, K.M., Farrow, N., Donnelley, M., Jaffe, A., and Waters, S.A. (2021). Treatment of Cystic Fibrosis: From Gene- to Cell-Based Therapies. *Front. Pharmacol.* 12. Available at: [/pmc/articles/PMC8007963/](#) [Accessed May 4, 2021].
37. Awatade, N.T., Wong, S.L., Hewson, C.K., Fawcett, L.K., Kicic, A., Jaffe, A., and Waters, S.A. (2018). Human Primary Epithelial Cell Models: Promising Tools in the Era of Cystic Fibrosis Personalized Medicine. *Front. Pharmacol.* 9, 1429. Available at: [www.frontiersin.org](#) [Accessed May 19, 2021].
38. Walasek, M.A., van Os, R., and de Haan, G. (2012). Hematopoietic stem cell expansion: Challenges and opportunities. *Ann. N. Y. Acad. Sci.* 1266, 138–150. Available at: [https://nyaspubs.onlinelibrary.wiley.com/doi/full/10.1111/j.1749-6632.2012.06549.x](#) [Accessed May 4, 2021].
39. Chafouri-Fard, S., Niazi, V., Taheri, M., and Basiri, A. (2021). Effect of Small Molecule on ex vivo Expansion of Cord Blood Hematopoietic Stem Cells: A Concise Review. *Front. Cell Dev. Biol.* 9, 875. Available at: [www.frontiersin.org](#) [Accessed May 4, 2021].
40. Asakura, A., Hirai, H., Kablar, B., Morita, S., Ishibashi, J., Piras, B.A., Christ, A.J., Verma, M., Vineretsky, K.A., and Rudnicki, M.A. (2007). Increased survival of muscle stem cells lacking the MyoD gene after transplantation into regenerating skeletal muscle. *Proc. Natl. Acad. Sci.* 104, 16552–16557. Available at: [https://www.pnas.org/content/104/42/16552.long](#) [Accessed January 14, 2019].
41. Qu, Z., Balkir, L., van Deutekom, J.C., Robbins, P.D., Pruchnic, R., and Huard, J. (1998). Development of approaches to improve cell survival in myoblast transfer therapy. *J. Cell Biol.* 142, 1257–67. Available at: [http://www.pubmedcentral.nih.gov/articlerender.fcgi?artid=2149359&tool=pmcentrez&rendertype=abstract](#) [Accessed February 9, 2016].
42. Yamanaka, S. (2020). Pluripotent Stem Cell-Based Cell Therapy—Promise and Challenges. *Cell Stem Cell* 27, 523–531. Available at: [http://www.cell.com/article/S1934590920304604/fulltext](#) [Accessed July 16, 2021].
43. Martincorena, I., and Campbell, P.J. (2015). Somatic mutation in cancer and normal cells. *Science* (80-.). 349, 1483–1489. Available at: [https://science.sciencemag.org/content/349/6255/1483](#) [Accessed July 16, 2021].
44. Bonin, M. von, Jambor, H.K., Teipel, R., Stölzel, F., Thiede, C., Damm, F., Kroschinsky, F., Schetelig, J., Chavakis, T., and Bornhäuser, M. (2021). Clonal hematopoiesis and its emerging effects on cellular therapies. *Leukemia*, 1. Available at: [/pmc/articles/PMC8249428/](#) [Accessed July 19, 2021].
45. Baumann, K. (2017). Stem cells: Stem cell-based therapies threatened by the accumulation of p53 mutations. *Nat. Rev. Mol. Cell Biol.* 2017 187.
46. Merkle, F.T., Ghosh, S., Kamitaki, N., Mitchell, J., Avior, Y., Mello, C., Kashin, S., Mekhoubad, S., Ilic, D., Charlton, M., *et al.* (2017). Human pluripotent stem cells recurrently acquire and expand dominant negative P53 mutations. *Nat.* 2017 5457653 545, 229–233. Available at: [https://www.nature.com/articles/nature22312](#) [Accessed July 16, 2021].
47. Yang, J., Liu, H., Wang, K., Li, L., Yuan, H., Liu, X., Liu, Y., and Guan, W. (2017). Isolation, culture and biological characteristics of multipotent porcine skeletal muscle satellite cells. *Cell Tissue Bank.* 2017 184 18, 513–525. Available at: [https://link.springer.com/article/10.1007/s10561-017-9614-9](#) [Accessed July 16, 2021].

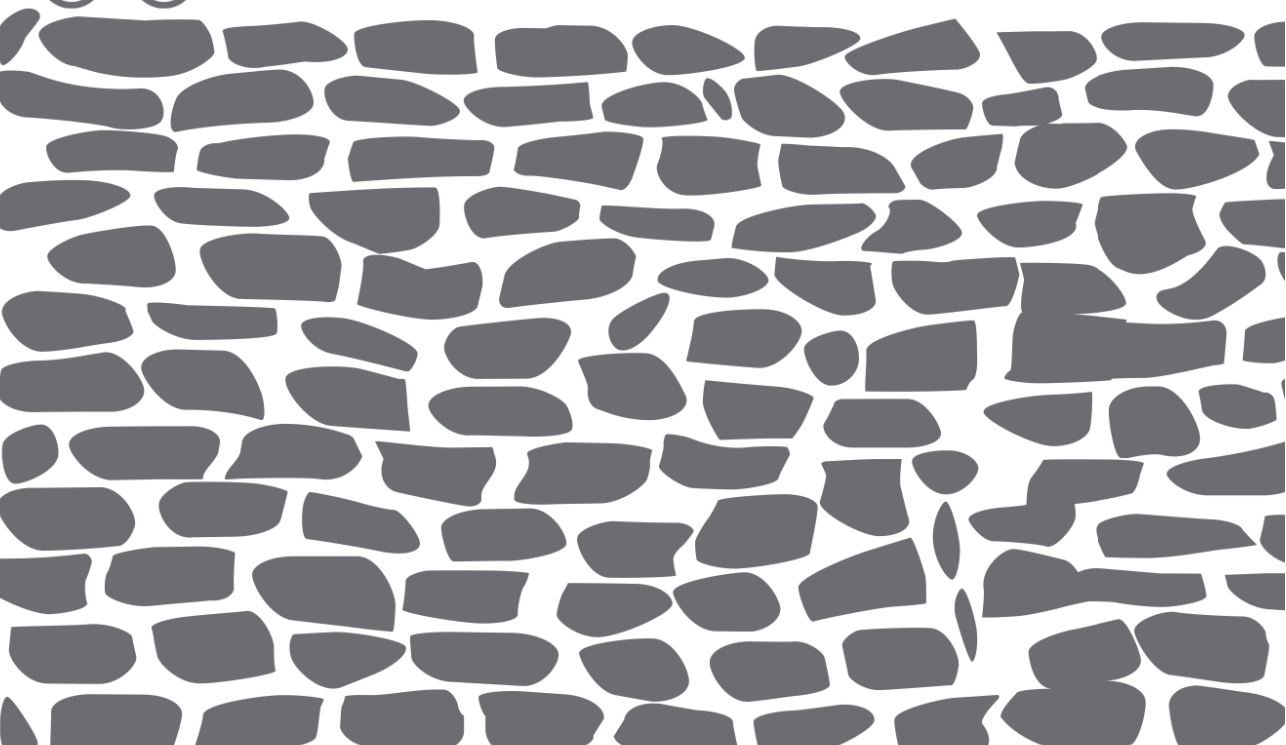
48. Périé, S., Trollet, C., Mouly, V., Vanneaux, V., Mamchaoui, K., Bouazza, B., Marolleau, J.P., Laforêt, P., Chapon, F., Eymard, B., et al. (2014). Autologous myoblast transplantation for oculopharyngeal muscular dystrophy: a phase I/IIa clinical study. *Mol. Ther.* 22, 219–25. Available at: <http://www.ncbi.nlm.nih.gov/pubmed/23831596> [Accessed November 16, 2016].
49. Tremblay, J.P., Bouchard, J.P., Malouin, F., Théau, D., Cottrell, F., Collin, H., Rouche, A., Gilgenkrantz, S., Abbadì, N., and Tremblay, M. (1993). Myoblast transplantation between monozygotic twin girl carriers of Duchenne muscular dystrophy. *Neuromuscul. Disord.* 3, 583–92. Available at: <http://www.ncbi.nlm.nih.gov/pubmed/8186717> [Accessed June 25, 2016].
50. Tremblay, J.P., Malouin, F., Roy, R., Huard, J., Bouchard, J.P., Satoh, A., and Richards, C.L. (1993). Results of a triple blind clinical study of myoblast transplantations without immunosuppressive treatment in young boys with Duchenne muscular dystrophy. *Cell Transplant.* 2, 99–112. Available at: <http://www.ncbi.nlm.nih.gov/pubmed/8143083> [Accessed June 25, 2016].
51. Tremblay, J., Skuk, D., Palmieri, and Rothstein (2009). A case for immunosuppression for myoblast transplantation in duchenne muscular dystrophy. *Mol. Ther.* 17, 1122–1124. Available at: <https://www.ncbi.nlm.nih.gov/pmc/articles/PMC19564866/?tool=EBI> [Accessed July 19, 2021].
52. Law, P.K., Bertorini, T.E., Goodwin, T.G., Chen, M., Fang, Q.W., Li, H.J., Kirby, D.S., Florendo, J.A., Herrod, H.G., and Golden, G.S. (1990). Dystrophin production induced by myoblast transfer therapy in Duchenne muscular dystrophy. *Lancet (London, England)* 336, 114–5. Available at: <http://www.ncbi.nlm.nih.gov/pubmed/1697393> [Accessed June 25, 2016].
53. Huard, J., Bouchard, J.P., Roy, R., Malouin, F., Dansereau, G., Labrecque, C., Albert, N., Richards, C.L., Lemieux, B., and Tremblay, J.P. (1992). Human myoblast transplantation: preliminary results of 4 cases. *Muscle Nerve* 15, 550–60. Available at: <http://www.ncbi.nlm.nih.gov/pubmed/1584246> [Accessed June 25, 2016].
54. Miller, R.G., Sharma, K.R., Pavlath, G.K., Gussoni, E., Mynhier, M., Lanctot, A.M., Greco, C.M., Steinman, L., and Blau, H.M. (1997). Myoblast implantation in Duchenne muscular dystrophy: the San Francisco study. *Muscle Nerve* 20, 469–78. Available at: <http://www.ncbi.nlm.nih.gov/pubmed/9121505> [Accessed June 25, 2016].
55. Law, P.K., Goodwin, T.G., Fang, Q., Deering, M.B., Duggirala, V., Larkin, C., Florendo, J.A., Kirby, D.S., Li, H.J., and Chen, M. (1993). Cell transplantation as an experimental treatment for Duchenne muscular dystrophy. *Cell Transplant.* 2, 485–505. Available at: <http://www.ncbi.nlm.nih.gov/pubmed/8167934> [Accessed June 25, 2016].
56. Karpatì, G., Ajdukovic, D., Arnold, D., Gledhill, R.B., Guttmann, R., Holland, P., Koch, P.A., Shoubridge, E., Spence, D., and Vanasse, M. (1993). Myoblast transfer in Duchenne muscular dystrophy. *Ann. Neurol.* 34, 8–17. Available at: <http://www.ncbi.nlm.nih.gov/pubmed/8517684> [Accessed June 25, 2016].
57. Taylor, C.J., Bolton, E.M., Pocock, S., Sharples, L.D., Pedersen, R.A., and Bradley, J.A. (2005). Banking on human embryonic stem cells: estimating the number of donor cell lines needed for HLA matching. *Lancet* 366, 2019–2025.
58. Nakatsujì, N., Nakajima, F., and Tokunaga, K. (2008). HLA-haplotype banking and iPS cells. *Nat. Biotechnol.* 2008 267 26, 739–740. Available at: <https://www.nature.com/articles/nbt0708-739> [Accessed July 20, 2021].

59. Beauchamp, J.R., Morgan, J.E., Pagel, C.N., and Partridge, T.A. (1999). Dynamics of myoblast transplantation reveal a discrete minority of precursors with stem cell-like properties as the myogenic source. *J. Cell Biol.* 144, 1113–1121.
60. Abou-Khalil, R., Le Grand, F., Pallafacchina, G., Valable, S., Authier, F.J., Rudnicki, M. a., Cherardi, R.K., Germain, S., Chretien, F., Sotiropoulos, A., *et al.* (2009). Autocrine and Paracrine Angiopoietin 1/Tie-2 Signaling Promotes Muscle Satellite Cell Self-Renewal. *Cell Stem Cell* 5, 298–309.
61. Baroffio, A., Hamann, M., Bernheim, L., Bochaton-Piallat, M.L., Gabbiani, G., and Bader, C.R. (1996). Identification of self-renewing myoblasts in the progeny of single human muscle satellite cells. *Differentiation*. 60, 47–57. Available at: <http://www.ncbi.nlm.nih.gov/pubmed/8935928>.
62. Laumonier, T., Bermont, F., Hoffmeyer, P., Kindler, V., and Menetrey, J. (2017). Human myogenic reserve cells are quiescent stem cells that contribute to muscle regeneration after intramuscular transplantation in immunodeficient mice. *Sci. Rep.* 7, 3462. Available at: <http://www.ncbi.nlm.nih.gov/pubmed/28615691> [Accessed June 20, 2017].
63. Sampaolesi, M., Torrente, Y., Innocenzi, A., Tonlorenzi, R., D'Antona, G., Pellegrino, M.A., Barresi, R., Bresolin, N., De Angelis, M.G.C., Campbell, K.P., *et al.* (2003). Cell therapy of α -sarcoglycan null dystrophic mice through intra-arterial delivery of mesoangioblasts. *Science* (80-.). 301, 487–492. Available at: <https://science.sciencemag.org/content/301/5632/487> [Accessed April 22, 2021].
64. Dellavalle, A., Sampaolesi, M., Tonlorenzi, R., Tagliafico, E., Sacchetti, B., Perani, L., Innocenzi, A., Galvez, B.G., Messina, G., Morosetti, R., *et al.* (2007). Pericytes of human skeletal muscle are myogenic precursors distinct from satellite cells. *Nat. Cell Biol.* 9, 255–267. Available at: <https://www.nature.com/articles/ncb1542> [Accessed April 20, 2021].
65. Miyagoe-Suzuki, Y., and Takeda, S. (2017). Skeletal muscle generated from induced pluripotent stem cells - Induction and application. *World J. Stem Cells* 9, 89–97. Available at: <http://www.worldscientific.com/doi/10.1002/wjst.1631> [Accessed June 16, 2021].
66. Muskiewicz, K.R., Frank, N.Y., Flint, A.F., and Gussoni, E. (2005). Myogenic potential of muscle side and main population cells after intravenous injection into sub-lethally irradiated mdx mice. *J. Histochem. Cytochem.* 53, 861–873. Available at: <http://journals.sagepub.com/doi/10.1369/jhc.4A6573.2005> [Accessed April 23, 2021].
67. Bachrach, E., Perez, A.L., Choi, Y.-H., Illigens, B.M.W., Jun, S.J., Nido, P. Del, McGowan, F.X., Li, S., Flint, A., Chamberlain, J., *et al.* (2006). Muscle engraftment of myogenic progenitor cells following intraarterial transplantation. *Muscle Nerve* 34, 44–52. Available at: <http://doi.wiley.com/10.1002/mus.20560> [Accessed April 23, 2021].
68. Cossu, G., Previtali, S.C., Napolitano, S., Cicalese, M.P., Tedesco, F.S., Nicastro, F., Noviello, M., Roostalu, U., Natali Sora, M.G., Scarlato, M., *et al.* (2015). Intra-arterial transplantation of HLA-matched donor mesoangioblasts in Duchenne muscular dystrophy. *EMBO Mol. Med.* 7, 1513–1528. Available at: <https://onlinelibrary.wiley.com/doi/10.15252/emmm.201505636> [Accessed April 20, 2021].
69. Cerletti, M., Jurga, S., Witczak, C. a., Hirshman, M.F., Shadrach, J.L., Goodyear, L.J., and Wagers, A.J. (2008). Highly Efficient, Functional Engraftment of Skeletal Muscle Stem Cells in Dystrophic Muscles. *Cell* 134, 37–47.
70. Mendell, J.R., Kissel, J.T., Amato, A.A., King, W., Signore, L., Prior, T.W., Sahenk, Z., Benson, S., McAndrew, P.E., and Rice, R. (1995). Myoblast transfer in the treatment of Duchenne's muscular dystrophy. *N. Engl. J. Med.* 333, 832–8. Available at: <http://www.ncbi.nlm.nih.gov/pubmed/7651473> [Accessed June 25, 2016].

71. Moyle, L.A., Tedesco, F.S., and Benedetti, S. (2019). Pericytes in Muscular Dystrophies. In *Advances in Experimental Medicine and Biology* (Springer New York LLC), pp. 319–344. Available at: https://link.springer.com/chapter/10.1007/978-3-030-16908-4_15 [Accessed April 20, 2021].
72. Relaix, F., Bencze, M., Borok, M.J., Der Vartanian, A., Gattazzo, F., Mademtzoglou, D., Perez-Diaz, S., Prola, A., Reyes-Fernandez, P.C., Rotini, A., et al. (2021). Perspectives on skeletal muscle stem cells. *Nat. Commun.* *12*, 1–11. Available at: <https://doi.org/10.1038/s41467-020-20760-6> [Accessed May 4, 2021].
73. Copley, M.R., Beer, P.A., and Eaves, C.J. (2012). Hematopoietic stem cell heterogeneity takes center stage. *Cell Stem Cell* *10*, 690–697.
74. Li, N., and Clevers, H. (2010). Coexistence of quiescent and active adult stem cells in mammals. *Science* (80-.). *327*, 542–545. Available at: <https://science.sciencemag.org/content/327/5965/542> [Accessed May 14, 2021].
75. Cornelison, D.D., and Wold, B.J. (1997). Single-cell analysis of regulatory gene expression in quiescent and activated mouse skeletal muscle satellite cells. *Dev. Biol.* *191*, 270–83. Available at: <http://www.ncbi.nlm.nih.gov/pubmed/9398440> [Accessed September 30, 2015].
76. Siegel, A.L., Kuhlmann, P.K., and Cornelison, D. (2011). Muscle satellite cell proliferation and association: new insights from myofiber time-lapse imaging. *Skelet. Muscle* *2011* *11*, 1–7. Available at: <https://skeletalmusclejournal.biomedcentral.com/articles/10.1186/2044-5040-1-7> [Accessed July 20, 2021].
77. Dell'Orso, S., Juan, A.H., Ko, K.-D., Naz, F., Gutierrez-Cruz, G., Feng, X., and Sartorelli, V. (2019). Single-cell analysis of adult skeletal muscle stem cells in homeostatic and regenerative conditions. *Development*, dev.174177. Available at: <http://dev.biologists.org/content/early/2019/03/18/dev.174177> [Accessed April 1, 2019].
78. Cho, D.S., and Doles, J.D. (2017). Single cell transcriptome analysis of muscle satellite cells reveals widespread transcriptional heterogeneity. *Gene* *636*, 54–63. Available at: <http://www.sciencedirect.com/science/article/pii/S0378111917307230?via%3Dihub> [Accessed December 6, 2017].
79. Collins, C. a., Olsen, I., Zammit, P.S., Heslop, L., Petrie, A., Partridge, T. a., and Morgan, J.E. (2005). Stem cell function, self-renewal, and behavioral heterogeneity of cells from the adult muscle satellite cell niche. *Cell* *122*, 289–301.
80. Ono, Y., Masuda, S., Nam, H.-S., Benezra, R., Miyagoe-Suzuki, Y., and Takeda, S. (2012). Slow-dividing satellite cells retain long-term self-renewal ability in adult muscle. *J. Cell Sci.* *125*, 1309–17. Available at: <http://www.ncbi.nlm.nih.gov/pubmed/22349695>.
81. Qu-Petersen, Z., Deasy, B., Jankowski, R., Ikezawa, M., Cummins, J., Pruchnic, R., Mytinger, J., Cao, B., Gates, C., Wernig, A., et al. (2002). Identification of a novel population of muscle stem cells in mice: potential for muscle regeneration. *J. Cell Biol.* *157*, 851–64. Available at: <http://www.ncbi.nlm.nih.gov/pubmed/12021255> [Accessed July 23, 2018].
82. Gharaibeh, B., Lu, A., Tebbets, J., Zheng, B., Feduska, J., Crisan, M., Péault, B., Cummins, J., and Huard, J. (2008). Isolation of a slowly adhering cell fraction containing stem cells from murine skeletal muscle by the preplate technique. *Nat. Protoc.* *3*, 1501–1509. Available at: <http://www.nature.com/doi/10.1038/nprot.2008.142> [Accessed September 25, 2017].
83. Rocheteau, P., Gayraud-Morel, B., Siegl-Cachedenier, I., Blasco, M.A., and Tajbakhsh, S. (2012). A subpopulation of adult skeletal muscle stem cells retains all template DNA strands after cell division. *Cell* *148*, 112–125.

84. Kitzmann, M., Carnac, G., Vandromme, M., Primig, M., Lamb, N.J.C., and Fernandez, A. (1998). The Muscle Regulatory Factors MyoD and Myf-5 Undergo Distinct Cell Cycle-specific Expression in Muscle Cells. *J. Cell Biol.* *142*, 1447–1459. Available at: <http://www.ncbi.nlm.nih.gov/pubmed/9744876> [Accessed May 29, 2019].
85. Yoshida, N., Yoshida, S., Koishi, K., Masuda, K., and Nabeshima, Y. (1998). Cell heterogeneity upon myogenic differentiation: down-regulation of MyoD and Myf-5 generates “reserve cells”. *J. Cell Sci.* *111*, 769–779.
86. Abou-Khalil, R., Le Grand, F., and Chazaud, B. (2013). Human and Murine Skeletal Muscle Reserve Cells. In *Methods in Molecular Biology* (Humana Press Inc.), pp. 165–177. Available at: http://link.springer.com/10.1007/978-1-62703-508-8_14 [Accessed April 21, 2020].
87. Carnac, G., Fajas, L., L honoré, A., Sardet, C., Lamb, N.J.C., and Fernandez, A. (2000). The retinoblastoma-like protein p130 is involved in the determination of reserve cells in differentiating myoblasts. *Curr. Biol.* *10*, 543–546. Available at: <https://www.sciencedirect.com/science/article/pii/S0960982200004711?via%3Dihub> [Accessed May 29, 2019].
88. Sandoval-Guzmán, T., Wang, H., Khattak, S., Schuez, M., Roensch, K., Nacu, E., Tazaki, A., Joven, A., Tanaka, E.M., and Simon, A. (2014). Fundamental differences in dedifferentiation and stem cell recruitment during skeletal muscle regeneration in two salamander species. *Cell Stem Cell* *14*, 174–187. Available at: <http://dx.doi.org/10.1016/j.stem.2013.11.007> [Accessed May 17, 2021].
89. Baghdadi, M.B., and Tajbakhsh, S. (2017). Regulation and phylogeny of skeletal muscle regeneration. *Dev. Biol.* Available at: <http://www.sciencedirect.com/science/article/pii/S0012160617304141> [Accessed August 18, 2017].
90. Bentzinger, C.F., Wang, Y.X., and Rudnicki, M.A. (2012). Building muscle: molecular regulation of myogenesis. *Cold Spring Harb. Perspect. Biol.* *4*. Available at: <http://www.ncbi.nlm.nih.gov/pubmed/22300977> [Accessed July 1, 2016].
91. Segalés, J., Perdiguerro, E., and Muñoz-Cánoves, P. (2016). Regulation of Muscle Stem Cell Functions: A Focus on the p38 MAPK Signaling Pathway. *Front. Cell Dev. Biol.* *4*, 91. Available at: <http://www.ncbi.nlm.nih.gov/pubmed/27626031> [Accessed January 26, 2017].
92. Allen, R.E., and Boxhorn, L.K. (1989). Regulation of skeletal muscle satellite cell proliferation and differentiation by transforming growth factor-beta, insulin-like growth factor I, and fibroblast growth factor. *J. Cell. Physiol.* *138*, 311–315. Available at: <http://doi.wiley.com/10.1002/jcp.1041380213> [Accessed April 7, 2021].
93. Schertzer, J.D., Ryall, J.G., and Lynch, G.S. (2006). Systemic administration of IGF-I enhances oxidative status and reduces contraction-induced injury in skeletal muscles of mdx dystrophic mice. *Am. J. Physiol. - Endocrinol. Metab.* *291*, 499–505. Available at: <http://www.ajpendo.org> [Accessed May 17, 2021].
94. Gehrig, S.M., van der Poel, C., Hoeflich, A., Naim, T., Lynch, G.S., and Metzger, F. (2012). Therapeutic potential of PEGylated insulin-like growth factor I for skeletal muscle disease evaluated in two murine models of muscular dystrophy. *Growth Horm. IGF Res.* *22*, 69–75.
95. Lala-Tabbert, N., Fu, D., and Wiper-Bergeron, N. (2016). Induction of CCAAT/Enhancer-Binding Protein β Expression With the Phosphodiesterase Inhibitor Isobutylmethylxanthine Improves Myoblast Engraftment Into Dystrophic Muscle. *Stem Cells Transl. Med.* *5*, 500–510. Available at: <http://doi.wiley.com/10.5966/sctm.2015-0169> [Accessed April 5, 2021].

96. Xu, C., Tabebordbar, M., Iovino, S., Ciarlo, C., Liu, J., Castiglioni, A., Price, E., Liu, M., Barton, E.R., Kahn, C.R., et al. (2013). XA zebrafish embryo culture system defines factors that promote vertebrate myogenesis across species. *Cell* 155, 909. Available at: <http://dx.doi.org/10.1016/j.cell.2013.10.023> [Accessed April 5, 2021].
97. Judson, R.N., and Rossi, F.M.V. (2020). Towards stem cell therapies for skeletal muscle repair. *npj Regen. Med.* 5, 1–6.



Appendices

Summary

Samenvatting

Resumen

Curriculum vitae

PhD portfolio

List of publications

Acknowledgements

Summary

Pompe disease is a rare metabolic myopathy characterized by deficiency of acid α -glucosidase due to disease-associated variants in the *GAA* gene, resulting in lysosomal glycogen accumulation. Enzyme replacement therapy (ERT) represents the standard of care for Pompe disease since 2006, consisting of intravenous infusion of recombinant human acid α -glucosidase (rhGAA). ERT treatment improves survival and ameliorates cardiomyopathy in children, and improves respiratory and muscle function in children and adult onset patients. However, treatment is not always effective and there is significant variability in response to treatment between patients. As a consequence of the variability in treatment outcome, the necessity of life-long (bi)weekly ERT infusions, and the high costs associated with therapy, new therapeutic avenues are necessary for Pompe disease. Furthermore, novel therapies are also necessary for other skeletal muscle disorders with unmet clinical needs. This thesis explores the molecular mechanisms that govern Pompe disease and investigates strategies for the development of regenerative cell-based therapies for muscle disorders.

In **chapter 1**, we introduced the features that characterize Pompe disease and its current gold-standard of care – ERT –, including its limitations. The role of glycogen metabolism in skeletal muscle and its disturbances in glycogen storage disorders (GSDs) were defined, as well as relevant metabolic pathways altered in Pompe disease and of relevance for the work presented in this thesis, such as autophagy. Furthermore, experimental outcomes amenable for development for Pompe disease were described. The biology of skeletal muscle was introduced, with a focus on satellite cells, the native skeletal muscle stem cells, along with their role in the muscle regenerative process. Additionally, innovative forthcoming therapeutic avenues for skeletal muscle were introduced, paying emphasis on cell therapies and descriptions of cell types amenable for this purpose. Last, the scope and aims of this thesis were delineated.

Although residual *GAA* enzyme activity largely affects disease onset and progression, other factors are suspected to modulate disease course. These factors include cytoplasmic glycogen metabolism, among others. In **chapter 2**, the metabolism of glycogen in muscle and brain of mouse and skeletal muscle of human patients with Pompe disease were analyzed. Enzymes involved in cytoplasmic glycogen synthesis including *GYG1*, *GS*, *GLUT4*, *GBE1*, and *UGP2* were upregulated in skeletal muscle, cardiac muscle, and brain of *Gaa^{-/-}* mice,

confirming dysregulation of glycogen metabolism in a mouse model of Pompe disease. In addition, certain changes were present before the onset of muscle pathology, while other changes developed through the life course of mice with Pompe disease. Quantitative mass spectrometry was performed in skeletal muscle biopsies of five patients that responded well to ERT both before and after treatment with ERT. Analyses of this data showed increased expression of GBE1 relative to healthy individuals. Furthermore, paired analysis of individual patients after ERT treatment showed reduction of GYG1, GS, and GBE1 compared to before ERT treatment. These results suggested that metabolic changes in Pompe disease precede muscle wasting, that dysregulation of glycogen metabolism also seemed to occur in humans with Pompe disease, and that ERT treatment resulted in attenuation of dysregulated enzyme levels.

Skeletal muscle has a remarkable regenerative capacity after damage in a process mediated by satellite cells. However, in muscle-degenerative conditions regeneration is often hampered due to disbalance between muscle degeneration and regeneration. In **chapter 3**, recent progress on the role of satellite cell-mediated repair in neuromuscular disorders was reviewed, with an emphasis in Pompe disease. We reported disease-specific abnormalities in satellite cell function in various neuromuscular disorders. A comparison was performed between muscle dystrophies (e.g., Duchenne muscular dystrophy) and Pompe disease. In addition, foreseeable targets for therapy such as autophagy, the muscle microenvironment, and activation of satellite cells were discussed. Last, experimental muscle regenerative approaches for Pompe disease were reviewed.

Satellite cell function is largely influenced by interactions with their microenvironment. Tools for the study of these interactions and their outcomes are necessary for a more complete understanding of the biology of muscle stem cells. In **chapter 4**, an *in vitro* assay for the evaluation of satellite cell activation through *ex vivo* isolation of murine skeletal muscle fibers was presented. This assay can be used to compare satellite cells across different mouse models or to evaluate their response to treatments, offering a valuable complementary tool for *in vitro* experimentation. Experimental approaches were optimized and discussed, as well as potential problems and proposed solutions for the adaptation of this assay to alternative experimental conditions. This assay allows partial preservation of the satellite cells' niche *in vitro*, allowing the study of satellite cell-niche interactions.

In Pompe disease, satellite cell-mediated regeneration is hampered due to reduced activation of skeletal muscle stem cells. In **chapter 5**, the relationship

between autophagy dysregulation, satellite cell activation, and regeneration was investigated in a mouse model of Pompe disease. Results showed that dysregulation of key autophagic proteins occurs before the onset of muscle pathology, confirming a causative role in the development of cellular pathology. Furthermore, we observed accumulation of autophagic debris in isolated *Gaa*^{-/-} skeletal muscle fibers and increased satellite cell activation in response to FGF2 treatment compared to wild-type. Treatment with rapamycin, an inducer of autophagy, stimulated autophagic flux, normalized activation, and improved myofiber morphology, yet failed to remove autophagic debris. Overall, modulation of autophagy was not sufficient to restore regeneration. However, induction of muscle regeneration by experimentally induced acute muscle injury transiently restored skeletal muscle histology and function and reduced lysosomal load. This study indicated that modulation of autophagy is not sufficient to overcome the satellite cell activation limit that is a feature of Pompe disease. Data also suggested that forcing satellite cell activation through induction of acute muscle injury could have sufficient potential to overcome the autophagic block caused by Pompe disease.

A large number of neuromuscular disorders are characterized for the lack of available therapies. In others, like Pompe disease, available therapies are not curative. These unmet needs warrant research and development of novel therapies. Cell therapy represents a promising therapeutic avenue for muscle disorders. However, the development of cell-based therapies for neuromuscular disorders is currently limited by the incapacity to expand regenerative cells *in vitro*. In **chapter 6**, we described a method to isolate murine regenerative myogenic cell fractions – termed reserve cells – from *ex vivo*-expanded muscle cultures with capacity to regenerate skeletal muscle *in vivo* upon transplantation. Reserve cell fractions possessed distinct *in vitro* and *in vivo* properties. Under differentiation conditions, fast-adhering reserve cells were enriched for myogenin-expressing cells and preferentially contributed to direct muscle regeneration after transplantation in pre-injured immunodeficient mice. Slow-adhering reserve cells were enriched for PAX7-expressing cells and primarily engrafted as skeletal muscle stem cells, displaying higher regenerative capacity after a second bout of injury. Transcriptomic profiling of these populations was characterized, which allowed to provide a first molecular characterization of reserve cell fractions and to provide insight in pathways involved in reserve-cell mediated muscle regeneration.

Last, in **chapter 7** results in the context of literature were discussed. We

highlighted the findings reported in this thesis and placed them in the context of the current state-of-the-art knowledge on the molecular mechanisms of Pompe disease and cell-based therapies for neuromuscular disorders. In addition, we discussed outlooks and future challenges that the work contained in this thesis faces towards therapy development and clinical application.

Samenvatting

De ziekte van Pompe is een zeldzame metabolische spierziekte die veroorzaakt wordt door ziekte-geassocieerde varianten in het GAA gen. Deze mutaties veroorzaken opeenhoping van glycogeen in het lysosoom. De standaard therapie voor de ziekte van Pompe is enzymvervangende therapie (ERT). Hierbij wordt intraveneus recombinant humaan zuur- α -glucosidase (rhGAA) toegediend. ERT behandeling vergroot de overlevingskans bij kinderen en helpt tegen cardiomyopathie. Ook helpt deze therapie bij ademhalingsfuncties en spierfuncties in kinderen en volwassenen die de ziekte op latere leeftijd hebben gekregen. Echter, de behandeling is niet altijd even effectief en er is veel verschil in hoe patiënten op de behandeling reageren. Hierdoor en mede doordat patiënten voor hun hele leven lang dure (twee)wekelijks ERT infusies nodig hebben, zijn er nieuwe therapeutische interventies nodig voor de ziekte van Pompe. Dit geldt ook voor andere spierziektes waar op dit moment geen genezing voor bestaat. In dit proefschrift worden de moleculaire mechanismen die ten grondslag liggen aan de ziekte van Pompe onderzocht. Tevens worden regeneratieve cel-gebaseerde methodes als therapie voor spierziektes onderzocht.

In **hoofdstuk 1** bespreken we de karakteristieken van de ziekte van Pompe en beperkingen van ERT als gouden standaard voor therapie. We beschrijven de rol van glycogeen metabolisme in skeletspieren en de verstoring ervan in glycogeen opslag ziektes (GSDs), aangedane metabolische mechanismes voor de ziekte van Pompe, en andere mechanismen van belang voor de context van dit proefschrift, zoals autofagie. Verder worden ook onderzoeksresultaten besproken die bij kunnen dragen aan de ziekte van Pompe. Daarnaast wordt de biologie van de skeletspier geïntroduceerd, met een focus op de satellietcellen, de stamcel van de skeletspiercellen, alsmede hun rol in het spierregeneratie proces. Ook worden innovatieve toekomstige therapeutische mogelijkheden voor skeletspieren geïntroduceerd, met een focus op cel-gebaseerde therapieën en beschrijvingen van cel types die hiervoor geschikt zijn. Tot slot, worden de scope en de doelen van dit proefschrift beschreven.

Alhoewel residuale GAA enzymactiviteit de start en het verloop van de ziekte van Pompe beïnvloedt, spelen andere factoren een grotere rol bij het moduleren van de ziekte. Een van deze factoren is o.a. cytosolaire glycogeen metabolisme. In **hoofdstuk 2**, wordt het metabolisme van glycogeen in spierweefsel en de hersenen van muizen en in de skeletspieren van patiënten met de ziekte van

Pompe geanalyseerd. Enzymen betrokken bij cytoplasmatische glycogeen aanmaak zoals GYG1, GS, GLUT4, GBE1, en UGP2 waren geüpereguleerd in skeletspieren, hartspieren, en in de hersenen van *Gaa^{-/-}* muizen. Dit bevestigde de deregulatie van glycogeen metabolisme in een muismodel voor de ziekte van Pompe. Daarnaast waren sommige veranderingen al aanwezig voor het tot uiting komen van de spier pathologie, terwijl andere veranderingen ontwikkelden in de loop van het leven van de muis met de ziekte van Pompe. Kwantitatieve massa spectrometrie werd toegepast op skeletspier biopten van vijf patiënten die goed op de therapie reageerden. Metingen werden gedaan zowel voor als na ERT behandeling. Er was een verhoogde expressie van GBE1 vergelijkbaar met gezonde individuen. Verder liet een gepaarde analyse van individuele patiënten na ERT behandeling een verlaging van GYG1, GS, en GBE1 zien vergeleken met voor de ERT behandeling. Deze resultaten suggereren dat metabolische veranderingen in de ziekte van Pompe vooraf gaan aan spierdegeneratie, dat disregulatie van glycogeen metabolisme ook plaats vindt in patiënten met de ziekte van Pompe, en dat ERT behandeling gedisreguleerde enzym levels tegengaat.

Skeletspier heeft een noemenswaardige regeneratieve capaciteit na schade in een proces ondersteunt door satellietcellen. Echter, in spierdegeneratieve condities is regeneratie vaak belemmerd door een disbalans tussen spierdegeneratie en regeneratie. In **hoofdstuk 3** wordt de vooruitgang op de rol van satellietcel-gebaseerde herstel van neuromusculaire ziektes gereviewed met een focus op de ziekte van Pompe. We rapporteren ziekte-specifieke abnormaliteiten in satellietcel functie in verschillende neuromusculaire ziektes. We vergelijken spierdystrofie (b.v. spierdystrofie van Duchenne) met de ziekte van Pompe. Daarnaast worden mogelijke targets voor therapie zoals autofagie, de spier micro-omgeving, en de activatie van satellietcellen besproken. Tot slot worden experimentele spierregeneratieve mogelijkheden voor de ziekte van Pompe besproken.

Satellietcel functie wordt grotendeels beïnvloedt door interactie met de micro-omgeving. Tools voor het bestuderen van deze interacties en de resultaten zijn nodig voor een volledig begrip van de biologie van de spierstamcel. In **hoofdstuk 4** presenteren we een *in vitro* assay voor de evaluatie van satellietcel activatie d.m.v. *ex vivo* isolatie van muisskeletspier vezels. Deze assay kan worden gebruikt om satellietcellen te vergelijken tussen verschillende muismodellen of om hun reactie op behandeling te evalueren. Dit biedt een complementaire kostbare tool voor *in vitro* experimenten. De experimentele benaderingen zijn geoptimaliseerd en worden besproken. Tevens worden potentiële problemen en oplossingen voor

adaptatie van deze assay voor andere experimentele condities behandeld. Deze assay staat het behoud van een deel van de niche van de satellietcel *in vitro* toe zodat satellietcel-niche interacties kunnen worden bestudeerd.

In de ziekte van Pompe wordt satelliet cel-ondersteunde regeneratie tegengegaan door een verminderde activiteit in skeletspierstamcellen. In **hoofdstuk 5**, wordt de relatie van autofagy disregulatie, satellietcel activatie en regeneratie bestudeerd in een muismodel van de ziekte van Pompe. De resultaten laten zien dat er disregulatie is van essentiële autofagy eiwitten voordat er spierpathologie is. Dit bevestigt de causale rol in de ontwikkeling van celpathologie. Verder zagen we accumulatie van autofage afval in geïsoleerde *Gaa*^{-/-} skeletspiervezels en een verhoogde satellietcel activatie als reactie op FGF2 behandeling vergeleken met wildtype muizen. Behandeling met rapamycin, een induceerder van autofagy, stimuleert de autofage flux, normaliseert activatie en verbetert myovezel morfologie, echter autofage afval werd niet opgeruimd. In opsomming, modulatie van autofagy was onvoldoende om regeneratie te herstellen. Echter, inductie van spierregeneratie door experimenteel geïnduceerde acute spierschade verbeterde tijdelijk de skeletspier histologie en functie en verminderde de lysosomale belasting. Deze studie laat zien dat modulatie van autofagy niet voldoende is om de satellietcel activatie limiet, welke zo karakteristiek is voor de ziekte van Pompe, te overkomen. De data suggereert dat geforceerde satellietcel activatie door inductie van acute spier schade voldoende potentie zou kunnen hebben om de autofage blokkade van de ziekte van Pompe te overkomen.

Voor een groot aantal aan neuromusculaire ziektes is geen therapie beschikbaar. Voor andere, zoals de ziekte van Pompe, geneest de therapie de ziekte niet. Deze onvervulde behoeftes vereisen onderzoek en ontwikkeling van nieuwe therapieën. Celtherapie is een veelbelovende therapeutische mogelijkheid voor spierziektes. Echter, de ontwikkeling van op cellen-gebaseerde therapieën voor neuromusculaire ziektes wordt momenteel tegengehouden door de uitdaging om regeneratieve cellen *in vitro* te vermeerderen. In **hoofdstuk 6** beschrijven we de methode om geïsoleerde muis-regeneratieve myogene celfracties, genaamd reserve cellen, van *ex vivo*-vermeerderde spierkweken te isoleren. Deze cellen kunnen nadat ze *in vivo* zijn getransplanteerd skeletspier regenereren. Met behulp van differentiatie condities werden snel-adherende reserve cellen verrijkt voor myogene-expresserende cellen en met name deze cellen dragen bij aan directe spierregeneratie na transplantatie in vooraf verwonde immunodeficiënte muizen. Langzaam-adherende reserve cellen werden verrijkt voor PAX7-expresserende

cellen en voornamelijk getransplanteerd als skeletspierstamcel. Deze cellen lieten een hogere regeneratieve capaciteit zien na een tweede verwonding. Het transcriptoom van deze cel populaties is gekarakteriseerd. Dit verzorgde een eerste moleculaire karakteristiek van reserve cel fracties en bracht inzichten in de mechanismes die betrokken zijn bij reserve-cel gebaseerde spierregeneratie.

Tot slot, in **hoofdstuk 7** worden de onderzoeksresultaten in de context van de literatuur besproken. We belichten de bevindingen in dit proefschrift en plaatsen ze in context van de huidige state-of-the-art kennis over de moleculaire mechanismen van de ziekte van Pompe en van op cellen-gebaseerde therapieën voor neuromusculaire ziektes. Daarnaast blikken we vooruit op de toekomstige uitdagingen die het werk beschreven in dit proefschrift tegen zal komen om door te kunnen ontwikkelen tot een therapie of klinische toepassing.

Resumen

La enfermedad de Pompe es una miopatía metabólica rara caracterizada por deficiencia de alfa-glucosidasa ácida debido a variantes patogénicas en el gen *GAA*, que causa en acumulación de glucógeno en los lisosomas. La terapia de reemplazo enzimático (ERT, por sus siglas en inglés) es el tratamiento estándar para la enfermedad de Pompe desde 2006. Esta consiste en infusión intravenosa de alfa-glucosidasa ácida recombinante humana (rhGAA). El tratamiento con ERT mejora la supervivencia y disminuye la cardiomiopatía en niños, y mejora la función respiratoria y muscular en pacientes pediátricos y adultos. Sin embargo, el tratamiento no es siempre efectivo, existiendo una variabilidad de respuesta al tratamiento entre diferentes pacientes significativa. Como consecuencia de esta variabilidad en la respuesta al tratamiento, de la necesidad de infusiones de ERT bisemanales de por vida y de los altos costes asociados a esta terapia, nuevas opciones terapéuticas son necesarias para tratar la enfermedad de Pompe. Además, también son necesarias nuevas terapias para otras enfermedades musculares con requerimientos médicos sin satisfacer. Esta tesis explora los mecanismos moleculares que participan en la enfermedad de Pompe e investiga estrategias para el desarrollo de terapias celulares regenerativas para enfermedades musculares.

En el **capítulo 1** se presentan las características de la enfermedad de Pompe y su tratamiento estándar – ERT –, incluyendo sus limitaciones. Se define el rol que juega el metabolismo del glucógeno en tejido muscular esquelético en enfermedades del almacenamiento del glucógeno (GSDs) (como la enfermedad de Pompe), así como la existencia de alteraciones en rutas metabólicas en la enfermedad de Pompe que son de relevancia para el trabajo presentado en esta tesis, tal y como la autofagia. Además, se describen opciones experimentales en desarrollo válidas para la enfermedad de Pompe. Asimismo, se describe la biología del tejido muscular esquelético, haciendo énfasis en las células satélite –, las células madre nativas del tejido muscular esquelético, incluyendo su rol en el proceso de regeneración muscular. Adicionalmente se presentan terapias innovadoras para su aplicación en músculo esquelético –, prestando especial interés en terapias celulares, con descripciones de tipos celulares válidos para este propósito. Por último, se delimitan el ámbito y los objetivos perseguidos en esta tesis.

Aunque la actividad enzimática residual de *GAA* afecta al inicio y progresión de la enfermedad, otros factores también podrían modular su curso. Entre estos factores se incluye el metabolismo del glucógeno citoplasmático, entre otros. En el

capítulo 2 se analiza el metabolismo del glucógeno en tejido muscular y cerebral de ratón y músculo esquelético de pacientes humanos de enfermedad de Pompe. Enzimas relacionadas con la síntesis de glucógeno citoplasmático, incluyendo GYG1, GS, GLUT4, GBE1 y UGP2 se encontraron elevadas en musculo esquelético, músculo cardíaco y cerebro de ratones *Gaa^{-/-}*, confirmando la desregulación del metabolismo del glucógeno en un modelo de ratón de la enfermedad de Pompe. Además, algunos cambios ya estaban presentes antes del inicio de la patología muscular, mientras que otros cambios se desarrollaron durante el curso de vida de ratones con enfermedad de Pompe. Se realizó espectrometría de masa cuantitativa en biopsias de tejido muscular esquelético antes y después de comenzar tratamiento con ERT en cinco pacientes que respondieron positivamente a dicho tratamiento. El análisis de estos datos mostró expresión de GBE1 elevada con respecto a individuos sanos. Además, análisis en par de pacientes mostraron niveles reducidos de GYG1, GS y GBE1 comparados con pacientes antes de ser tratados con ERT. Estos resultados sugieren que los cambios metabólicos en enfermedad de Pompe preceden al debilitamiento muscular, que la desregulación del metabolismo de glucógeno también parece afectar a humanos, y que el tratamiento con ERT resulta en una atenuación en la desregulación de los niveles enzimáticos.

Tras sufrir daño, el músculo esquelético tiene una alta capacidad de regeneración, en un proceso mediado por células satélite. Sin embargo, en condiciones musculares degenerativas la regeneración se ve a menudo afectada debido al desequilibrio entre episodios de degeneración y regeneración muscular. En el **capítulo 3** se revisa el progreso reciente acerca del rol de la reparación muscular mediada por células satélite en enfermedades neuromusculares, haciendo énfasis en la enfermedad de Pompe. Se describen anomalías que afectan a la función de células satélite en varias enfermedades neuromusculares. Se establecen comparaciones entre distrofias musculares (ej., distrofia muscular de Duchenne) y enfermedad de Pompe. Además, son objeto de debate potenciales dianas terapéuticas tal y como la autofagia, el nicho muscular y la activación de células satélite. Por último, se debaten propuestas experimentales de regeneración muscular aplicadas a la enfermedad de Pompe.

La función de células satélite está altamente influenciada por las interacciones con su microambiente. En este momento herramientas para el estudio de esas interacciones son necesarias con el fin de mejorar nuestro entendimiento de la biología de las células madre musculares. En el **capítulo 4** se presenta un ensayo *in vitro* para evaluar la activación de células satélite mediante aislamiento

ex vivo de fibras de músculo esquelético de ratón. Este ensayo puede utilizarse para comparar células satélite de distintos modelos de ratón, o para evaluar su respuesta a tratamientos, ofreciendo una herramienta complementaria para experimentación *in vitro*. Se debate sobre distintos enfoques experimentales, así como sobre problemas potenciales y sus posibles soluciones en cuanto a la adaptación de este ensayo a condiciones experimentales alternativas. Por último, el ensayo descrito en este capítulo permite preservar parcialmente el nicho de las células satélite *in vitro*, permitiendo el estudio de las interacciones entre células satélite y su microambiente.

En la enfermedad de Pompe la regeneración mediada por células satélite esta obstaculizada debido a una activación reducida de células madre de músculo esquelético. En el **capítulo 5** se investiga en un modelo de ratón de enfermedad de Pompe la relación entre desregulación de la autofagia, activación de células satélite y regeneración. Los resultados mostraron que la desregulación de proteínas con una importante función autofágica ocurrió ya antes del inicio de la patología muscular, confirmando un rol causativo en el desarrollo de la patología celular. Además, se observó acumulación de residuos autofágicos en fibras aisladas de musculo esquelético *Gaa*^{-/-} así como un incremento en la activación de células satélite en respuesta a tratamiento con FGF2 en comparación con ratones de tipo silvestre. Tratamiento con rapamicina, un inductor de la autofagia, estimuló el flujo autofágico, normalizó la activación de células madre musculares y mejoró la morfología de fibras musculares, aunque no fue capaz de eliminar los residuos autofagicos. En general, la modulación de la autofagia no fue suficiente para restaurar el proceso regenerativo. Sin embargo, inducción experimental del proceso de regeneración mediante daño muscular agudo fue capaz de restaurar transitoriamente la histología y función del musculo esquelético, así como de reducir la carga lisosomal. Este estudio indica que la modulación de autofagia no es suficiente para superar la limitación en la activación de células satélite que caracteriza la enfermedad de Pompe. Los datos también sugieren que forzar la activación de células satélite mediante inducción de daño muscular agudo podría tener suficiente capacidad para superar el bloqueo autofágico propio de la enfermedad de Pompe.

Un alto número de enfermedades neuromusculares están caracterizadas por la ausencia de terapias. En otras, como la enfermedad de Pompe, las terapias disponibles no son curativas. Estas necesidades médicas sin satisfacer justifican la investigación y el desarrollo de nuevos tratamientos. La terapia celular representa

una opción terapéutica prometedora para las enfermedades musculares. Sin embargo, el desarrollo de terapias celulares para enfermedades neuromusculares está actualmente limitado por la incapacidad de expandir células regenerativas *in vitro*. En el **capítulo 6** se describe un método para aislar fracciones celulares miogénicas de ratón – llamadas células de reserva – a partir de cultivos celulares expandidos *ex vivo* con capacidad de regenerar musculo esquelético *in vivo* al ser trasplantadas. Las diferentes fracciones de células de reserva tuvieron diferentes propiedades *in vitro* e *in vivo*. En condiciones de diferenciación, las células de reserva de adhesión rápida estaban enriquecidas en células que expresaban miogenina, y contribuyeron preferencialmente a la regeneración muscular de manera directa tras ser trasplantadas en ratones inmunodeficientes previamente heridos. Las células de reserva de adhesión lenta estaban enriquecidas con células que expresaban PAX7, e injertaron primariamente como células madre de musculo esquelético tras ser trasplantadas, mostrando una capacidad regenerativa más alta tras una segunda ronda de daño muscular. Se caracterizó el perfil transcriptómico de estas poblaciones celulares, lo cual permite proveer la primera caracterización molecular de fracciones de células reserva, así como revelar información sobre rutas moleculares mediadas o r células de reserva relacionadas con la regeneración muscular.

Por último, en el **capítulo 7** se debaten los resultados con respecto a la literatura existente. Subrayamos los descubrimientos realizados en esta tesis y los ponemos en contexto con el estado del arte actual acerca de los mecanismos moleculares que gobiernan la enfermedad de Pompe y con las terapias celulares aplicadas a enfermedades neuromusculares. Además, se debate el panorama y los futuros retos que el trabajo contenido en esta tesis encuentra con respecto al desarrollo y aplicación clínica de terapias.

Curriculum vitae

Personal information

Name: Rodrigo Cañibano Fraile

Date of birth: 2nd November 1989

Nationality: Spanish

Telephone: (+31) 61 731 6446 / (+34) 691 413 423

E-mail: rodrigo.canibano.fraile@gmail.com

Professional experience

2021 – present **Life Science and Health Consultant.** FFUND, Abcoude, the Netherlands

Education

2016 – 2022 **PhD Biomedical Sciences.** Department of Pediatrics / Department of Clinical Genetics. **Erasmus Medical Center. Erasmus University Rotterdam**, the Netherlands.

Promotor: Prof. dr. A. van der Ploeg

Co-promotors: Dr. Gerben Schaaf and Dr. Pim Pijnappel

2014 – 2016 **Research Master Molecular Medicine (MSc.). Erasmus University Rotterdam**, the Netherlands.

MSc. Research thesis: Towards a cell-based therapy. Cellular and molecular characterization of muscle regenerative cells expanded *ex vivo*.

Department of Clinical Genetics, Erasmus MC, Rotterdam, Netherlands.

Supervisor: Dr. Gerben Schaaf

Principal investigator: Dr. Pim Pijnappel

MSc. Research internship: Role of integrin alpha 6 in mesenchymal stromal cells of pediatric acute lymphoblastic leukemia.

Department of Pediatric Oncology, Erasmus MC, Rotterdam, Netherlands.

Supervisor: Dr. Cesca van de Ven

Principal investigator: Prof. dr. Monique den Boer

2007 – 2013 **BSc. Biology** (Fundamental Biology specialization). **Universidad de León**, Spain.
Amicus exchange scholarship: University of Wisconsin-Green Bay, Wisconsin, U.S.A.
BSc. Industrial Research Internship – ITACyL, Palencia, Spain.

PhD portfolio

Personal details

Name PhD candidate: Rodrigo Cañibano Fraile

PhD period: October 2016 – March 2021

Erasmus MC department(s): Pediatrics / Clinical Genetics

Research school: Medical Genetics Centre South-West Netherlands (MGC)

Promotor: Prof. Dr. Ans T. van der Ploeg

Co-promotors: Dr. W.W.M. Pim Pijnappel; Dr. Gerben J. Schaaf

PhD training

Courses	Year	Workload (ECTS)
Genetics	2017	3
Laboratory animal science	2017	3
Introduction course R2: Genomics Analysis and Visualization Platform	2017	0.5
Biostatistical Methods I	2018	2
Safe laboratory techniques	2018	0.5
Integrity in science	2019	0.3

Workshops and Seminars	Year	Workload (ECTS)
Department meetings	2016 - 2021	2
Clinical Genetics seminars	2016 - 2021	1
Journal Clubs	2016 - 2021	1.5
Centre Lysosomal Storage Disorders meetings	2016 - 2021	1
24 th MGC PhD Workshop, Leuven, Belgium	2017	1
25 th MGC PhD Workshop, Texel	2018	1
MolMed PhD Day	2018	0.3
26 th MGC PhD Workshop, Maastricht	2019	1
Entrepreneurship Awakening	2020	0.5
Venture Challenge	2020	1.5

Inter(national) meetings	Year	Workload (ECTS)
European Symposium Steps Forward in Pompe disease, Schiphol	2016	1
International Glycogen Storage Disease Conference (IGSD), Groningen	2017	1
Dutch Society for Stem Cell Research (DSSCR) annual meeting, Utrecht	2017-2019	1.5
Muscles2Meet Neuromuscular Young Talent Symposium, Zeist	2017, 2019	2
Society for the Study of Inborn Errors of Metabolism (SSIEM) Annual Symposium, Rotterdam	2019	1
European Study Group on Lysosomal Diseases (ESGLD), Vic, Spain	2019	1
MGC Symposium, Rotterdam	2019	0.5

Presentations	Year	Workload (ECTS)
Oral presentation 24 th MGC workshop, Leuven, Belgium	2017	0.25
Poster presentation 25 th MGC Workshop, Texel	2018	0.25
Poster presentation SSIEM, Rotterdam	2019	0.25
Oral presentation 26 th MGC workshop, Maastricht	2019	0.25
Oral Presentation ESGLD, Vic, Spain	2019	0.25
Poster Presentation ESGLD, Vic, Spain	2019	0.25
Oral Presentation MGC Day, Rotterdam	2019	0.25

Education	Year	Workload (ECTS)
Teaching assistant Junior Med School, Erasmus MC	2018 - 2020	0.75
Supervision Claudia Milazzo, MSc. Molecular Medicine, Internship Year 2 & MSc. Thesis	2018-2019	2
Teaching assistant BSc. Nanobiology, Erasmus MC / TU Delft	2019	0.5
Supervision Carlos A. dos Santos, BA Sc. Life Sciences Hogeschool Utrecht, Internship Year 4 & BA Sc. project	2019-2020	2
Co-supervision Faidra Karkala, MSc. Molecular Medicine, Internship Year 1	2019-2020	1
		Total 36.1

List of publications

Publications:

Schaaf GJ, Canibano-Fraile R, van Gestel TJM, van der Ploeg AT, Pijnappel WWMP. Restoring the regenerative balance in neuromuscular disorders: satellite cell activation as therapeutic target in Pompe disease. *Ann Transl Med.* 2019;7(13):280. doi:10.21037/atm.2019.04.48

Canibano-Fraile R, Boertjes E, Bozhilova S, Pijnappel WWMP, Schaaf GJ. An in vitro assay to quantify satellite cell activation using isolated mouse myofibers. *STAR Protoc.* 2021;2(2):100482. doi:10.1016/j.xpro.2021.100482

Submitted manuscripts:

Ex vivo generation of reserve cell populations with enhanced muscle regenerative properties. Rodrigo Canibano-Fraile, Wesley Huisman, Jip Zonderland, Claudia Milazzo, Tom J.M. van Gestel, Ans T. van der Ploeg, W. W. M. Pim Pijnappel, Gerben J. Schaaf. *Stem Cell Reports.*

Lysosomal glycogen accumulation in Pompe disease results in disturbed cytoplasmic glycogen metabolism. Rodrigo Canibano-Fraile, Laurike Harlaar, Esther Brusse, Nadine A. M. E. van der Beek, Carlos A. dos Santos, Marianne Hoogeveen-Westerveld, Ans T. van der Ploeg, Gerben J. Schaaf, W. W. M. Pim Pijnappel. *Journal of Inherited Metabolic Diseases.*

Manuscripts in preparation:

Provoked muscle regeneration transiently rescues the Pompe disease phenotype: the role of autophagy. Gerben J. Schaaf, Rodrigo Canibano-Fraile, Tom J.M, van Gestel, Ans T. van der Ploeg; W. W. M. Pim Pijnappel. *Manuscript in preparation.*

Acknowledgements

I would like to thank my promotor Prof. dr. Ans van der Ploeg and co-promotors Dr. Gerben Schaaf and Dr. Pim Pijnappel for giving me the opportunity to perform my PhD at their groups and for their support during the past years.

I would also like to extend my acknowledgements to the members of my doctoral committee, former and current members of our research group, and paranymphs. Thank you for your time and dedication. Last, I would not like to forget to thank those who came before us, for they laid the ground that made this work possible.

To my teachers and mentors.

To my friends.

To my family.

Rodrigo.